Universitat de Girona

KSL-W ANALOGUES, PEPTIDE CONJUGATES AND TRYPTOPHAN-CONTAINING CYCLIC PEPTIDES WITH ACTIVITY AGAINST PLANT PATHOGENS

Cristina Camó Marín

Universitat de Girona

Doctoral thesis

KSL-W ANALOGUES, PEPTIDE CONJUGATES AND TRYPTOPHAN-CONTAINING CYCLIC PEPTIDES WITH ACTIVITY AGAINST PLANT PATHOGENS

Cristina Camó Marín

2019

Doctoral Programme in Chemistry

Supervised by:

Dr. Marta Planas Grabuleda

Dr. Lidia Feliu Soley

Tutor:

Dr. Marta Planas Grabuleda

This manuscript has been presented to opt for the doctoral degree from the University of Girona

Dr. Marta Planas Grabuleda and Dr. Lidia Feliu Soley, of the Universitat de Girona,

WE DECLARE:

That the thesis entitled “KSL-W analogues, peptide conjugates and tryptophan-containing cyclic peptides with activity against plant pathogens”, presented by Cristina Camó Marín to obtain a doctoral degree, has been completed under our supervision.

For all intents and purposes, we hereby sign this document.

Dr. Marta Planas Grabuleda

Dr. Lidia Feliu Soley

Girona, 5 March 2019

A la meva família

ACKNOWLEDGEMENTS

I ha arribat el moment que em costava pensar que arribés, el moment en que em trobo escrivint les últimes línies de la tesi. Un llarg camí que ha costat, que ha estat un repte dia rere dia, que m'ha donat moltes alegries però també moltes llàgrimes, però sobretot m'ha permès APRENDRE, no només a nivell de coneixements, si no com a PERSONA.

Per aquest camí hi ha passat molta gent, persones que l'han viscut des d'abans de començar (si ho se... els meus nervis infinits per tot), persones que he conegut durant la carrera i la tesi, persones que han passat de puntetes i també persones amb qui no ha estat fàcil, però de cada una d'elles he intentat aprendre, fer-me millor persona i "quedar-me" amb tot el positiu d'aquesta experiència així que GRÀCIES!!!

Intentaré posar ordre perquè si no ... començo pel principi (i espero no deixar-me a ningú)!

Primer de tot voldria agrair a les meves directores, la Dra. Marta Planas i la Dra. Lídia Feliu, la confiança que van dipositar en mi i tota la seva ajuda al llarg d'aquests anys, no només de Doctorat, si no també de Treball Experimental. Recordo com si fos ara el dia que vaig rebre el vostre correu dient-me si volia fer el doctorat (i efectivament, encara no m'ho crec). També m'agradaria donar les gràcies a la Dra. Montse Heras, per tot el que m'ha ensenyat i per totes les estones compartides al laboratori.

Tot seguit, voldria agrair a totes les persones que formen part dels Serveis Tècnics de la UdG el seu suport, però sobretot a l'Anna Costa per tots els ESI-MS realitzats, per tota la seva ajuda i paciència amb nosaltres. Per altra banda, no em puc oblidar de donar les gràcies a la Dra. Esther Badosa i en general al grup CIDSAV per haver realitzat les proves biològiques de tots els meus productes de la tesi.

I fins aquí la part més "formal" dels agraïments ...

A partir d'aquí, m'agradaria donar les gràcies a totes aquelles persones, que d'una manera o una altre, m'han "aguantat" poc o molt al llarg d'aquesta tesi (que no han estat poques). Començaré per la Cris R. qui em va introduir en el món dels pèptids i de la fase sòlida durant el meu treball experimental, i si, qui primer em va sentir dir que estava nerviosa per la presentació el primer dia que entrava al lab. A la Sílvia, per les nostres converses i els nostres farts de riure; i a la Nerea, una persona forta, amb molta empenta

Ja endinsada en el camí de la tesi, no em puc oblidar de tots els meus "nens" (com els hi dèiem, els Minions), que m'han fet suar, però de qui he après moltíssim i m'ha fet millorar com a persona. Sempre ho dic, per mi, el més complicat de la tesi ha estat "gestionar" els nens. En Joel i l'Elena, que van començar a posar les bases en aquesta tesi; en Zeus, que va ser el primer de tots a patir-me, en Christian, l'Eila, l'Àlex, la Leila, l'Anna Clopés, la Kristy, la Maria i en Marcel.

ACKNOWLEDGMENTS

Va arribar el moment de quedar-me "sola" com a doctorant del lippso i això va propiciar encara més les trobades de passadís i conèixer a l'Ester i en Martí i, òbviament els nostres enanitos treballadors. Gràcies per totes i cadascunes de les estones compartides, pel nostre grup "batalla de les verdures", pels nostres farts de riure i per les nostres "desfogades", i els nostres esmorzars amb en Pep i la Montse que eren el millor moment dia. Gràcies a aquests esmorzars va aparèixer a la petita del grup, l'Anna V. , qui des del minut 1 em va demostrar tenir un enorme cor dins d'un cos petit. Gràcies per ser-hi sempre petita.

Però a qui li he d'agraïr tota aquesta tesi i tots els moments viscuts és a la meva "mami lipssiana" Iteng. Gràcies per tot el que m'has ensenyat, gràcies per totes i cada unes de les tonteries que hem fet juntes (no recordaré el moment Skype entre despatxos o l'iteng està apagada o fora de cobertura ...), gràcies per tots els moments de tancament de porta, pels "momentos punkis", per les abraçades just en el moment que feien falta, per les paraules que necessitava escoltar just quan me les deies. I sobretot per ajudar-me quan més ho necessitat. He sigut capaç d'acabar la tesi gràcies a tu, perquè no m'ha sigut fàcil combinar escriure la tesi amb la feina, però en tots i cada un dels moments hi has estat. De veritat que GRÀCIES!!

Dins l'àmbit més personal, no em puc oblidar de donar les gràcies al meu compi Ivan, amb qui hem compartit mil riures dins i fora de la pista de pàdel. Per cert, no cal que vagis preparant les receptes perquè seré doctora en Química i no metge eeh.

I endinsada en l'àmbit familiar, no em puc deixar als meus pares i al meu germà "petit" Marc per tot el seu recolzament i l'ajuda en els bons, però sobretot en els no tant bons (que no són pocs). Sense vosaltres no hauria estat possible: US ESTIMO!!

I per acabar, GRÀCIES Miquel per aquests 13 anys junts, per "aguantar-me", i més sobretot durant el final de la tesi, que no ha estat fàcil. Gràcies per estar sempre al meu costat pet, T'ESTIMO !!

A tots vosaltres, MOLTÍSSIMES GRÀCIES!!!!

The development of this Doctoral Thesis has been funded by the following research projects of "Ministerio de Ciencia e Innovación":

- ✓ "Nuevas estrategias de control del fuego bacteriano. Péptidos sintéticos estimuladores de defensa en el huésped" (AGL2012-39880-C02-02)

- ✓ Péptidos conjugados para el control de bacterias fitopatógenas de cuarentena (METAPEP) (AGL2015-69876-C2-2-R)

Cristina Camó Marín thanks to a Doctoral grant of the Ministerio de Ciencia e Innovación (BES-2013-065571)

Publications derived from this thesis:

- ✓ Badosa, E.; Montesinos, L.; Camó, C.; Ruz, L.; Cabrefiga, J.; Francés, J.; Gascón, B.; Planas, M.; Feliu, L.; Montesinos, E. Control of fire blight infections with synthetic peptides that elicit plant defense responses. *J. Plant Pathol.* **2017**, *99*, 65-73.

- ✓ Camó, C.; Torné, M.; Besalú, E.; Rosés, C.; Cirac, A.; Moiset, G.; Badosa, E.; Bardají, E.; Montesinos, E.; Planas, M.; Feliu, F. Tryptophan-containing cyclic decapeptides with activity against plant pathogenic bacteria. *Molecules,* **2017**, *22*, 1817.

- ✓ Camó, C.; Bonaterra, A.; Badosa, E.; Baró, A.; Montesinos, L.; Montesinos, E.; Planas, M.; Feliu, L. Antimicrobial peptide KSL-W and analogues: Promising agents to control plant diseases. *Peptides,* **2019**, *112*, 85-95.

Publications in preparation derived from this thesis:

- ✓ Camó, C.; Planas, M.; Feliu, L. Design and synthesis of peptide conjugates. *In preparation.*

Publications derived from other projects:

- ✓ Crous-Masó, J.; Palomeras, S.; Camó, C.; Martínez-Garza, Ú.; Planas, M.; Feliu, L.; Puig, T. (-)-Epigallocatechin 3-gallate synthetic analogues inhibit fatty acid synthase and show anticancer activity in triple negative breast cancer. *Molecules*, **2018**, *23*, 1160.

- ✓ Rosés, C.; Camó, C.; Oliveras, À.; Moll, L.; López, N.; Feliu, L.; Planas, M. Total solid-phase synthesis of dihydroxy fengycin derivatives. *J. Org. Chem*. **2018**, *83-24*, 15297-15311.

- ✓ Rosés, C.; Camó, C.; Vogels, K.; Planas, M.; Feliu, L. Solid-phase synthesis of cyclic depsipeptides containing a tyrosine phenyl ester bond. *Org. Lett*. **2016**, *18*, 4140-4143.

- ✓ Vilà, S.; Camó, C.; Figueras, E.; Badosa, E.; Montesinos, E.; Planas, M.; Feliu, L. Solid-phase synthesis of cyclic lipopeptidotriazoles. *Eur. J. Org. Chem*. **2014**, 4785-4794.

aa	Amino Acid
Ac	Acetyl
All	Allyl
ASM	Acibenzolar-S-methyl
Boc	*tert*-Butyloxycarbonyl
^{t}Bu	*tert*-Butyl
CM	Aminomethyl ChemMatrix
CPP	Cell-penetrating Peptide
DIPCDI	*N,N'*-Diisopropylcarbodiimide
DIEA	*N,N'*-Diisopropylethylamine
DMF	*N,N'*-Dimethylformamide
Equiv	Equivalent
ESI-MS	Electrospray Ionization-mass Spectrometry
Fmoc	9-Fluorenylmethyloxycarbonyl
HPLC	High Performance Liquid Chromatography
HRMS	High Resolution Mass Spectrometry
ivDde	1-(4,4-dimetyl-2,6-dioxocyclohex-1-ylidine)-3-methylbutyl
JA	Jasmonic Acid
m/z	Mass-to-charge Ratio
MAMPs	Microbe-associated Molecular Patterns
MBHA	4-Methylbenzhydrylamine
MIC	Minimum Inhibitory Concentration
NMM	*N*-Methylmorpholine
NMP	*N*-Methyl-2-pyrrolidinone
Oxyma	Ethyl 2-cyano-2-(hydroxyamino)acetate
PAC linker	3-(4-Hydroxymethylphenoxi)propionic acid
PAMP	Pathogen-associated Molecular Patterns
PRRs	Pattern Recognition Receptors

PyOxim	[Ethyl cyano(hydroxyimino)acetato-O^2]tri-1-pyrrolidinylphosphonium hexafluorophosphate
Rink	4-[Amino(2,4-dimethoxyphenyl)methyl]phenoxyacetic acid
ROS	Reactive Oxygen Species
TFA	Trifluoroacetic Acid
THF	Tetrahydrofuran
TIS	Triisopropylsilane
t_R	Retention Time
Tr	Trityl

Name	Three letter code	One letter code
Aspartic acid	Asp	D
Glutamic acid	Glu	E
Alanine	Ala	A
Arginine	Arg	R
Asparagine	Asn	N
Cysteine	Cys	C
Phenylalanine	Phe	F
Glycine	Gly	G
Glutamine	Gln	Q
Histidine	His	H
Isoleucine	Ile	I
Leucine	Leu	L
Lysine	Lys	K
Methionine	Met	M
Proline	Pro	P
Serine	Ser	S
Tyrosine	Tyr	Y
Threonine	Thr	T
Tryptophan	Trp	W
Valine	Val	V

ABSTRACT

One of the main reasons for the economic losses in the agriculture system are diseases caused by pathogenic microorganisms which are responsible for crop devastation and a low and poor quality of the fruits. Nowadays, the control of plant diseases is mainly based on the use of antibiotics, but they are not authorized in the European Union and some bacterial strains have developed resistance to them. In this context, the LIPPSO group in collaboration, with the CIDSAV group, is studying the use of peptides to control diseases caused by pathogens such as *Xanthomonas axonopodis* pv. *vesicatoria, Erwinia amylovora*, *Pseudomonas syringae* pv. *syringae*, *Xanthomonas fragariae*, *Pseudomonas syringae* pv. *actinidiae or Xanthomonas arboricola* pv. *pruni* as an alternative to traditional antibiotics.

With the aim of identifying new agents active against plant pathogens of economic importance, in this thesis 15 peptides reported as plant defense elicitors, promiscuous, multifunctional or antimicrobial were selected, synthesized and tested against the six plant pathogenic bacteria mentioned above. Among them, KKVVFWVKFK-NH_2 (**KSL-W**) displayed the highest antimicrobial activity against all the tested pathogens, low hemolysis and low phytotoxicity in tobacco leaves. This peptide was taken as a lead and 49 analogues were designed and synthesized in order to improve its biological activity profile. The designed analogues included N-terminal deletion sequences, and peptides incorporating a D-amino acid or an acyl chain. The screening of these sequences revealed that a nine amino acid length was the minimum for activity. The presence of a D-amino acid significantly decreased the hemolysis and endowed **KSL-W** within the capacity of inducing the expression of defense-related genes in tomato plants. The incorporation of an acyl chain led to sequences with high activity against *Xanthomonas* strains, low hemolysis and phytotoxicity. Therefore, this study demonstrates that **KSL-W** constitutes an excellent candidate as new agent to control plant diseases and can be considered as a lead to develop derivatives with multifunctional properties, including antimicrobial and plant defense elicitation.

Additionally, we studied the use of peptide conjugates incorporating an antimicrobial peptide, a plant defense elicitor peptide and/or a cell-penetrating peptide (CPP) as a strategy to find new leads with improved properties. In particular, 28 peptide conjugates were designed using **BP100** and **BP16** as CPPs, **KSL-W** as antimicrobial peptide; and **Pep13**, **flg15**, **Pip1** and **BP13** as elicitor peptides. Moreover, the order of the sequences was analysed in order to study the influence of this order on the biological activity. Taking all the activity results together, we concluded that peptides **BP100-Pep13** and **KSLW-BP16** showed the best biological profile with MIC values ranging from 0.8 to 6.2 μM and hemolysis below 7% at 50 μM. These peptides also had low phytotoxicy causing a necrosis area of 0.04 and 0.34 cm, respectively, at 50 μM.

The third part of the thesis was centred on the synthesis of cyclic decapeptides incorporating a Trp residue. Selected members of a library of 66 cyclic peptides were prepared on solid phase. All this library was then screened against the phytopathogenic bacteria *Pseudomonas syringae* pv. *syringae*, *Xanthomonas axonopodis* pv. *vesicatoria* and *Erwinia amylovora*. The hemolytic activity of these peptides was also tested. The results obtained were compared with those of a collection of Phe analogues

previously reported. The analysis of the data showed that the replacement of Phe for a Trp residue improved the antimicrobial activity against these three pathogens. In particular, around 40 Trp analogues showed lower MIC values than their corresponding Phe derivatives. Interestingly, 26 Trp-containing sequences exhibited MIC of 0.8 to 3.1 µM against *X. axonopodis* pv. *vesicatoria*, 21 peptides MIC of 1.6 to 6.2 µM against *P. syringae* pv. *syringae* and six peptides MIC of 6.2 to 12.5 µM against *E. amylovora*. Regarding the hemolysis, in general, Trp derivatives displayed a percentage of hemolysis comparable to that of their Phe analogues. Notably, 40 Trp-containing cyclic peptides showed a hemolysis below 20% at 125 µM. The peptides with the best biological activity profile were c(LKKKLWKKLQ) (**BPC086W**) and c(LKKKKWLLKQ) (**BPC108W**), which displayed MIC values ranging from 0.8 µM to 125 µM. Therefore, it is evident that these Trp sequences constitute promising candidates for the development of new agents for use in plant protection.

Moreover, with the same aim of finding new antimicrobial cyclic peptides containing a Trp residue, a second library was designed, based on a computational method called *Superposing Significant Interaction Rules* (SSIR). After applying this method to the previously Trp-containing cyclic peptides library, 22 new sequences were obtained. Among them, c(KKKKKWLKLQ) (**BPC870W**) leads to MIC values ranging from 3.1 to 6.2 µM against *P. syringae* pv. *syringae* and *X. axonopodis* pv. *vesicatoria*, and from 12.5 to 25 µM against *E. amylovora*. In addition, it only caused 19% of hemolysis at 125 µM.

This thesis allowed the identification of new lead peptides with a good biological profile which can be used to control phytopathogenic diseases, including **KSL-W** and analogues, conjugate peptides and Trp-containing cyclic peptides.

RESUM

Una de les raons principals de les pèrdues econòmiques en el sistema agrícola són les malalties causades per microorganismes patògens responsables de la devastació dels cultius i d'una baixa i pobre qualitat dels fruits. Actualment, el control de les malalties vegetals es basa principalment en l'ús d'antibiòtics, però no estan autoritzades a la Unió Europea i algunes soques bacterianes han desenvolupat resistència. En aquest context, el grup LIPPSO, en col·laboració amb el grup CIDSAV, estudia l'ús de pèptids per controlar les malalties causades per agents patògens com *Xanthomonas axonopodis* pv. *vesicatoria*, *Erwinia amylovora*, *Pseudomonas syringae* pv. *syringae*, *Xanthomonas fragariae*, *Pseudomonas syringae* pv. *actinidiae* o *Xanthomonas arboricola* pv. *pruni* com una alternativa als antibiòtics tradicionals.

Amb l'objectiu d'identificar nous agents actius contra patògens vegetals d'importància econòmica, en aquesta tesi, es van seleccionar, sintetitzar i provar contra els patògens descrits 15 pèptids definits com a estimuladors de defenses en plantes, promiscus, multifuncionals o antimicrobians, contra els sis bacteris patògens vegetals esmentats anteriorment. Entre elles, KKVVFWVKFK-NH_2 (**KSL-W**) va mostrar la major activitat antimicrobiana contra tots els patògens provats, baixa hemòlisi i baixa fitotoxicitat a les fulles de tabac. A partir de l'estructura del KSL-W es van dissenyar i sintetitzar 49 anàlegs per millorar el seu perfil d'activitat biològica. Els anàlegs dissenyats van incloure seqüències on es realitzava una eliminació dels residus d'aminoàcids de l'extrem N-terminal, i pèptids que incorporaven un D-aminoàcid o una cadena d'acil. L'anàlisi de les activitats antimicrobianes va demostrar que es requereix una longitud de nou aminoàcids per tal de la seqüència sigui activa. A més, la presència d'un D-aminoàcid va disminuir significativament l'hemòlisi i va dotar al **KSL-W** la capacitat d'induir l'expressió de gens relacionats amb la defensa en plantes de tomàquet. Per altra banda, la incorporació d'una cadena d'acil va conduir a seqüències amb elevada activitat contra les soques de *Xanthomonas*, baixa hemòlisis i fitotoxicitat. Per tant, aquest estudi demostra que KSL-W és un excel·lent candidat com a nou agent per controlar les malalties de plantes i es pot considerar un pèptid *lead* per desenvolupar nous derivats amb propietats multifuncionals, incloent l'estimulació de defenses en plantes.

A més, es va estudiar l'ús de pèptids conjugats que incorporaven un pèptid antimicrobià, un pèptid estimulador de defenses i/o un *cell-penetrating peptide* (CPP) com a estratègia per l'obtenció de nous pèptids *lead* amb propietats millorades. Concretament, s'han dissenyat 28 pèptids conjugats utilitzant **BP100** i **BP16** com a CPPs, **KSL-W** com a pèptid antimicrobià, i **Pep13**, **flg15**, **Pip-1** i **BP13** com a estimuladors de defenses. A més, es va analitzar l'ordre de les seqüències en la conjugació per estudiar la influència d'aquest ordre en l'activitat biològica. Tenint en compte totes les activitats juntes, vam concloure que els pèptids BP100-Pep13 i KSLW-BP16 van mostrar el millor perfil biològic amb valors de concentració mínima inhibitòria (CMI) d'entre 0,8 i 6,2 µM i hemòlisi per sota del 7% a 50 µM. Aquests pèptids també eren poc fitotòxics, causant una àrea de necrosi de 0,04 i 0,34 cm, respectivament, a 50 µM.

La tercera part de la tesi es va centrar en la síntesi de decapèptids cíclics que incorporaven un residu de Trp. Els membres seleccionats d'una quimioteca de 66 pèptids cíclics es van sintetitzar en fase sòlida. Tota

aquesta biblioteca es va provar contra els bacteris fitopatògens *Pseudomonas syringae* pv. *syringae*, *Xanthomonas axonopodis* pv. *vesicatoria* i *Erwinia amylovora*. També es va determinar l'activitat hemolítica d'aquests pèptids. Els resultats obtinguts es van comparar amb els d'una col lecció d'anàlegs contenint un residu de Phe anteriorment estudiats. L'anàlisi de les dades va mostrar que la substitució del residu de Phe per un de Trp va millorar l'activitat antimicrobiana contra aquests tres patògens. En concret, prop de 40 anàlegs de Trp presentaven valors de CMI més baixos que els seus derivats amb Phe. De forma interessant, 26 seqüències que contenen Trp mostraven una MIC de 0,8 a 3,1 µM contra *X. axonopodis* pv. *vesicatoria*, 21 pèptids una MIC d'1,6 a 6,2 µM contra *P. syringae* pv. *syringae* i sis pèptids una CMI de 6,2 a 12,5 µM contra *E. amylovora*. Pel que fa a la hemòlisi, en general, els derivats de Trp mostren un percentatge d'hemòlisis comparable al dels seus anàlegs amb Phe. Notablement, 40 pèptids cíclics que contenen Trp mostren una hemòlisis inferior al 20% a 125 µM. Els pèptids amb el millor perfil d'activitat biològica van ser c(LKKKLWKKLQ) (**BPC086W**) i c(LKKKKWLLKQ) (**BPC108W**), que mostraven valors de CMI que van des de 0,8 µM a 125 µM. Per tant, és evident que aquestes seqüències de Trp constitueixen candidats prometedors per al desenvolupament de nous agents per a l'ús en protecció fitosanitària.

A més, amb el mateix objectiu de trobar nous pèptids cíclics antimicrobians que contenen un residu de Trp, es va dissenyar una segona quimioteca, basada en un mètode computacional anomenat *Superposing Commonwealth Rules* (SSIR). Després d'aplicar aquest mètode a l'anterior quimioteca de pèptids cíclics que contenia Trp, es van obtenir 22 noves seqüències. Entre ells, c(KKKKKWLKLQ) (**BPC870W**) condueixen a valors MIC que oscil·len entre 3.1 i 6.2 µM contra *P. syringae* pv. *syringae* i *X. axonopodis* pv. *vesicatoria* i de 12,5 a 25 µM contra E. amylovora. A més, només va causar un 19% d'hemòlisis a 125 µM.

Aquesta tesi va permetre identificar nous pèptids lead amb un bon perfil biològic que es poden utilitzar per controlar les malalties fitopatogèniques, incloent **KSL-W** i anàlegs, pèptids conjugats i pèptids cíclics que contenen Trp.

RESUMEN

Una de las razones principales de las pérdidas económicas en el sistema agrícola son las enfermedades causadas por microorganismos patógenos responsables de la devastación de los cultivos y de una baja y pobre calidad de los frutos. Actualmente, el control de las enfermedades vegetales se basa principalmente en el uso de antibióticos, pero no están autorizados en la Unión Europea y algunas cepas bacterianas han desarrollado resistencia. En este contexto, el grupo LIPPSO, en colaboración con el grupo CIDSAV, estudia el uso de péptidos para controlar las enfermedades causadas por agentes patógenos como *Xanthomonas axonopodis* pv. *vesicatoria*, *Erwinia amylovora*, *Pseudomonas syringae* pv. *syringae*, *Xanthomonas fragariae*, *Pseudomonas syringae* pv. *actinidiae* o *Xanthomonas arboricola* pv. *pruni* como una alternativa a los antibióticos tradicionales.

Con el objetivo de identificar nuevos agentes activos contra patógenos vegetales de importancia económica, en esta tesis, se han seleccionado, sintetizado y probado contra los patógenos descritos 15 péptidos definidos como estimuladores de defensas en plantas, promiscuos, multifuncionales o antimicrobianos, contra las seis bacterias patógenos vegetales mencionados anteriormente. Entre ellos, KKVVFWVKFK-NH_2 (**KSL-W**) mostró la mayor actividad antimicrobiana contra todos los patógenos probados, baja hemólisis y baja fitotoxicidad en las hojas de tabaco. A partir de la estructura del **KSL-W** se diseñaron y sintetizaron 49 análogos para mejorar su perfil de actividad biológica. Los análogos diseñados incluyeron secuencias donde se realizaba una eliminación de los residuos de aminoácidos del extremo N-terminal, y péptidos que incorporaban un D-aminoácido o una cadena de acilo. El análisis de las actividades antimicrobianas demostró que se requiere una longitud de nueve aminoácidos para que la secuencia sea activa. Además, la presencia de un D-aminoácido disminuyó significativamente la hemólisis y dotó al **KSL-W** de la capacidad de inducir la expresión de genes relacionados con la defensa en plantas de tomate. Por otra parte, la incorporación de una cadena de acilo condujo a secuencias con elevada actividad contra las cepas de *Xanthomonas*, baja hemólisis y fitotoxicidad. Por tanto, este estudio demuestra que **KSL-W** es un excelente candidato como nuevo agente para controlar las enfermedades de plantas y se puede considerar un péptido *lead* para desarrollar nuevos derivados con propiedades multifuncionales, incluyendo la estimulación de defensas en plantas.

Además, se estudió el uso de péptidos conjugados que incorporaban un péptido antimicrobiano, un péptido estimulador de defensas y/o un *cell-penetrating peptide* (CPP) como estrategia para la obtención de nuevos péptidos *lead* con propiedades mejoradas. Concretamente, se han diseñado 28 péptidos conjugados utilizando **BP100** y **BP16** como CPPS, **KSL-W** como péptido antimicrobiano, y **Pep13**, **flg15**, **Pip-1** y **BP13** como estimuladores de defensas. Además, se analizó el orden de las secuencias en la conjugación para estudiar la influencia de este orden en la actividad biológica. Teniendo en cuenta todas las actividades juntas, concluimos que los péptidos **BP100-Pep13** y **KSLW-BP16** mostraron el mejor perfil biológico con valores de concentración mínima inhibitoria (CMI) de entre 0,8 y 6,2 µM y hemólisis por debajo del 7% a 50 µM. Estos péptidos también eran poco fitotóxicos, causando un área de necrosis de 0,04 y 0,34 cm, respectivamente, a 50 µM.

La tercera parte de la tesis se centró en la síntesis de decapéptidos cíclicos que incorporaban un residuo de Trp. Los miembros seleccionados de una quimioteca de 66 péptidos cíclicos se sintetizaron en fase sólida. Toda esta quimioteca se probó contra las bacterias fitopatógenos *Pseudomonas syringae* pv. *syringae*, *Xanthomonas axonopodis* pv. *vesicatoria* y *Erwinia amylovora*. También se determinó la actividad hemolítica de estos péptidos. Los resultados obtenidos se compararon con los de una colección de análogos conteniendo un residuo de Phe anteriormente estudiados. El análisis de los datos mostró que la sustitución del residuo de Phe por uno de Trp mejoró la actividad antimicrobiana contra estos tres patógenos. En concreto, cerca de 40 análogos de Trp presentaban valores de CMI más bajos que sus derivados con Phe. De manera interesante, 26 secuencias que contienen Trp mostraban una MIC de 0,8 a 3,1 µM contra *X. axonopodis* pv. *vesicatoria*, 21 péptidos una MIC de 1,6 a 6,2 µM contra *P. syringae* pv. *syringae* y seis péptidos una CMI de 6,2 a 12,5 µM contra *E. amylovora*. En cuanto a la hemólisis, en general, los derivados de Trp muestran un porcentaje de hemólisis comparable al de sus análogos con Phe. Notablemente, 40 péptidos cíclicos que contienen Trp muestran una hemólisis inferior al 20% a 125 µM. Los péptidos con el mejor perfil de actividad biológica fueron c(LKKKLWKKLQ) (**BPC086W**) y c(LKKKKWLLKQ) (**BPC108W**), que mostraban valores de CMI que van desde 0,8 µM a 125 µM. Por lo tanto, es evidente que estas secuencias de Trp constituyen candidatos prometedores para el desarrollo de nuevos agentes para el uso en protección fitosanitaria.

Además, con el mismo objetivo de encontrar nuevos péptidos cíclicos antimicrobianos que contienen un residuo de Trp, se diseñó una segunda quimioteca, basada en un método computacional llamado *Superposing Commonwealth Rules* (SSIR). Después de aplicar este método a la anterior quimioteca de péptidos cíclicos que contenía Trp, se obtuvieron 22 nuevas secuencias. Entre ellos, c(KKKKKWLKLQ) (**BPC870W**) conducen a valores MIC que oscilan entre 3.1 y 6.2 µM contra *P. syringae* pv. *syringae* y *X. axonopodis* pv. *vesicatoria* y de 12,5 a 25 µM contra *E. amylovora*. Además, sólo causó un 19% de hemólisis a 125 µM.

Esta tesis permitió identificar nuevos péptidos *lead* con un buen perfil biológico que se pueden utilizar para controlar las enfermedades fitopatogénicas, incluyendo **KSL-W** y análogos, péptidos conjugados y péptidos cíclicos que contienen Trp.

1. INTRODUCTION

1.1. Plant diseases

Many plant diseases caused by bacteria and fungi are responsible for large economic losses in fruit and vegetable crops (Agrios 2005). It is estimated that in current crop fields over a third of the total potential production is lost because of pests (Oerke 2006). Efforts are placed on securing or increasing crop yield and increasing the half-life span of harvests due to their extremely important economic and social impact. Weeds lead to the highest productivity loss (34%), but, while animal and pathogens pests have less impact (18 and 16% of crops loss, respectively), their management greatly relies on the extensive use of chemical pesticides.

In the European Union there are few products based on chemical compounds authorized for the control of plant diseases and those available have a reduced effectiveness. Moreover, some bacterial strains have developed resistance to those treatments. Therefore, due to the lack of available products to control these pathologies there is a great need to find alternatives to these treatments. For this reason, the LIPPSO group together with the Plant Pathology group CIDSAV of the UdG, have focused their research on the development of new sustainable and effective agents to control plant diseases caused by the following pathogens.

Erwinia amylovora

Erwinia amylovora is a gram-negative bacterium that causes the disease called fire blight, which is the most serious bacteriosis that affects fruit trees of the *Rosacea*e family, and also ornamental plants of great economic and commercial interest (Figure 1). The bacteria penetrate the plant through the flowers or wounds and can affect all the organs of the plant. The infection causes the flower buds and leaves to appear burnt. Depending on the degree of the infection that the tree presents, direct death may occur. Fire blight can be spread both in long and short distances. Bacteria can be spread by air currents and migratory birds or by insects, gardening machines, rain or wind. The control of fire blight is not very effective when plants are affected. Therefore, current investigation is focused on finding strategies to avoid the dispersion of the bacterium (Piqué 2015).

Figure 1. Leaves and pear affected by *Erwinia amylovora*

Xanthomonas axonopodis* pv. *vesicatoria

Xanthomonas axonopodis pv. *vesicatoria* is a gram-negative bacterium which causes the disease called bacterial spot. This pathology is typical of warm and humid climates, and mainly affects tomato and pepper crops (Figure 2). The infection causes the appearance of black spots on the leaves, on the stalk or on the fruits that end up causing plant's plucking or death (Mitrev 2006).

Figure 2. Tomato and leaves affected by *Xanthomonas axonopodis* pv. *vesicatoria*

Xanthomonas fragariae

Xanthomonas fragariae is a bacterium that causes diseases in strawberries. Since Spain is one of the main producers of strawberries, this pathogen is a major economic threat. In general, the disease spreads from the planting of stocks infected by the pathogen. Usually it affects the leaves and the fruits producing a series of spots around the crown of the strawberry that starts as small points that become bigger (Figure 3) (Vandroemmeab 2008).

Figure 3. Spots on strawberry leaves causes by *Xanthomonas fragariae*

Xanthomonas arboricola pv. pruni

Xanthomonas arboricola pv. pruni is a gram-negative bacterium that causes bacterial blight in stone fruits. This pathology is characterized by the appearance of spots in fruits and leaves (Figure 4), making the affected fruits difficult to market. In addition, the production of the affected trees is considerably reduced (EPPO 2005).

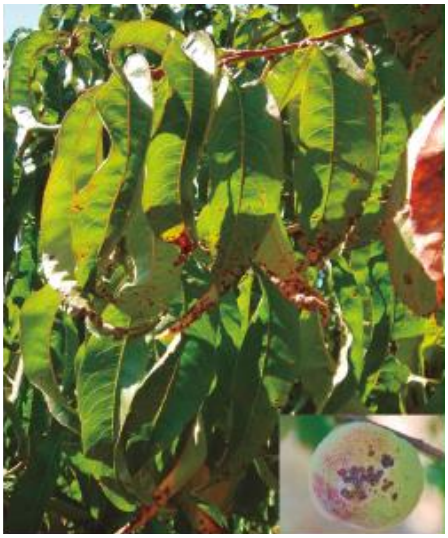

Figure 4. Bacterial blight in stone fruits caused by *Xanthomanas arboricola* pv. *pruni*

Pseudomonas syringae pv. syringae

Pseudomonas syringae pv. *syringae* is a gram-negative bacterium responsible for a large number of diseases called bacterial necrosis. These diseases affect plants and horticultural crops (Figure 5). *P. syringae* pv. *syringae* produces the nucleation of the ice, enhancing the damage caused by frost to the plants. Symptoms are spots on leaves and fruits that prevent their growth (Agrios 2005).

Figure 5. Cherry and leaves infected by *Pseudomonas syringae* pv. *syringae*

Pseudomonas syringae pv. actinidiae

Pseudomonas syringae pv. actinidiae is a bacterium which causes kiwi canker. This pathogen was first described in Japan and is currently beginning to be present in the Mediterranean area. Symptoms

include the brown discoloration of the shoots, the appearance of spots on the leaves and the rapid deterioration of the fruit. The affectation depends on the variety of kiwi (Figure 6) (Abelleira 2015).

Figure 6. Spots on the kiwi leaves caused by *Pseudomonas syringae* pv. *actinidiae*

1.2. Antimicrobial peptides

Antimicrobial peptides are short and cationic sequences, usually less than 50 amino acids (2 - 10 kDa), and many of them are part of the plant immune system. They display a wide range of biological activities, from antibacterial and antifungal to antitumor. In addition, they have important structural characteristics for their activity, such as a positive charge, an amphipathic character, hydrophobicity and a particular secondary structure.

A crucial characteristic for the antimicrobial activity of peptides is their net positive charge, which, in most cases, oscillates between +2 and +9 (Hancock 1997). It is believed that the first step for the activity of this type of sequences is the electrostatic interaction between their positive charge and the negative charge of the surface of the bacterial membrane (Monroc 2006). Consequently, the presence of positively charged residues, such as arginine and lysine, is a crucial feature in the primary structure of antimicrobial peptides (Yeaman 2003). In fact, there are some studies that show that there is a strong relationship between cationicity and antimicrobial activity. However, this ratio is not linear and the lack of a direct correlation has been confirmed by biophysical experiments with membrane models (Toke 2005, Yeaman 2003).

A peptide is amphipathic if it is able to adopt a conformation in which the hydrophobic residues are placed on one side of its structure and the hydrophilic ones, on the opposite side. This property is important since the membranes also presents an amphipathic nature. It has been described that the hydrophobic residues of the peptides interact with the lipid tails of the cell membrane, while the hydrophilic residues of the peptides interact with the polar membrane groups and the aqueous medium (Wu 1999). An increase in the amphipathicity of the peptides leads to an increase in their affinity for all types of membranes and results in a reduction in their selectivity (Wieprecht 1997).

The percentage of hydrophobic residues in a sequence is a measure of its overall hydrophobicity. This characteristic determines the degree of insertion of the peptides into the lipid bilayer of the cell membranes: an increase in the hydrophobicity of a peptide results in its binding to all types of membranes, causing a reduction in the selectivity between the different types of membranes. Therefore, generally the antimicrobial peptides have a moderate number of hydrophobic residues (approximately 50%) to achieve a greater affinity towards the membranes of the microbial cells (Wieprecht 1997).

Many antimicrobial peptides adopt an unstructured or spread out conformation in aqueous medium (Straus 2006), while others adopt a secondary structure of α-helix or β-sheet through the formation of intramolecular hydrogen bonds. The α-helix structure consists of a helical disposition of the peptide chain stabilized by the formation of intracatenary hydrogen bonds. The central structure is formed by the skeleton of the peptide while the side chains extend out of the helix (Grant 1992). The β-sheet structure is characterized by an alignment of two or more peptide chains segments forming a sheet. This structure is stabilized by the formation of hydrogen interactions between the carbonyl groups of the amino acids of a peptide chain and the N-H groups of a second peptide chain. Depending on the relative position of the chains there are two types of β-sheets: parallel and antiparallel sheets. However, it should be noted that antimicrobial peptides present an anti-parallel conformation (Grant 1992).

The importance of the secondary structure in peptide activity has been studied. It has been observed that the alteration of the secondary structure of a peptide modifies the antimicrobial activity and, at the same time, dissociates the antimicrobial activity from the hemolysis. In addition, the loss of a rigid and stable conformation can reduce the activity of a peptide (Oren 1999).

The mechanism of action of antimicrobial peptides is not fully understood, but several models have been proposed. Among them, the most accepted are the barrel-stave model (Figure 7A), in which the peptides create a pore across the membrane ; the carpet model (Figure 7B), where the peptides cover the membrane surface and induce a detergent-like effect, creating micelles with the membrane lipids; and the toroidal pore model (Figure 7C), in which the pores created are transient, with varied duration, and contain both peptides and lipids (Chan 2006).

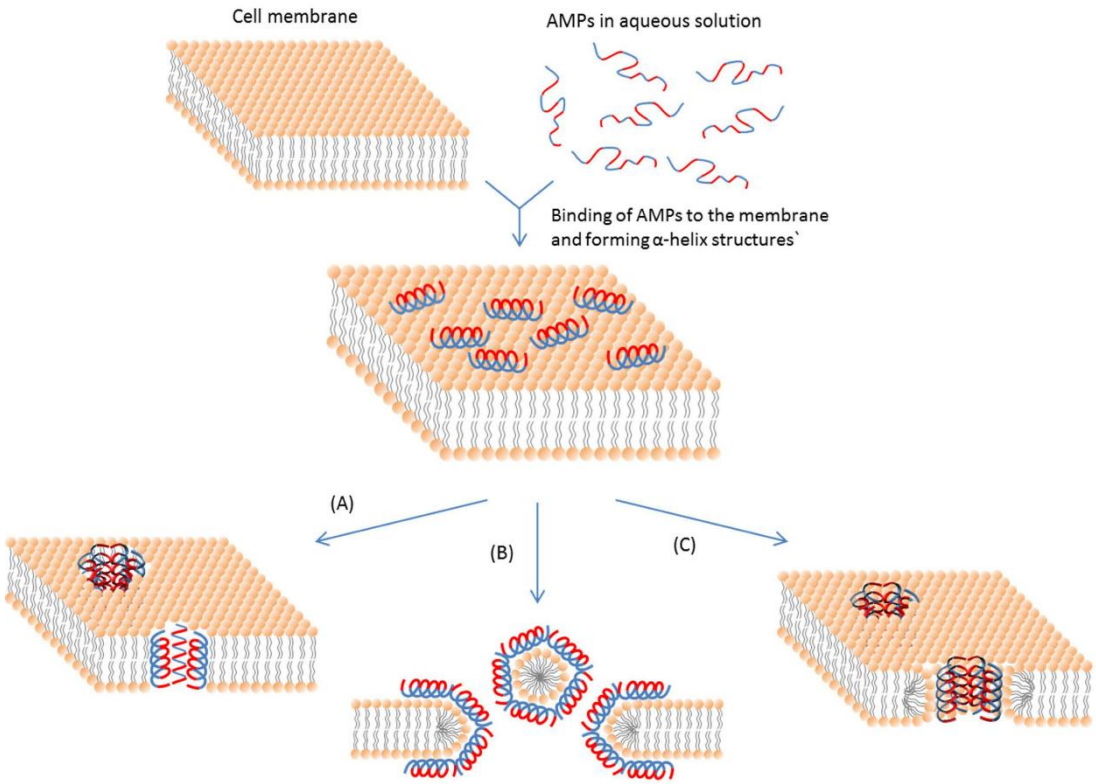

Figure 7. Membrane disruptive models for antimicrobial peptides. The red part of the peptides represents a hydrophilic surface, while the blue colour corresponds to a hydrophobic part. A: the barrel-stave model; B: the carpet model; and C: the toroidal pore model (Bahar 2013)

Antimicrobial peptides have attracted much interest, because the appearance of resistant strains is more difficult since it would require major changes in the cell membrane structure.

In more recent years, it has been proven that some antimicrobial peptides have intracellular targets, interfering with vital processes of the microorganism, such as DNA transcription, RNA translation, protein folding or cell wall synthesis (Brogden 2005). Antimicrobial peptides can inhibit these processes solely or concomitantly with cell disruption activity, which also depend on the species of the targeted microorganism (Hale 2007). This non-cell disrupting mechanism still requires the peptide interaction with the cell membrane to penetrate into the cytoplasm, but it is similar to the mechanism of action antibiotics.

In this context, the LIPPSO group, in collaboration with the CIDSAV group, are interested in finding new antimicrobial peptides as agents to control plant diseases caused by the bacteria described in section 1.1. For this purpose, the LIPPSO group designed a family of 125 linear undecapeptides based on the general structure R-X^1KLFKKILKX^{10}L-NH_2, where X^1 and X^{10} correspond to amino acids with various degrees of hydrophilicity and hydrophobicity (Leu, Lys, Phe, Trp, Tyr or Val) and R includes different N-terminal derivatizations (H, Ac, Ts, Bz or Bn) (Badosa 2007). This library of undecapeptides was synthesized and tested against *E. amylovora*, *X. axonopodis* pv. *vesicatoria* and *P. syringae* pv. *syringae*.

Among them, KKLFKKILKL-NH_2 (**BP100**) displays excellent antimicrobial activity against these phytopathogenic bacteria (MIC of 2.5-7.5 µM) and it is low hemolytic (3% at 50 µM).

The LIPPSO group also designed and synthesized a library of 56 cyclic decapeptides (Monroc 2006), with the general structure c(X_5PheX_3Gln), where X corresponds to Leu or Lys. Among these cyclic peptides, c(KKLKKFKKLQ) (**BPC194**) was identified as a lead peptide. **BPC194** displays excellent antimicrobial activity against *E. amylovora*, *P. syringae* pv. *syringae* and *X. axonopodis* pv. *vesicatoria* (MIC of 3.1-12.5 µM). This peptide also exhibits a low hemolysis (17% at 375 µM).

1.3. Plant defense elicitor peptides

Several peptides have been described to stimulate innate plant immune responses (Markus 2013). These sequences promote molecular mechanisms in plants that lead to an alkalinization of the medium, the production of reactive oxygen species (ROS) or the overexpression of specific genes.

Although plants do not have defense specialized cells against the invasion of pathogens like animals, they present a first barrier of defense located on their surface and formed by impermeable walls, cuticular lipids, antimicrobial enzymes and secondary metabolites (Muthamilarasan 2013). In addition, plants can produce a defensive response through two interconnected defense mechanisms that microorganisms have to overcome in order to survive and promote an infection.

The first mechanism of defense in plants is known as pathogen-associated molecular patterns (PAMP) – triggered immunity (Figure 8a) (Wei 2012 and Pieterse 2009). PAMPs are essential molecular structures that are conserved in different pathogens and are recognized by a group of receptors that are called pattern recognition receptors (PRRs). This recognition promotes different processes that are the basis of the defensive response, such as the alkalinization of the growth medium, the increase of the cytoplasmatic calcium concentration that causes the closure of stomata to avoid the entry of pathogens, the production of ROS and the synthesis of salicylic acid, jasmonic acid and ethylene, which are involved in the regulation of defense mechanisms.

Pathogens can overcome the previous mechanisms and promote a pathogenesis by injecting effector proteins to the cytoplasm of plant cells through the cell wall (Figure 8b). In this case, plants have a second level of defense that can detect and inhibit these effectors, which is known as effector-triggered immunity (Figure 8c) (Nomura 2011). The activation of the effector-triggered immunity mechanisms promotes the synthesis of salicylic acid, jasmonic acid and ethylene, as well as the reinforcement of the cell wall and the production of antimicrobial compounds in the endoplasmic reticulum.

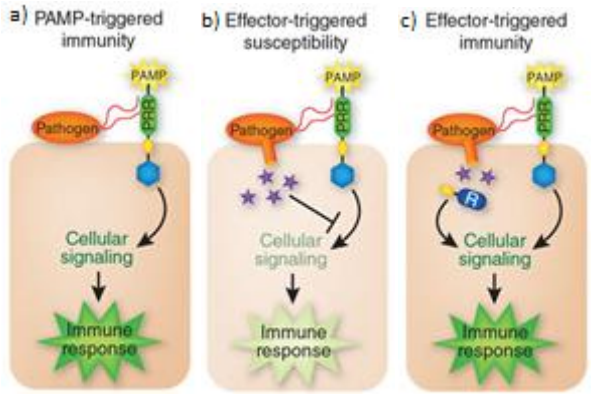

Figure 8. Defense mechanisms of plants (Pieterse 2009)

Several studies have reported that a strategy for the control of plant diseases is the use of peptides that act indirectly protecting plants from pathogens through the induction of the expression of genes involved in defense mechanisms. In particular, natural peptides that act as molecular messengers (MAMPs), endogenous elicitor peptides and synthetic peptides that stimulate the immune system of plants have been described. The MAMPs alert the plant of the potential attack by a microorganism and induce the production of defenses. MAMPs include peptides derived from microbial proteins such as flg22, derived from flagellin (Felix 1999); elf18, derived from EF-Tu (Lacombe 2010); Pep13, derived from transglutaminase (Brunner 2002); or the csp15 derived from a cold shock protein (Felix 2003). Endogenous elicitor peptides regulate the defense mechanisms of plants and are released when damage or infection occurs. Within these endogenous elicitor peptides are the systemins, HypSys, AtPeps, ZmPeps, GmPeps, GmSubPep and the inceptins (Yamaguchi 2011). Some examples of synthetic peptides able to activate the immune system of plants include antimicrobial peptides, hexapeptides and ultrashort cationic lipopeptides (Miyashita 2011, Brotman 2009).

1.4. Strategies to improve the biological profile of antimicrobial peptides

There are several strategies to improve the biological profile of antimicrobial peptides. In particular, these approaches have the aim of increasing their bioavailability and stability towards proteases and/or, of reducing their toxicity. These strategies include, among others, the introduction into the peptide sequence of non-natural amino acids, such as D-isomers, the acylation of the peptide sequence, the preparation of peptide conjugates and the synthesis of analogues containing a tryptophan residue (Ng-Choi 2014).

a) Incorporation of a D-amino acid

The introduction of D-isomers in a peptide sequence is a widely used strategy to improve the biological profile of peptides. Although this modification destabilizes the secondary structure, other structural properties, such as the hydrophobicity and the charge distribution, are maintained. Moreover, this strategy leads to less hemolytic and more stable peptides towards proteolytic enzymes, while maintaining their antimicrobial activity (Oren 1997, Matsuzaki 2009).

The LIPPSO group synthesized a collection of peptides derived from **BP100** incorporating a D-amino acid (Güell 2011). Among them, **BP143** (KKLfKKILKL-NH_2), **BP145** (KkLFKKILKL-NH_2) and **BP147** (kKLFKKILKL-NH_2) showed a similar antimicrobial activity to that of the parent peptide **BP100** (<7.5 μM) against E. *amylovora*, *P. syringae* pv. *syringae* and *X. axonopodis* pv. *vesicatoria.* Interestingly, all the sequences synthesized, except for **BP147**, exhibited lower hemolysis values than **BP100** and all of them were more stable to the degradation by proteases.

b) Incorporation of a fatty acid chain

The acylation of peptides with a fatty acid chain has been demonstrated to be a useful strategy to improve their antimicrobial activity. This has been observed for lipopeptides resulting from the acylation of the N-terminus of cationic antimicrobial peptides with fatty acids of 8 to 18 carbons (Malina 2005).

The general mechanism of action of lipopeptides is similar to that of antimicrobial peptides. They also target the microbial membrane and act by inhibiting the synthesis of cell wall compounds or by inducing membrane lysis by forming channels or pores. In addition, it has been observed that the acyl group is a key point for their antimicrobial activity, because it increases the affinity of the peptides towards the membrane, favouring their insertion into the hydrophobic core of the bilayer (Mandal 2013).

The LIPPSO group synthesized a library of cyclic lipopeptides derived from **BPC194**. In this study, it was reported that the length of the hydrophobic chain influenced the antimicrobial activity of the peptide. The most active cyclic lipopeptides were those bearing an acyl chain of 4 to 6 carbons (Vilà 2014). **BPC500** (c(KKLKK(CO-C_3H_7)FKKLQ), bearing a butyric acid group, displayed MIC values ranging from 3.1 to 12.5 μM against *E. amylovora*, *P. syringae pv. syringae* and *X. axonopodis pv. vesicatoria* and an hemolysis value of 15% at 50 μM. Other studies revealed the importance of the length of the hydrophobic chain on the antimicrobial activity of peptides derivatized with an acyl chain. However, their findings pointed out that the highest activity was observed for those lipopeptides containing an acyl chain of 14 to 16 carbon. (Vilà 2013).

c) Peptide conjugates

A strategy to increase the efficacy of peptides consists on the conjugation of two peptides (identical or different). It has been shown that in these homo- or heterodimeric peptides, the intermolecular bonding of the sequences reinforces the activity of the two individual peptides, while increasing the stability to degradation by proteases as well as the solubility (Lorenzón 2012).

The LIPPSO group is investigating the efficacy of synthetic peptide conjugates based on the combination of two sequences with different activities. In particular, the conjugation between antimicrobial peptides, elicitor peptides, cell-penetrating peptides and multifunctional peptides is studied. The application of those conjugates in plants could lead to the elimination of the corresponding pathogen and, at the same

time, to the stimulation of the defenses of the plant, with an effective prevention of the corresponding disease.

d) Incorporation of a tryptophan residue

Some authors have described that tryptophan plays an important role in the activity of antimicrobial peptides, since it has been observed that peptides rich in this amino acid have a relevant and broad spectrum of biological activity. This behaviour has been attributed to the hydrophilic and hydrophobic characteristics of the tryptophan indole ring that favour their insertion in the lipid bilayer through hydrogen bonding and π-cation interactions (Muñoz 2007).

In order to increase the biological activity of the cyclic decapeptides of the library described in section 1.2, the LIPPSO group designed and synthesized a library of 66 cyclic peptides incorporating a tryptophan residue instead of phenylalanine. Thus, the general structure of these peptides is c(X_5-Trp-X_3-Gln), where X is lysine or leucine. Specifically, 50 peptides contain all combinations of 3 leucines and 5 lysines, and 16 peptides incorporate the substructure K^5WKKLQ^{10}, and all possible combinations of leucine and lysine in positions 1 to 4.

The evaluation of the antimicrobial activity of this library of peptides against *E. amylovora*, *P. syringae* pv. *syringae* and *X. axonopodis* pv. *vesicatoria*, as well as of their hemolytic activity led to peptides with a good biological profile (**BPC072W**, **BPC098W**, **BPC120W** and **BPC132W**), which displayed MIC values ranging from 1.6 to 25 µM, and a hemolysis lower than 20% at 125 µM (Table 1). Cyclic peptides with the best biological profile were **BPC086W** and **BPC108W**, with MIC between 0.8 and 12.5 µM, and a low hemolytic activity (≤ 8% at 125 µM).

Moreover, since more active sequences were identified than those previously described bearing a phenylalanine, these results revealed that the presence of a tryptophan residue in the sequence of this family of cyclic peptides enhanced the antimicrobial activity against the three pathogens tested.

Table 1. Antimicrobial activity (MIC) and hemolysis of cyclic peptides containing a Trp residue

Peptide	Sequence	MIC (µM)			Hemolysis (%) (125 µM)
		Pss[a]	*Xav*[a]	*Ea*[a]	
BPC072W	c(KKKLKWLKLQ)	3.1-6.2	1.6-3.1	12.5-25	9
BPC086W	c(LKKKLWKKLQ)	3.1-6.2	0.8-1.6	6.2-12.5	8
BPC098W	c(LLKKKWKKLQ)	3.1-6.2	1.6-3.1	12.5-25	18
BPC108W	c(LKKKKWLLKQ)	1.6-3.1	1.6-3.1	6.2-12.5	5
BPC120W	c(LKKLKWKLKQ)	3.1-6.2	1.6-3.1	12.5-25	9
BPC132W	c(KLKKLWLKKQ)	3.1-6.2	1.6-3.1	12.5-25	8

[a] *Pss*, *Pseudomonas syringae* pv. *syringae*; *Xav*, *Xanthomonas axonopodis* pv. *vesicatoria; Ea, Erwinia amylovora.*

1.5. Solid-phase peptide synthesis

Solid-phase synthesis meant a breakthrough in the field of the preparation of peptides. This simple and practical methodology was developed by Robert Bruce Merrifield, a biochemist who received the Nobel Prize in Chemistry in 1984 for this achievement (Merrifield 1963). Currently, it is the most commonly used procedure for the synthesis of peptides.

Compared to the synthesis in solution, solid-phase synthesis presents a number of advantages (Kates 2000). In this synthetic methodology an excess of reagents is used, allowing the reactions to be quantitative in each reaction step. This excess of reagents and the soluble by-products can be removed by filtration and washes of the solid support. According to this methodology, solvents of high boiling points, such as *N,N'*-dimethylformamide (DMF) or *N*-methyl-2-pyrrolidinone (NMP), can be used. In addition, all reactions are carried out within the same container, which avoids the loss of peptide by manipulation. Moreover, the solid-phase synthesis allows easy automation of the process and is a convenient method to be used in combinatorial chemistry.

Generally, solid-phase peptide synthesis is performed from the C- to the N-terminus of the peptide, that is, in the C → N sense. The synthesis consists of sequential steps of coupling and deprotection of the different amino acids in order to obtain the desired peptide (Scheme 1). Thus, after coupling the first amino acid conveniently protected to the solid support, the protecting group of the α-amino is removed in order to proceed to the coupling of the next amino acid. Once the sequence is completed, the peptide is cleaved from the support (Scheme 1).

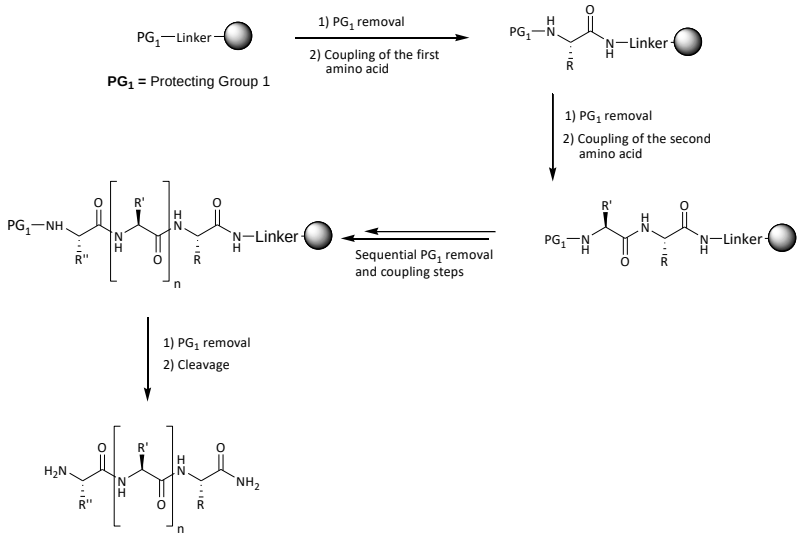

Scheme 1. General strategy for the synthesis of linear peptides on solid phase

The solid-phase synthesis of cyclic peptides involves the preparation of the corresponding protected linear sequence (Scheme 2). In this case, the first amino acid of the sequence (C-terminal) is linked to

the resin through its side-chain. Next, the protecting groups of the N and C-terminus are removed, which is followed by the cyclization and the cleavage of the peptide from the support.

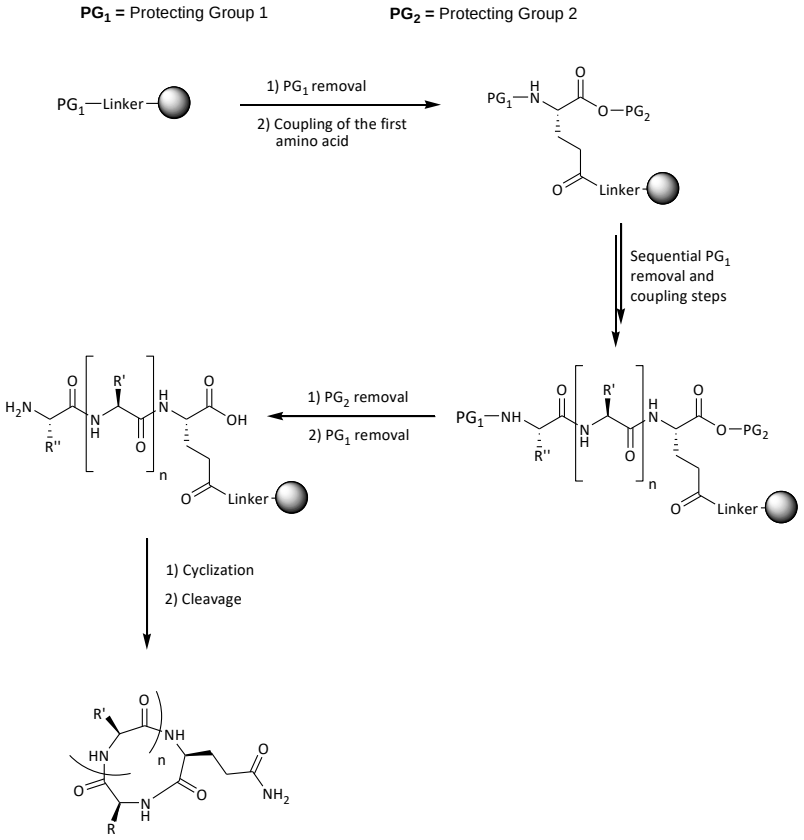

Scheme 2. Synthesis of cyclic peptides on solid phase

The key points of the solid-phase synthesis are the solid support, the linker, the protecting groups, the coupling reagents and the cleavage.

a) Solid support

The solid support is the insoluble polymeric matrix where the chemical reactions necessary for the synthesis of the peptide occur. Certain physical and chemical properties are required for a solid support to be useful for peptide synthesis. It must be chemically stable, it must be composed of particles of a convenient size and shape to allow its manipulation and the rapid filtration of solvents, and it must be inert to the reagents and solvents used in the synthesis. In addition, the support must be conveniently functionalized to allow the coupling of the linker (Grant 1992).

Nowadays, the most common types of solid supports are: polystyrene-divinylbenzene-based resins and polyethylene glycol-based resins. The resins used in this work are shown in Table 2.

Table 2. Representative resins used in solid-phase peptide synthesis

Structure	Name
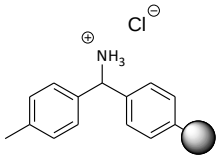	*p*-Methylbenzhydrylamine (**MBHA**)
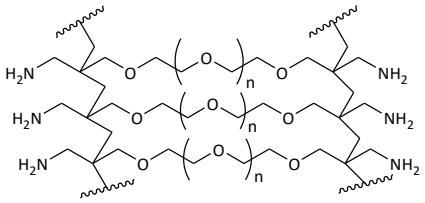	Aminomethyl ChemMatrix (**CM**)

b) Linker

The linker is a bifunctional molecule which, on the one hand, is attached to the solid support and, on the other hand, is attached to the first amino acid of the sequence. The bond between the linker and the solid support must be stable throughout the different steps of the synthesis and to the conditions of the cleavage. On the other hand, the linkage of the linker with the peptide must be stable during the synthesis, but it must be labile to the cleavage conditions.

The linkers used in this work, their cleavage conditions and the resulting C-terminal functional group are shown in Table 3.

Table 3. Linkers used in this work and cleavage conditions

Structure	Name	Cleavage conditions	Resulting C-terminus
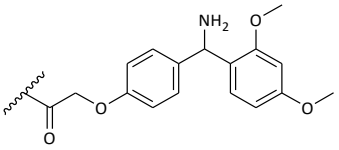	Rink amide	TFA	Amide
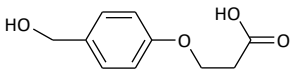	PAC	TFA	Carboxylic acid

c) Protecting groups

In order to avoid side reactions during the coupling steps of the different amino acids, it is necessary to use protecting groups for the α-amino group and for the functional groups of the side chains of the trifunctional amino acids.

There are two types of protecting groups. On the one hand, the temporary groups protect the α-amino group and are removed before the coupling of the next amino acid. On the other hand, the permanent groups are used to protect the side-chain functional groups and are usually removed during the cleavage step. It is important that the conditions for the removal of these two types of protecting groups are completely different in order to be able to remove them selectively.

In general, for the synthesis of linear peptides, a 9-fluorenylmethoxycarbonyl (Fmoc)/*tert*-butyl (^{t}Bu) strategy is used. This strategy is based on the orthogonality between these two protecting groups. Two protecting groups are orthogonal when their removal mechanisms are different and, therefore, one can be removed in the presence of the other and in any order. In order to synthesize cyclic peptides, a third level of orthogonality must be introduced, therefore, a three-dimensional orthogonal strategy is followed. In this work a Fmoc/^{t}Bu/allyl (All) strategy was used. In some cases, the synthesis of peptides requires the use of protecting groups which can be removed selectively. In this work, has been used the group 1-(4,4-dimethyl-2,6-dioxocyclohex-1-ylidene)-3-methylbutyl (ivDde) for the protection of the N^{ε}-amino group of a Lys residue. This group can be removed with 2% hydrazine in DMF or NMP and it is stable to the conditions of the peptide synthesis. Some representative protecting groups are shown in Table 4.

Table 4. Protecting groups used in this work and removal conditions

Structure	Name	Removal conditions	Protected group
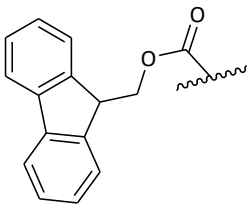	9-Fluorenylmethoxycarbonyl (**Fmoc**)	30% Piperidine	Amine
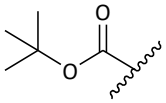	*tert*-Butyloxycarbonyl (**Boc**)	95% TFA	Amine
	*tert*-Butyl (**^{t}Bu**)	95% TFA	Hydroxyl
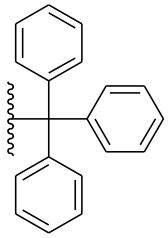	Trityl (**Tr**)	1% TFA	Amine
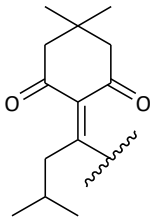	1-(4,4-Dimethyl-2,6-dioxocyclohex-1-ylidene)-3-methylbutyl (**ivDde**)	2% Hydrazine	Amine
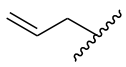	Allyl (**All**)	$Pd(PPh_3)_4$	Carboxylic acid

d) Coupling reagents

Couplings of the amino acids need to be mediated by coupling reagents. These reagents activate the α-carboxyl group of the amino acid to be coupled, because they increase the electrophilic character of this group, facilitating the formation of the amide bond.

One of the most commonly used coupling reagents is *N,N'*-diisopropylcarbodiimide (DIPCDI) (Figure 9). Additionally, the ethyl 2-cyano-2-(hydroxyamino)acetate (Oxyma) is added in order to avoid secondary reactions.

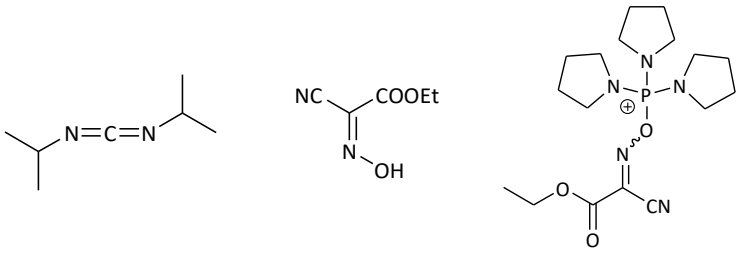

Figure 9. Structure of DIPCDI, Oxyma and PyOxim

In order to synthesize cyclic peptides, [ethyl cyano(hydroxyimino)acetato-O^2]tri-1-pyrrolidinylphosphonium hexafluorophosphate (PyOxim) is used as reagent coupling, Oxyma as additive and *N,N*-diisopropylethylamine (DIEA) as a base.

e) Cleavage

The last step of the solid-phase synthesis of peptides consists in the cleavage of the peptide from the support. In general, an acidolytic solution is used, specifically a solution of trifluoroacetic acid (TFA)/H_2O/triisopropylsilane (TIS) (95:2.5:2.5). H_2O and TIS have the purpose of capturing carbocations formed at this stage, avoiding secondary reactions.

These conditions, besides disassociating the peptide from the solid support, also promote the simultaneous removal of the acid labile protecting groups present in the side chains of the trifunctional amino acids. Therefore, as a final product, the peptide is obtained completely unprotected.

2. OBJECTIVES

The main objectives of this PhD thesis are:

a) Identification of new lead peptides active against plant pathogens from sequences described in the literature with interesting biological activity. The selected peptides will be tested for their antibacterial activity, hemolysis and phytotoxicity. The structure of the peptide with the best biological activity profile will be optimized. These analogues will also be screened for their capacity to induce plant defense responses.

b) Design and synthesis of peptide conjugates incorporating a cell-penetrating peptide (CPP), an antimicrobial peptide and/or a plant defense peptide elicitor. The influence of the order of conjugation on the antimicrobial activity, hemolysis and phytotoxicity will be evaluated.

c) Study of the influence on the biological activity of the replacement of a phenylalanine with a tryptophan in a library of cyclic decapeptides.

d) Design and synthesis of new tryptophan-containing cyclic decapeptides.

3. RESULTS AND DISCUSSION

3.1. KSL-W and analogues:

Promising agents to control plant diseases

*This chapter is based on the article "*Camó, C.; Bonaterra, A.; Badosa, E.; Baró, A.; Montesinos, L.; Montesinos, E.; Planas, M.; Feliu, L. Antimicrobial peptide KSL-W and analogues: Promising agents to control plant diseases*. *Peptides,* **2019**, 85".

The finding of new antimicrobial peptides active *in vivo* against plant pathogens demands the accessibility to a wide range of sequences with high activity *in vitro*. Realizing this need, we selected sequences described in the literature as plant defense elicitors, promiscuous, multifunctional or antimicrobial to be further tested against our target plant pathogens. Moreover, these sequences have been also described as low hemolytic and toxic.

3.1.1. Selection of peptides

The selected peptides are described below and included in Table 5.

- ✓ *Antimicrobial peptides*

***Bm*LAO-f1** (IKFEPPLPPKKAH-NH_2) is a fragment of a multifunctional enzyme called LAO protein isolated from *Bothropoides mattogrosensis* venom which displays antimicrobial activity against Gram-positive and Gram-negative bacteria and is low hemolytic (Okubo 2012). Apart from having antimicrobial activity, LAO enzyme is able to decrease platelet aggregation, stimulate edema formation, control tumorous cells, and play an important role in host innate immunity for other organisms. For these reasons, LAO enzyme is described as a multifunctional enzyme.

Api88 (Gu-ONNRPVYIPRPRPPHPRL-NH_2) is a Pro-rich antimicrobial peptide derived from apidaecin 1b with improved activity against Gram-negative bacteria, both in vitro and in vivo, and without toxicity towards human cells (Czihal 2012, Volke 2015, Ostorhazi 2014).

JCpep7 (KVFLGLK-OH) is a short cationic antimicrobial peptide isolated from *Jatropha curcas* that displays activity against Gram-positive and Gram-negative bacteria (Xiao 2011).

The decapeptide **KSL** (KKVVFKVKFK-NH_2) was identified from a combinatorial library and shows a wide range of antimicrobial activity being low hemolytic. Moreover, it effectively blocks oral biofilm formation and inhibits the activity of several oral bacteria involved in caries development (Hong 1998, Concannon 2003 and Na 2007). Later, an improved KSL analogue in terms of stability in the oral cavity was reported (Na 2007). This analogue, known as **KSL-W** (KKVVFWVKFK-NH_2), incorporates a Trp residue at position 6 instead of a Lys, preserves a high activity against a range of oral bacteria and fungi, prevents the development of oral biofilms, and is nontoxic against normal human gingival epithelial cells (Na 2007, Theberge 2013, Semlali 2011, Bernegossi 2016). In addition, it has been shown that KSL-W is also effective towards other bacteria associated with wound healing (Gawande 2014).

- ✓ *Multifunctional peptides*

Peptides QKALNEINQF-NH_2 (**p10**) and TKKTKLTEEEKNRL-NH_2 (**p14**) isolated from bovine milk display multifunctional activity. They show angiotensin-converting enzyme inhibition, prolyl endopeptidase inhibition, antioxidant and antimicrobial activities (Sistla 2013, Srinivas 2010).

Preprotemporin-1CEa (FVDLKKIANIINSIFGK-NH_2) and temporin-1CEa (FVDLKKIANIINSIF-NH_2) are short, hydrophobic peptides that inhibit the growth of Gram-positive bacteria. They are also active against a wide range of human cancer cell lines and show a moderate hemolysis (Shang 2009, Wang 2012, Wang 2013, Wang 2016).

The lactoferrin-derived peptide WFRKQLKW-OH (**L10**) is a multifunctional compound that possesses antimicrobial, anti-inflammatory and antiendotoxin activities being also low hemolytic (Mishra 2013).

Frenatin 2.1S (GLVGTLLGHIGKAILG-NH_2) and **frenatin 2.2S** (GLVGTLLGHIGKAILS-NH_2) were isolated from skin secretions of the frog *Sphaenorhynchus lacteus* and display antibacterial activity against methicillin-resistant bacterial strains, are low hemolytic and have also been reported as immunostimulatory agents (Conlon 2014, Pantic 2015).

- ✓ *Promiscuous peptides*

The antimicrobial peptides ***Cn*-AMP1** (SVAGRAQGM-NH_2), ***Cn*-AMP2** (TESYFVFSVGM-NH_2) and ***Cn*-AMP3** (YCSYTMEA-NH_2) identified from green coconut (*Cocos nucifera*) water have been described to be active against Gram-positive and Gram-negative bacteria as well as to display immunomodulatory activity (Mandal 2009 and Silva 2012). In addition, *Cn*-AMP1 and *Cn*-AMP2 have also been shown to be effective against cancerous cells (Silva 2012, Prabhu 2014, Gour 2016). Moreover, due to these diverse biological activities, these peptides have been termed as promiscuous (Silva 2012).

- ✓ *Defense elicitors*

Peptide elicitor **Pip-1** (YGIHTH-NH_2), identified through combinatorial chemistry, induces various defense responses in plant cells (Miyashita 2011, Kim 2014, Kim 2015, Kim 2016).

Pep-13 (VWNQPVRGFKVYE-OH), a pathogen-associated molecular pattern from *Phytophthora sojae*, triggers multiple defense responses in parsley and potato (Nürnberger 1994, Brunner 2002, Halim 2009, Landgraf 2014).

Table 5. Sequences of the selected peptides

Peptide	Sequence
Plant defense elicitors	
Pip-1	YGIHTH-NH_2
Pep13	VWNQPVRGFKVYE-OH
Promiscuous peptides	
Cn-AMP1	SVAGRAQGM-NH_2
Cn-AMP2	TESYFVFSVGM-NH_2
Cn-AMP3	YCSYTMEA-NH_2
Multifunctional peptides	
p10	QKALNEINQF-NH_2
p14	TKKTKLTEEEKNRL-NH_2
Preprotemporin-1CEa	FVDLKKIANIINSIFGK-NH_2
L10	WFRKQLKW-OH
Frenatin 2.1S	GLVGTLLGHIGKAILG-NH_2
Frenatin 2.2S	GLVGTLLGHIGKAILS-NH_2
Antimicrobial peptides	
dGu-Api88	ONNRPVYIPRPRPPHPRL-NH_2[c]
JCpep7	KVFLGLK-OH
KSL	KKVVFKVKFK-NH_2
KSL-W	KKVVFWVKFK-NH_2

[a]O stands for 4-hydroxyproline.

3.1.2. Synthesis of the selected peptides

Peptides were manually synthesized on solid-phase using standard Fmoc/^{t}Bu strategy (Scheme 3). A Fmoc-Rink MBHA resin (0.55 mmol/g), a MBHA resin (0.4 mmol/g) or a ChemMatrix resin (0.66 mmol/g) was used as solid support. The ChemMatrix resin was selected for the synthesis of peptides containing more than 11 residues. The PAC-derivatized resins were employed to prepare C-terminal carboxylic acid whereas the Rink-derivatized ones served for C-terminal peptide amides. The coupling of the first amino acid onto the PAC-derivatized resins was performed in presence of DIPCDI, 4-dimethylaminopyridine (DMAP) and DIEA in DMF at room temperature for 2 h under stirring. This treatment was repeated twice and the completion of the coupling was checked using a Fmoc test. Peptide elongation was carried out through sequential Fmoc removal and coupling steps of the corresponding Fmoc-protected amino acid. The Fmoc removal was performed by exposure of the peptidyl resin to a mixture of piperidine/DMF (3:7, 2 + 2x10 min). Couplings of the corresponding amino acids were mediated by Oxyma and DIPCDI in DMF. The completion of the couplings was checked using the Kaiser or the chloranil test (Kaiser 1970, Vojkovsky 1995).

Once the peptide sequence was completed, the resin was treated with piperidine/NMP (3:7, 2 + 2x10 min). Finally, the resulting resin was treated with TFA/H_2O/TIS (95:2.5:2.5) for 2 h at room temperature. In the case of peptides containing a tryptophan residue a mixture of TFA/phenol/H_2O/TIS (92.5:2.5:2.5:2.5) was used. For peptides containing a methionine residue a solution of TFA/dithiothreitol (DTT)/H_2O/TIS (92.5:2.5:2.5:2.5) was employed.

Following TFA evaporation and diethyl ether extraction, the crude peptide was dissolved in H_2O, lyophilized, purified by reverse-phase column chromatography and analysed by HPLC, obtaining excellent purities (90 - >99% HPLC purity) (Table 6). All peptides were characterized by ESI-MS and HRMS.

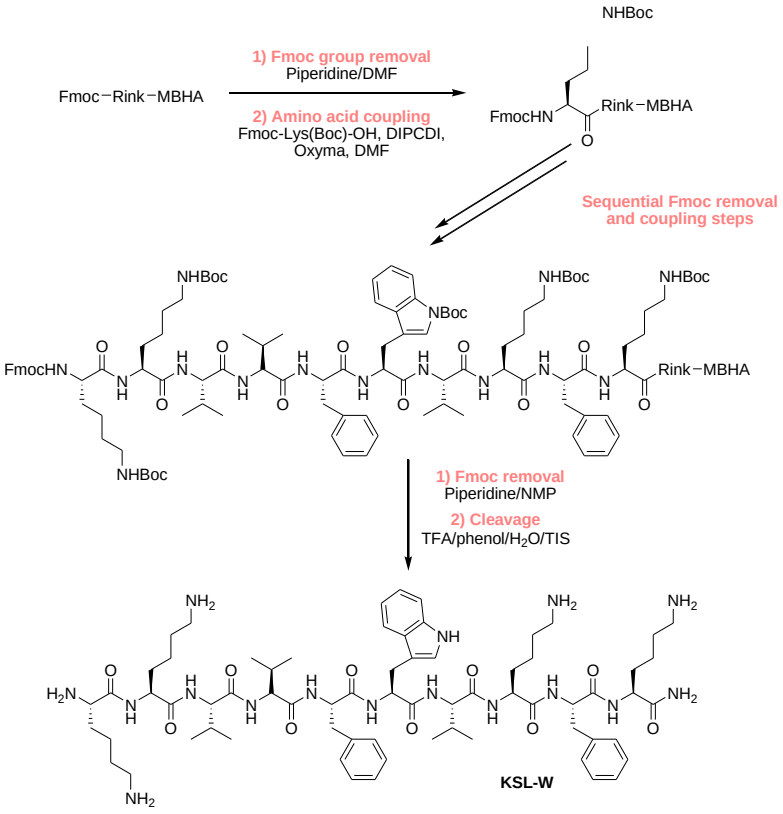

Scheme 3 Solid-phase strategy for the synthesis of linear peptides

Table 6. Sequences, retention times (t_R) and purities on HPLC, ESI-MS and HRMS data of the peptides

Peptide	t_R (min)	Purity[a] (%)	ESI-MS	HRMS[c]
Plant defense elicitors				
Pip-1	5.38	72 (>99[b])	726.4 $[M+H]^+$	726.3688 $[M+H]^+$
Pep13	6.31	63 (>99[b])	811.5 $[M+2H]^{2+}$	811.4266 $[M+2H]^{2+}$
Promiscuous peptides				
Cn-AMP1	5.33	43 (>99[b])	875.5 $[M+H]^+$	-
Cn-AMP2	6.97	65 (>99[b])	1265.6 $[M+H]^+$	1287.5670 $[M+Na]^+$
Cn-AMP3	5.78	73 (>99[b])	966.4 $[M+H]^+$	988.3481 $[M+Na]^+$
Multifunctional peptides				
p10	5.76	73 (>99[b])	1203.7 $[M+H]^+$	1203.6445 $[M+H]^+$
p14	5.38	42 (>99[b])	859.0 $[M+2H]^{2+}$	1716.9983 $[M+H]^+$
Preprotemporin-1CEa	7.07	90	960.6 $[M+2H]^{2+}$	1919.1473 $[M+H]^+$
L10	6.27	96 (>99[b])	1191.8 $[M+H]^+$	607.3312 $[M+H+Na]^{2+}$
Frenatin 2.1S	7.90	95 (>99[b])	1518.0 $[M+H]^+$	759.4799 $[M+2H]^{2+}$
Frenatin 2.2S	7.17	73 (>99[b])	774.5 $[M+2H]^{2+}$	785.4745 $[M+H+Na]^{2+}$
Antimicrobial peptides				
Api88	5.73	93	1096.7 $[M+2H]^{2+}$	2191.2430 $[M+H]^+$
JCpep7	6.01	98 (>99[b])	804.6 $[M+H]^+$	804.5332 $[M+H]^+$
KSL	5.81	63 (>99[b])	1250.0 $[M+H]^+$	625.4278 $[M+2H]^{2+}$
KSLW	6.19	55 (>99[b])	1307.9 $[M+H]^+$	654.4198 $[M+2H]^{2+}$

[a] Percentage determined by HPLC calculated as the area under the peak with respect to total area under peaks at 220 nm from the crude reaction mixture
[b] Percentage determined by HPLC calculated as the area under the peak with respect to total area under peaks at 220 nm from the purified peptide
[c] The calculated theoretical values are available in the experimental section

3.1.3. Biological activity of the selected peptides

The fifteen selected peptides from the literature were tested for *in vitro* growth inhibition of the plant pathogenic bacteria *E. amylovora*, *P. syringae* pv. *syringae*, *P. syringae* pv. *actinidiae*, *X. arboricola* pv. *pruni*, *X. fragariae* and *X. axonopodis* pv. *vesicatoria* at 0.8, 1.6, 3.1, 6.2, 12.5, 25 and 50 µM (Table 7). All these tests were performed by the Plant Pathology group. The results are expressed as the minimum inhibitory concentration (MIC) which is the lowest peptide concentration for which there is no bacterial growth at the end of the experiment.

Table 7. Antimicrobial activity of the selected peptides

Peptide	MIC (μM)					
	Ea[a]	*Pss*[a]	Psa[a]	*Xap*[a]	*Xf*[a]	*Xav*[a]
Plant defense elicitors						
Pip-1	>50	>50	>50	>50	>50	>50
Pep13	>50	>50	>50	>50	>50	>50
Promiscuous peptides						
Cn-AMP1	>50	>50	>50	>50	>50	>50
Cn-AMP2	>50	>50	12.5-25	12.5-25	>50	>50
Cn-AMP3	>50	>50	>50	>50	>50	>50
Multifunctional peptides						
p10	>50	>50	>50	>50	>50	>50
p14	>50	>50	>50	>50	>50	>50
Preprotemporin-1CEa	25-50	>50	>50	3.1-6.2	>50	3.1-6.2
L10	>50	>50	>50	>50	>50	>50
Frenatin 2.1S	25-50	>50	>50	>50	>50	3.1-6.2
Frenatin 2.2S	25-50	>50	>50	6.2-12.5	25-50	6.2-12.5
Antimicrobial peptides						
dGu-Api88	25-50	>50	12.5-25	>50	>50	>50
JCpep7	>50	>50	>50	>50	>50	>50
KSL	>50	6.2-12.5	1.6-3.1	6.2-12.5	6.2-12.5	12.5-25
KSL-W	6.2-12.5	6.2-12.5	1.6-3.1	0.8-1.6	3.1-6.2	6.2-12.5

[a] *Ea, Erwinia amylovora; Pss, Pseudomonas syringae* pv. *syringae; Psa, Pseudomonas syringae* pv. *actinidiae; Xap, Xantomonas arboricola* pv. *pruni; Xf, Xanthomonas fragariae; Xav, Xanthomonas axonopodis* pv. *vesicatoria.*

The plant defense elicitor peptides **Pip-1** and **Pep-13** were not active against these bacteria. Among the other sequences, seven exhibited activity against at least one of the above pathogens (MIC < 25 μM). In particular, the promiscuous peptide ***Cn*-AMP2** showed MIC of 12.5 to 25 μM against *P. syringae* pv. *actinidiae* and *X. arboricola* pv. *pruni*. Among the multifunctional peptides, **preprotemporin-1CEa** and **frenatin 2.2S** displayed MIC values ranging from 3.1 to 12.5 μM against *X. arboricola* pv. *pruni* and *X. axonopodis* pv. *vesicatoria*, and **frenatin 2.1S** was active against the latter pathogen with MIC of 3.1 to 6.2 μM. Concerning the tested antimicrobial peptides, the deguanylated **Api88** (**dGu-Api88**) analogue was active against *P. syringae* pv. *actinidiae* with MIC of 12.5 to 25 μM. Interestingly, **KSL** and **KSL-W** were highly active against the pathogens tested. **KSL** showed MIC values ranging from 1.6 to 25 μM against all bacteria except for *E. amylovora*. **KSL-W** was more active with MIC values between 0.8 to 12.5 μM against all the pathogens, highlighting *P. syringae* pv. *actinidiae* and *X. arboricola* pv. *pruni* (MIC of 1.6 to 3.1 μM and 0.8 to 1.6 μM, respectively).

The toxicity of these peptides to eukaryotic cells was determined as the ability to lyse erythrocytes in comparison to melittin which causes a 100% hemolysis. Percent hemolysis at 375 µM is shown in Table 8. Notably, the best peptides, **KSL** and **KSL-W** were also low hemolytic with a percent hemolysis of 5 and 20%, respectively, at this concentration.

This set of selected peptides was also screened for their effect on tobacco leaves by infiltrating each compound into the mesophylls of the leaves (Table 8). The nonspecific and nonselective toxic melittin was used as positive control, which caused a brown necrotic area of around 2 cm diameter at 250 µM after 48 h of infiltration. In contrast, **KSL** and **KSLW** had a significantly lower effect than melittin at this concentration being the size of the lesions of 0.34 and 0.62 cm, respectively.

Table 8. Hemolysis and phytotoxicity of the selected peptides

Peptide	Hemolysis (%) (375 µM)	Phytotoxicity (cm) (250 µM)
Plant defense elicitors		
Pip-1	0 ± 0.1	0 ± 0
Pep13	0 ± 0.1	0 ± 0
Promiscuous peptides		
Cn-AMP1	0 ± 0.4	0.11 ± 1.0
Cn-AMP2	8 ± 2.7	0 ± 0
Cn-AMP3	95 ± 2.5	0.11 ± 0
Multifunctional peptides		
p10	0 ± 0.1	0 ± 0
p14	0 ± 0.2	0 ± 0
Preprotemporin-1CEa	100 ± 2.6	0.71 ± 0.1
L10	1 ± 0.2	0 ± 0
Frenatin 2.1S	86 ± 2.4	1.10 ± 0.1
Frenatin 2.2S	84 ± 1.8	0.97 ± 0.2
Antimicrobial peptides		
dGu-Api88	1 ± 0.2	0 ± 0
JCpep7	5 ± 0.4	0 ± 0
KSL	5 ± 1.3	0.34 ± 1.0
KSL-W	20 ± 1.8	0.62 ± 0.4

Taken together, these results allowed the identification of **KSL-W**, a short cationic peptide with a suitable activity profile to be considered as an excellent antimicrobial agent against plant pathogenic bacteria. It displayed high antibacterial activity, low hemolysis and phytotoxicity and, therefore, was selected for further studies. It is noteworthy to mention that this is the first report on the antimicrobial activity of **KSL-W** against plant pathogens. Previous studies were focused on its use to fight bacteria present in the oral cavity or in wounds (Concannon 2003, Na 2007, Semlali 2011, Theberge 2013, Bernegossi 2016, Gawande 2014).

3.1.4. Design of KSL-W analogues

Based on **KSL-W** sequence (KKVVFWVKFK-NH_2), a total of 49 analogues were designed. Specifically, N-terminal deletion derivatives containing 4 to 9 amino acids (**BP403** to **BP408**) were synthesized to examine whether the entire sequence of **KSL-W** is necessary for its full antibacterial activity. Moreover, analogues incorporating a D-amino acid at each position of the original peptide (**BP442** to **BP451**) were prepared. This substitution was considered because it constitutes a strategy to protect peptides against enzymatic hydrolysis while reducing their hemolytic activity (Güell 2011). In addition, lipopeptides (**BP409** to **BP441**) were designed by acylating the N-terminus or by replacing each amino acid of the sequence with a lysine residue acylated at its side-chain with butyric, hexanoic or lauric acid. In particular, these acyl groups were chosen because they promoted the best results in a previous work based on studying the antimicrobial activity of cyclic lipopeptides (Vilà 2016). Thus, the influence on the biological activity of the hydrophobic chain length and its position was evaluated. The incorporation of an acyl chain to a peptide has been described as an approach to increase the affinity of peptides towards microbial membranes enhancing their antimicrobial activity (Vilà 2016, Makovitzki 2006, Jerala 2007, Mangoni 2011).

3.1.5. Synthesis of KSL-W analogues

The synthesis of the N-terminal deletion sequences and of the peptides incorporating a D-amino acid was performed manually on solid-phase using a standard Fmoc/^{t}Bu strategy, with a Fmoc-Rink-MBHA resin as solid support. The same protocol described in section 3.1.2 was followed.

The resulting peptides corresponding to the N-terminal deletion were analysed by HPLC obtaining purities between 62 and 85%, and characterized by ESI-MS and HRMS. On the other hand, peptides incorporating a D-amino acid were purified by reverse-phase column chromatography being obtained in excellent HPLC purities (>99%) and characterized by mass spectrometry. All results are shown in Tables 9 and 10.

Table 9. Sequences, retention times and purities on HPLC, ESI and HRMS data of N-terminal deletion analogues.

Peptide	Sequence	t_R (min)	Purity[a] (%)	ESI-MS	HRMS[b]
BP403	VKFK-NH_2	5.29	62	520.3 $[M+H]^+$	260.6844 $[M+2H]^{2+}$
BP404	WVKFK-NH_2	5.78	82	706.4 $[M+H]^+$	353.7226 $[M+2H]^{2+}$
BP405	FWVKFK-NH_2	6.11	85	853.5 $[M+H]^+$	427.2569 $[M+2H]^{2+}$
BP406	VFWVKFK-NH_2	6.21	76	952.5 $[M+H]^+$	318.1966 $[M+3H]^{3+}$
BP407	VVFWVKFK-NH_2	6.33	82	1051.6 $[M+H]^+$	351.2210 $[M+3H]^{3+}$
BP408	KVVFWVKFK-NH_2	6.19	67	1179.7 $[M+H]^+$	393.9165 $[M+3H]^{3+}$

[a] Percentage determined by HPLC calculated as the area under the peak with respect to total area under peaks at 220 nm from the crude reaction mixture
[b] The calculated theoretical values are available in the experimental section

Table 10. Sequences, retention times and purities on HPLC, ESI and HRMS data of D-analogues.

Peptide	Sequence[a]	t_R (min)	Purity[b] (%)	ESI-MS	HRMS[d]
BP442	KKVVFWVKFk-NH_2	6.07	88 (>99[c])	1330.0 $[M+Na]^+$	436.6179 $[M+3H]^{3+}$
BP443	KKVVFWVKfK-NH_2	6.02	90 (>99[c])	1308.0 $[M+H]^+$	436.6179 $[M+3H]^{3+}$
BP444	KKVVFWVkFK-NH_2	5.98	49 (>99[c])	1330.0 $[M+Na]^+$	436.6176 $[M+3H]^{3+}$
BP445	KKVVFWvKFK-NH_2	6.09	67 (>99[c])	654.5 $[M+2H]^{2+}$	436.6169 $[M+3H]^{3+}$
BP446	KKVVFwVKFK-NH_2	6.26	91 (>99[c])	1330.0 $[M+Na]^+$	436.6159 $[M+3H]^{3+}$
BP447	KKVVfWVKFK-NH_2	6.25	93 (>99[c])	1330.0 $[M+Na]^+$	436.6155 $[M+3H]^{3+}$
BP448	KKVvFWVKFK-NH_2	6.27	91 (>99[c])	1330.0 $[M+Na]^+$	436.6155 $[M+3H]^{3+}$
BP449	KKvVFWVKFK-NH_2	6.18	71 (>99[c])	1330.0 $[M+Na]^+$	436.6157 $[M+3H]^{3+}$
BP450	KkVVFWVKFK-NH_2	6.11	61 (>99[c])	1330.0 $[M+Na]^+$	436.6169 $[M+3H]^{3+}$
BP451	kKVVFWVKFK-NH_2	6.13	68 (>99[c])	1308.0 $[M+H]^+$	436.6167 $[M+3H]^{3+}$

[a] Lower-case letters are D-enantiomers.
[b] Percentage determined by HPLC calculated as the area under the peak with respect to total area under peaks at 220 nm from the crude mixture peptide
[c] Percentage determined by HPLC calculated as the area under the peak with respect to total area under peaks at 220 nm from the purified peptide
[d] The calculated theoretical values are available in the experimental section

The synthesis of the N-terminal acylated sequences followed a similar protocol and, once peptide chain elongation was completed, the N-terminal Fmoc group was removed and the free amino group was derivatized with butanoic, hexanoic or lauric acid (10 equiv) in presence of DIPCDI (10 equiv) and Oxyma (10 equiv) in NMP for 1 h under stirring. Peptides were cleaved from the resin by acidolytic treatment, purified by reverse-phase column chromatography and were obtained in excellent purities (>99%), as determined by analytical HPLC (Table 11). Their identity was confirmed by mass spectrometry.

Table 11. Sequences, retention times and purities on HPLC, and MS data of N-terminal acylated sequences

Peptide	Sequence	t_R (min)	Purity[a] (%)	ESI-MS	HRMS[c]
BP409	$C_5H_{11}CO$-KKVVFWVKFK-NH_2	6.53	71 (>99[b])	1427.9 $[M+Na]^+$	469.3072 $[M+3H]^{3+}$
BP410	C_3H_7CO-KKVVFWVKFK-NH_2	6.30	59 (>99[b])	1399.8 $[M+Na]^+$	459.9627 $[M+3H]^{3+}$
BP411	$C_{11}H_{23}CO$-KKVVFWVKFK-NH_2	7.36	71 (>99[b])	1513.0 $[M+Na]^+$	497.3374 $[M+3H]^{3+}$

[a] Percentage determined by HPLC calculated as the area under the peak with respect to total area under peaks at 220 nm from the crude mixture peptide
[b] Percentage determined by HPLC calculated as the area under the peak with respect to total area under peaks at 220 nm from the purified peptide
[c] The calculated theoretical values are available in the experimental section

In the case of the side-chain acylated peptides, the lysine to be derivatized was incorporated as Fmoc-Lys(ivDde)-OH, because the removal of this group can be achieved by treatment with hydrazine and it is stable towards the conditions used to remove Fmoc in the peptide synthesis (Scheme 4). After completion of the peptide sequence, the N-terminus was acetylated yielding peptidyl resins **1**-**10**. An aliquot of these resins was treated with TFA and the resulting peptides were analysed by HPLC and characterized by ESI-MS (Table 12).

Table 12. Sequences, retention time and HPLC purities, and ESI-MS data.

Sequence	t_R (min)	Purity[a] (%)	ESI-MS
CH_3CO-KKVVFWVKFK(ivDde)-NH_2	6.97	79	778.9 $[M+2H]^{2+}$
CH_3CO-KKVVFWVKK(ivDde)K-NH_2	6.46	70	1537.0 $[M+H]^+$
CH_3CO-KKVVFWVK(ivDde)FK-NH_2	6.94	79	1555.9 $[M+H]^+$
CH_3CO-KKVVFWK(ivDde)KFK-NH_2	6.58	72	1585.0 $[M+H]^+$
CH_3CO-KKVVFK(ivDde)VKFK-NH_2	6.45	52	1498.0 $[M+H]^+$
CH_3CO-KKVVK(ivDde)WVKFK-NH_2	6.47	73	1537.0 $[M+H]^+$
CH_3CO-KKVK(ivDde)FWVKFK-NH_2	6.61	83	1585.0 $[M+H]^+$
CH_3CO-KKK(ivDde)VFWVKFK-NH_2	6.59	83	1585.0 $[M+H]^+$
CH_3CO-KK(ivDde)VVFWVKFK-NH_2	6.98	73	1556.0 $[M+H]^+$
CH_3CO-K(ivDde)KVVFWVKFK-NH_2	6.94	73	1556.0 $[M+H]^+$

[a] Percentage determined by HPLC calculated as the area under the peak with respect to total area under peaks at 220 nm from the crude mixture peptide

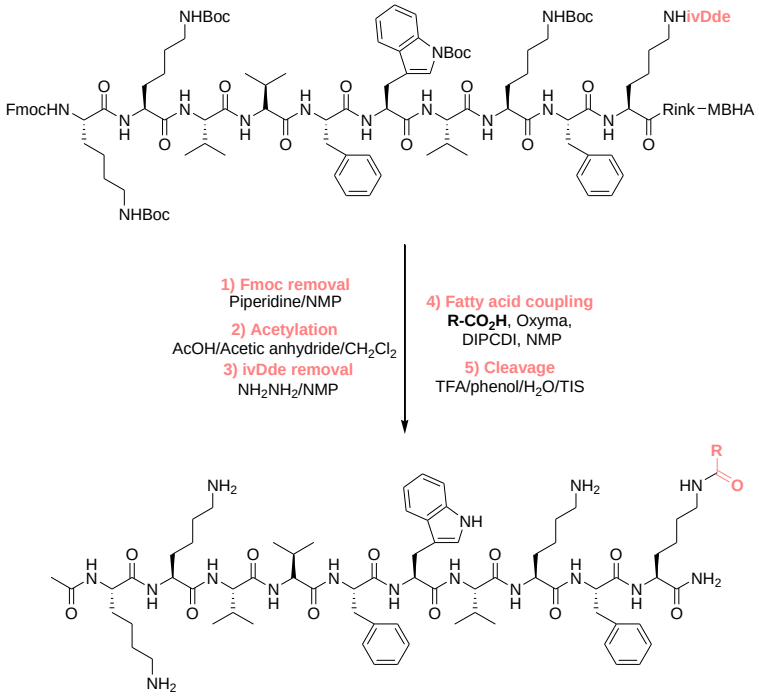

Scheme 4. General strategy for the solid-phase peptide synthesis for lipopeptides

Next, the ivDde group was removed by treatment with hydrazine and the resulting free amino group was acylated with the corresponding fatty acid. After acidolytic cleavage, lipopeptides were purified by reserve-phase column chromatography being obtained in excellent HPLC purities (93->99%) and characterized by mass spectrometry (Table 13).

Table 13. Sequences, retention time and HPLC purity, ESI-MS and HRMS data of lipopeptides derived from **KSL-W**.

Peptide	Sequence	t_R (min)	Purity[a] (%)	ESI-MS	HRMS[c]
BP412	CH_3CO-KKVVFWVKFK(CO-C_5H_{11})-NH_2	6.74	65 (>99[b])	724.4 $[M+2H]^{2+}$	483.3111 $[M+3H]^{3+}$
BP413	CH_3CO-KKVVFWVKFK(CO-C_3H_7)-NH_2	6.53	64 (>99[b])	1442.1 $[M+Na]^{+}$	473.9678 $[M+3H]^{3+}$
BP414	CH_3CO-KKVVFWVKFK(CO-$C_{11}H_{23}$)-NH_2	7.72	68 (>99[b])	766.6 $[M+2H]^{2+}$	511.3431 $[M+3H]^{3+}$
BP415	CH_3CO-KKVVFWVKK(CO-C_5H_{11})K-NH_2	6.34	57 (>99[b])	715.0 $[M+2H]^{2+}$	476.9874 $[M+3H]^{3+}$
BP416	CH_3CO-KKVVFWVKK(CO-C_3H_7)K-NH_2	6.11	50 (>99[b])	701.0 $[M+2H]^{2+}$	467.6437 $[M+3H]^{3+}$
BP417	CH_3CO-KKVVFWVKK(CO-$C_{11}H_{23}$)K-NH_2	7.18	59 (>99[b])	757.6 $[M+2H]^{2+}$	505.0202 $[M+3H]^{3+}$
BP418	CH_3CO-KKVVFWVK(CO-C_5H_{11})FK-NH_2	6.76	58 (>99[b])	1448.1 $[M+H]^{+}$	483.3118 $[M+3H]^{3+}$
BP419	CH_3CO-KKVVFWVK(CO-C_3H_7)FK-NH_2	6.52	50 (>99[b])	710.5 $[M+2H]^{2+}$	473.9685 $[M+3H]^{3+}$
BP420	CH_3CO-KKVVFWVK(CO-$C_{11}H_{23}$)FK-NH_2	7.66	69 (>99[b])	767.1 $[M+2H]^{2+}$	511.3422 $[M+3H]^{3+}$
BP421	CH_3CO-KKVVFWK(CO-C_5H_{11})KFK-NH_2	6.44	60 (>99[b])	739.1 $[M+2H]^{2+}$	492.9859 $[M+3H]^{3+}$
BP422	CH_3CO-KKVVFWK(CO-C_3H_7)KFK-NH_2	6.23	48 (>99[b])	725.0 $[M+2H]^{2+}$	483.6428 $[M+3H]^{3+}$
BP423	CH_3CO-KKVVFWK(CO-$C_{11}H_{23}$)KFK-NH_2	7.25	68 (>99[b])	781.2 $[M+2H]^{2+}$	521.0187 $[M+3H]^{3+}$
BP424	CH_3CO-KKVVFK(CO-C_5H_{11})VKFK-NH_2	6.26	45 (>99[b])	1390.2 $[M+H]^{+}$	463.9834 $[M+3H]^{3+}$
BP425	CH_3CO-KKVVFK(CO-C_3H_7)VKFK-NH_2	6.05	49 (>99[b])	681.5 $[M+2H]^{2+}$	454.6387 $[M+3H]^{3+}$
BP426	CH_3CO-KKVVFK(CO-$C_{11}H_{23}$)VKFK-NH_2	7.11	63 (>99[b])	738.1 $[M+2H]^{2+}$	492.0150 $[M+3H]^{3+}$
BP427	CH_3CO-KKVVK(CO-C_5H_{11})WVKFK-NH_2	6.33	43 (>99[b])	715.1 $[M+2H]^{2+}$	736.9569 $[M+2Na]^{2+}$
BP428	CH_3CO-KKVVK(CO-C_3H_7)WVKFK-NH_2	6.12	46 (>99[b])	701.1 $[M+2H]^{2+}$	467.6417 $[M+3H]^{3+}$
BP429	CH_3CO-KKVVK(CO-$C_{11}H_{23}$)WVKFK-NH_2	7.21	57 (>99[b])	757.6 $[M+2H]^{2+}$	505.0172 $[M+3H]^{3+}$
BP430	CH_3CO-KKVK(CO-C_5H_{11})FWVKFK-NH_2	6.46	74 (>99[b])	739.1 $[M+2H]^{2+}$	492.9852 $[M+3H]^{3+}$
BP431	CH_3CO-KKVK(CO-C_3H_7)FWVKFK-NH_2	6.26	58 (>99[c])	725.1 $[M+2H]^{2+}$	724.9612 $[M+2H]^{2+}$
BP432	CH_3CO-KKVK(CO-$C_{11}H_{23}$)FWVKFK-NH_2	7.26	80 (>99[c])	781.6 $[M+2H]^{2+}$	521.0162 $[M+3H]^{3+}$
BP433	CH_3CO-KKK(CO-C_5H_{11})VFWVKFK-NH_2	6.46	63 (>99[b])	739.1 $[M+2H]^{2+}$	492.9874 $[M+3H]^{3+}$
BP434	CH_3CO-KKK(CO-C_3H_7)VFWVKFK-NH_2	6.26	46 (>99[b])	1471.1 $[M+Na]^{+}$	483.6433 $[M+3H]^{3+}$
BP435	CH_3CO-KKK(CO-$C_{11}H_{23}$)VFWVKFK-NH_2	7.27	70 (>99[b])	781.6 $[M+2H]^{2+}$	521.0198 $[M+3H]^{3+}$
BP436	CH_3CO-KK(CO-C_5H_{11})VVFWVKFK-NH_2	6.85	63 (>99[b])	724.5 $[M+2H]^{2+}$	483.3102 $[M+3H]^{3+}$
BP437	CH_3CO-KK(CO-C_3H_7)VVFWVKFK-NH_2	6.62	49 (>99[b])	710.5 $[M+2H]^{2+}$	710.4447 $[M+2H]^{2+}$
BP438	CH_3CO-KK(CO-$C_{11}H_{23}$)VVFWVKFK-NH_2	7.74	73 (93[b])	766.6 $[M+2H]^{2+}$	511.3408 $[M+3H]^{3+}$
BP439	CH_3CO-K(CO-C_5H_{11})KVVFWVKFK-NH_2	6.81	62 (>99[b])	725.0 $[M+2H]^{2+}$	483.3096 $[M+3H]^{3+}$
BP440	CH_3CO-K(CO-C_3H_7)KVVFWVKFK-NH_2	6.58	50 (>99[b])	710.5 $[M+2H]^{2+}$	473.9675 $[M+3H]^{3+}$
BP441	CH_3CO-K(CO-$C_{11}H_{23}$)KVVFWVKFK-NH_2	7.73	65 (>99[b])	766.6 $[M+2H]^{2+}$	511.3411 $[M+3H]^{3+}$

[a] Percentage determined by HPLC calculated as the area under the peak with respect to total area under peaks at 220 nm from the crude mixture peptide

[b] Percentage determined by HPLC calculated as the area under the peak with respect to total area under peaks at 220 nm from the purified peptide

[c] The calculated theoretical values are available in the experimental section

3.1.6. Biological activity of KSL-W derivatives

The antibacterial activity of the 49 **KSL-W** analogues was examined against *E. amylovora*, *P. syringae* pv. syringae, *P. syringae* pv. *actinidiae*, *X. aroboricola* pv. *pruni*, *X. fragariae* and *X. axonopodis* pv. *vesicatoria* (Tables 14, 15 and 16). Their toxicity against red blood cells and tobacco leaves was also evaluated. These analogues included 6 N-terminal deletion sequences, 10 peptides incorporating a D-amino acid and 33 lipopeptides.

The N-terminal deletion analogues containing 4 to 7 amino acids were inactive against all the pathogens (MIC >25 µM) (Table 14). The peptide incorporating 8 amino acids (**BP407**) showed activity against 4 pathogens with MIC of 6.2 to 25 µM. In the case of the 9-residue peptide (**BP408**), activity was observed against all the pathogens (MIC of 3.1 to 25 µM) except for *P. syringae* pv. *actinidiae*.

Table 14. Antimicrobial activity of N-terminal deletion analogues.

Peptide	MIC (µM)					
	Ea[a]	***Pss***[a]	***Psa***[a]	***Xap***[a]	***Xf***[a]	***Xav***[a]
KSL-W	*6.2-12.5*	*6.2-12.5*	*1.6-3.1*	*0.8-1.6*	*3.1-6.2*	*6.2-12.5*
BP403	>50	>50	>50	>50	>50	>50
BP404	>50	>50	>50	>50	>50	>50
BP405	>50	>50	>50	>50	>50	>50
BP406	>50	25-50	>50	>50	25-50	25-50
BP407	12.5-25	>50	25-50	6.2-12.5	12.5-25	6.2-12.5
BP408	12.5-25	6.2-12.5	25-50	6.2-12.5	6.2-12.5	3.1-6.2

[a] *Ea, Erwinia amylovora; Pss, Pseudomonas syringae* pv. *syringae; Psa, Pseudomonas syringae* pv. *actinidiae; Xap, Xantomonas arboricola* pv. *pruni; Xf, Xanthomonas fragariae; Xav, Xanthomonas axonopodis* pv. *vesicatoria.*

In the case of the analogues incorporating a D-amino acid, compared to **KSL-W**, in general, a decrease of the activity was observed. The most active analogues were **BP442**, **BP448**, **BP450** and **BP451** bearing the D-amino acid at positions 10, 4, 2 and 1, respectively (MIC of 0.8 to 25 µM). Among them highlighted **BP442** which was as active as **KSL-W** against *P. syringae* pv. syringae, *X. arboricola* pv. pruni and *X. fragariae*, and more active against *X. axonopodis* pv. vesicatoria (MIC of 1.6 to 3.1 µM). Moreover, all D-diastereoisomers were less hemolytic than the parent peptide with a percent hemolysis ≤12% at 375 µM. In addition, they were less phytotoxic than melittin, causing a necrotic area between 0.12 to 0.90 cm at 250 µM. Interestingly, the best peptide **BP442** was neither hemolytic (2% to 375 µM) nor phytotoxic (size of lesion of 0.18 cm at 250 µM).

Table 15. Antimicrobial activity (MIC), hemolysis and phytotoxicity of the peptides derived from **KSL-W** containing a D-amino acid.

Peptide	MIC (μM)						Hemolysis[b] (%) (375 μM)	Phytotoxicity[c] (cm) (250 μM)
	Ea[a]	*Pss*[a]	*Psa*[a]	*Xap*[a]	*Xf*[a]	*Xav*[a]		
KSL-W	*6.2-12.5*	*6.2-12.5*	*1.6-3.1*	*0.8-1.6*	*3.1-6.2*	*6.2-12.5*	*20 ± 1.8*	*0.62 ± 0.4*
BP442	12.5-25	6.2-12.5	3.1-6.2	0.8-1.6	3.1-6.2	1.6-3.1	2 ± 0.2	0.18 ± 0.1
BP443	>50	>50	25-50	12.5-25	12.5-25	12.5-25	0 ± 1.1	0.12 ± 1.1
BP444	>50	25-50	25-50	25-50	>50	>50	0 ± 0	0.50 ± 0.1
BP445	>50	12.5-25	6.2-12.5	6.2-12.5	12.5-25	6.2-12.5	1 ± 0.2	0.53 ± 0.1
BP446	>50	>50	25-50	>50	12.5-25	>50	4 ± 0.5	0.83 ± 0.1
BP447	>50	12.5-25	6.2-12.5	25-50	25-50	12.5-25	12 ± 0.9	0.90 ± 0.1
BP448	12.5-25	12.5-25	6.2-12.5	6.2-12.5	6.2-12.5	6.2-12.5	3 ± 0.7	0.68 ± 0.1
BP449	>50	12.5-25	6.2-12.5	12.5-25	12.5-25	12.5-25	2 ± 0.3	0.26 ± 0.1
BP450	12.5-25	6.2-12.5	3.1-6.2	1.6-3.1	3.1-6.2	3.1-6.2	5 ± 0.8	0.44 ± 0.1
BP451	12.5-25	6.2-12.5	3.1-6.2	1.6-3.1	3.1-6.2	3.1-6.2	4 ± 0.4	0.47 ± 0.1

[a]*Ea*, *Erwinia amylovora; Pss*, *Pseudomonas syringae* pv. *syringae*; *Psa*, *Pseudomonas syringae* pv. *actinidiae*; *Xap*, *Xanthomonas arboricola* pv. *pruni*; *Xf*, *Xanthomonas fragariae*; *Xav*, *Xanthomonas axonopodis* pv. *vesicatoria*.
[b]Percent hemolysis at 375 μM plus confidence interval (α = 0.05).
[c]Phytotoxicity at 250 μM determined as the lesion diameter (cm) in infiltrated tobacco leaves plus confidence interval.

Regarding lipopeptides derived from **KSL-W**, the antimicrobial activity depended on the pathogen. Whereas, in general, they displayed high activity against the *Xanthomonas* strains, they were not active against *E. amylovora* and the two *Pseudomonas* species (Table 16 and Figure 10). As previously reported, this different sensitivity was attributed to the different composition of the bacterial membrane (Badosa 2007, Güell 2017 and Güell 2011). Only 2, 1 and 6 lipopeptides displayed MIC values of 12.5 to 25 μM against *E. amylovora*, *P. syringae* pv. *syringae* and *P. syringae* pv. *actinidiae*, respectively. In contrast, these derivatives were significantly active against the *Xanthomonas* species. MIC values <25 μM were found for 20 peptides against at least two of these species. Interestingly, lipopeptides with MIC of 3.1 to 6.2 μM were obtained, namely: **BP417** and **BP432** against *X. arboricola* pv*. pruni*; **BP411**, **BP417** and **BP432** against *X. fragariae*; **BP409**, **BP410**, **BP411** and **BP432** against *X. axonopodis* pv. *vesicatoria*. It is noteworthy to mention, that the latter peptides displayed higher activity than the parent peptide **KSL-W** against this bacterium.

Table 16. Antimicrobial activity of lipopeptides derived from **KSL-W**

Peptide	MIC (μM)					
	Ea[a]	***Pss***[a]	***Psa***[a]	***Xap***[a]	***Xf***[a]	***Xav***[a]
KSL-W	*6.2-12.5*	*6.2-12.5*	*1.6-3.1*	*0.8-1.6*	*3.1-6.2*	*6.2-12.5*
BP409	12.5-25	>50	12.5-25	25-50	6.2-12.5	3.1-6.2
BP410	12.5-25	25-50	12.5-25	12.5-25	6.2-12.5	3.1-6.2
BP411	>50	>50	>50	>50	3.1-6.2	3.1-6.2
BP412	>50	>50	>50	6.2-12.5	>50	12.5-25
BP413	>50	>50	12.5-25	12.5-25	12.5-25	12.5-25
BP414	>50	>50	>50	>50	>50	>50
BP415	>50	>50	>50	>50	>50	>50
BP416	>50	>50	>50	25-50	25-50	>50
BP417	>50	>50	>50	3.1-6.2	3.1-6.2	6.2-12.5
BP418	>50	>50	>50	6.2-12.5	6.2-12.5	12.5-25
BP419	>50	12.5-25	12.5-25	6.2-12.5	12.5-25	6.2-12.5
BP420	>50	>50	>50	>50	>50	>50
BP421	>50	>50	>50	>50	>50	>50
BP422	>50	>50	>50	>50	>50	>50
BP423	>50	>50	>50	6.2-12.5	6.2-12.5	12.5-25
BP424	>50	25-50	>50	25-50	12.5-25	12.5-25
BP425	>50	>50	>50	25-50	25-50	12.5-25
BP426	>50	>50	>50	6.2-12.5	12.5-25	6.2-12.5
BP427	>50	>50	>50	12.5-25	25-50	25-50
BP428	>50	>50	>50	>50	>50	>50
BP429	>50	>50	>50	6.2-12.5	12.5-25	12.5-25
BP430	25-50	25-50	12.5-25	6.2-12.5	12.5-25	12.5-25
BP431	>50	25-50	25-50	6.2-12.5	25-50	12.5-25
BP432	>50	>50	25-50	3.1-6.2	3.1-6.2	3.1-6.2
BP433	>50	>50	12.5-25	6.2-12.5	12.5-25	6.2-12.5
BP434	>50	>50	25-50	12.5-25	25-50	12.5-25
BP435	>50	>50	>50	6.2-12.5	12.5-25	6.2-12.5
BP436	>50	>50	>50	>50	25-50	>50
BP437	>50	>50	>50	25-50	6.2-12.5	12.5-25
BP438	>50	>50	>50	>50	>50	>50
BP439	>50	>50	>50	25-50	12.5-25	12.5-25
BP440	>50	>50	>50	25-50	>50	12.5-25
BP441	>50	>50	>50	>50	>50	>50

[a]*Ea*, *Erwinia amylovora; Pss*, *Pseudomonas syringae* pv. *syringae*; *Psa*, *Pseudomonas syringae* pv. *actinidiae*; *Xap*, *Xanthomonas arboricola* pv. *pruni*; *Xf*, *Xanthomonas fragariae*; *Xav*, *Xanthomonas axonopodis* pv. *vesicatoria*.

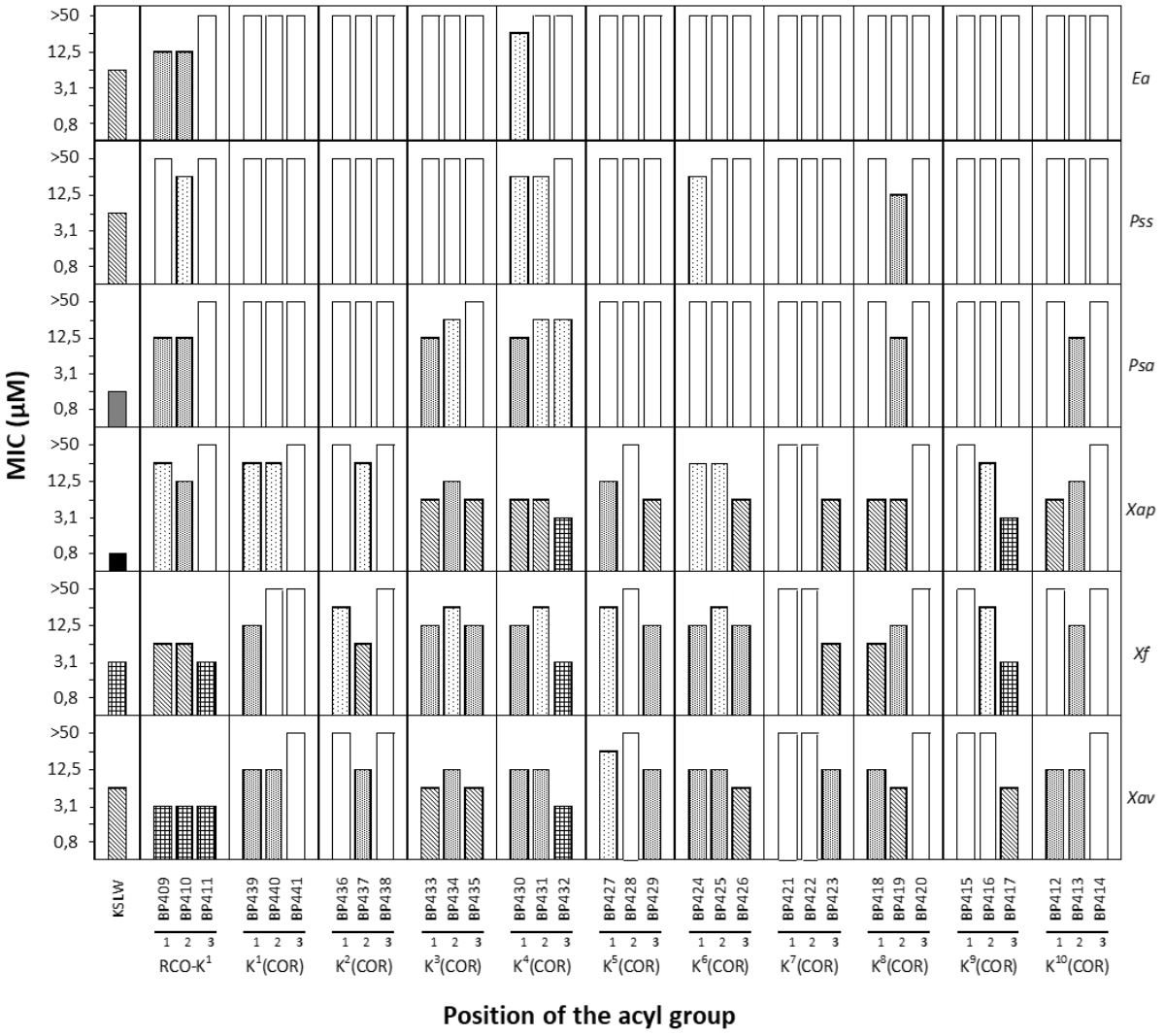

Figure 10. MICs of the lipopeptides derived from KSL-W against the bacteria *E. amylovora* (*Ea*), *P. syringae* pv. *syringae* (*Pss*), *P. syringae* pv. *actinidiae* (*Psa*), *X. arboricola* pv. *pruni* (*Xap*), *X. fragariae* (*Xf*) and *X. axonopodis* pv. *vesicatoria* (*Xav*). The position of the acyl group is indicated with a superscript. The type of the acyl group is indicated at the bottom of each peptide code as: 1: R = C_5H_{11}; 2: R = C_3H_7 and 3: R = $C_{11}H_{23}$.

In agreement with previous reports, both the position and the type of acyl chain influenced the antibacterial activity of the lipopeptides (Vilà 2016, Makovitzki 2006, Jerala 2007, Mangoni 2011, Mandal 2013, Malina 2005).

The analogues derivatized at the N-terminus and at the side-chain of the residues at positions 3 and 4 displayed the highest activity. For these derivatives, peptides with MIC <50 µM against 4 or 5 pathogens were identified and most of them displayed high activity against the three *Xanthomonas* species (MIC <12.5 µM). In general, the analogues incorporating a lauroyl group were clearly the most active. In fact, 6 out of 11 sequences displayed MIC <12.5 µM against at least two *Xanthomonas* species. Among them, highlighted **BP411**, **BP417** and **BP432** which exhibited MIC values of 3.1 to 6.2 µM against these bacteria. Within the hexanoyl and butanoyl derivatives, although no significant differences were observed between these peptides, **BP410** showed the best antibacterial profile,

being active against 5 pathogens with MIC <25 µM. Accordingly, the best peptides were **BP409**, **BP410** and **BP411**, incorporating the acyl chain at the N-terminus, **BP417** and **BP432** with a lauroyl group at position 9 and 4, respectively.

Lipopeptides were, in general, low toxic (Table 17, Figure 11). Regarding their toxicity against erythrocytes, at 50 µM, 26 out of 33 peptides displayed a hemolysis percentage ≤13%, and for the rest of peptides this percentage ranged from 22 to 63%. At the highest concentration tested, 375 µM, the hemolysis of 23 peptides did not exceed 50% and, among them, 15 sequences exhibited only ≤16% hemolysis.

Table 17. Hemolysis and phytotoxicity of KSL-W and lipopeptides **BP409-BP441**

Peptide	Hemolysis[a] (%) (375 µM)	Phytotoxicity (cm)[b] (250 µM)
KSL-W	20 ± 1.8	0.62 ± 0.4
BP409	16 ± 0.9	0.84 ± 0.1
BP410	2 ± 0	0.30 ± 0.1
BP411	32 ± 1.9	0.52 ± 0.3
BP412	87 ± 5.8	0.46 ± 0.1
BP413	4 ± 0.3	0.60 ± 1.9
BP414	75 ± 1.7	0 ± 0
BP415	7 ± 0.8	0.4 ± 0
BP416	8 ± 0.8	0 ± 0
BP417	68 ± 2.3	0 ± 0
BP418	42 ± 6.6	0 ± 0
BP419	1 ± 0.7	0.51 ± 0.1
BP420	6 ± 0.1	0.50 ± 0.1
BP421	8 ± 0.5	0.46 ± 0.1
BP422	1 ± 0.3	0.34 ± 0
BP423	64 ± 2.0	0.80 ± 0.2
BP424	7 ± 1.1	0.52 ± 0.1
BP425		0.50 ± 0.1
BP426	60 ± 1.8	0.86 ± 0.1
BP427	65 ± 6.6	0.20 ± 0.2
BP428	42 ± 4.6	0.14 ± 0.2
BP429	77 ± 4.6	0.48 ± 0.3
BP430	31 ± 1.6	0.44 ± 0.2
BP431	13 ± 1.5	0.56 ± 0.2
BP432	47 ± 4.3	0.53 ± 0.2
BP433	56 ± 18.3	0.64 ± 0.2
BP434	39 ± 5.0	0.58 ± 0.2
BP435	53 ± 0.2	0 ± 0
BP436	11 ± 0.2	0.63 ± 0.3
BP437	26 ± 9.2	0.63 ± 0.2
BP438	5 ± 0.3	0.40 ± 0.3
BP439	55 ± 7.0	0.76 ± 0.2
BP440	48 ± 7.9	0.65 ± 0.2
BP441	11 ± 0.3	0.60 ± 0.2

[a] Percent hemolysis at 375 µM plus confidence interval (α = 0.05).

[b] Phytotoxicity at 250 µM determined as the lesion diameter (cm) in infiltrated tobacco leaves plus confidence interval.

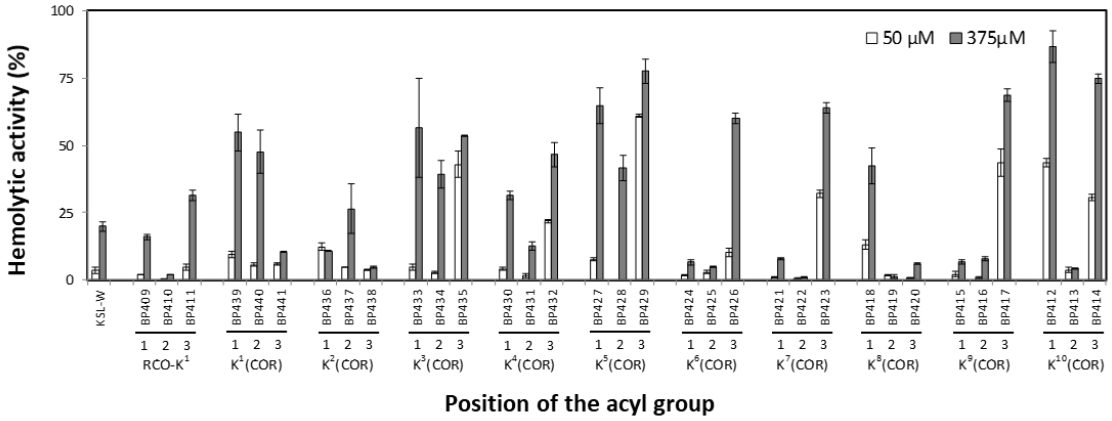

Figure 11. Hemolytic activity of the lipopeptides derived from KSL-W at 50 and 375 µM. Vertical bars within each column indicate confidence interval at the mean. The position of the acyl group is indicated with a superscript. The type of the acyl group is indicated at the bottom of each peptide code as: 1: R = C_5H_{11}, 2: R = C_3H_7 and 3: R = $C_{11}H_{23}$.

Analysis of the results pointed out that, in general, the hemolysis increased with increasing the length of the acyl chain. A percentage of hemolysis <50% at 375 µM was obtained for all lipopeptides derivatized with a butanoyl group. In contrast, only 6 sequences containing a lauroyl chain displayed similar percentages. Thus, the incorporation of a butanoyl group rendered the least hemolytic lipopeptides, whereas a lauroyl yielded the most hemolytic ones. These results are in good agreement with previous studies reporting that an increase of the peptide hydrophobicity is related to an increase in the cytotoxicity (Vilà 2016, Blondelle 2000, Oh 2000).

Moreover, the position of the acyl chain also influenced the hemolysis, being the least hemolytic the sequences acylated at the N-terminus or at positions 2 and 8, and the most hemolytic those derivatized at positions 3, 5 or 10. It is noteworthy to mention that the hemolysis was determined at concentrations up to 375 µM, which is 7 to 120-fold higher than the MIC values.

Concerning their effect in tobacco leaves, these acylated derivatives were not phytotoxic at 50 µM: only 6 peptides caused a necrotic area of 0.25 to 0.44 cm. At 250 µM, they were significantly less phytotoxic than melittin, being the size of the lesion <1 cm for all peptides, ranging from 0 – 0.60 cm for 25 of them.

Comparable results were described in previous reports on short cationic lipopeptides, which revealed that a high activity against plant pathogens is not necessarily associated with a damage in plant tissues even when applied directly at the infection area (Makovitzki 2007). Moreover, similarly to previous results on cyclic lipopeptides, no correlation was observed between phytotoxicity and hemolysis (Vilà 2016).

Notably, among the lipopeptides with the highest antibacterial activity (**BP409**, **BP410**, **BP411**, **BP417** and **BP432**), highlighted **BP410**, **BP411** and **BP432** because they are not toxic towards both erythrocytes (<50% at 375 μM) and tobacco leaves (size of lesion of 0.30 to 0.53 cm at 250 μM).

The capacity of inducing the expression of genes related to plant defense responses of **KSL-W** and its D-diastereoisomers was evaluated (Table 17). Flagellin 15 (**flg15**), jasmonic acid (JA) and acibenzolar-S-methyl (ASM) were included in this study as positive controls due to their described capacity to enhance the plant immune system (Bektas 2015). **Pip-1** and **Pep13**, previously described as plant defense elicitors, were also tested.

Tabla 18. Expression of genes related to defense/stress response in tomato after the treatment with the reference products flagellin 15 (**flg15**), jasmonic acid (JA), and acybenzolar-*S*-methyl (ASM), with the plant defense elicitors **Pip-1** and **Pep-13**, and with **KSL-W** and ten **KSL-W** derivatives. Fold induction above 2 is considered overexpression in the relative quantification by the $\Delta\Delta Ct$ method. Significant values are indicated in bold.

Genes	Reference products[a]			Plant defense elicitors[b]		Peptides[b]										
	flg15	JA	ASM	Pip-1	Pep-13	KSL-W	BP442	BP443	BP444	BP445	BP446	BP447	BP448	BP449	BP450	BP451
Harp	**3.3**	1.9	**2.8**	0.4	0.6	0.5	1.4	1.6	**2.4**	1.9	1.7	**3.8**	1.4	**2.3**	1.3	1.0
PR1	**30.4**	2.9	**16.4**	0.1	0.1	0.1	2.7	1.5	0.6	0.6	0.8	**2.3**	0.5	1.7	**2.2**	0.5
GluA	**12.7**	0.2	**7.5**	0.1	0.1	0.7	0.6	1.7	1.4	**4.6**	1.9	**6.1**	1.7	**2.9**	**2.5**	0.4
PPO	**4.3**	**>50**	**7.8**	1.1	**3.2**	1.0	0.7	0.9	**2.1**	1.4	1.0	1.3	0.9	1.7	1.2	1.4
LOX	1.6	**9.7**	**2.4**	1.0	1.1	1.3	0.9	0.9	0.7	0.6	1.1	1.2	**3.2**	1.1	1.9	1.0
PinII	**5.2**	**>50**	**3.6**	0.2	0.8	0.3	0.4	0.7	1.2	1.3	1.3	**2.4**	1.4	**3.5**	1.2	2.0
Sub1	**12.3**	**4.0**	**4.1**	1.4	0.8	0.4	0.6	0.9	0.6	0.4	1.0	1.0	0.6	0.8	1.0	1.0
ERT3	**3.6**	**41.3**	**3.7**	0.4	0.3	0.2	0.1	1.5	1.5	1.6	1.6	**2.1**	**3.7**	1.9	**2.1**	1.0
BCB	**11.3**	**6.6**	**2.6**	0.7	1.6	1.1	**2.8**	0.8	0.9	0.6	1.1	1.1	0.4	1.3	0.9	1.4
Osm2	**11.3**	**48.4**	**2.8**	**2.0**	0.7	1.2	0.9	1.9	1.1	1.0	**2.1**	1.1	**4.0**	0.6	1.7	1.6
Tas14	**2.3**	0.9	1.1	0.9	**4.1**	1.2	1.2	1.1	1.5	**6.1**	1.4	**6.0**	0.6	**9.0**	0.7	1.4

[a] The reference products were tested at 125 µM (**flg15**), 2.5 mM (JA), and 300 mg/L (ASM)

[b] Plant defense elicitors and peptides were tested at 125 µM

Table 18 summarizes the relative quantification for the expression of the selected genes calculated by the *ΔΔCt* method. Positive controls clearly overexpressed the majority of genes. JA induced expression of all the genes except for *Harp*, *PR1*, *GluA* and *Tas14*. ASM and flg15 overexpressed all the genes tested except for *Tas14* and *LOX*, respectively. Pip1 and Pep13 overexpressed only one (*Osm2*) or two (*PPO* and *Tas14*) of the tested genes, respectively.

Concerning **KSLW** and its derivatives, the parent peptide, **BP443** and **BP451** did not induce the overexpression of any of the genes. The other eight peptides overexpressed from 1 to 6 genes. In particular, **BP442** and **BP446** only induced the overexpression of *BCB* and *Osm2*, respectively. **BP444** and **BP445** overexpressed 2 genes; *Harp* and *LOX* (**BP444**) and *PPO* and *Tas14* (**BP445**). Peptides **BP448** and **BP450** promoted the overexpression of 3 genes. Apart from *ERT3*, **BP450** also overexpressed *PR1* and *GluA*, and **BP448**, *Osm2* and *LOX*. The latter was the only peptide that induce overexpression of *LOX*. The KSL-W analogues **BP447** and **BP449** overexpressed 6 and 4 genes, respectively, that were also induced by flg15. These two peptides overexpressed *Harp*, *GluA*, *PinII* and *Tas14*, and **BP447** also overexpressed *PR1* and *ERT3*.

Therefore, the presence of a D-amino in the **KSL-W** favoured the capacity of inducing the expression of defense-related genes on tomato plants. Some of these **KSL-W** analogues overexpressed more genes than the parent peptide and than other defense response elicitors described in the literature (**Pip1** or **Pep13**). This modification resulted to be more effective when the D-amino acid was incorporated at positions 2 to 5, peptides **BP447**, **BP448**, **BP449** and **BP450** being the ones that showed the best results.

Taking all the results of the **KSL-W** derivatives together (Table 19), it can be concluded that the incorporation of a D-amino acid at position 10 affords a peptide (**BP442**) with a significant activity against all the bacteria tested that is neither hemolytic nor phytotoxic. It can also be observed that when a D-amino acid is present at position 5, the resulting peptide **BP447** induces the expression of 6 defense-related genes. On the other hand, it has been demonstrated that the acylation of KSL-W renders peptides selective towards *Xanthomonas* strains. In particular, those bearing a butanoyl at the N-terminus (**BP410**), or a lauroyl at the N-terminus (**BP411**) or at position 4 (**BP432**) are highly active against these bacteria and also low toxic against erythrocytes or plant tissues.

Table 19. Peptides with the best biological activity profile

Biological activity properties	Peptides					
	KSL-W	**BP410**	**BP411**	**BP432**	**BP442**	**BP447**
Structure[a]		C_3H_7CO-K[1]	$C_{11}H_{23}CO$-K[1]	K[4]($COC_{11}H_{23}$)	D-K[10]	D-F[5]
Antibacterial activity (MIC)						
Ea[b]	6.2-12.5	12.5-25	>50	>50	12.5-25	>50
Pss[b]	6.2-12.5	25-50	>50	>50	6.2-12.5	12.5-25
Psa[b]	1.6-3.1	12.5-25	>50	25-50	3.1-6.2	6.2-12.5
Xap[b]	0.8-1.6	12.5-25	>50	3.1-6.2	0.8-1.6	25-50
Xf[b]	3.1-6.2	6.2-12.5	3.1-6.2	3.1-6.2	3.1-6.2	25-50
Xav[b]	6.2-12.5	3.1-6.2	3.1-6.2	3.1-6.2	1.6-3.1	12.5-25
Hemolysis (%)[c]	20 ± 1.8	2 ± 0	32 ± 1.9	47 ± 4.3	2 ± 0.2	12 ± 0.9
Size of the lesions (cm) in infiltrated tobacco leaves[d]	0.62 ± 0.4	0.30 ± 0.1	0.52 ± 0.3	0.53 ± 0.2	0.18 ± 0.1	0.90 ± 0.1
Defense gene expression in tomato plants[e]	none	nd[f]	nd[f]	nd[f]	*BCB*	*Harp, PR1a, GluA, PinII, ERT3, Tas14*

[a] KSL-W sequence: KKVVFWVKFK-NH_2; for the other peptides is indicated the modification that was incorporated.
[b] *Ea*, *Erwinia amylovora*; *Pss*, *Pseudomonas syringae* pv. syringae; *Psa*, *Pseudomonas syringae* pv. actinidiae; *Xap*, *Xanthomonas arboricola* pv. pruni; *Xf*, *Xanthomonas fragariae*; *Xav*, *Xanthomonas axonopodis* pv. vesicatoria.
[c] Percent hemolysis at 375 μM plus confidence interval (α = 0.05).
[d] Diameter of the lesions (cm) measured after 48 h infiltration of lipopeptides at 250 μM.
[e] Expression of genes in tomato plants after the treatment with the peptides at 125 μM.
[f] nd, not determined.

In summary, this study has allowed the identification of **KSL-W** as a new lead to control plant pathogens of economic importance. This peptide is highly active against a range of bacteria being also low hemolytic and phytotoxic. It has also been demonstrated that the incorporation of a D-amino acid constitutes a suitable strategy to obtain derivatives with an improved biological activity profile or with the capacity to induce the expression of defense-related genes. Based on these promising data, we envisage that these peptides may open up an alternative approach to the challenging task of developing novel peptides with multifunctional properties like antimicrobial activity or plant defense elicitation properties. According to our previous experience with similar sequences, our peptides would be applied by spraying the plants.

3.2. Design and synthesis of peptide conjugates

*This chapter corresponds to a manuscript in preparation:

Camó, C.; Planas, M.; Feliu, L. Design and synthesis of peptide conjugates. *In preparation.*

3.3. Tryptophan-containing cyclic decapeptides with activity against plant pathogenic bacteria

*This chapter is based on the article “Camó, C.; Torné, M.; Besalú, E.; Rosés, C.; Cirac, A.; Moiset, G.; Badosa, E.; Bardají, E.; Montesinos, E.; Planas, M.; Feliu, F. Tryptophan-containing cyclic decapeptides with activity against plant pathogenic bacteria. *Molecules* **2017**, 1817.”

Cyclic peptides are interesting candidates as new antimicrobial agents to fight plant pathogens due to their high conformational rigidity and proteolytic stability (Lee 2015, Russo 2016, de Veer 2017). In a previous work, a library of 66 Phe-containing cyclic decapeptides with general structure c(X_5-Phe-X_3-Gln) where X = Lys or Leu was synthesized. (Monroc 2006). From this library sequences with high activity against *E. amylovora*, *P. syringae* pv. *syringae* and *X. axonopodis* pv. *vesicatoria* were identified, highlighting c(LysLysLeuLysLysPheLysLysLeuGln) (**BPC194**) and c(LysLeuLysLysLysPheLysLysLeuGln) (**BPC198**) (MIC of 3.1 to 25 μM).

Several studies reported that antimicrobial peptides containing a Trp display more potent antimicrobial activity than those with a Phe. In line with this argument, analogues of LL-37, cathelicidin-2, cecropin A-melittin hybrid and of temporin 1-T1 with Phe → Trp substitutions exhibited increased antimicrobial activities (Rajasekaran 2015, Strömsted 2009, Molhoek 2010, Nan 2012 and Ji 2014). This trend was attributed to the bulkier hydrophobic side chain of Trp compared to Phe that would favour the interaction with the cell membrane facilitating a deeper embedding of the peptides (Hu 1993, Chan 2006, Domalaon 2016, Rajasekaran 2015, Saravanan 2014, Wessolowski 2004, Choi 2014, Grau-Campistany 2016, Xie 2017).

Thus, with the aim of finding new leads and in view of the key role of Trp in the activity of antimicrobial peptides, the Phe in the aforementioned library was replaced with a Trp. The resulting 66-member library was screened for its antimicrobial and hemolytic activities and peptides with a good biological activity profile were identified (BPC086W, BPC108W) (see section 1.4). In view of these results, in this PhD thesis, on the one hand, an analysis of the influence of the replacement of the Phe with a Trp was undertaken. On the other hand, new cyclic peptides containing a Trp were designed and synthesized.

3.3.1. Study of the influence of the replacement of a Phe with a Trp on the biological activity of cyclic decapeptides

3.3.1.1. Synthesis of selected cyclic peptides containing a Trp

In this work, 15 out of the 66 Trp analogues were selected and resynthesized in order to confirm the results of the antimicrobial and hemolytic activities and to perform a thorough comparison of these data with those of the Phe library.

These cyclic peptides containing a Trp residue were prepared on solid-phase following a three-dimensional orthogonal Fmoc/^{t}Bu/All strategy depicted in Schemes (6 and 7). A Fmoc-Rink-MBHA was used as solid support. Fmoc removal was followed by side-chain anchoring of Fmoc-Glu-OAll, which resulted in a Gln residue after peptide cleavage from the resin. Peptide elongation was then performed through sequential Fmoc removal and coupling steps of the corresponding protected amino acids. The Fmoc group was removed by treatment with piperidine/DMF (3:7). Coupling of the amino acids were mediated by DIPCDI and Oxyma. Once the linear peptidyl sequence was assembled, an aliquot of the

resulting peptidyl resin was treated with TFA/phenol/H_2O/TIS (92.5:2.5:2.5:2.5) and the crude was analyzed by HPLC and characterized by ESI-MS. The expected linear peptides were obtained in HPLC purities between 93 and >99% (Table 27).

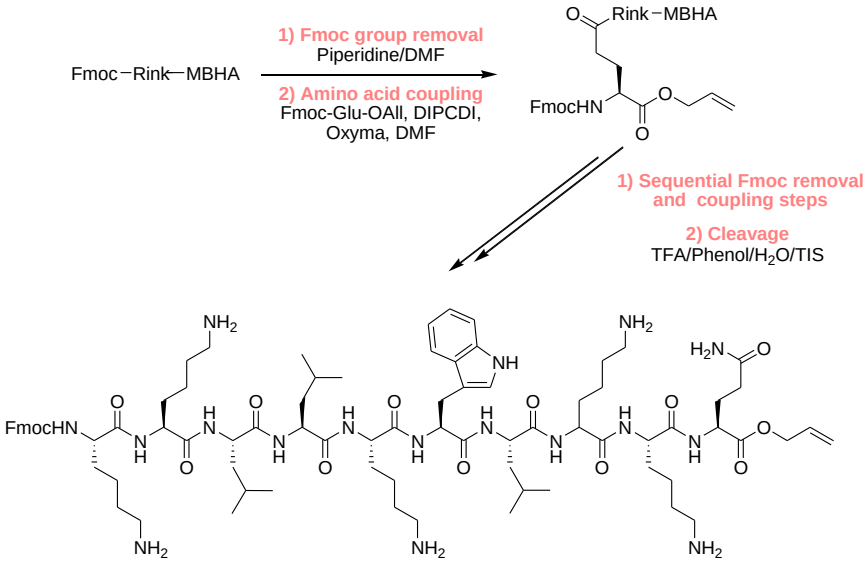

Scheme 6. Synthesis of the linear precursors

Table 27. Characterization of the linear peptides

Sequence	t_R (min)	Purity[a] (%)	ESI-MS
Fmoc-KKLLKWLKKQ-OAll	7.21	98	1597.0 $[M+Na]^+$
Fmoc-LKKLKWLKKQ-OAll	6.90	>99	1597.0 $[M+Na]^+$
Fmoc-KLLKKWLKKQ-OAll	7.08	>99	1598.0 $[M+Na]^+$
Fmoc-LKLKKWLKKQ-OAll	6.97	>99	1598.0 $[M+Na]^+$
Fmoc-LLKKKWLKKQ-OAll	6.93	>99	788.0 $[M+2H]^{2+}$
Fmoc-LKLKLWKKKQ-OAll	6.93	>99	1597.0 $[M+Na]^+$
Fmoc-LLKLKWKKKQ-OAll	7.07	>99	788.5 $[M+2H]^{2+}$
Fmoc-LLLKKWKKKQ-OAll	7.23	96	788.5 $[M+2H]^{2+}$
Fmoc-KLLLKWKKLQ-OAll	7.37	97	780.5 $[M+2H]^{2+}$
Fmoc-KKKLKWKKLQ-OAll	6.61	97	796.0 $[M+2H]^{2+}$
Fmoc-LLLKKWKKLQ-OAll	6.94	>99	781.0 $[M+2H]^{2+}$
Fmoc-KKLKKWKKLQ-OAll	6.64	96	795.5 $[M+2H]^{2+}$
Fmoc-LLKLKWKKLQ-OAll	7.44	95	781.0 $[M+2H]^{2+}$
Fmoc-KLKKKWKKLQ-OAll	6.67	93	795.5 $[M+2H]^{2+}$
Fmoc-LLLLKWKKLQ-OAll	8.49	>99	1545.0 $[M+H]^+$

[a] Percentage determined by HPLC calculated as the area under the peak with respect to total area under peaks at 220 nm from the crude reaction mixture

Next, the C-terminal allyl ester was removed by treatment with $Pd(PPh_3)_4$ in $CHCl_3$/AcOH/*N*-methylmorpholine (NMM) (3:2:1) for 3 h (Scheme 7). After Fmoc removal, cyclization was carried out using PyOxym, Oxyma and DIEA in NMP for 24 h. Acidolytic cleavage of the resulting resin provided the

desired cyclic peptides in HPLC purities between 81 and > 99% (Table 28). Moreover, peptides were characterized by ESI-MS and HRMS and, in all cases, the signal corresponding to the expected ions was observed.

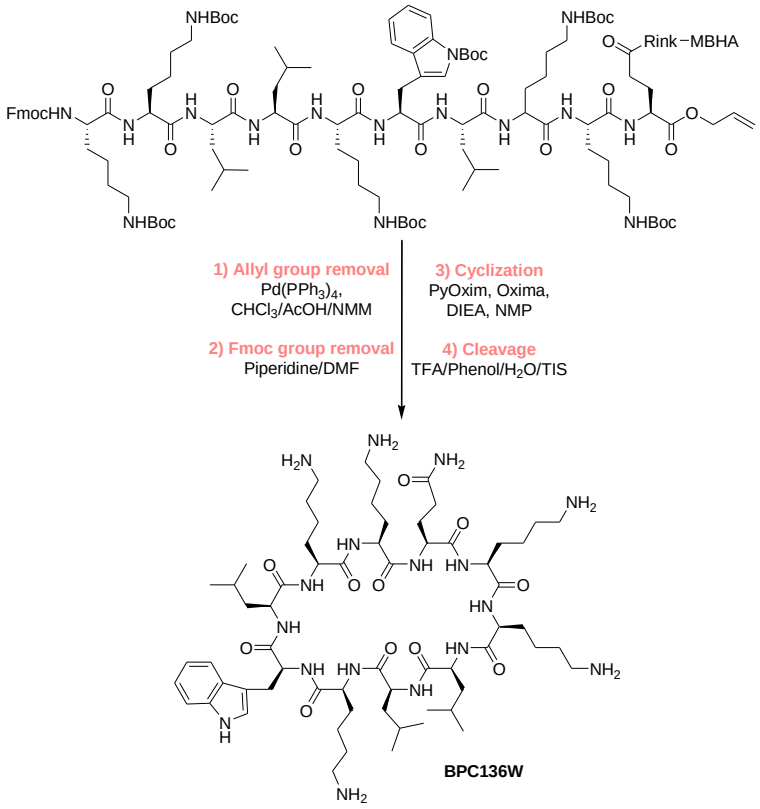

Scheme 7. Strategy for the solid-phase synthesis of the cyclic peptides depicted for **BPC136W**

Table 28. Characterization of the cyclic peptides synthesized in this PhD thesis

Peptide	Sequence	t_R (min)	Purity[a] (%)	ESI-MS	HRMS[b]
BPC136W	c(KKLLKWLKKQ)	6.87	89	1316.9 $[M+Na]^+$	647.9401 $[M+2H]^{2+}$
BPC140W	c(LKKLKWLKKQ)	6.95	81	1317.0 $[M+Na]^+$	647.9406 $[M+2H]^{2+}$
BPC142W	c(KLLKKWLKKQ)	6.76	87	1317.0 $[M+Na]^+$	647.9424 $[M+2H]^{2+}$
BPC144W	c(LKLKKWLKKQ)	6.72	87	1317.0 $[M+Na]^+$	647.9381 $[M+2H]^{2+}$
BPC146W	c(LLKKKWLKKQ)	6.45	80	1317.0 $[M+Na]^+$	647.9419 $[M+2H]^{2+}$
BPC156W	c(LKLKLWKKKQ)	6.37	>99	1317.0 $[M+Na]^+$	647.9422 $[M+2H]^{2+}$
BPC164W	c(LLKLKWKKKQ)	6.38	>99	1317.0 $[M+Na]^+$	647.9417 $[M+2H]^{2+}$
BPC166W	c(LLLKKWKKKQ)	6.38	83	1316.9 $[M+Na]^+$	647.9423 $[M+2H]^{2+}$
BPC184W	c(KLLLKWKKLQ)	6.97	93	1301.8 $[M+Na]^+$	640.4371 $[M+2H]^{2+}$
BPC186W	c(KKKLKWKKLQ)	5.94	92	1331.9 $[M+Na]^+$	655.4473 $[M+2H]^{2+}$
BPC188W	c(LLLKKWKKLQ)	6.97	93	1301.9 $[M+Na]^+$	640.4352 $[M+2H]^{2+}$
BPC194W	c(KKLKKWKKLQ)	6.21	91	1331.9 $[M+Na]^+$	655.4456 $[M+2H]^{2+}$
BPC196W	c(LLKLKWKKLQ)	6.60	99	1301.9 $[M+Na]^+$	640.4362 $[M+2H]^{2+}$
BPC198W	c(KLKKKWKKLQ)	6.26	93	1309.8 $[M+H]^+$	655.4468 $[M+2H]^{2+}$
BPC200W	c(LLLLKWKKLQ)	7.40	96	1264.8 $[M+H]^+$	632.9303 $[M+2H]^{2+}$

[a] Percentage determined by HPLC calculated as the area under the peak with respect to total area under peaks at 220 nm from the crude reaction mixture
[b] The calculated theoretical values are available in the experimental section

3.3.1.2. Antimicrobial activity

The Trp-containing library was tested for in vitro growth inhibition of *X. axonopodis* pv. *vesicatoria*, *P. syringae* pv. *syringae* and *E. amylovora* (Table 29). All peptides were active against at least one pathogen with MIC < 25 µM, being *X. axonopodis* pv. *vesicatoria* the most sensitive bacteria. Notably, 60 out of 66 sequences displayed MIC < 12.5 µM against this bacterium. In particular, 23 peptides showed MIC of 1.6 to 3.1 µM, while **BPC078W**, **BPC080W**, and **BPC086W** were the most active with MIC of 0.8 to 1.6 µM. In contrast, this library was slightly less active against *P. syringae* pv. *syringae*, although 52 cyclic peptides displayed MIC < 12.5 µM, being **BPC108W** the most active sequence (MIC of 1.6 to 3.1 µM). *E. amylovora* was the least sensitive bacteria, but 34 peptides showed MIC < 25µM. Notably, six sequences displayed MIC of 6.2 to 12.5 µM.

Table 29. Antimicrobial activity (MIC) of the cyclic peptides containing a Trp residue

Peptide	Sequence	MIC (µM)		
		Pss[a]	*Xav*[a]	*Ea*[a]
BPC016W	c(KLKLKWKLKQ)	12.5-25	3.1-6.2	>100
BPC058W	c(KKKKKWLLLQ)	12.5-25	25-50	50-75
BPC060W	c(KKKKLWKLLQ)	3.1-6.2	6.2-12.5	12.5-25
BPC062W	c(KKKLKWKLLQ)	3.1-6.2	6.2-12.5	12.5-25
BPC064W	c(KKLKKWKLLQ)	3.1-6.2	6.2-12.5	6.2-12.5
BPC066W	c(KLKKKWKLLQ)	6.2-12.5	6.2-12.5	6.2-12.5
BPC068W	c(LKKKKWKLLQ)	6.2-12.5	1.6-3.1	25-50
BPC070W	c(KKKKLWLKLQ)	6.2-12.5	1.6-3.1	12.5-25
BPC072W	c(KKKLKWLKLQ)	3.1-6.2	1.6-3.1	12.5-25
BPC074W	c(KKLKKWLKLQ)	6.2-12.5	1.6-3.1	12.5-25
BPC076W	c(KLKKKWLKLQ)	6.2-12.5	1.6-3.1	6.2-12.5
BPC078W	c(LKKKKWLKLQ)	6.2-12.5	0.8-1.6	25-50
BPC080W	c(KKKLLWKKLQ)	6.2-12.5	0.8-1.6	12.5-25
BPC082W	c(KKLKLWKKLQ)	6.2-12.5	1.6-3.1	12.5-25
BPC084W	c(KLKKLWKKLQ)	12.5-25	1.6-3.1	12.5-25
BPC086W	c(LKKKLWKKLQ)	3.1-6.2	0.8-1.6	6.2-12.5
BPC088W	c(KKLLKWKKLQ)	6.2-12.5	1.6-3.1	12.5-25
BPC090W	c(KLKLKWKKLQ)	6.2-12.5	1.6-3.1	12.5-25
BPC092W	c(LKKLKWKKLQ)	6.2-12.5	3.1-6.2	50-75
BPC094W	c(KLLKKWKKLQ)	6.2-12.5	3.1-6.2	25-50
BPC096W	c(LKLKKWKKLQ)	6.2-12.5	1.6-3.1	12.5-25
BPC098W	c(LLKKKWKKLQ)	3.1-6.2	1.6-3.1	12.5-25
BPC100W	c(KKKKLWLLKQ)	12.5-25	6.2-12.5	>100
BPC102W	c(KKKLKWLLKQ)	3.1-6.2	6.2-12.5	12.5-25
BPC104W	c(KKLKKWLLKQ)	6.2-12.5	6.2-12.5	12.5-25
BPC106W	c(KLKKKWLLKQ)	3.1-6.2	3.1-6.2	25-50
BPC108W	c(LKKKKWLLKQ)	1.6-3.1	1.6-3.1	6.2-12.5
BPC110W	c(KKKLLWKLKQ)	3.1-6.2	6.2-12.5	12.5-25
BPC112W	c(KKLKLWKLKQ)	3.1-6.2	6.2-12.5	50-75
BPC114W	c(KLKKLWKLKQ)	3.1-6.2	1.6-3.1	12.5-25
BPC116W	c(LKKKLWKLKQ)	3.1-6.2	3.1-6.2	12.5-25
BPC118W	c(KKLLKWKLKQ)	6.2-12.5	12.5-25	12.5-25
BPC120W	c(LKKLKWKLKQ)	3.1-6.2	1.6-3.1	12.5-25
BPC122W	c(KLLKKWKLKQ)	3.1-6.2	6.2-12.5	12.5-25
BPC124W	c(LKLKKWKLKQ)	6.2-12.5	3.1-6.2	50-75
BPC126W	c(LLKKKWKLKQ)	6.2-12.5	1.6-3.1	25-50
BPC128W	c(KKKLLWLKKQ)	6.2-12.5	1.6-3.1	12.5-25

BPC130W	c(KKLKLWLKKQ)	6.2-12.5	1.6-3.1	12.5-25
BPC132W	c(KLKKLWLKKQ)	3.1-6.2	1.6-3.1	12.5-25
BPC134W	c(LKKKLWLKKQ)	6.2-12.5	3.1-6.2	25-50
BPC136W	c(KKLLKWLKKQ)	6.2-12.5	3.1-6.2	6.2-12.5
BPC138W	c(KLKLKWLKKQ)	6.2-12.5	3.1-6.2	25-50
BPC140W	c(LKKLKWLKKQ)	6.2-12.5	3.1-6.2	12.5-25
BPC142W	c(KLLKKWLKKQ)	6.2-12.5	3.1-6.2	12.5-25
BPC144W	c(LKLKKWLKKQ)	3.1-6.2	1.6-3.1	12.5-25
BPC146W	c(LLKKKWLKKQ)	3.1-6.2	3.1-6.2	25-50
BPC148W	c(KKLLLWKKKQ)	12.5-25	12.5-25	>100
BPC150W	c(KLKLLWKKKQ)	12.5-25	6.2-12.5	>100
BPC152W	c(LKKLLWKKKQ)	6.2-12.5	6.2-12.5	75-100
BPC154W	c(KLLKLWKKKQ)	3.1-6.2	1.6-3.1	25-50
BPC156W	c(LKLKLWKKKQ)	6.2-12.5	3.1-6.2	>100
BPC158W	c(LLKKLWKKKQ)	12.5-25	1.6-3.1	12.5-25
BPC160W	c(KLLLKWKKKQ)	6.2-12.5	6.2-12.5	>100
BPC162W	c(LKLLKWKKKQ)	6.2-12.5	3.1-6.2	>100
BPC164W	c(LLKLKWKKKQ)	6.2-12.5	6.2-12.5	>100
BPC166W	c(LLLKKWKKKQ)	6.2-12.5	6.2-12.5	>100
BPC184W	c(KLLLKWKKLQ)	3.1-6.2	1.6-3.1	25-50
BPC186W	c(KKKLKWKKLQ)	12.5-25	6.2-12.5	>100
BPC188W	c(LLLKKWKKLQ)	6.2-12.5	12.5-25	50-75
BPC190W	c(LKKKKWKKLQ)	25-50	12.5-25	>100
BPC192W	c(LKLLKWKKLQ)	12.5-25	6.2-12.5	25-50
BPC194W	c(KKLKKWKKLQ)	12.5-25	6.2-12.5	12.5-25
BPC196W	c(LLKLKWKKLQ)	3.1-6.2	1.6-3.1	>100
BPC198W	c(KLKKKWKKLQ)	25-50	3.1-6.2	25-50
BPC200W	c(LLLLKWKKLQ)	>50	3.1-6.2	75-100
BPC202W	c(KKKKKWKKLQ)	25-50	12.5-25	>100

[a] *Pss, Pseudomonas syringae* pv. *syringae; Xav, Xanthomonas axonopodis* pv. *vesicatoria; Ea, Erwinia amylovora*

Next, a comparison study of the antibacterial activities of the Phe- and Trp-containing libraries was carried out (Figure 12). In this figure, the lowest value of the MIC range for the Phe analogues is represented in white symbols, whereas black symbols are used for Trp derivatives. Grey symbols stand for peptides displaying the same activity. This analysis revealed that the presence of the Trp greatly enhanced the antimicrobial activity against the bacteria tested. In fact, compared with the collection of Phe analogues, the Trp-containing peptide library included a larger number of active sequences. In particular, the screening of the Phe-containing cyclic peptide library led to the identification of two sequences with MIC of 1.6 to 3.1 µM against *X. axonopodis* pv. *vesicatoria*, four with MIC of 3.1 to 6.2 µM against *P. syringae* pv. *syringae*, and one with MIC of 6.2 to 12.5 µM against *E. amylovora*. In the case of the Trp analogues, these MIC values were observed for 23, 20 and 6 cyclic peptides, respectively.

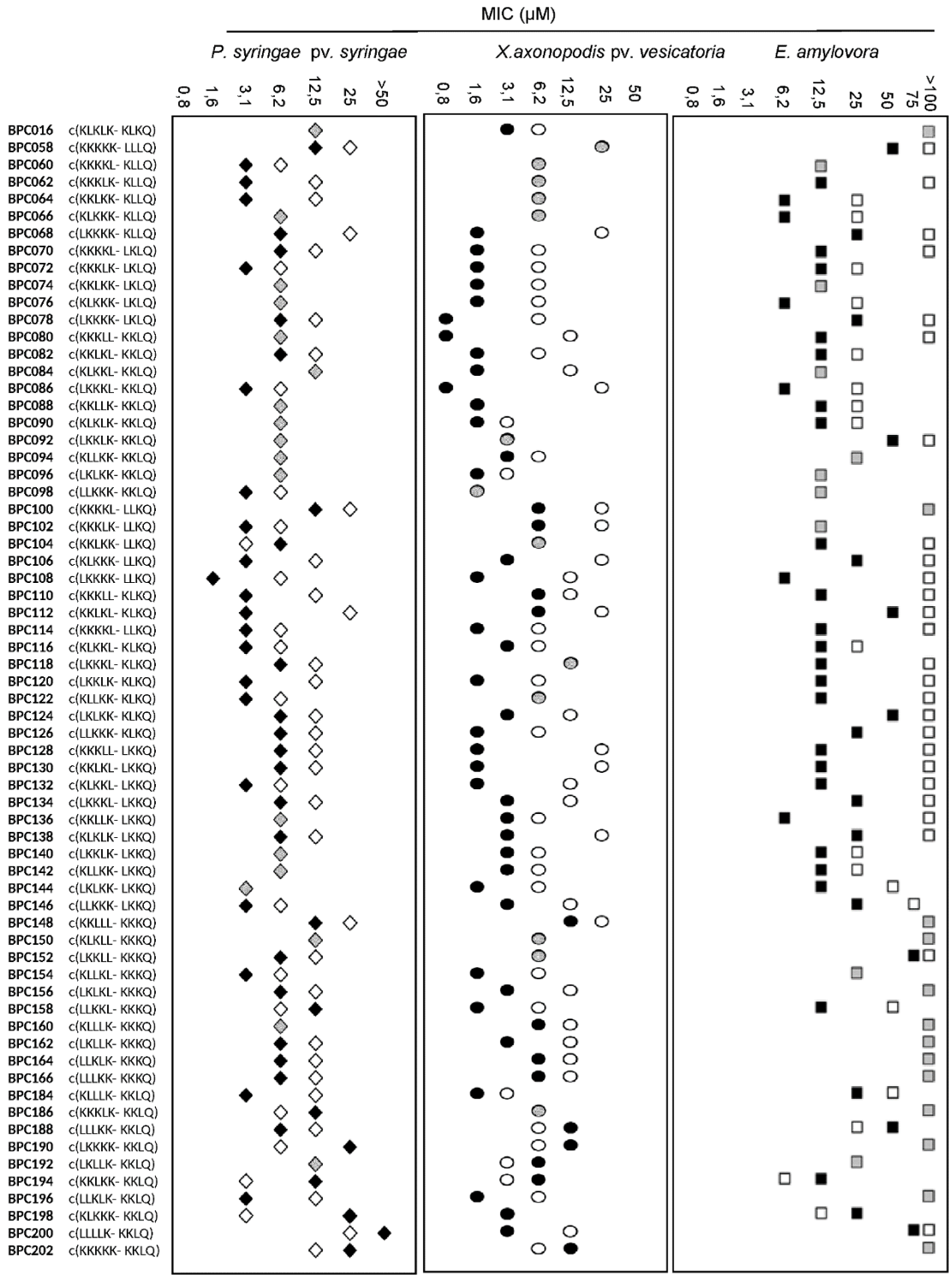

Figure 12. Antibacterial activity of the cyclic peptides incorporating a Trp or a Phe. Sequences and codes of the cyclic peptides are depicted, "-" for Trp (W) or Phe (F). Antimicrobial activity is given as the minimal concentration that inhibits growth (MIC). The MIC axis is in logarithmic scale and for each sequence the lowest value of the MIC range is represented. Black symbols correspond to peptides with a Trp, white symbols to peptides with a Phe and grey symbols to peptides that exhibit the same MIC values.

Moreover, a second analysis was performed in which the activity of each Phe-containing peptide was correlated with that of its Trp derivative. This correlation is represented in Figure 13 where the Phe peptides are placed on the left and the Trp sequences on the right. A negative slope was obtained in most cases clearly pointing out to an increase of the activity. This trend was observed for 40, 41 and 46 Trp analogues against *P. syringae* pv. *syringae*, *E. amylovora* and *X. axonopodis* pv. *vesicatoria*, respectively, which displayed lower MIC values than their corresponding Phe counterparts. Moreover, for 15 to 22 compounds, the Phe → Trp substitution did not influence the activity, as shown from the resulting horizontal lines in Figure 13.

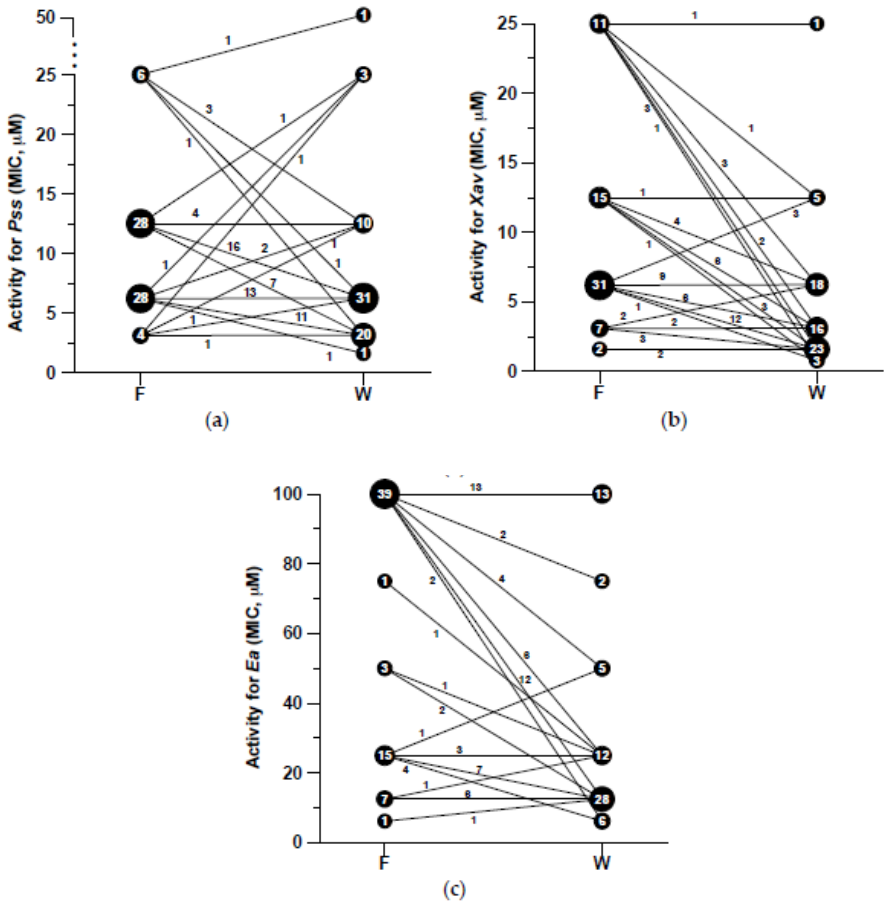

Figure 13. Graphical representation of the antibacterial activity of the cyclic peptides incorporating a Phe or a Trp. Antibacterial activity against (a) *P. syringae* pv. *syringae*, (b) *X. axonopodis* pv. *vesicatoria*, (c) *E. amylovora*. The antibacterial activity is given as the minimal concentration that inhibits growth (MIC), and the lowest values of the MIC range is represented. The numbers in the black circles indicate the number of compounds with a given activity, the segment connectors link each Phe-containing peptide with its corresponding Trp-derivative, and the segment labels stand for the number of peptides that follow the same activity trend.

Remarkably, within the Trp-containing cyclic peptides we found sequences with highest activity than the Phe derivatives against *X. axonopodis* pv. *vesicatoria* (**BPC078W**, **BPC080W**, and **BPC086W**, MIC of 0.8 to 1.6 µM) and *P. syringae* pv. *vesicatoria* (**BPC108W**, MIC of 1.6 to 3.1 µM).

3.3.1.3. Hemolytic activity

The toxicity of this library was evaluated as the ability to lyse erythrocytes in comparison to melittin at 50 and 125 µM (Table 30). In general, all cyclic decapeptides displayed low hemolysis values. In particular, 39 out of 66 sequences displayed a hemolysis ≤ 10% at 125µM and 10 sequences, hemolysis between 11 and 20%.

Table 30. Sequences and cytotoxicity data of library of Trp-containing cyclic peptides

Peptide	Sequence	Hemolysis (%)	
		50 µM	125 µM
BPC016W	c(KLKLKWKLKQ)	25	32
BPC058W	c(KKKKKWLLLQ)	2	3
BPC060W	c(KKKKLWKLLQ)	22	29
BPC062W	c(KKKLKWKLLQ)	3	4
BPC064W	c(KKLKKWKLLQ)	17	25
BPC066W	c(KLKKKWKLLQ)	33	41
BPC068W	c(LKKKKWKLLQ)	6	7
BPC070W	c(KKKKLWLKLQ)	6	9
BPC072W	c(KKKLKWLKLQ)	7	9
BPC074W	c(KKLKKWLKLQ)	39	50
BPC076W	c(KLKKKWLKLQ)	15	21
BPC078W	c(LKKKKWLKLQ)	3	6
BPC080W	c(KKKLLWKKLQ)	3	4
BPC082W	c(KKLKLWKKLQ)	26	34
BPC084W	c(KLKKLWKKLQ)	54	60
BPC086W	c(LKKKLWKKLQ)	4	8
BPC088W	c(KKLLKWKKLQ)	14	19
BPC090W	c(KLKLKWKKLQ)	9	15
BPC092W	c(LKKLKWKKLQ)	2	3
BPC094W	c(KLLKKWKKLQ)	35	42
BPC096W	c(LKLKKWKKLQ)	10	15
BPC098W	c(LLKKKWKKLQ)	12	18
BPC100W	c(KKKKLWLLKQ)	19	27
BPC102W	c(KKKLKWLLKQ)	12	17
BPC104W	c(KKLKKWLLKQ)	2	3
BPC106W	c(KLKKKWLLKQ)	2	2
BPC108W	c(LKKKKWLLKQ)	4	5
BPC110W	c(KKKLLWKLKQ)	3	4
BPC112W	c(KKLKLWKLKQ)	3	4
BPC114W	c(KLKKLWKLKQ)	29	38
BPC116W	c(LKKKLWKLKQ)	9	14

BPC118W	c(KKLLKWKLKQ)	4	4
BPC120W	c(LKKLKWKLKQ)	6	9
BPC122W	c(KLLKKWKLKQ)	2	6
BPC124W	c(LKLKKWKLKQ)	2	2
BPC126W	c(LLKKKWKLKQ)	5	9
BPC128W	c(KKKLLWLKKQ)	2	2
BPC130W	c(KKLKLWLKKQ)	1	2
BPC132W	c(KLKKLWLKKQ)	5	8
BPC134W	c(LKKKLWLKKQ)	3	4
BPC136W	c(KKLLKWLKKQ)	1	2
BPC138W	c(KLKLKWLKKQ)	7	14
BPC140W	c(LKKLKWLKKQ)	31	37
BPC142W	c(KLLKKWLKKQ)	16	18
BPC144W	c(LKLKKWLKKQ)	16	21
BPC146W	c(LLKKKWLKKQ)	4	7
BPC148W	c(KKLLLWKKKQ)	1	2
BPC150W	c(KLKLLWKKKQ)	17	32
BPC152W	c(LKKLLWKKKQ)	1	3
BPC154W	c(KLLKLWKKKQ)	4	7
BPC156W	c(LKLKLWKKKQ)	1	2
BPC158W	c(LLKKLWKKKQ)	10	14
BPC160W	c(KLLLKWKKKQ)	3	6
BPC162W	c(LKLLKWKKKQ)	57	56
BPC164W	c(LLKLKWKKKQ)	6	6
BPC166W	c(LLLKKWKKKQ)	1	1
BPC184W	c(KLLLKWKKLQ)	22	32
BPC186W	c(KKKLKWKKLQ)	1	1
BPC188W	c(LLLKKWKKLQ)	33	48
BPC190W	c(LKKKKWKKLQ)	1	3
BPC192W	c(LKLLKWKKLQ)	13	17
BPC194W	c(KKLKKWKKLQ)	3	5
BPC196W	c(LLKLKWKKLQ)	2	3
BPC198W	c(KLKKKWKKLQ)	2	4
BPC200W	c(LLLLKWKKLQ)	6	7
BPC202W	c(KKKKKWKKLQ)	0	1

A comparison study similar to that of the antibacterial activity was carried out for the Phe- and the Trp-containing peptides (Figure 14). The percent hemolysis at 125 µM were represented. White symbols were used for the Phe analogues, black symbols for the Trp derivatives and grey symbols for peptides with the

same hemolysis. This analysis pointed out that it cannot be defined a general trend for the hemolysis when replacing a Phe with a Trp.

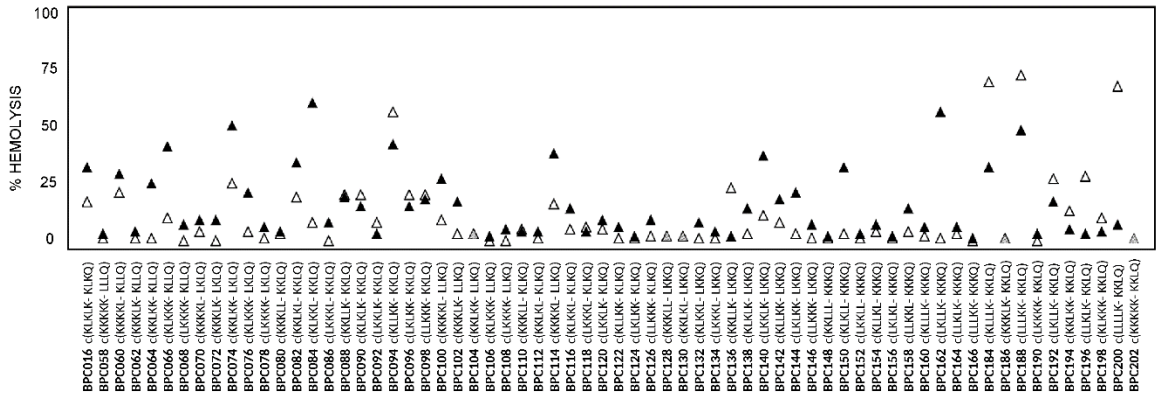

Figure 14. Hemolytic activity of the cyclic peptides incorporating a Trp or a Phe. Sequences and codes of the cyclic peptides are depicted, "-" stands for W or F. Hemolytic activity was measured at 125 μM and is expressed as a percentage compared to melittin as a standard. Black triangles correspond to peptides with a Trp, white triangles to peptides with a Phe and grey triangles to peptides that display the same hemolysis.

Moreover, similarly to the antimicrobial activity, the percent hemolysis at 125 μM of the Phe analogues was correlated with that of the Trp derivatives (Figure 15). It was observed that 40 Trp derivatives displayed a percentage of hemolysis comparable to that of their Phe counterparts. Moreover, 49 Trp-containing cyclic peptides vs. 56 Phe analogues showed a hemolysis ≤20% at 125 μM.

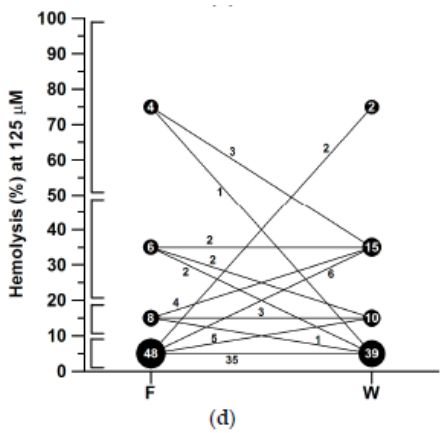

Figure 15. Graphical representation of the hemolytic activity of the cyclic peptides incorporating a Phe or a Trp. Hemolytic activity was measured at 125 μM and is expressed as a percentage compared to melittin as a standard. The numbers in the black circles indicate the number of compounds with a given activity, the segment connectors link each Phe-containing peptide with its corresponding Trp-derivative, and the segment labels stand for the number of peptides that follow the same hemolysis. The brackets in the y-axis of the hemolytic activity stand for hemolysis percentage ranges.

Taking into account all the activity and hemolysis results, peptides **BPC072W**, **BPC098W**, **BPC120W** and **BPC132W** showed a good biological activity profile with MIC values ranging from 1.6 to 25 µM and a hemolysis below 20% at 125 µM. The best peptides were **BPC086W** and **BPC108W**, which displayed MIC values ranging from 0.8 to 12.5 µM. These peptides were also low hemolytic (≤ 8% at 125 µM).

This work supports the notion that subtle changes in a peptide sequence may lead to a significant modification of its biological activity (Monroc 2006, Vilà 2016). Thus, for example, the Phe → Trp substitution in the lead peptides c(LysLysLeuLysLysPheLysLysLeuGln) (**BPC194**) and c(LysLeuLysLysLysPheLysLysLeuGln) (**BPC198**) caused a reduction of the activity. In contrast, this substitution in c(LeuLysLysLysLeuPheLysLysLeuGln) (**BPC086**) and c(LeuLysLysLysLysPheLeuLeuLysGln) (**BPC108**), which were poorly active, afforded the Trp analogues **BPC086W** and **BPC108W** with the best biological activity profile.

3.3.2. Design and synthesis of new tryptophan-containing cyclic decapeptides

3.3.2.1. Design of cyclic peptides

In this PhD thesis, with the aim of improving the antimicrobial activity of the cyclic decapeptides containing a Trp residue described in the previous section, a second library was designed. This study was carried out in collaboration with Dr. Emili Besalú. A computational method called Superposing Significant Interaction Rules (SSIR) was used, which consists on searching for rules of order 1, 2, 3 or higher that are significant for a particular property. In this case, the properties were the antibacterial activity and the hemolysis. For example, a rule of order 2 is one that simultaneously involves two residues of the sequence. The method recounts how many peptides in the library obey this pattern and, among them, how many are active. Thus, it can be determined which are the significant rules that will allow to predict the structure of new peptides to be synthesized. Then, the number of significant rules that each of these new peptides obey is determined. This method gives a ranking of sequences for each given property (antibacterial activity or hemolysis). In our study, when applying this computational method to the 66-member library of cyclic peptides, the 22 sequences included in Table 31 were obtained.

MANUSCRIPT IN PREPARATION. EMBARGO UNTIL PUBLICATION DATE

4. CONCLUSIONS

- ✓ From sequences described in the literature, it has been identified KKVVFWVKFK-NH_2 (**KSL-W**) as a new lead peptide active against plant pathogens. **KSL-W** showed MIC values between 0.8 to 12.5 μM against all the pathogens tested, being more active against *P. syringae* pv. *actinidiae* and *X. arboricola* pv. *pruni* (MIC of 1.6 to 3.1 μM and 0.8 to 1.6 μM, respectively). Moreover, it inhibited a hemolysis of 20% at 375 μM, and a phytotoxicity of 0.62 cm at 250 μM.

- ✓ The nine residues at the C-terminus of **KSL-W** are required for its antibacterial activity. Thus, KVVFWVKFK-NH_2 (**BP408**) showed activity against five of the bacteria tested with MIC values between 3.1 and 25 μM.

- ✓ The presence of a D-amino acid in **KSL-W** significantly decreased the hemolysis and endowed it with the capacity to induce the expression of defense-related genes in tomato plants. KKVVFWVKFk-NH_2 (**BP442**) was the best derivative, displaying only a 2% hemolysis at 375 μM and inducing the expression of the blue copper binding protein (*BCB*).

- ✓ The incorporation of an acyl chain in **KSL-W** led to sequences with high activity against *Xanthomonas* strains, low hemolysis and phytotoxicity. In particular, best derivatives were C_3H_7CO-KKVVFWVKFK-NH_2 (**BP410**), $C_{11}H_{23}CO$-KKVVFWVKFK-NH_2 (**BP411**) and CH_3CO-KKVK(CO-$C_{11}H_{23}$)FWVKFK-NH_2 (**BP432**), which displayed higher activity than **KSL-W** against *X. axonopodis* pv. *vesicatoria* (MICs of 3.1 to 25 μM, of 3.1 to >50 μM and of 3.1 to >50 μM, respectively), a percent hemolysis between 2 and 47% at 375 μM, and a phytotoxicity ranging from 0.3 and 0.53 cm at 250 μM.

- ✓ A library of 28 peptide conjugates incorporating a CPP (**BP100**, **BP16**), an antimicrobial peptide (**KSL-W**, **BP143**) and/or a plant defense peptide elicitor (**BP13**, **flg15**, **Pep13**, **Pip-1**) was designed and synthesized. Peptide conjugates **BP100-Pep13** and **KSLW-BP16** were the most active against all the bacteria tested (MICs of 0.8 to 6.2 μM), and displayed low hemolysis (5 and 6% at 50 μM, respectively) and low phytotoxicity (necrotic area of 0.04 and 0.34 cm at 50 μM, respectively).

- ✓ We have studied the influence on the biological activity of the replacement of a Phe with a Trp in a library of cyclic decapeptides. This study demonstrated that this replacement provided peptides with higher antimicrobial activity against the bacteria tested than those of the Phe-containing library. In particular, the Phe derivatives included two sequences with MIC of 1.6 to 3.1 μM against *X. axonopodis* pv. *vesicatoria*, four with MIC of 3.1 to 6.2 μM against *P. syringae* pv. *syringae*, and one with MIC of 6.2 to 12.5 μM against *E. amylovora*. In contrast, in the case of the Trp analogues, these MIC values were observed for 23, 20 and 6 cyclic peptides, respectively.

- ✓ The use of the Superposing Significant Interaction Rules (SSIR) computational method allowed the design of a library of 22 cyclic decapeptides containing a Trp residue and the identification of c(KKKKKWLKLQ) (**BPC870W**). This cyclic decapeptide showed MIC values ranging from 3.1 to 6.2

μM against *P. syringae* pv. *syringae* and *X. axonopodis* pv. *vesicatoria*, and from 12.5 to 25 μM against *E. amylovora*. Moreover, it only caused 19% of hemolysis at 125 μM.

5. EXPERIMENTAL SECTION

5.1. MATERIALS AND METHODS

5.1.1. Ninhydrin or Kaiser test (Kaiser 1970)

The ninhydrin test is a qualitative colorimetric test that is used to detect the presence of free primary amines in a peptidyl resin. This test has a great application in the field of synthesis of peptides on solid phase since it allows to know qualitatively if the amino acid coupling has been completed.

This test is based on a transamination-decarboxylation reaction between the amine group of the amino acid and ninhydrin, resulting in a conjugated imine product, a chromophore with a deep blue or Ruhemann's purple color.

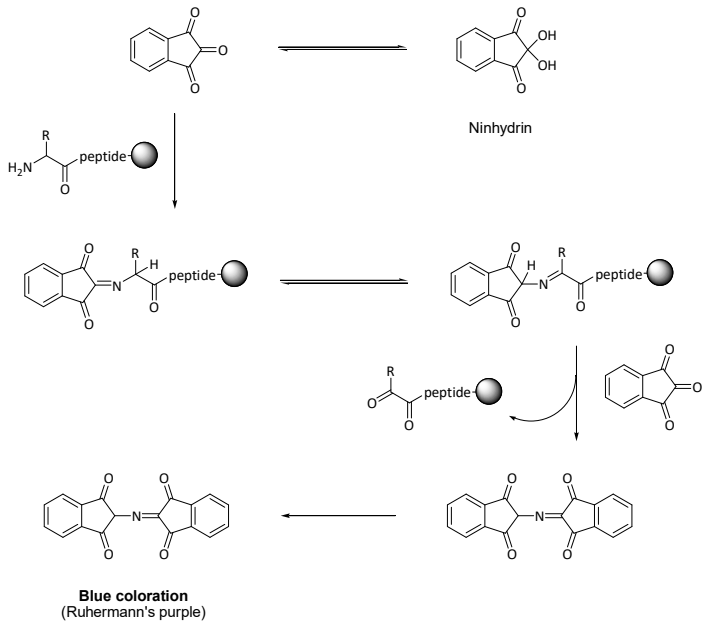

Scheme 8. Ninhydrin test

Three reagents are used to perform the test:

- ✓ **Reagent A:** 500 mg of ninhydrin solved in 10 ml of absolute ethanol.
- ✓ **Reagent B:** 100 mg of phenol solved in 25 ml of absolute ethanol.
- ✓ **Reagent C:** 1ml of 1mM NaCN solution in 49 ml of pyridine distilled on ninhydrin.

A few resin beads from the reaction vessel are transferred into an Eppendorf tube and 3 drops of each solution of the test kit are added. Next, the suspension is mixed well and heated at 100°C for 3 min. The resin beads and the solution turn dark blue when free primary amines are present. The color of the resin beads doesn't change and the solution stays yellow when no free primary amines are present.

5.1.2. Chloranil test (Vojkovsky 1995)

The chloranil test is a qualitative colorimetric test used to detect the presence of free secondary amines attached to a solid support. Like the ninhydrin test, the chloranil test is used to check if the coupling of an amino acid onto a secondary amine has been completed.

The mechanism of the reaction that promotes blue coloration is the addition of enamine, formed by the reaction between acetaldehyde and the secondary amine of the amino acid, and chloranil that results in the loss of hydrochloric acid (Scheme 9).

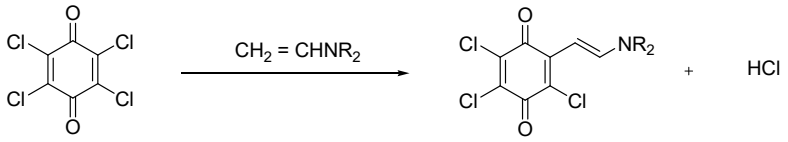

Scheme 9. Chloranil test

Two reagents are used to perform the test:

- ✓ **Reagent A:** 2% acetaldehyde in DMF.
- ✓ **Reagent B:** 2% chloranil in DMF.

A few resin beads from the reaction vessel are transferred into an Eppendorf tube and 4 drops of each solution of the test are added. Then, the suspension is mixed well and is incubated at room temperature for 5 min. A negative result is indicated by the solution remaining yellow, while a positive result is indicated by either the solution, the beads or both, having turned into an intense deep blue.

5.1.3. Fmoc test

The Fmoc test allows to determine the loading of the resin in any stages of the peptide synthesis. Loading refers to the µmol of amino groups per mg of resin. To carry out the test, an aliquot of the resin (between 4 and 5 mg) is weighed in an Eppendorf and treated with piperidine/DMF (3:7, 0.5 ml) for 30 min under stirring. This mixture is transferred to a tube containing methanol (6.5 ml). Then, the absorbance is measured in a UV-Vis spectrophotometer at 301 nm. As a blank, a solution of methanol (6.5 ml) + piperidine/DMF (3:7, 0.5 ml) is used. To determine the loading of the resin, the following formula is applied:

$$Loading\ \left(\frac{\mu mol}{mg}\right) = \frac{Abs_{301} \cdot\ 10^6\ \frac{\mu mol}{g} \cdot\ 0.007\ L}{7800\ M^{-1} \cdot\ 1\ cm^{-1} \cdot\ x\ mg\ of\ resin}$$

5.1.4. High-performance liquid chromatography (HPLC)

The HPLC analysis were carried out on a Dionex equipment consisting of an ASI-100 automatic injector, a P680 binary pump and a variable UV/Vis wavelength UVD10OU detector. The separation was performed in reverse phase, using a Kromasil 100 C_{18} (3.5 µm, 4.6 mm x 40 mm) column and a mobile phase containing H_2O (solvent A) and CH_3CN (solvent B) with 0.1% of TFA. The flow used was 1 ml/min and a linear gradient of 2-100% B was applied. The detection was carried out at 220 nm.

5.1.5. Electrospray ionization mass spectrometry (ESI/MS)

The ESI-MS experiments were carried out at the Technical Research Services (STR) of the UdG, with a Bruker Daltonics Esquire 6000 mass spectrometer with a precision of ± 0.2 m/z, formed by a source of ionization by electrospray (ESI), an ion trap analyser and an electron multiplier detector. It works in negative or positive ionization mode, in a range of 50 to 3.000 m/z. The samples were solved in CH_3CN/H_2O (80:20) and were introduced to the instrument through a HPLC automatic injector of Agilent Technologies (1200 Series), at a flow rate of 100 µl/min.

5.1.6. High resolution mass spectrometry (HRMS)

The HRMS experiments were carried out using the same conditions as those of the ESI-MS, with a Bruker microTOF-Q IITM instrument using a hybrid quadrupole-flight time analyser (STR-UdG). The introduction of the samples was performed by direct infusion and were externally calibrated using sodium formate. The experiments were performed in positive ionization mode ESI (+).

5.1.7. Purification

The purification of peptides was carried out with a CombiFlash Rf200 device which operates at pressures above 200 psi. A reverse-phase C_{18} RediSep RfGold column was used, with a flow rate of 18 ml/min, and the detection was performed at 220 nm. Conditioning of the column was carried out with MeOH, H_2O and H_2O/CH_3CN mixtures. The samples were solved in H_2O:CH_3CN (98:2). A linear gradient of 2-100% CH_3CN for 22 min was used.

5.2. General method for solid-phase peptide synthesis

The synthesis was carried out manually on solid-phase in polypropylene syringes equipped with a polyethylene filter. An orthogonal Fmoc/^{t}Bu strategy was followed. A Fmoc-Rink-MBHA (0.55 mmol/g), a MBHA (0.4 mmol/g) or a ChemMatrix resin (0.66 mmol/g) was used as solid support. The ChemMatrix resin was selected for the synthesis of peptides containing more than 11 residues. The Fmoc-Rink-MBHA resin was swollen with CH_2Cl_2 (1 x 20 min) and DMF (1 x 20 min), the MBHA resin was swollen with CH_2Cl_2 (1 × 20 min) and DMF (1 × 20 min) and washed with piperidine/DMF (3:7, 1 × 5 min), DMF (6 × 1 min) and CH_2Cl_2 (3 × 1 min), and the ChemMatrix resin was swollen with MeOH (2 x 1 min), DMF (2 x 1 min), CH_2Cl_2 (2 x 1 min), CH_2Cl_2/TFA (99:1) (3 x 1 min), CH_2Cl_2/DIEA (19:1) (3 x 1 min), CH_2Cl_2 (3 x 1 min) and DMF (6 x

1 min). A Fmoc-Rink-amide linker was used to prepare C-terminal peptide amides whereas a PAC linker was employed for C-terminal carboxylic acid peptides. Once the resin MBHA or ChemMatrix was swollen, it was treated with the corresponding linker (4 equiv), Oxyma (4 equiv) and DIPCDI (4 equiv) in DMF overnight. After this time, the resin was washed with DMF (6 x 1 min) and CH_2Cl_2 (3 x 1 min). This step was monitored by the Kaiser test (Kaiser 1970).

Peptide elongation was carried out through sequential Fmoc removal and coupling steps of the corresponding protected amino acid. The Fmoc group was removed with piperidine/DMF (3:7, 1 x 2 min and 2 x 10 min). The coupling of the first amino acid (5 equiv) onto a PAC-ChemMatrix or a PAC-MBHA resin was performed in presence of *N,N'*-diisopropylcarbodiimide (DIPCDI) (5 equiv.), 4-dimethylaminopyridine (DMAP) (0.5 equiv.) and *N,N'*-diisopropylethylamine (DIEA) (1 equiv.) in DMF at room temperature for 2 h under stirring. This treatment was repeated twice and, then, the resin was washed with DMF (6 x 1 min) and CH_2Cl_2 (3 x 1 min) and dried with diethyl ether (3 x 2 min). The completion of the reaction was checked using a Fmoc test. Then, the resin was acetylated with CH_2Cl_2/pyridine/acetic anhydride (18:1.35:1.35, 2 x 30 min) and washes with CH_2Cl_2 (3 x 2 min), DMF (3 x 2 min), MeOH (2 x 2 min), CH_2Cl_2 (2 x 2 min) and DMF (6 x 1 min). Couplings of the other amino acids were carried out by treating the resin with the corresponding protected amino acid (4 equiv), Oxyma (4 equiv) and DIPCDI (4 equiv) in DMF under stirring for 1 h at room temperature. These reactions were monitored by the Kaiser test (Kaiser 1970) if the coupling was performed on a primary amine or by the chloranil test (Vojkovsky 1995) if the coupling was performed on a secondary amine. After each coupling and Fmoc removal step, the resin was washed with DMF (6 x 1 min) and CH_2Cl_2 (2 x 1 min). After the sixth coupling, NMP was employed instead of DMF.

Once the peptidyl resin was completed, the Fmoc group was removed and peptides were cleaved from the resin by treatment with TFA/H_2O/TIS (95:2.5:2.5) for 2 h at room temperature. Peptides incorporating a tryptophan residue were cleaved with TFA/phenol/H_2O/TIS (92.5:2.5:2.5:2.5) and peptides incorporating a methionine residue were cleaved with TFA/DTT/H_2O/TIS (92.5:2.5:2.5:2.5). Following evaporation of the acidic solution, the crude peptides were washed with cold diethyl ether. The mixture was centrifuged and the supernatant was removed. This procedure was repeated three times. The resulting peptides were dissolved in H_2O, lyophilized, purified by reverse-phase chromatography with a CombiFlash® Rf equipment, analysed by HPLC and characterized by ESI-MS and HRMS.

Tyr-Gly-Ile-His-Thr-His-NH_2 (Pip-1)

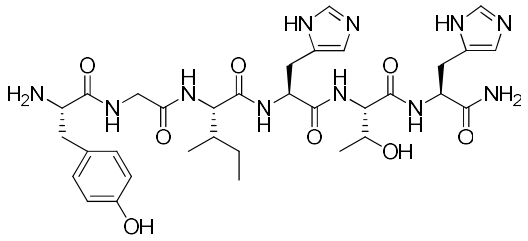

A Fmoc-Rink-MBHA resin (200 mg, 0.55 mmol/g) was swollen with CH_2Cl_2 (1 x 20 min) and with DMF (1 x 20 min). Removal of the Fmoc group and coupling of the amino acids were performed using the conditions described in the above general method. The cleavage provided **Pip-1** in 72% HPLC purity. Elution with H_2O/CH_3CN (87:13) yielded **Pip-1** in >99% HPLC purity.

HPLC (λ = 220 nm): t_R = 5.38 min. ESI-MS (*m/z*): 363.7 $[M+2H]^{2+}$, 726.4 $[M+H]^+$, 748.4 $[M+Na]^+$. HRMS (*m/z*): calculated for $C_{33}H_{48}N_{11}O_8$ $[M+H]^+$ 726.3682, found 726.3688; calculated for $C_{33}H_{47}N_{11}O_8Na$ $[M+Na]^+$ 748.3501, found 748.3503.

Val-Trp-Asn-Gln-Pro-Val-Arg-Gly-Phe-Lys-Val-Tyr-Glu-OH (Pep13)

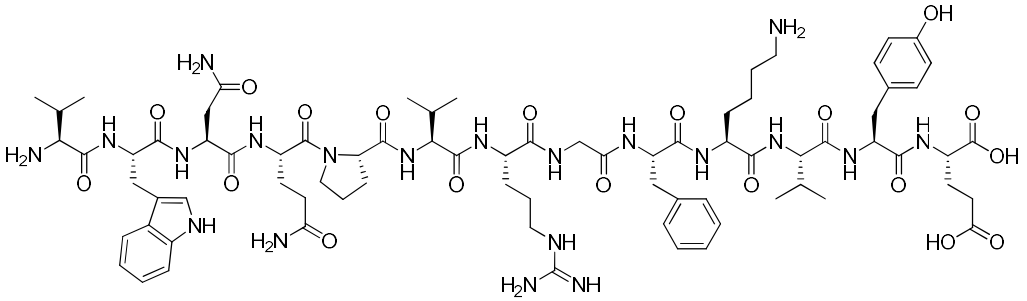

A PAC-ChemMatrix resin (200 mg, 0.66 mmol/g) was swollen with CH_2Cl_2 (1 x 20 min) and with DMF (1 x 20 min). Coupling of the amino acids and removal of the Fmoc group were performed using the conditions described in the above general method. The cleavage provided **Pep13** in 63% HPLC purity. Elution with H_2O/CH_3CN (78:22) yielded **Pep13** in >99% HPLC purity.

HPLC (λ = 220 nm): t_R = 6.31 min. ESI-MS (*m/z*): 811.5 $[M+2H]^{2+}$, 822.9 $[M+H+Na]^{2+}$, 833.4 $[M+2Na]^{2+}$, 1621.9 $[M+H]^+$, 1644.8 $[M+Na]^+$. HRMS (m/z): calculated for $C_{77}H_{114}N_{20}O_{19}$ $[M+2H]^{2+}$ 811.4279, found 811.4266; calculated for $C_{77}H_{113}N_{20}O_{19}Na$ $[M+H+Na]^{2+}$ 822.4189, found 822.4170; calculated for $C_{77}H_{113}N_{20}O_{19}K$ $[M+H+K]^{2+}$ 830.4058, found 830.4016; calculated for $C_{77}H_{113}N_{20}O_{19}Cu$ $[M+H+Cu]^{2+}$ 841.8849, found 841.8860; calculated for $C_{77}H_{113}N_{20}O_{19}$ $[M+H]^+$ 1621.8485, found 1621.8475.

Ser-Val-Ala-Gly-Arg-Ala-Gln-Gly-Met-NH_2 (Cn-AMP1)

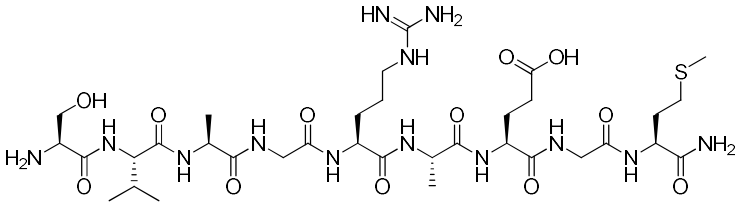

A Fmoc-Rink-MBHA resin (200 mg, 0.55 mmol/g) was swollen with CH_2Cl_2 (1 x 20 min) and with DMF (1 x 20 min). Removal of the Fmoc group and coupling of the amino acids were performed using the conditions described in the above general method. The cleavage provided **Cn-AMP1** in 43% HPLC purity. Elution with H_2O/CH_3CN (88:12) yielded **Cn-AMP1** in >99% HPLC purity.

HPLC (λ = 220 nm): t_R = 5.33 min. ESI-MS (*m/z*): 438.2 $[M+2H]^{2+}$, 449.2 $[M+H+Na]^{2+}$, 875.5 $[M+H]^{+}$, 897.4 $[M+Na]^{+}$.

Ser-Val-Ala-Gly-Arg-Ala-Gln-Gly-Met-NH_2 (Cn-AMP2)

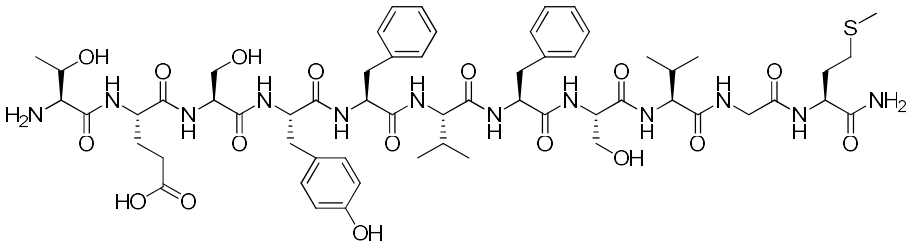

A Fmoc-Rink-MBHA resin (200 mg, 0.55 mmol/g) was swollen with CH_2Cl_2 (1 x 20 min) and with DMF (1 x 20 min). Removal of the Fmoc group and coupling of the amino acids were performed using the conditions described in the above general method. The cleavage provided **Cn-AMP2** in 65% HPLC purity. Elution with H_2O/CH_3CN (66:34) yielded **Cn-AMP2** in >99% HPLC purity.

HPLC (λ = 220 nm): t_R = 6.97 min. ESI-MS (*m/z*): 1265.6 $[M+H]^{+}$, 1287.6 $[M+Na]^{+}$, 1303.6 $[M+K]^{+}$. HRMS (*m/z*): calculated for $C_{59}H_{85}N_{12}O_{17}SNa$ $[M+H+Na]^{2+}$ 644.2882, found 644.2873; calculated for $C_{59}H_{84}N_{12}O_{17}SNa_2$ $[M+2Na]^{2+}$ 655.2791, found 655.2787; calculated for $C_{59}H_{85}N_{12}O_{17}S$ $[M+H]^{+}$ 1265.5871, found 1265.5850; calculated for $C_{59}H_{84}N_{12}O_{17}SNa$ $[M+Na]^{+}$ 1287.5690, found 1287.5670.

Tyr-Cys-Ser-Tyr-Thr-Met-Glu-Ala-NH_2 (Cn-AMP3)

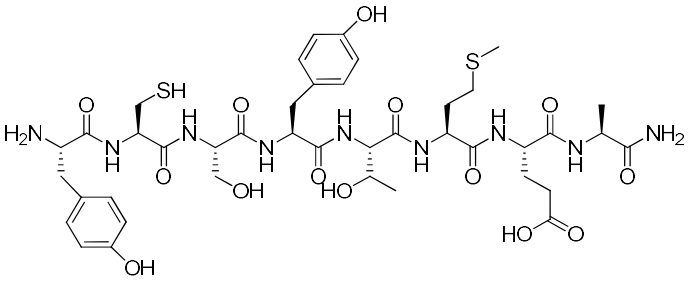

A Fmoc-Rink-MBHA resin (200 mg, 0.55 mmol/g) was swollen with CH_2Cl_2 (1 x 20 min) and with DMF (1 x 20 min). Removal of the Fmoc group and coupling of the amino acids were performed using the conditions described in the above general method. The cleavage provided **Cn-AMP3** in 73% HPLC purity. Elution with H_2O/CH_3CN (80:20) yielded **Cn-AMP3** in >99% HPLC purity.

HPLC (λ = 220 nm): t_R = 5.78 min. ESI-MS (*m/z*): 966.4 $[M+H]^{+}$, 988.4 $[M+Na]^{+}$, 1004.4 $[M+K]^{+}$. HRMS (*m/z*): calculated for $C_{41}H_{59}N_9O_{14}S_2Na$ $[M+Na]^{+}$ 988.3515, found 988.3481.

Gln-Lys-Ala-Leu-Asn-Glu-Ile-Asn-Gln-Phe-NH_2 (p10)

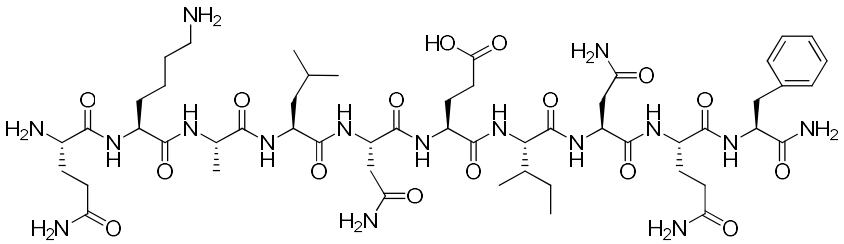

A Fmoc-Rink-MBHA resin (200 mg, 0.55 mmol/g) was swollen with CH_2Cl_2 (1 x 20 min) and with DMF (1 x 20 min). Removal of the Fmoc group and coupling of the amino acids were performed using the conditions described in the above general method. The cleavage provided **p10** in 73% HPLC purity. Elution with H_2O/CH_3CN (82:18) yielded **p10** in >99% HPLC purity.

HPLC (λ = 220 nm): t_R = 5.76 min. ESI-MS (*m/z*): 602.3 $[M+2H]^{2+}$, 613.3 $[M+H+Na]^{2+}$, 1203.7 $[M+H]^+$, 1225.7 $[M+Na]^+$. HRMS (*m/z*): calculated for $C_{53}H_{87}N_{16}O_{16}$ $[M+H]^+$ 1203.6480, found 1203.6445; calculated for $C_{53}H_{86}N_{16}O_{16}Na$ $[M+Na]^+$ 1225.6300, found 1225.6262.

Thr-Lys-Lys-Thr-Lys-Leu-Thr-Glu-Glu-Glu-Lys-Asn-Arg-Leu-NH_2 (p14)

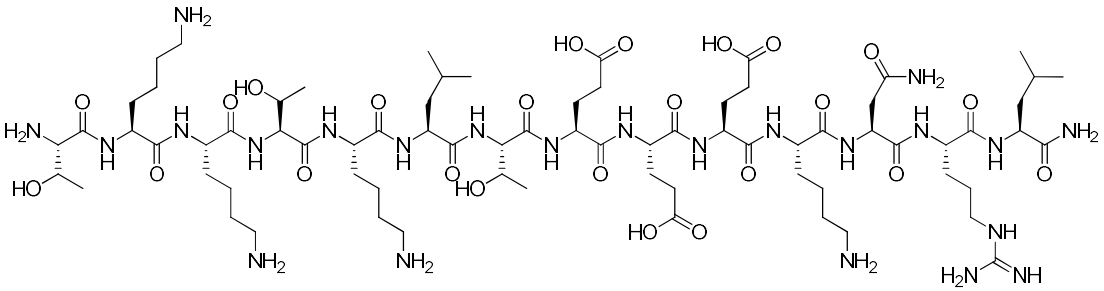

A Fmoc-Rink-ChemMatrix resin (200 mg, 0.66 mmol/g) was swollen with CH_2Cl_2 (1 x 20 min) and with DMF (1 x 20 min). Removal of the Fmoc group and coupling of the amino acids were performed using the conditions described in the above general method. The cleavage provided **p14** in 42% HPLC purity. Elution with H_2O/CH_3CN (92:8) yielded **p14** in >99% HPLC purity.

HPLC (λ = 220 nm): t_R = 5.38 min. ESI-MS (*m/z*): 573.1 $[M+3H]^{3+}$, 859.0 $[M+2H]^{2+}$, 1718.0 $[M+H]^+$. HRMS (*m/z*): calculated for $C_{73}H_{134}N_{23}O_{24}$ $[M+H]^+$ 1716.9967, found 1716.9983.

Phe-Val-Asp-Leu-Lys-Lys-Ile-Ala-Asn-Ile-Ile-Asn-Ser-Ile-Phe-Gly-Lys-NH_2 (preproTemporin-1CEa)

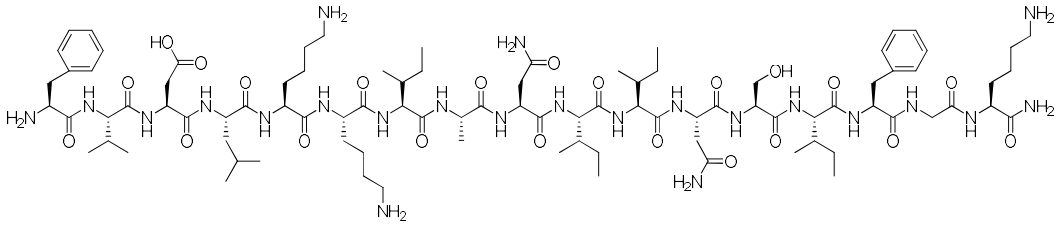

A Fmoc-Rink-ChemMatrix resin (200 mg, 0.66 mmol/g) was swollen with CH_2Cl_2 (1 x 20 min) and with DMF (1 x 20 min). Removal of the Fmoc group and coupling of the amino acids were performed using the conditions described in the above general method. The cleavage provided **preproTemporin-1Cea** in 90% HPLC purity.

HPLC (λ = 220 nm): t_R = 7.07 min. ESI-MS (*m/z*): 640.7 $[M+3H]^{3+}$, 960.6 $[M+2H]^{2+}$, 1920.2 $[M+H]^+$, 1941.2 $[M+Na]^+$.HRMS (*m/z*): calculated for $C_{91}H_{152}N_{23}O_{22}$ $[M+H]^+$ 1919.1477, found 1919.1473.

Trp-Phe-Arg-Lys-Gln-Leu-Lys-Trp-OH (L10)

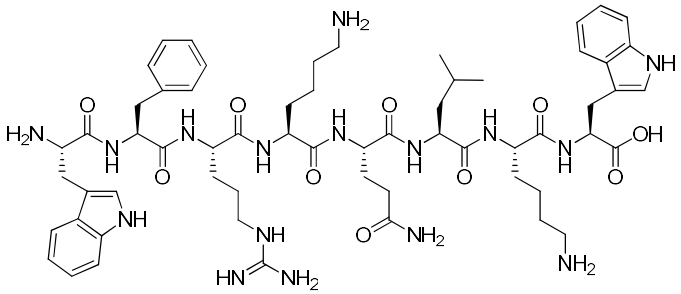

Fmoc-PAC-MBHA resin (200 mg, 0.55 mmol/g) was swollen with CH_2Cl_2 (1 x 20 min) and with DMF (1 x 20 min). Coupling of the amino acids and removal of the Fmoc group were performed using the conditions described in the above general method. The cleavage provided **L10** in 96% HPLC purity. Elution with H_2O/CH_3CN (76:24) yielded **L10** in >99% HPLC purity.

HPLC (λ = 220 nm): t_R = 6.27 min. ESI-MS (*m/z*): 596.4 $[M+2H]^{2+}$, 607.3 $[M+H+Na]^{2+}$, 615.8 $[M+H+K]^{2+}$, 1191.8 $[M+H]^+$, 1213.7 $[M+Na]^+$. HRMS (*m/z*): calculated for $C_{60}H_{88}N_{16}O_{10}$ $[M+2H]^{2+}$ 596.3429, found 596.3406; calculated for $C_{60}H_{87}N_{16}O_{10}Na$ $[M+H+Na]^{2+}$ 607.3339, found 607.3312; calculated for $C_{64}H_{86}N_{16}O_{10}Na_2$ $[M+2H]^{2+}$ 618.3249, found 618.3224; calculated for $C_{60}H_{87}N_{16}O_{10}$ $[M+H]^+$ 1191.6786, found 1191.6753; calculated for $C_{60}H_{86}N_{16}O_{10}Na$ $[M+Na]^+$ 1213.6605, found 1213.6586.

Gly-Leu-Val-Gly-Thr-Leu-Leu-Gly-His-Ile-Gly-Lys-Ala-Ile-Leu-Gly-NH_2 (Frenatin 2.1S)

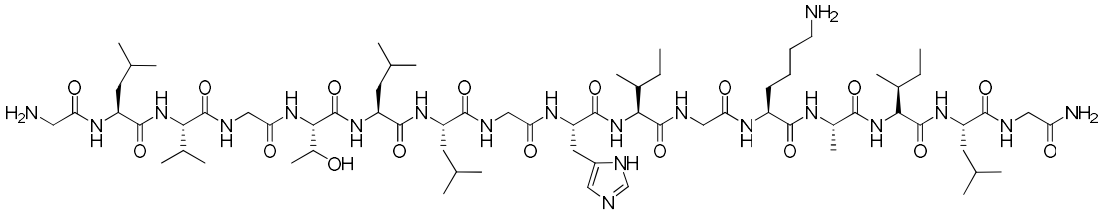

A Fmoc-Rink-ChemMatrix resin (50 mg, 0.66 mmol/g) was swollen with CH_2Cl_2 (1 x 20 min) and with DMF (1 x 20 min). Removal of the Fmoc group and coupling of the amino acids were performed using the conditions described in the above general method. The cleavage provided **Frenatin 2.1S** in 95% HPLC purity. Elution with H_2O/CH_3CN (68:32) yielded **Frenatin 2.1S** in >99% HPLC purity.

HPLC (λ = 220 nm): t_R = 7.90 min. ESI-MS (*m/z*): 759.6 $[M+2H]^{2+}$, 770.5 $[M+H+Na]^{2+}$, 1518.0 $[M+H]^+$, 1540.0 $[M+Na]^+$. HRMS (*m/z*): calculated for $C_{70}H_{126}N_{20}O_{17}$ $[M+2H]^{2+}$ 759.4799, found 759.4799; calculated for $C_{70}H_{125}N_{20}O_{17}$ $[M+H]^+$ 1517.9526, found 1517.9536.

Gly-Leu-Val-Gly-Thr-Leu-Leu-Gly-His-Ile-Gly-Lys-Ala-Ile-Leu-Ser-NH_2 (Frenatin 2.2S)

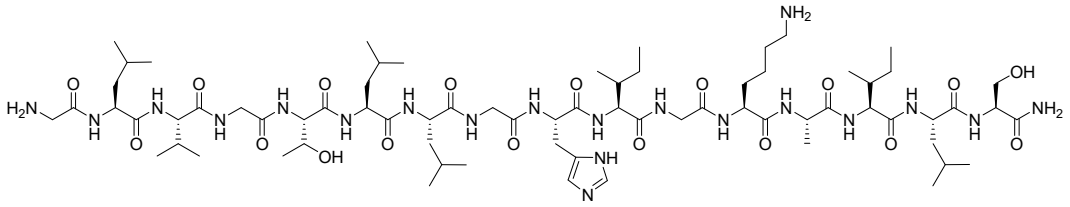

A Fmoc-Rink-ChemMatrix resin (200 mg, 0.66 mmol/g) was swollen with CH_2Cl_2 (1 x 20 min) and with DMF (1 x 20 min). Removal of the Fmoc group and coupling of the amino acids were performed using the conditions described in the above general method. The cleavage provided **Frenatin 2.2S** in 73% HPLC purity. Elution with H_2O/CH_3CN (72:28) yielded **Frenatin 2.2S** in >99% HPLC purity.

HPLC (λ = 220 nm): t_R = 7.17 min. ESI-MS (*m/z*): 774.5 $[M+2H]^{2+}$, 786.0 $[M+H+Na]^{2+}$, 1548.0 $[M+H]^+$, 1570.0 $[M+Na]^+$, 1587.0 $[M+K]^+$. HRMS (*m/z*): calculated for $C_{71}H_{128}N_{20}O_{18}$ $[M+2H]^{2+}$ 774.4852, found 774.4836; calculated for $C_{71}H_{127}N_{20}O_{18}Na$ $[M+H+Na]^{2+}$ 785.4762, found 785.4745; calculated for $C_{71}H_{127}N_{20}O_{18}$ $[M+H]^+$ 1547.9632, found 1547.9655; calculated for $C_{71}H_{126}N_{20}O_{18}Na$ $[M+Na]^+$ 1569.9451, found 1569.9449.

dGu-Hyp-Asn-Asn-Arg-Pro-Val-Tyr-Ile-Pro-Arg-Pro-Arg-Pro-Pro-His-Pro-Arg-Leu-NH_2 (dGu-Api88)

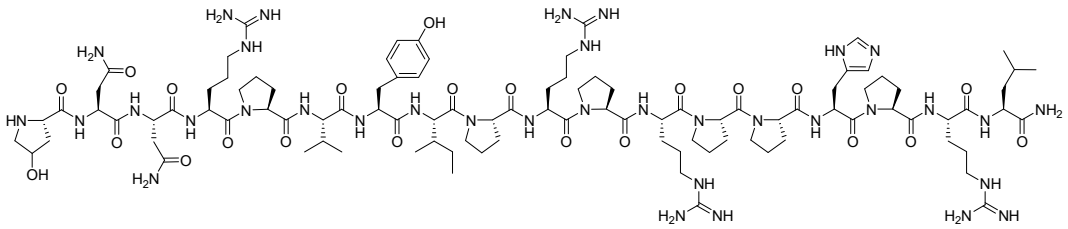

A Fmoc-Rink-MBHA resin (200 mg, 0.55 mmol/g) was swollen with CH_2Cl_2 (1 x 20 min) and with DMF (1 x 20 min). Removal of the Fmoc group and coupling of the amino acids were performed using the conditions described in the above general method. The cleavage provided **dGu-Api88** in 93% HPLC purity.

HPLC (λ = 220 nm): t_R = 5.73 min. ESI-MS (*m/z*): 1096.7 $[M+2H]^{2+}$, 1107.7 $[M+H+Na]^{2+}$, 1118.6 $[M+2Na]^{2+}$.

HRMS (*m/z*): calculated for $C_{99}H_{160}N_{35}O_{22}$ $[M+H]^+$ 2191.2472, found 2191.2430.

Lys-Val-Phe-Leu-Gly-Leu-Lys-OH (JCpep7)

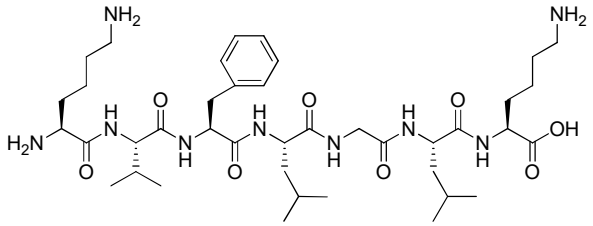

A PAC-MBHA resin (200 mg, 0.55 mmol/g) was swollen with CH_2Cl_2 (1 x 20 min) and with DMF (1 x 20 min). Coupling of the amino acids and removal of the Fmoc group were performed using the conditions described in the above general method. The cleavage provided **JCPep7** in 98% HPLC purity. Elution with H_2O/CH_3CN (80:20) yielded **JCPep7** in >99% HPLC purity.

HPLC (λ = 220 nm): t_R = 6.01 min. ESI-MS (*m/z*): 402.8 $[M+2H]^{2+}$, 804.6 $[M+H]^+$, 826.6 $[M+Na]^+$. HRMS (*m/z*): calculated for $C_{40}H_{70}N_9O_8$ $[M+H]^+$ 804.5342, found 804.5332.

Lys-Lys-Val-Val-Phe-Lys-Val-Lys-Phe-Lys-NH_2 (KSL)

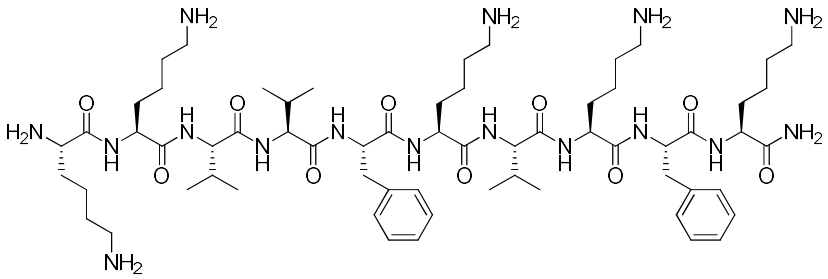

A Fmoc-Rink-MBHA resin (200 mg, 0.55 mmol/g) was swollen with CH_2Cl_2 (1 x 20 min) and with DMF (1 x 20 min). Removal of the Fmoc group and coupling of the amino acids were performed using the conditions described in the above general method. The cleavage provided **KSL** in 63% HPLC purity. Elution with H_2O/CH_3CN (85:15) yielded **KSL** in >99% HPLC purity.

HPLC (λ = 220 nm): t_R = 5.81 min. ESI-MS (*m/z*): 626.0 $[M+2H]^{2+}$, 1250.0 $[M+H]^+$, 1271.9 $[M+Na]^+$. HRMS (*m/z*): calculated for $C_{63}H_{110}N_{16}O_{10}$ $[M+2H]^{2+}$ 625.4290, found 625.4278; calculated for $C_{63}H_{109}N_{16}O_{10}$ $[M+H]^+$ 1249.8507, found 1249.8494.

Lys-Lys-Val-Val-Phe-Trp-Val-Lys-Phe-Lys-NH_2 (KSL-W)

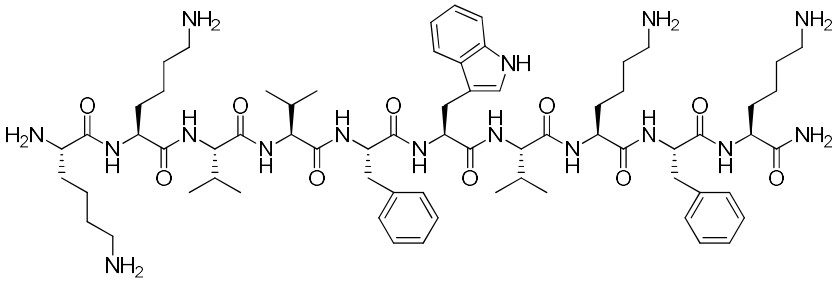

A Fmoc-Rink-MBHA resin (200 mg, 0.55 mmol/g) was swollen with CH_2Cl_2 (1 x 20 min) and with DMF (1 x 20 min). Removal of the Fmoc group and coupling of the amino acids were performed using the conditions described in the above general method. The cleavage provided **KSL-W** in 55% HPLC purity. Elution with H_2O/CH_3CN (88:12) yielded **KSLW** in >99% HPLC purity.

HPLC (λ = 220 nm): t_R = 6.19 min. ESI-MS (*m/z*): 654.9 $[M+2H]^{2+}$, 1307.9 $[M+H]^+$, 1329.9 $[M+Na]^+$. HRMS (*m/z*): calculated for $C_{68}H_{108}N_{16}O_{10}$ $[M+2H]^{2+}$ 654.4212, found 654.4198; calculated for $C_{68}H_{107}N_{16}O_{10}$ $[M+H]^+$ 1307.8351, found 1307.8339.

Val-Lys-Phe-Lys-NH_2 (BP403)

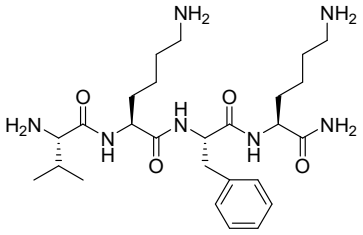

A Fmoc-Rink-MBHA resin (50 mg, 0.55 mmol/g) was swollen with CH_2Cl_2 (1 x 20 min) and with DMF (1 x 20 min). Removal of the Fmoc group and coupling of the amino acids were performed using the conditions described in the above general method. The cleavage provided **BP403** in 62% HPLC purity.

HPLC (λ = 220 nm): t_R = 5.29 min. ESI-MS (*m/z*): 260.6 $[M+2H]^{2+}$, 520.3 $[M+H]^+$. HRMS (*m/z*): calculated for $C_{26}H_{47}N_7O_4$ $[M+2H]^{2+}$ 260.6839, found 260.6844; calculated for $C_{26}H_{46}N_7O_4$ $[M+H]^+$ 520.3606, found 520.3590.

Trp-Val-Lys-Phe-Lys-NH_2 (BP404)

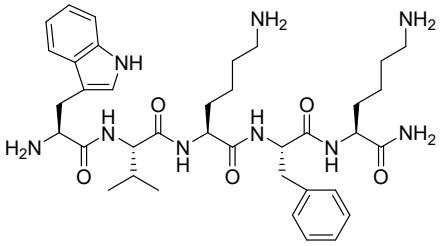

A Fmoc-Rink-MBHA resin (50 mg, 0.55 mmol/g) was swollen with CH_2Cl_2 (1 x 20 min) and with DMF (1 x 20 min). Removal of the Fmoc group and coupling of the amino acids were performed using the conditions described in the above general method. The cleavage provided **BP404** in 82% HPLC purity.

HPLC (λ = 220 nm): t_R = 5.78 min. ESI-MS (*m/z*): 353.7 $[M+2H]^{2+}$, 706.4 $[M+H]^+$, 728.4 $[M+Na]^+$. HRMS (*m/z*): calculated for $C_{37}H_{58}N_9O_5$ $[M+3H]^{3+}$ 236.1515, found 236.1506; calculated for $C_{37}H_{57}N_9O_5$ $[M+2H]^{2+}$ 353.7236, found 353.7226; calculated for $C_{37}H_{56}N_9O_5$ $[M+H]^+$ 706.4399, found 706.4388.

Phe-Trp-Val-Lys-Phe-Lys-NH_2 (BP405)

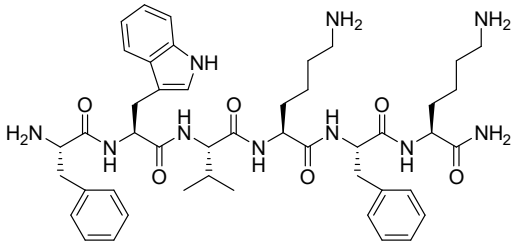

A Fmoc-Rink-MBHA resin (50 mg, 0.55 mmol/g) was swollen with CH_2Cl_2 (1 x 20 min) and with DMF (1 x 20 min). Removal of the Fmoc group and coupling of the amino acids were performed using the conditions described in the above general method. The cleavage provided **BP405** in 85% HPLC purity.

HPLC (λ = 220 nm): t_R = 6.11 min. ESI-MS (*m/z*): 427.2 $[M+2H]^{2+}$; 853.5 $[M+H]^+$, 875.4 $[M+Na]^+$. HRMS (*m/z*): calculated for $C_{46}H_{67}N_{10}O_6$ $[M+3H]^{3+}$ 285.1743, found 285.1737; calculated for $C_{46}H_{66}N_{10}O_6$ $[M+2H]^{2+}$ 427.2578, found 427.2569; calculated for $C_{46}H_{65}N_{10}O_6$ $[M+H]^+$ 853.5083, found 853.5065.

Val-Phe-Trp-Val-Lys-Phe-Lys-NH_2 (BP406)

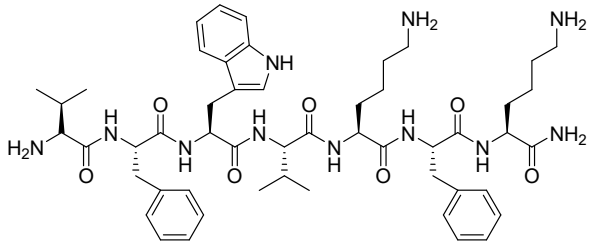

A Fmoc-Rink-MBHA resin (50 mg, 0.55 mmol/g) was swollen with CH_2Cl_2 (1 x 20 min) and with DMF (1 x 20 min). Removal of the Fmoc group and coupling of the amino acids were performed using the conditions described in the above general method. The cleavage provided **BP406** in 76% HPLC purity.

HPLC (λ = 220 nm): t_R = 6.21 min. ESI-MS (*m/z*): 476.7 $[M+2H]^{2+}$, 952.5 $[M+H]^+$, 974.5 $[M+Na]^+$. HRMS (*m/z*): calculated for $C_{51}H_{76}N_{11}O_7$ $[M+3H]^{3+}$ 318.1971, found 318.1966; calculated for $C_{51}H_{75}N_{11}O_7$ $[M+2H]^{2+}$ 476.7920, found 476.7908; calculated for $C_{51}H_{74}N_{11}O_7$ $[M+H]^+$ 952.5767, found 952.5796.

Val-Val-Phe-Trp-Val-Lys-Phe-Lys-NH_2 (BP407)

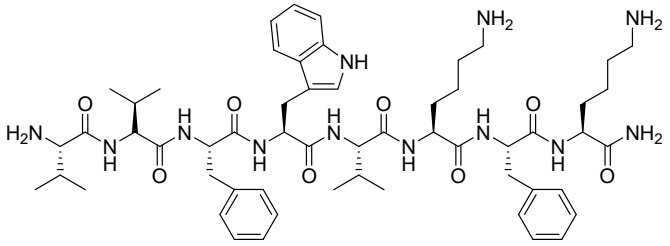

A Fmoc-Rink-MBHA resin (50 mg, 0.55 mmol/g) was swollen with CH_2Cl_2 (1 x 20 min) and with DMF (1 x 20 min). Removal of the Fmoc group and coupling of the amino acids were performed using the conditions described in the above general method. The cleavage provided **BP407** in 82% HPLC purity.

HPLC (λ = 220 nm): t_R = 6.33 min. ESI-MS (*m/z*): 526.3 $[M+2H]^{2+}$, 1051.6 $[M+H]^+$, 1073.6 $[M+Na]^+$. HRMS (*m/z*): calculated for $C_{56}H_{85}N_{12}O_8$ $[M+3H]^{3+}$ 351.2199, found 351.2210; calculated for $C_{56}H_{84}N_{12}O_8$ $[M+2H]^{2+}$ 526.3262, found 526.3263; calculated for $C_{56}H_{83}N_{12}O_8$ $[M+H]^+$ 1051.6451, found 1051.6436.

Lys-Val-Val-Phe-Trp-Val-Lys-Phe-Lys-NH_2 (BP408)

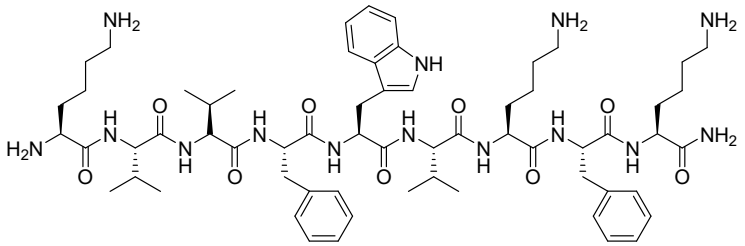

A Fmoc-Rink-MBHA resin (50 mg, 0.55 mmol/g) was swollen with CH_2Cl_2 (1 x 20 min) and with DMF (1 x 20 min). Removal of the Fmoc group and coupling of the amino acids were performed using the conditions described in the above general method. The cleavage provided **BP408** in 67% HPLC purity.

HPLC (λ = 220 nm): t_R = 6.19 min. ESI-MS (*m/z*): 590.8 $[M+2H]^{2+}$, 1179.7 $[M+H]^+$, 1201.7 $[M+Na]^+$. HRMS (*m/z*): calculated for $C_{62}H_{97}N_{14}O_9$ $[M+3H]^{3+}$ 393.9182, found 393.9165; calculated for $C_{62}H_{96}N_{14}O_9$ $[M+2H]^{2+}$ 590.3737, found 590.3710; calculated for $C_{62}H_{95}N_{14}O_9$ $[M+H]^+$ 1179.7401, found 1179.7355.

Lys-Lys-Val-Val-Phe-Trp-Val-Lys-Phe-D-Lys-NH_2 (BP442)

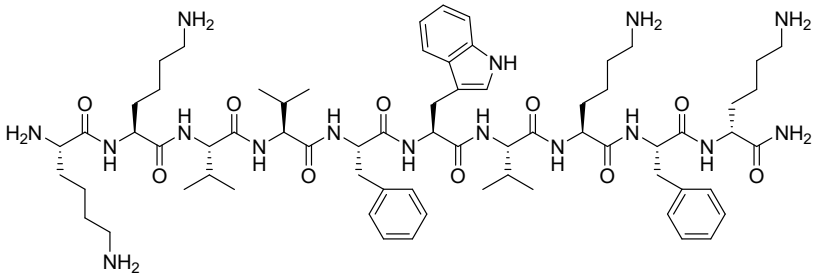

A Fmoc-Rink-MBHA (200 mg, 0.55 mmol/g) was swollen in CH_2Cl_2 (1 x 20 min) and DMF (1 x 20 min). Following the strategy described in the above general method, this peptide was synthesized incorporating a D-amino acid at position 10. The cleavage provided **BP442** in 88% HPLC purity. Elution with H_2O/CH_3CN (88:12) yielded **BP442** in >99% HPLC purity.

HPLC (λ = 220 nm): t_R = 6.07 min. ESI-MS (*m/z*): 654.5 $[M+2H]^{2+}$, 665.5 $[M+H+Na]^{2+}$, 1308.0 $[M+H]^+$, 1330.0 $[M+Na]^+$. HRMS (*m/z*): calculated for $C_{68}H_{109}N_{16}O_{10}$ $[M+3H]^{3+}$ 436.6165, found 436.6179; calculated for $C_{68}H_{108}N_{16}O_{10}$ $[M+2H]^{2+}$ 654.4212, found 654.4211; calculated for $C_{68}H_{107}N_{16}O_{10}$ $[M+H]^+$ 1307.8351, found 1307.8342.

Lys-Lys-Val-Val-Phe-Trp-Val-Lys-D-Phe-Lys-NH_2 (BP443)

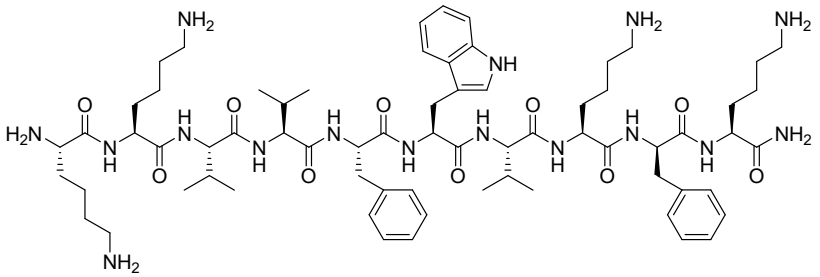

A Fmoc-Rink-MBHA (200 mg, 0.55 mmol/g) was swollen in CH_2Cl_2 (1 x 20 min) and DMF (1 x 20 min). Following the strategy described in the above general method, this peptide was synthesized incorporating a D-amino acid at position 9. The cleavage provided **BP443** in 90% HPLC purity. Elution with H_2O/CH_3CN (88:12) yielded **BP443** in >99% HPLC purity.

HPLC (λ = 220 nm): t_R = 6.02 min. ESI-MS (*m/z*): 1308.0 $[M+H]^+$, 1330.0 $[M+Na]^+$. HRMS (*m/z*): calculated for $C_{68}H_{109}N_{16}O_{10}$ $[M+3H]^{3+}$ 436.6165, found 436.6179; calculated for $C_{68}H_{108}N_{16}O_{10}$ $[M+2H]^{2+}$ 654.4212, found 654.4213; calculated for $C_{68}H_{107}N_{16}O_{10}$ $[M+H]^+$ 1307.8351, found 1307.8338.

Lys-Lys-Val-Val-Phe-Trp-Val-D-Lys-Phe-Lys-NH_2 (BP444)

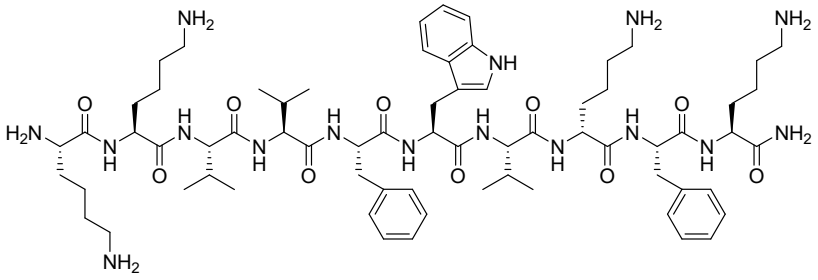

A Fmoc-Rink-MBHA (200 mg, 0.55 mmol/g) was swollen in CH_2Cl_2 (1 x 20 min) and DMF (1 x 20 min). Following the strategy described in the above general method, this peptide was synthesized incorporating a D-amino acid at position 8. The cleavage provided **BP444** in 49% HPLC purity. Elution with H_2O/CH_3CN (88:12) yielded **BP444** in >99% HPLC purity.

HPLC (λ = 220 nm): t_R = 5.98 min. ESI-MS (*m/z*): 655.0 $[M+2H]^{2+}$, 666.0 $[M+H+Na]^{2+}$, 673.5 $[M+H+K]^{2+}$, 1308.0 $[M+H]^+$, 1330.0 $[M+Na]^+$, 1345.9 $[M+K]^+$. HRMS (*m/z*): calculated for $C_{68}H_{109}N_{16}O_{10}$ $[M+3H]^{3+}$ 436.6165, found 436.6176; calculated for $C_{68}H_{108}N_{16}O_{10}$ $[M+2H]^{2+}$ 654.4212, found 654.4213; calculated for $C_{68}H_{107}N_{16}O_{10}$ $[M+H]^+$ 1307.8351, found 1307.8340.

Lys-Lys-Val-Val-Phe-Trp-D-Val-Lys-Phe-Lys-NH_2 (BP445)

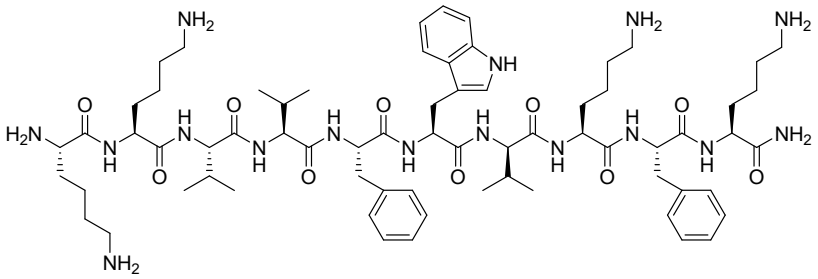

A Fmoc-Rink-MBHA (200 mg, 0.55 mmol/g) was swollen in CH_2Cl_2 (1 x 20 min) and DMF (1 x 20 min). Following the strategy described in the above general method, this peptide was synthesized incorporating a D-amino acid at position 7. The cleavage provided **BP445** in 67% HPLC purity. Elution with H_2O/CH_3CN (88:12) yielded **BP445** in >99% HPLC purity.

HPLC (λ = 220 nm): t_R = 6.09 min. ESI-MS (*m/z*): 437.2 $[M+3H]^{3+}$, 654.5 $[M+2H]^{2+}$, 1308.1 $[M+H]^+$, 1330.0 $[M+Na]^+$. HRMS (*m/z*): calculated for $C_{68}H_{109}N_{16}O_{10}$ $[M+3H]^{3+}$ 436.6165, found 436.6169; calculated for $[M+2H]^{2+}$ $C_{68}H_{108}N_{16}O_{10}$ 654.4212, found 654.4205; calculated for $C_{68}H_{107}N_{16}O_{10}$ $[M+H]^+$ 1307.8351, found 1307.8356.

Lys-Lys-Val-Val-Phe-D-Trp-Val-Lys-Phe-Lys-NH_2 (BP446)

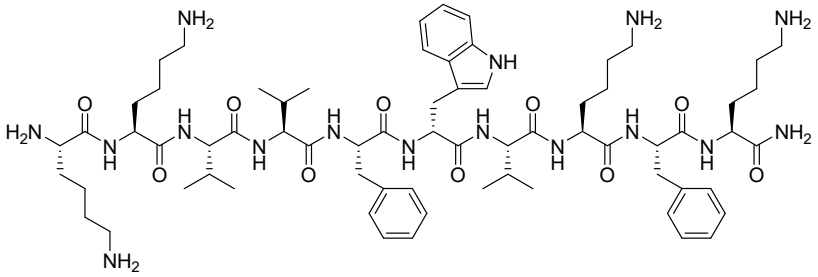

A Fmoc-Rink-MBHA (200 mg, 0.55 mmol/g) was swollen in CH_2Cl_2 (1 x 20 min) and DMF (1 x 20 min). Following the strategy described in the above general method, this peptide was synthesized incorporating a D-amino acid at position 6. The cleavage provided **BP446** in 91% HPLC purity. Elution with H_2O/CH_3CN (89:11) yielded **BP446** in >99% HPLC purity.

HPLC (λ = 220 nm): t_R = 6.26 min. ESI-MS (*m/z*): 654.5 $[M+2H]^{2+}$, 1308.0 $[M+H]^+$, 1330.0 $[M+Na]^+$. HRMS (*m/z*): calculated for $C_{68}H_{109}N_{16}O_{10}$ $[M+3H]^{3+}$ 436.6165, found 436.6159; calculated for $C_{68}H_{108}N_{16}O_{10}$ $[M+2H]^{2+}$ 654.4212, found 654.4195; calculated for $C_{68}H_{107}N_{16}O_{10}$ $[M+H]^+$ 1307.8351, found 1307.8337.

Lys-Lys-Val-Val-D-Phe-Trp-Val-Lys-Phe-Lys-NH_2 (BP447)

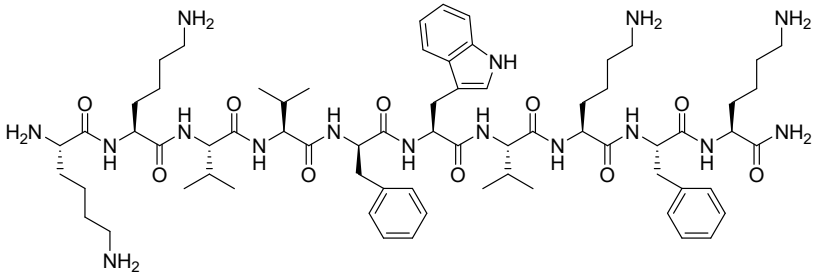

A Fmoc-Rink-MBHA (200 mg, 0.55 mmol/g) was swollen in CH_2Cl_2 (1 x 20 min) and DMF (1 x 20 min). Following the strategy described in the above general method, this peptide was synthesized incorporating a D-amino acid at position 5. The cleavage provided **BP447** in 93% HPLC purity. Elution with H_2O/CH_3CN (88:12) yielded **BP447** in >99% HPLC purity.

HPLC (λ = 220 nm): t_R = 6.25 min. ESI-MS (*m/z*): 654.5 $[M+2H]^{2+}$, 665.4 $[M+H+Na]^{2+}$, 1308.0 $[M+H]^+$, 1330.0 $[M+Na]^+$. HRMS (*m/z*): calculated for $C_{68}H_{109}N_{16}O_{10}$ $[M+3H]^{3+}$ 436.6165, found 436.6155; calculated for $C_{68}H_{108}N_{16}O_{10}$ $[M+2H]^{2+}$ 654.4212, found 654.4193; calculated for $C_{68}H_{107}N_{16}O_{10}$ $[M+H]^+$ 1307.8351, found 1307.8332.

Lys-Lys-Val-D-Val-Phe-Trp-Val-Lys-Phe-Lys-NH_2 (BP448)

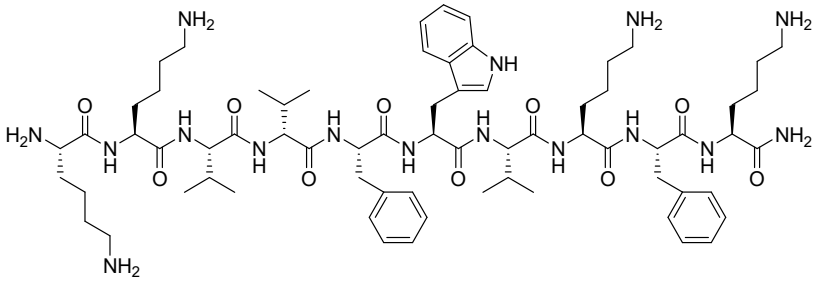

A Fmoc-Rink-MBHA (200 mg, 0.55 mmol/g) was swollen in CH_2Cl_2 (1 x 20 min) and DMF (1 x 20 min). Following the strategy described in the above general method, this peptide was synthesized incorporating a D-amino acid at position 4. The cleavage provided **BP448** in 91% HPLC purity. Elution with H_2O/CH_3CN (87:13) yielded **BP448** in >99% HPLC purity.

HPLC (λ = 220 nm): t_R = 6.27 min. ESI-MS (*m/z*): 654.5 $[M+2H]^{2+}$, 1308.0 $[M+H]^+$, 1330.0 $[M+Na]^+$. HRMS (*m/z*): calculated for $C_{68}H_{109}N_{16}O_{10}$ $[M+3H]^{3+}$ 436.6165, found 436.6155; calculated for $C_{68}H_{108}N_{16}O_{10}$ $[M+2H]^{2+}$ 654.4212, found 654.4193; calculated for $C_{68}H_{107}N_{16}O_{10}$ $[M+H]^+$ 1307.8351, found 1307.8333.

Lys-Lys-D-Val-Val-Phe-Trp-Val-Lys-Phe-Lys-NH_2 (BP449)

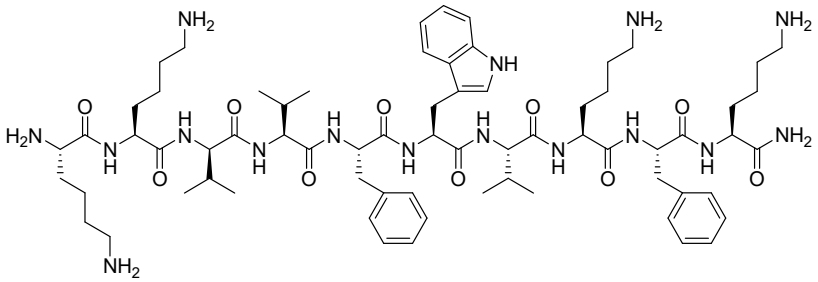

A Fmoc-Rink-MBHA (200 mg, 0.55 mmol/g) was swollen in CH_2Cl_2 (1 x 20 min) and DMF (1 x 20 min). Following the strategy described in the above general method, this peptide was synthesized incorporating a D-amino acid at position 3. The cleavage provided **BP449** in 71% HPLC purity. Elution with H_2O/CH_3CN (88:12) yielded **BP449** in >99% HPLC purity.

HPLC (λ = 220 nm): t_R = 6.18 min. ESI-MS (*m/z*): 1308.0 $[M+H]^+$, 1330.0 $[M+Na]^+$, 654.5 $[M+2H]^{2+}$, 665.5 $[M+H+Na]^{2+}$. HRMS (*m/z*): calculated for $C_{68}H_{109}N_{16}O_{10}$ $[M+3H]^{3+}$ 436.6165, found 436.6157; calculated for $C_{68}H_{108}N_{16}O_{10}$ $[M+2H]^{2+}$ 654.4212, found 654.4196; calculated for $C_{68}H_{107}N_{16}O_{10}$ $[M+H]^+$ 1307.8351, found 1307.8327;

Lys-D-Lys-Val-Val-Phe-Trp-Val-Lys-Phe-Lys-NH_2 (BP450)

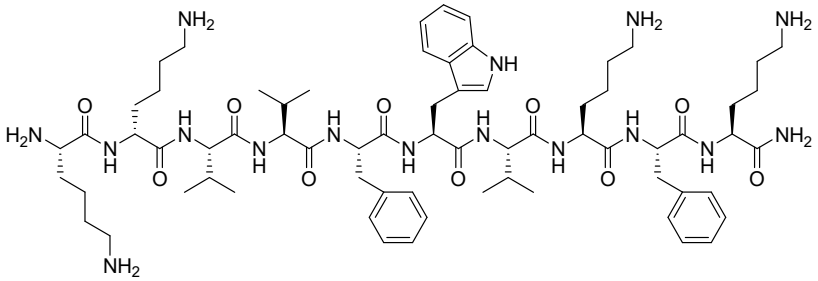

A Fmoc-Rink-MBHA (200 mg, 0.55 mmol/g) was swollen in CH_2Cl_2 (1 x 20 min) and DMF (1 x 20 min). Following the strategy described in the above general method, this peptide was synthesized incorporating a D-amino acid at position 2. The cleavage provided **BP450** in 61% HPLC purity. Elution with H_2O/CH_3CN (89:11) yielded **BP450** in >99% HPLC purity.

HPLC (λ = 220 nm): t_R = 6.11 min. ESI-MS (*m/z*): 655.0 $[M+2H]^{2+}$, 1308.0 $[M+H]^+$, 1330.0 $[M+Na]^+$. HRMS (*m/z*): calculated for $C_{68}H_{109}N_{16}O_{10}$ $[M+3H]^{3+}$ 436.6165, found 436.6169; calculated for $C_{68}H_{108}N_{16}O_{10}$ $[M+2H]^{2+}$ 654.4212, found 654.4201; calculated for $C_{68}H_{107}N_{16}O_{10}$ $[M+H]^+$ 1307.8351, found 1307.8326.

D-Lys-Lys-Val-Val-Phe-Trp-Val-Lys-Phe-Lys-NH_2 (BP451)

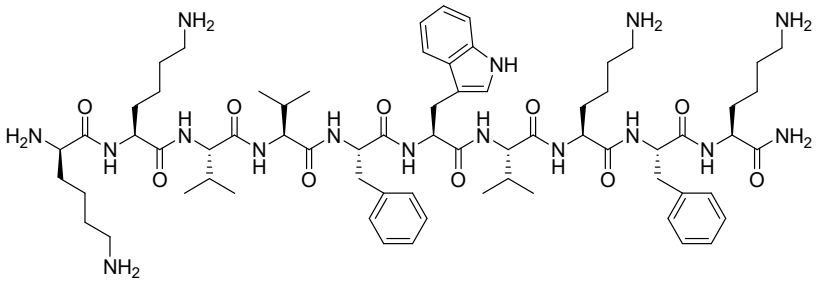

A Fmoc-Rink-MBHA (200 mg, 0.55 mmol/g) was swollen in CH_2Cl_2 (1 x 20 min) and DMF (1 x 20 min). Following the strategy described in the above general method, this peptide was synthesized incorporating a D-amino acid at position 1. The cleavage provided **BP451** in 68% HPLC purity. Elution with H_2O/CH_3CN (88:12) yielded **BP451** in >99% HPLC purity.

HPLC (λ = 220 nm): t_R = 6.13 min. ESI-MS (*m/z*): 654.5 $[M+2H]^{2+}$, 1308.0 $[M+H]^+$, 1330.0 $[M+Na]^+$. HRMS (*m/z*): calculated for $C_{68}H_{109}N_{16}O_{10}$ $[M+3H]^{3+}$ 436.6165, found 436.6167; calculated for $C_{68}H_{108}N_{16}O_{10}$ $[M+2H]^{2+}$ 654.4212, found 654.4200; calculated for $C_{68}H_{107}N_{16}O_{10}$ $[M+H]^+$ 1307.8351, found 1307.8334.

5.1. Solid-phase synthesis of lipopeptides derived from KSLW

5.3.1. Synthesis of lipopeptides derived from KSLW acylated at the N-terminus

Fmoc-Rink-MBHA resin (50 mg, 0.55 mmol/g) was swollen with CH_2Cl_2 (1 x 20 min) and DMF (1 x 20 min). Fmoc group removal and coupling of the amino acids were performed following the conditions described in section 1. After removal of the N-terminal Fmoc group, the peptidyl resin was acylated with the corresponding fatty acid (10 equiv) in presence of DIPCDI (10 equiv) and Oxyma (10 equiv) in NMP for 1 h under stirring. Washings were performed with NMP (6 x 1 min) and CH_2Cl_2 (2 x 1 min). The completion of the reactions was monitored by the Kaiser test (Kaiser 1970). At the end of the synthesis the resulting peptide was cleaved from the resin, purified, analysed and characterized following the procedure described in section 1.

C_5H_{11}CO-Lys-Lys-Val-Val-Phe-Trp-Val-Lys-Phe-Lys-NH_2 (BP409)

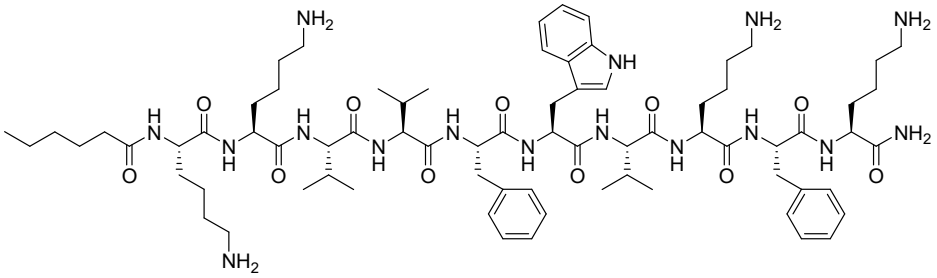

This lipopeptide was synthesized following the procedure described above using hexanoic acid. The cleavage provided **BP409** in 71% HPLC purity. Elution with H_2O/CH_3CN (82:18) yielded **BP409** in >99% HPLC purity.

HPLC (λ = 220 nm): t_R = 6.53 min. ESI-MS (*m/z*): 1405.9 $[M+H]^+$, 1427.9 $[M+Na]^+$. HRMS (*m/z*): calculated for $C_{74}H_{119}N_{16}O_{11}$ $[M+3H]^{3+}$ 469.3076, found 469.3072; calculated for $C_{74}H_{118}N_{16}O_{11}$ $[M+2H]^{2+}$ 703.4578, found 703.4552.

C_3H_7CO-Lys-Lys-Val-Val-Phe-Trp-Val-Lys-Phe-Lys-NH_2 (BP410)

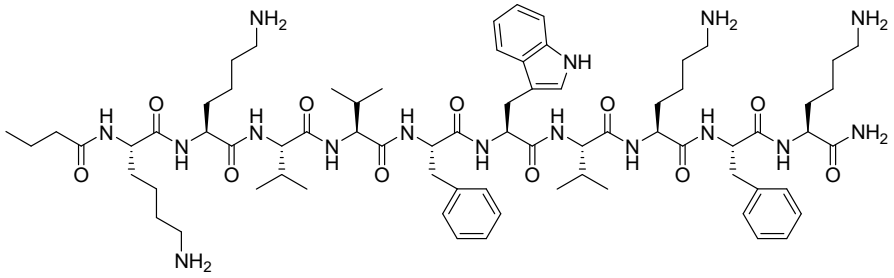

This lipopeptide was synthesized following the procedure described above using butyric acid. The cleavage provided **BP410** in 59% HPLC purity. Elution with H_2O/CH_3CN (85:15) yielded **BP410** in >99% HPLC purity.

HPLC (λ = 220 nm): t_R = 6.30 min. ESI-MS (*m/z*): 689.4 $[M+2H]^{2+}$; 1377.9 $[M+H]^+$, 1399.8 $[M+Na]^+$. HRMS (*m/z*): calculated for $C_{72}H_{115}N_{16}O_{11}$ $[M+3H]^{3+}$ 459.9638, found 459.9627; calculated for $C_{72}H_{114}N_{16}O_{11}$ $[M+2H]^{2+}$ 689.4421, found 689.4398.

$C_{11}H_{23}CO$-Lys-Lys-Val-Val-Phe-Trp-Val-Lys-Phe-Lys-NH_2 (BP411)

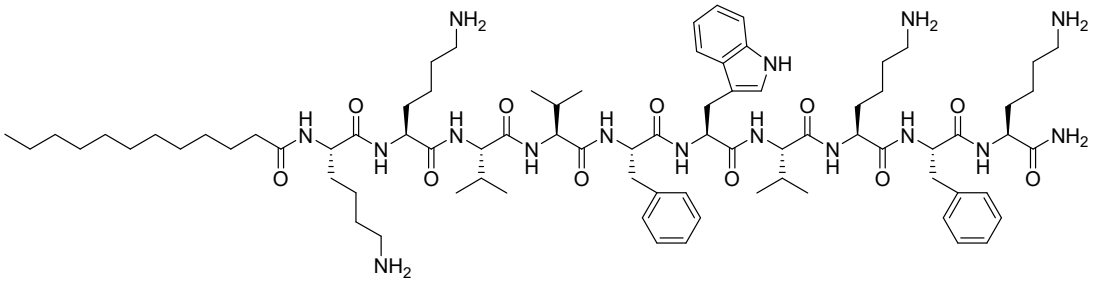

This lipopeptide was synthesized following the procedure described above using lauric acid. The cleavage provided **BP411** in 71% HPLC purity. Elution with H_2O/CH_3CN (83:17) yielded **BP411** in >99% HPLC purity.

HPLC (λ = 220 nm): t_R = 7.36 min. ESI-MS (*m/z*): 497.3 $[M+3H]^{3+}$, 745.5 $[M+2H]^{2+}$, 1490.0 $[M+H]^+$, 1513.0 $[M+Na]^+$. HRMS (*m/z*): calculated for $C_{80}H_{131}N_{16}O_{11}$ $[M+3H]^{3+}$ 497.3389, found 497.3374; calculated for $C_{80}H_{130}N_{16}O_{11}$ $[M+2H]^{2+}$ 745.5047, found 745.5023.

5.3.2. Synthesis of lipopeptides derived from KSLW containing an acyl group at the side-chain of a lysine residue

5.3.2.1. Synthesis of the peptidyl resins 1-10

A Fmoc-Rink-MBHA resin (50 mg, 0.55 mmol/g) was swollen with CH_2Cl_2 (1 x 20 min) and DMF (1 x 20 min). Fmoc group removal and coupling of the amino acids were performed following the conditions described in section 1. After removal of the N-terminal Fmoc group, the peptidyl resin was acetylated with Ac_2O/pyridine/CH_2Cl_2 (1:1:10) (2 x 30 min) followed by washings with NMP (6 x 1 min) and CH_2Cl_2 (2 x 1 min). The completion of the reaction was monitored by the Kaiser test (Kaiser 1970). An aliquot of the peptidyl resin was treated with TFA/phenol/H_2O/TIS (92.5:2.5:2.5:2.5) for 2 h. After evaporation of the acidic solution and washes with cold diethyl ether, the crude peptide was analysed by HPLC and characterized by ESI-MS.

CH_3CO-Lys(Boc)-Lys(Boc)-Val-Val-Phe-Trp(Boc)-Val-Lys(Boc)-Phe-Lys(ivDde)-Rink-MBHA (1)

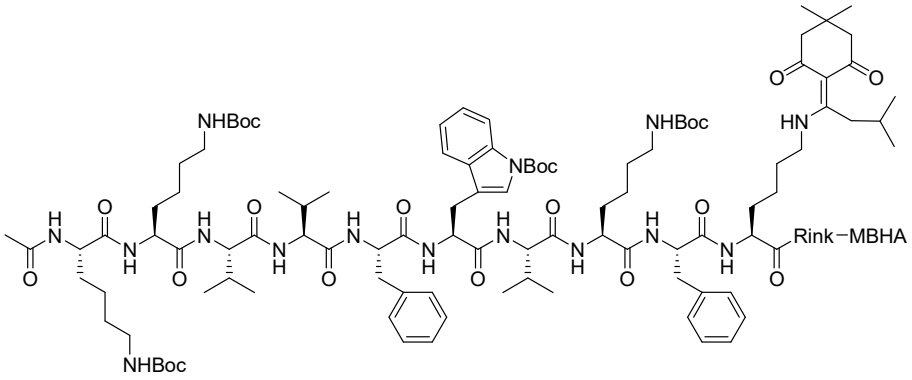

The peptidyl resin **1** was synthesized following the procedure described above incorporating Fmoc-Lys(ivDde)-OH at position 10. After cleavage of an aliquot of the peptidyl resin, the corresponding peptide was obtained in 79% HPLC purity.

HPLC (λ = 220 nm): t_R = 6.97 min. ESI-MS (*m/z*): 778.9 $[M+2H]^{2+}$,1555.9 $[M+H]^+$, 1577.9 $[M+Na]^+$.

CH_3CO-Lys(Boc)-Lys(Boc)-Val-Val-Phe-Trp(Boc)-Val-Lys(Boc)-Lys(ivDde)-Lys(Boc)-Rink-MBHA (2)

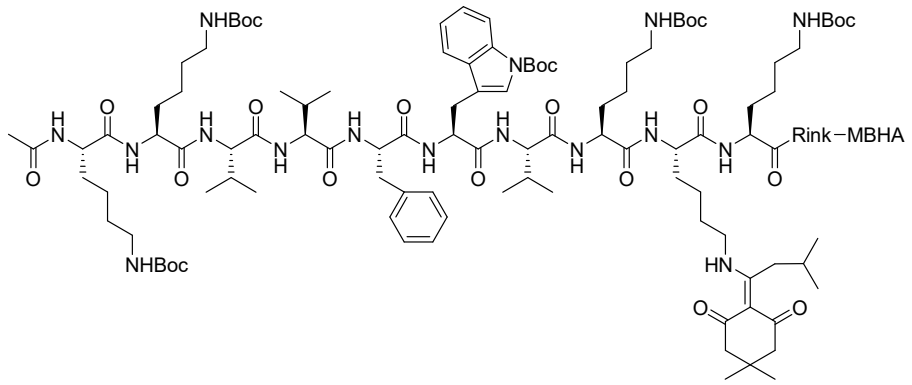

The peptidyl resin **2** was synthesized following the procedure described above incorporating Fmoc-Lys(ivDde)-OH at position 9. After cleavage of an aliquot of the peptidyl resin, the corresponding peptide was obtained in 70% HPLC purity.

HPLC (λ = 220 nm): t_R = 6.46 min. ESI-MS (*m/z*): 513.2 $[M+3H]^{3+}$, 769.4 $[M+2H]^{2+}$, 1537.0 $[M+H]^+$, 1559.9 $[M+Na]^+$.

CH_3CO-Lys(Boc)-Lys(Boc)-Val-Val-Phe-Trp(Boc)-Val-Lys(ivDde)-Phe-Lys(Boc)-Rink-MBHA (3)

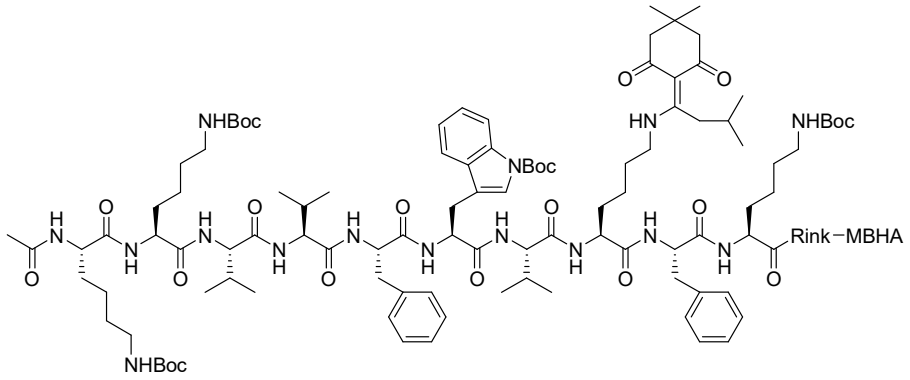

The peptidyl resin **3** was synthesized following the procedure described above incorporating Fmoc-Lys(ivDde)-OH at position 8. After cleavage of an aliquot of the peptidyl resin, the corresponding peptide was obtained in 79% HPLC purity.

HPLC (λ = 220 nm): t_R = 6.94 min. ESI-MS (*m/z*): 519.3 $[M+3H]^{3+}$, 778.9 $[M+2H]^{2+}$, 1555.9 $[M+H]^{+}$, 1577.9 $[M+Na]^{+}$.

CH_3CO-Lys(Boc)-Lys(Boc)-Val-Val-Phe-Trp(Boc)-Lys(ivDde)-Lys(Boc)-Phe-Lys(Boc)-Rink-MBHA (4)

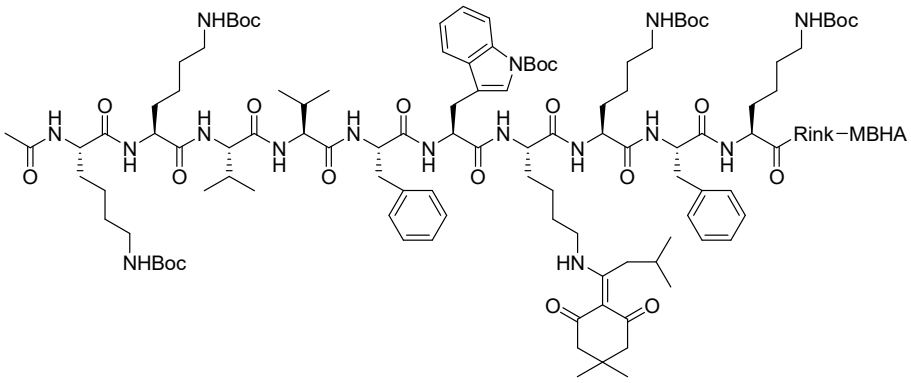

The peptidyl resin **4** was synthesized following the procedure described above incorporating Fmoc-Lys(ivDde)-OH at position 7. After cleavage of an aliquot of the peptidyl resin, the corresponding peptide was obtained in 72% HPLC purity.

HPLC (λ = 220 nm): t_R = 6.58 min. ESI-MS (*m/z*): 528.9 $[M+3H]^{3+}$, 792.9 $[M+2H]^{2+}$, 1585.0 $[M+H]^{+}$, 1607.9 $[M+Na]^{+}$.

CH_3CO-Lys(Boc)-Lys(Boc)-Val-Val-Phe-Lys(ivDde)-Val-Lys(Boc)-Phe-Lys(Boc)-Rink-MBHA (5)

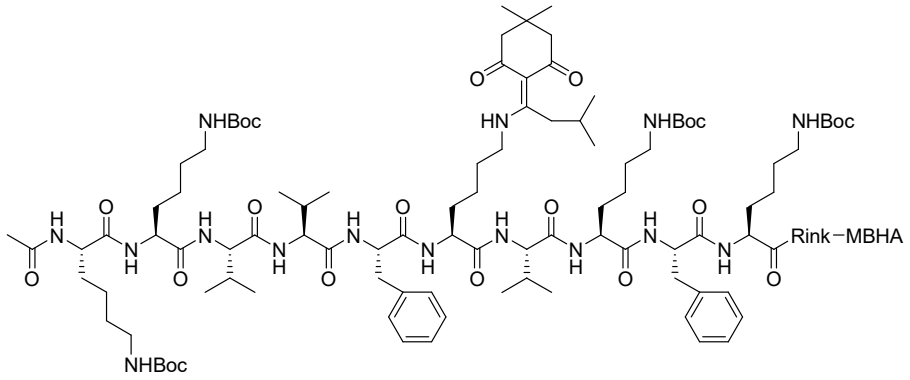

The peptidyl resin **5** was synthesized following the procedure described above incorporating Fmoc-Lys(ivDde)-OH at position 6. After cleavage of an aliquot of the peptidyl resin, the corresponding peptide was obtained in 52% HPLC purity.

HPLC (λ = 220 nm): t_R = 6.45 min. ESI-MS (*m/z*): 749.5 $[M+2H]^{2+}$, 1498.0 $[M+H]^+$, 1520.0 $[M+Na]^+$.

CH_3CO-Lys(Boc)-Lys(Boc)-Val-Val-Lys(ivDde)-Trp(Boc)-Val-Lys(Boc)-Phe-Lys(Boc)-Rink-MBHA (6)

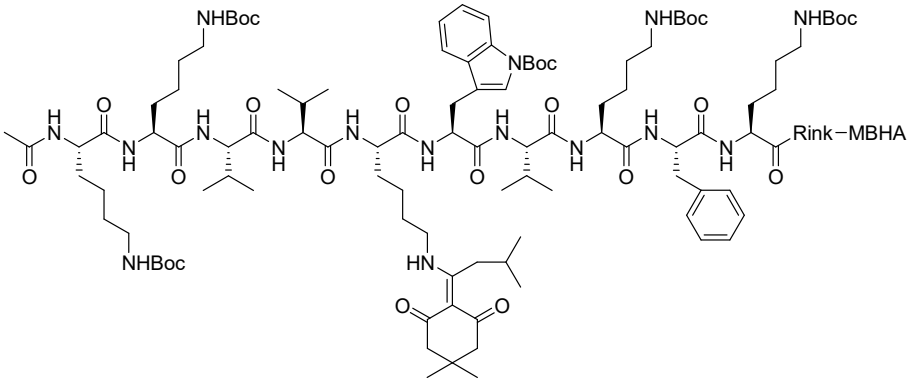

The peptidyl resin **6** was synthesized following the procedure described above incorporating Fmoc-Lys(ivDde)-OH at position 5. After cleavage of an aliquot of the peptidyl resin, the corresponding peptide was obtained in 73% HPLC purity.

HPLC (λ = 220 nm): t_R = 6.47 min. ESI-MS (*m/z*): 769.5 $[M+2H]^{2+}$, 1537.0 $[M+H]^+$, 1559.0 $[M+Na]^+$.

CH_3CO-Lys(Boc)-Lys(Boc)-Val-Lys(ivDde)-Phe-Trp(Boc)-Val-Lys(Boc)-Phe-Lys(Boc)-Rink-MBHA (7)

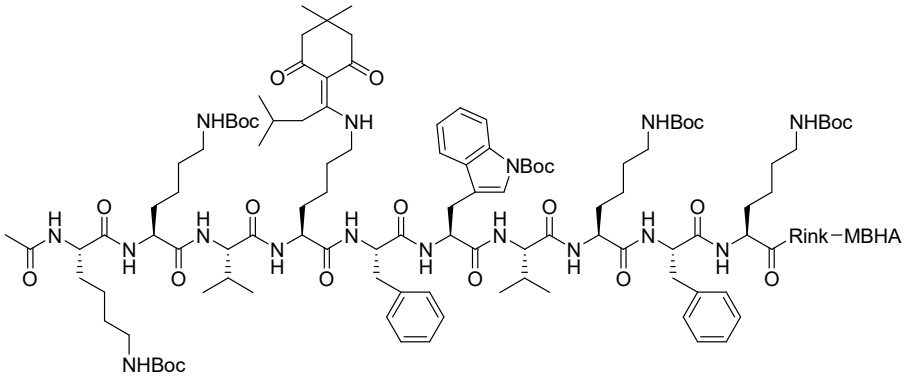

The peptidyl resin **7** was synthesized following the procedure described above incorporating Fmoc-Lys(ivDde)-OH at position 4. After cleavage of an aliquot of the peptidyl resin, the corresponding peptide was obtained in 83% HPLC purity.

HPLC (λ = 220 nm): t_R = 6.61 min. ESI-MS (*m/z*): 529.0 $[M+3H]^{3+}$, 793.0 $[M+2H]^{2+}$, 1585.0 $[M+H]^{+}$, 1607.0 $[M+Na]^{+}$.

CH_3CO-Lys(Boc)-Lys(Boc)-Lys(ivDde)-Val-Phe-Trp(Boc)-Val-Lys(Boc)-Phe-Lys(Boc)-Rink-MBHA (8)

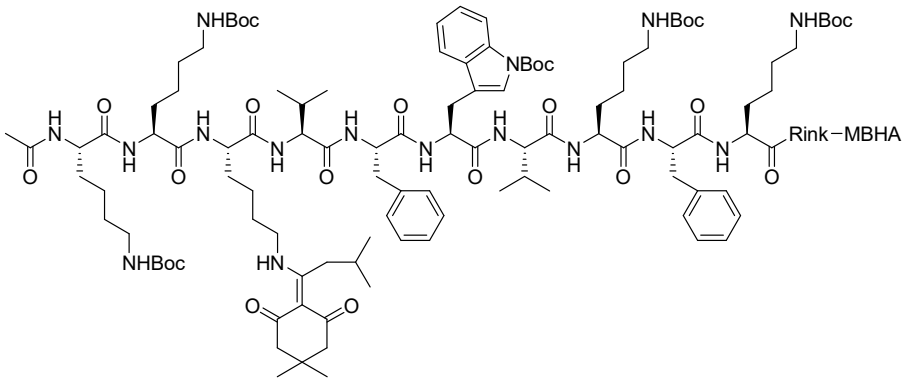

The peptidyl resin **8** was synthesized following the procedure described above incorporating Fmoc-Lys(ivDde)-OH at position 3. After cleavage of an aliquot of the peptidyl resin, the corresponding peptide was obtained in 83% HPLC purity.

HPLC (λ = 220 nm): t_R = 6.59 min. ESI-MS (*m/z*): 529.2 $[M+3H]^{3+}$, 793.0 $[M+2H]^{2+}$, 1585.0 $[M+H]^{+}$, 1607.0 $[M+Na]^{+}$.

CH_3CO-Lys(Boc)-Lys(ivDde)-Val-Val-Phe-Trp(Boc)-Val-Lys(Boc)-Phe-Lys(Boc)-Rink-MBHA (9)

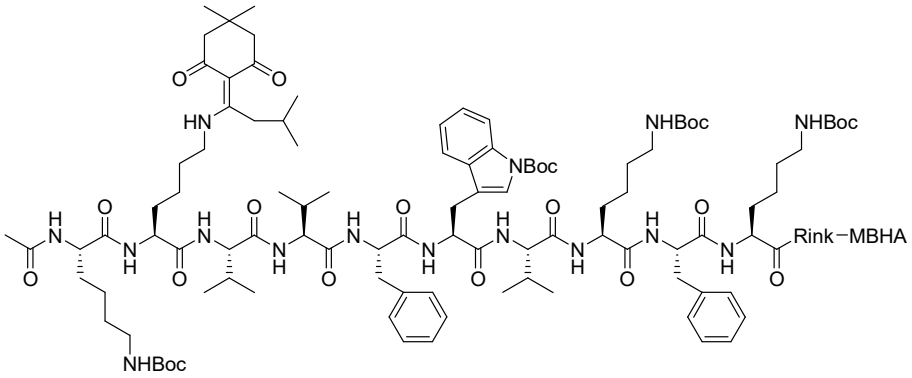

The peptidyl resin **9** was synthesized following the procedure described above incorporating Fmoc-Lys(ivDde)-OH at position 2. After cleavage of an aliquot of the peptidyl resin, the corresponding peptide was obtained in 73% HPLC purity.

HPLC (λ = 220 nm): t_R = 6.98 min. ESI-MS (*m/z*): 519.6 $[M+3H]^{3+}$, 778.5 $[M+2H]^{2+}$, 1556.0 $[M+H]^{+}$, 1578.0 $[M+Na]^{+}$.

CH_3CO-Lys(ivDde)-Lys(Boc)-Val-Val-Phe-Trp(Boc)-Val-Lys(Boc)-Phe-Lys(Boc)-Rink-MBHA (10)

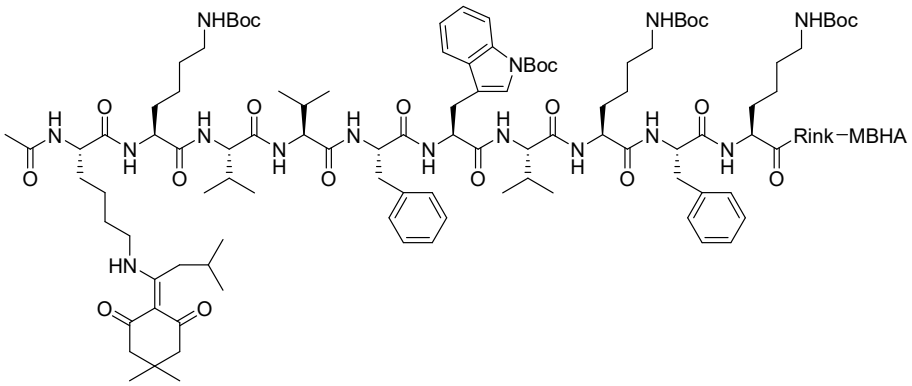

The peptidyl resin **10** was synthesized following the procedure described above incorporating Fmoc-Lys(ivDde)-OH at position 1. After cleavage of an aliquot of the peptidyl resin, the corresponding peptide was obtained in 73% HPLC purity.

HPLC (λ = 220 nm): t_R = 6.94 min. ESI-MS (*m/z*): 519.3 $[M+3H]^{3+}$, 778.5 $[M+2H]^{2+}$, 1556.0 $[M+H]^{+}$, 1578.0 $[M+Na]^{+}$.

5.3.2.2. Synthesis of lipopeptides derived from KSLW

The corresponding peptidyl resin **1-10** was treated with $NH_2NH_2.H_2O$/NMP (5:95, 10 x 20 min) under stirring and it was washed with NMP (2 x 1 min), CH_2Cl_2 (2 x 1 min), MeOH (2 x 1 min) and NMP (2 x 1 min). Then, the resulting peptidyl resin was acylated with the corresponding fatty acid (10 equiv) in

presence of DIPCDI (10 equiv) and Oxyma (10 equiv) in NMP for 1 h under stirring. The resulting resin was washed with NMP (6 x 1 min) and CH_2Cl_2 (2 x 1 min). The completion of the reaction was monitored by the Kaiser test (Kaiser 1970). The peptidyl resin was treated with TFA/phenol/H_2O/TIS (9.5:2.5:2.5:2.5) for 2 h. After evaporation of the TFA solution, the resulting crude peptide was washed with cold diethyl ether, dissolved in H_2O and lyophilised. Then, it was purified by reverse-phase chromatography with a CombiFlash®Rf instrument, analysed by HPLC and characterized by ESI-MS and HRMS.

CH_3CO-Lys-Lys-Val-Val-Phe-Trp-Val-Lys-Phe-Lys(CO-C_5H_{11})-NH_2 (BP412)

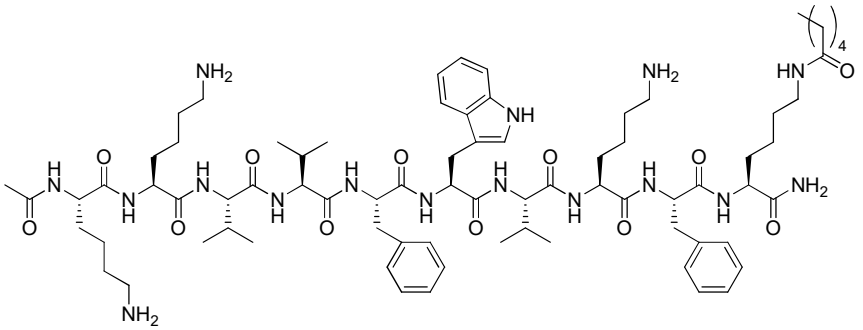

This peptide was synthesized from resin **1** following the strategy described above using hexanoic acid. The cleavage provided **BP412** in 65% HPLC purity. Elution with H_2O/CH_3CN (81:19) yielded **BP412** in >99% HPLC purity.

HPLC (λ = 220 nm): t_R = 6.74 min. ESI-MS (*m/z*): 724.4 $[M+2H]^{2+}$, 1447.9 $[M+H]^+$, 1469.9 $[M+Na]^+$. HRMS (*m/z*): calculated for $C_{76}H_{121}N_{16}O_{12}$ $[M+3H]^{3+}$ 483.3111, found 483.3109; calculated for $C_{76}H_{120}N_{16}O_{12}$ $[M+2H]^{2+}$ 724.4630, found 724.4609.

CH_3CO-Lys-Lys-Val-Val-Phe-Trp-Val-Lys-Phe-Lys(CO-C_3H_7)-NH_2 (BP413)

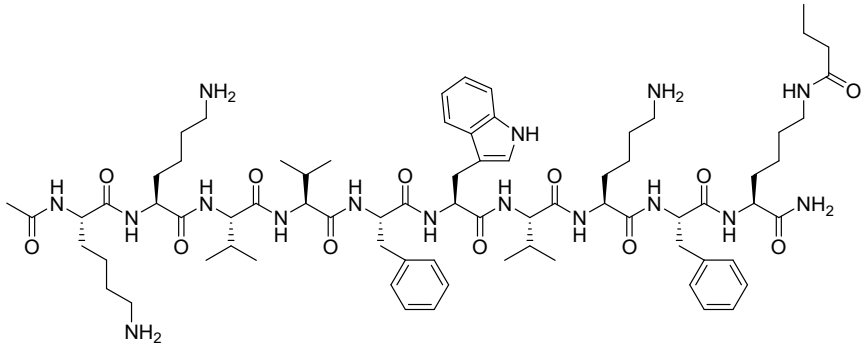

This peptide was synthesized from resin **1** following the strategy described above using butyric acid. The cleavage provided **BP413** in 64% HPLC purity. Elution with H_2O/CH_3CN (85:15) yielded **BP413** in >99% HPLC purity.

HPLC (λ = 220 nm): t_R = 6.53 min. ESI-MS (*m/z*): 710.5 $[M+2H]^{2+}$, 1420.1 $[M+H]^+$, 1442.1 $[M+Na]^+$, 1458.0 $[M+K]^+$. HRMS (*m/z*): calculated for $C_{74}H_{117}N_{16}O_{12}$ $[M+3H]^{3+}$ 473.9673, found 473.9678; calculated for

$C_{74}H_{116}N_{16}O_{12}$ $[M+2H]^{2+}$ 710.4474, found 710.4464; calculated for $C_{74}H_{115}N_{16}O_{12}$ $[M+H]^{+}$ 1419.8875, found 1419.8853.

CH_3CO-Lys-Lys-Val-Val-Phe-Trp-Val-Lys-Phe-Lys(CO-$C_{11}H_{23}$)-NH_2 (BP414)

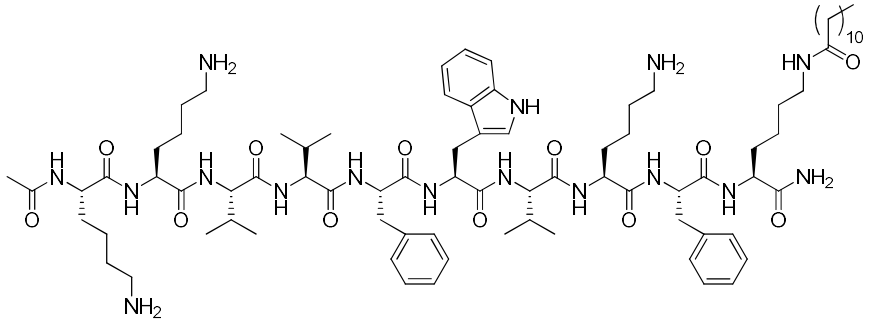

This peptide was synthesized from resin **1** following the strategy described above using lauric acid. The cleavage provided **BP414** in 68% HPLC purity. Elution with H_2O/CH_3CN (78:22) yielded **BP414** in >99% HPLC purity.

HPLC (λ = 220 nm): t_R = 7.72 min. ESI-MS (*m/z*): 1532.2 $[M+H]^{+}$, 1554.2 $[M+Na]^{+}$, 766.6 $[M+2H]^{2+}$. HRMS (*m/z*): calculated for $C_{82}H_{133}N_{16}O_{12}$ $[M+3H]^{3+}$ 511.3424, found 511.3431; calculated for $C_{82}H_{132}N_{16}O_{12}$ $[M+2H]^{2+}$ 766.5100, found 766.5086; calculated for $C_{82}H_{131}N_{16}O_{12}$ $[M+H]^{+}$ 1532.0127, found 1532.0102.

CH_3CO-Lys-Lys-Val-Val-Phe-Trp-Val-Lys-Lys(CO-C_5H_{11})-Lys-NH_2 (BP415)

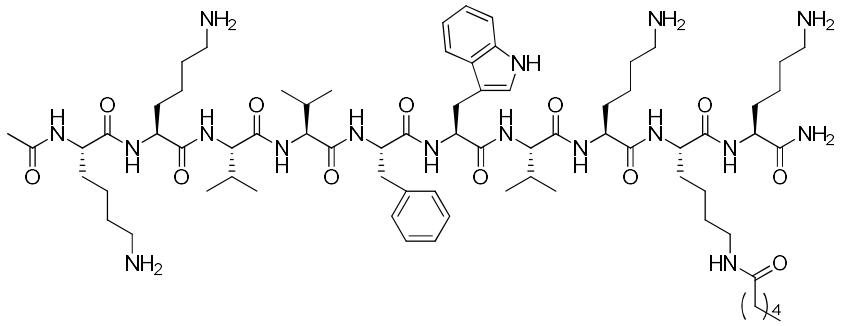

This peptide was synthesized from resin **2** following the strategy described above using hexanoic acid. The cleavage provided **BP415** in 57% HPLC purity. Elution with H_2O/CH_3CN (85:15) yielded **BP415** in >99% HPLC purity.

HPLC (λ = 220 nm): t_R = 6.34 min. ESI-MS (*m/z*): 477.1 $[M+3H]^{3+}$, 715.0 $[M+2H]^{2+}$, 726.0 $[M+H+Na]^{2+}$, 1429.1 $[M+H]^{+}$, 1451.1 $[M+Na]^{+}$. HRMS (*m/z*): calculated for $C_{73}H_{124}N_{17}O_{12}$ $[M+3H]^{3+}$ 476.9866, found 476.9874; calculated for $C_{73}H_{123}N_{17}O_{12}$ $[M+2H]^{2+}$ 714.9763, found 714.9749; calculated for $C_{73}H_{122}N_{17}O_{12}$ $[M+H]^{+}$ 1428.9453, found 1428.9423.

CH_3CO-Lys-Lys-Val-Val-Phe-Trp-Val-Lys-Lys(CO-C_3H_7)-Lys-NH_2 (BP416)

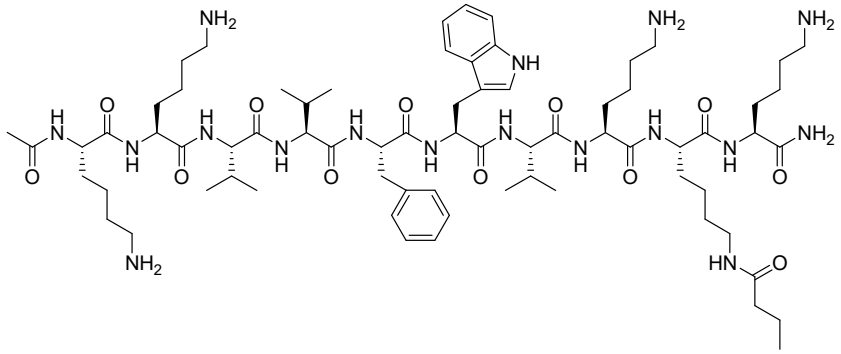

This peptide was synthesized from resin **2** following the strategy described above using butyric acid. The cleavage provided **BP416** in 50% HPLC purity. Elution with H_2O/CH_3CN (88:12) yielded **BP416** in >99% HPLC purity.

HPLC (λ = 220 nm): t_R = 6.11 min. ESI-MS (*m/z*): 701.0 $[M+2H]^{2+}$, 712.0 $[M+H+Na]^{2+}$, 1401.1 $[M+H]^+$, 1423.1 $[M+Na]^+$. HRMS (*m/z*): calculated for $C_{71}H_{120}N_{17}O_{12}$ $[M+3H]^{3+}$ 467.6429, found 467.6437; calculated for $C_{71}H_{119}N_{17}O_{12}$ $[M+2H]^{2+}$ 700.9607, found 700.9595; calculated for $C_{71}H_{118}N_{17}O_{12}$ $[M+H]^+$ 1400.9140, found 1400.9129.

CH_3CO-Lys-Lys-Val-Val-Phe-Trp-Val-Lys-Lys(CO-$C_{11}H_{23}$)-Lys-NH_2 (BP417)

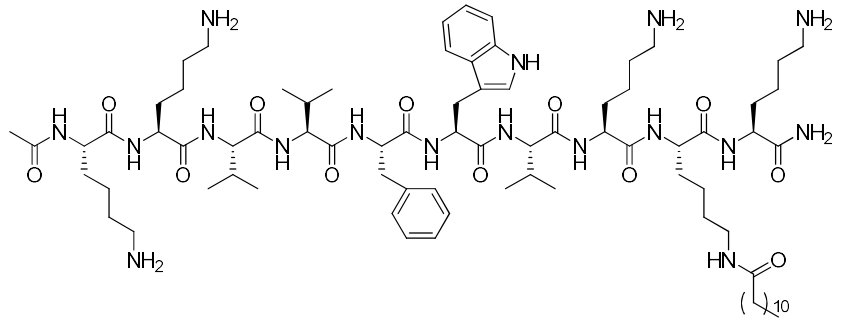

This peptide was synthesized from resin **2** following the strategy described above using lauric acid. The cleavage provided **BP417** in 59% HPLC purity. Elution with H_2O/CH_3CN (82:18) yielded **BP417** in >99% HPLC purity.

HPLC (λ = 220 nm): t_R = 7.18 min. ESI-MS (*m/z*): 757.6 $[M+2H]^{2+}$; 1513.2 $[M+H]^+$, 1535.2 $[M+Na]^+$. HRMS (*m/z*): calculated for $C_{79}H_{136}N_{17}O_{12}$ $[M+3H]^{3+}$ 505.0179, found 505.0202; calculated for $C_{79}H_{135}N_{17}O_{12}$ $[M+2H]^{2+}$ 757.0233, found 757.0225; calculated for $C_{79}H_{134}N_{17}O_{12}$ $[M+H]^+$ 1513.0392, found 1513.0379.

CH_3CO-Lys-Lys-Val-Val-Phe-Trp-Val-Lys(CO-C_5H_{11})-Phe-Lys-NH_2 (BP418)

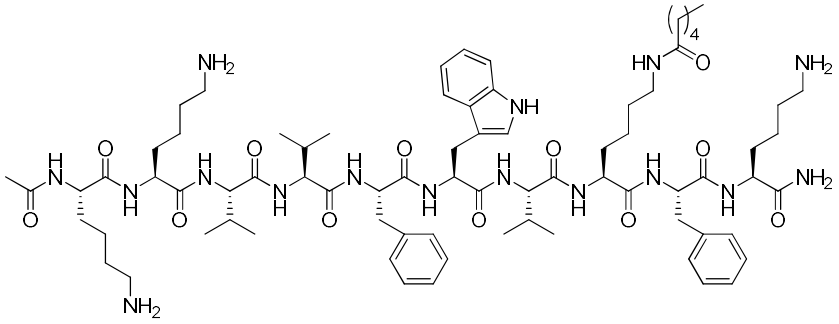

This peptide was synthesized from resin **3** following the strategy described above using hexanoic acid. The cleavage provided **BP418** in 58% HPLC purity. Elution with H_2O/CH_3CN (79:21) yielded **BP418** in >99% HPLC purity.

HPLC (λ = 220 nm): t_R = 6.76 min. ESI-MS (*m/z*): 1448.1 $[M+H]^+$, 1470.1 $[M+Na]^+$. HRMS (*m/z*): calculated for $C_{76}H_{121}N_{16}O_{12}$ $[M+3H]^{3+}$ 483.3111, found 483.3118; calculated for $C_{76}H_{120}N_{16}O_{12}$ $[M+2H]^{2+}$ 724.4630, found 724.4622; calculated for $C_{76}H_{119}N_{16}O_{12}$ $[M+H]^+$ 1447.9188, found 1447.9134.

CH_3CO-Lys-Lys-Val-Val-Phe-Trp-Val-Lys(CO-C_3H_7)-Phe-Lys-NH_2 (BP419)

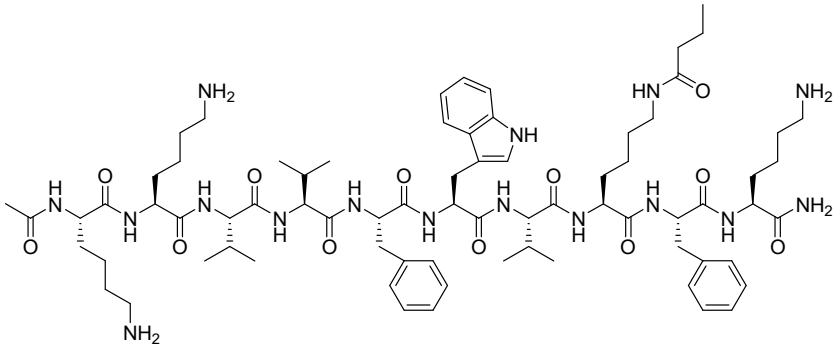

This peptide was synthesized from resin **3** following the strategy described above using butyric acid. The cleavage provided **BP419** in 50% HPLC purity. Elution with H_2O/CH_3CN (81:19) yielded **BP419** in >99% HPLC purity.

HPLC (λ = 220 nm): t_R = 6.52 min. ESI-MS (*m/z*): 710.5 $[M+2H]^{2+}$, 1420.1 $[M+H]^+$, 1442.1 $[M+Na]^+$. HRMS (*m/z*): calculated for $C_{74}H_{117}N_{16}O_{12}$ $[M+3H]^{3+}$ 473.9673, found 473.9685; calculated for $C_{74}H_{116}N_{16}O_{12}$ $[M+2H]^{2+}$ 710.4474, found 710.4469; calculated for $C_{74}H_{115}N_{16}O_{12}$ $[M+H]^+$ 1419.8875, found 1419.8862.

CH_3CO-Lys-Lys-Val-Val-Phe-Trp-Val-Lys(CO-$C_{11}H_{23}$)-Phe-Lys-NH_2 (BP420)

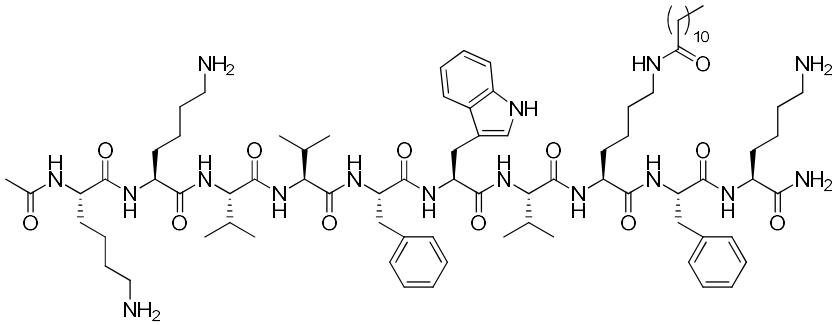

This peptide was synthesized from resin **3** following the strategy described above using lauric acid. The cleavage provided **BP420** in 69% HPLC purity. Elution with H_2O/CH_3CN (75:25) yielded **BP420** in >99% HPLC purity.

HPLC (λ = 220 nm): t_R = 7.66 min. ESI-MS (*m/z*): 767.1 $[M+2H]^{2+}$; 1532.2 $[M+H]^+$, 1554.3 $[M+Na]^+$. HRMS (*m/z*): calculated for $C_{82}H_{133}N_{16}O_{12}$ $[M+3H]^{3+}$ 511.3424, found 511.3422; calculated for $[M+2H]^{2+}$ $C_{82}H_{132}N_{16}O_{12}$ 766.5100, found 766.5082; calculated for $C_{82}H_{131}N_{16}O_{12}$ $[M+H]^+$ 1532.0127, found 1532.0064.

CH_3CO-Lys-Lys-Val-Val-Phe-Trp-Lys(CO-C_5H_{11})-Lys-Phe-Lys-NH_2 (BP421)

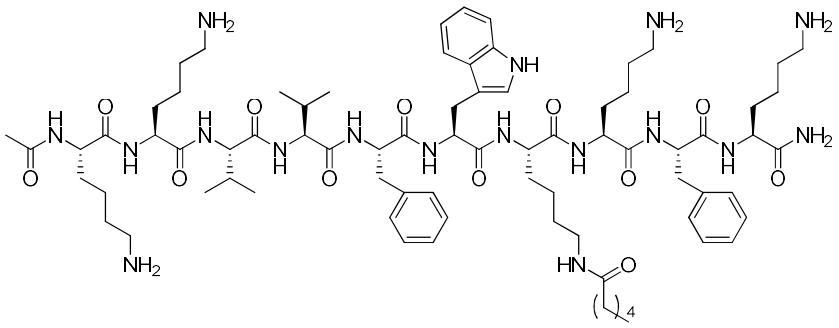

This peptide was synthesized from resin **4** following the strategy described above using hexanoic acid. The cleavage provided **BP421** in 60% HPLC purity. Elution with H_2O/CH_3CN (85:15) yielded **BP421** in >99% HPLC purity.

HPLC (λ = 220 nm): t_R = 6.44 min. ESI-MS (*m/z*): 739.1 $[M+2H]^{2+}$; 1477.2 $[M+H]^+$, 1499.2 $[M+Na]^+$. HRMS (*m/z*): calculated for $C_{77}H_{124}N_{17}O_{12}$ $[M+3H]^{3+}$ 492.9866, found 492.9859; calculated for $C_{77}H_{123}N_{17}O_{12}$ $[M+2H]^{2+}$ 738.9763, found 738.9734; calculated for $C_{77}H_{122}N_{17}O_{12}$ $[M+H]^+$ 1476.9453, found 1476.9423.

CH_3CO-Lys-Lys-Val-Val-Phe-Trp-Lys(CO-C_3H_7)-Lys-Phe-Lys-NH_2 (BP422)

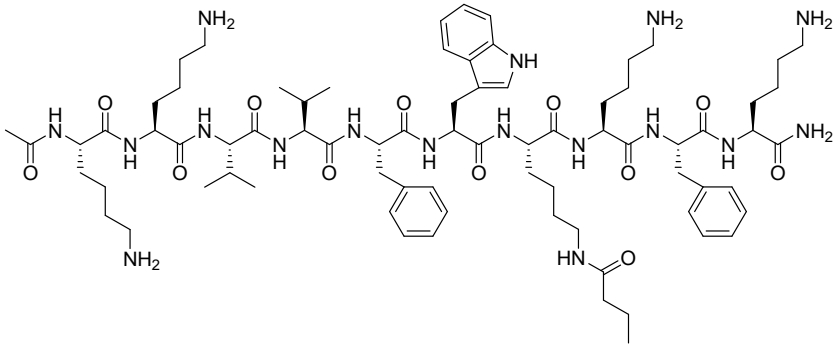

This peptide was synthesized from resin **4** following the strategy described above using butyric acid. The cleavage provided **BP422** in 48% HPLC purity. Elution with H_2O/CH_3CN (87:13) yielded **BP422** in >99% HPLC purity.

HPLC (λ = 220 nm): t_R = 6.23 min. ESI-MS (*m/z*): 725.0 $[M+2H]^{2+}$; 1449.1 $[M+H]^+$, 1471.1 $[M+Na]^+$. HRMS (*m/z*): calculated for $C_{75}H_{120}N_{17}O_{12}$ $[M+3H]^{3+}$ 483.6429, found 483.6428; calculated for $[M+2H]^{2+}$ $C_{75}H_{119}N_{17}O_{12}$ 724.9607, found 724.9596.

CH_3CO-Lys-Lys-Val-Val-Phe-Trp-Lys(CO-$C_{11}H_{23}$)-Lys-Phe-Lys-NH_2 (BP423)

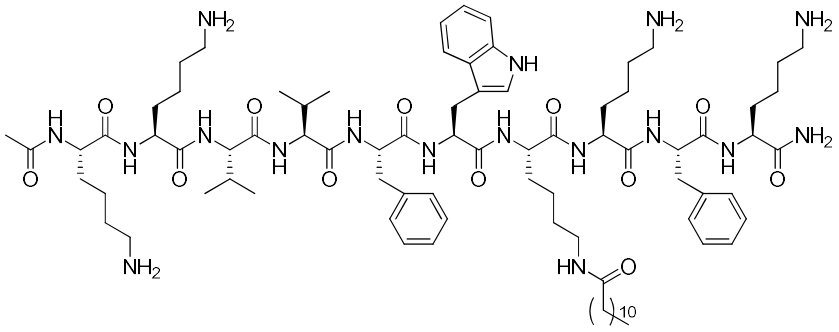

This peptide was synthesized from resin **4** following the strategy described above using lauric acid. The cleavage provided **BP423** in 68% HPLC purity. Elution with H_2O/CH_3CN (81:19) yielded **BP423** in >99% HPLC purity.

HPLC (λ = 220 nm): t_R = 7.25 min. ESI-MS (*m/z*): 781.2 $[M+2H]^{2+}$; 1561.3 $[M+H]^+$, 1583.3 $[M+Na]^+$. HRMS (*m/z*): calculated for $C_{83}H_{136}N_{17}O_{12}$ $[M+3H]^{3+}$ 521.0179, found 521.0187; calculated for $C_{83}H_{135}N_{17}O_{12}$ $[M+2H]^{2+}$ 781.0233, found 781.0226; calculated for $C_{83}H_{134}N_{17}O_{12}$ $[M+H]^+$ 1561.0392, found 1561.0381.

CH_3CO-Lys-Lys-Val-Val-Phe-Lys(CO-C_5H_{11})-Val-Lys-Phe-Lys-NH_2 (BP424)

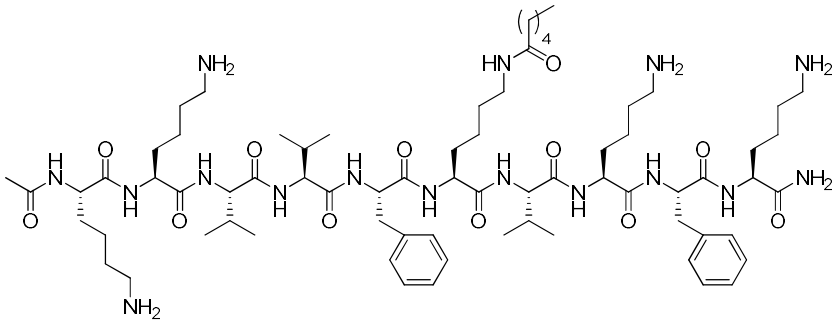

This peptide was synthesized from resin **5** following the strategy described above using hexanoic acid. The cleavage provided **BP424** in 45% HPLC purity. Elution with H_2O/CH_3CN (85:15) yielded **BP424** in >99% HPLC purity.

HPLC (λ = 220 nm): t_R = 6.26 min. ESI-MS (*m/z*): 695.6 $[M+2H]^{2+}$; 1390.2 $[M+H]^+$, 1412.2 $[M+Na]^+$. HRMS (*m/z*): calculated for $C_{71}H_{123}N_{16}O_{12}$ $[M+3H]^{3+}$ 463.9830, found 463.9834; calculated for $C_{71}H_{122}N_{16}O_{12}$ $[M+2H]^{2+}$ 695.4709, found 695.4695; calculated for $C_{71}H_{121}N_{16}O_{12}$ $[M+H]^+$ 1389.9344, found 1389.9318.

CH_3CO-Lys-Lys-Val-Val-Phe-Lys(CO-C_3H_7)-Val-Lys-Phe-Lys-NH_2 (BP425)

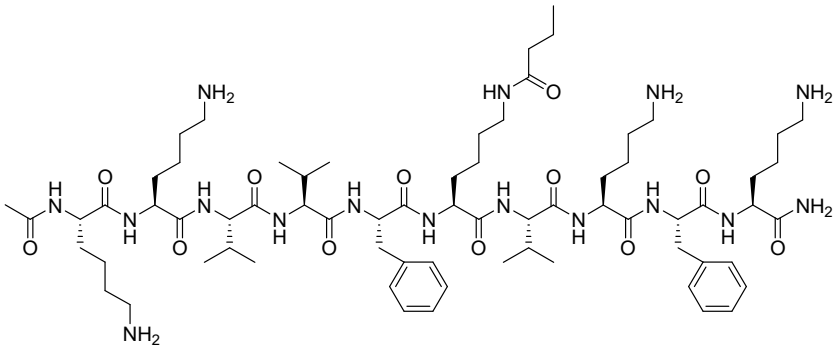

This peptide was synthesized from resin **5** following the strategy described above using butyric acid. The cleavage provided **BP425** in 49% HPLC purity. Elution with H_2O/CH_3CN (88:12) yielded **BP425** in >99% HPLC purity.

HPLC (λ = 220 nm): t_R = 6.05 min. ESI-MS (*m/z*): 681.5 $[M+2H]^{2+}$; 1362.1 $[M+H]^+$, 1384.0 $[M+Na]^+$. HRMS (*m/z*): calculated for $C_{69}H_{119}N_{16}O_{12}$ $[M+3H]^{3+}$ 454.6392, found 454.6387; calculated for $C_{69}H_{118}N_{16}O_{12}$ $[M+2H]^{2+}$ 681.4552, found 681.4533; calculated for $C_{69}H_{117}N_{16}O_{12}$ $[M+H]^+$ 1361.9031, found 1361.9022.

CH_3CO-Lys-Lys-Val-Val-Phe-Lys(CO-$C_{11}H_{23}$)-Val-Lys-Phe-Lys-NH_2 (BP426)

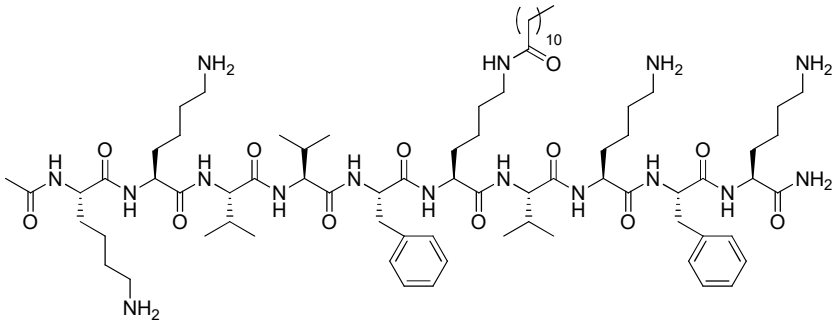

This peptide was synthesized from resin **5** following the strategy described above using lauric acid. The cleavage provided **BP426** in 63% HPLC purity. Elution with H_2O/CH_3CN (80:20) yielded **BP426** in >99% HPLC purity.

HPLC (λ = 220 nm): t_R = 7.11 min. ESI-MS (*m/z*): 738.1 $[M+2H]^{2+}$; 1474.2 $[M+H]^+$, 1496.2 $[M+Na]^+$. HRMS (*m/z*): calculated for $C_{77}H_{135}N_{16}O_{12}$ $[M+3H]^{3+}$ 492.0143, found 492.0150; calculated for $C_{77}H_{134}N_{16}O_{12}$ $[M+2H]^{2+}$ 737.5178, found 737.5167; calculated for $C_{77}H_{133}N_{16}O_{12}$ $[M+H]^+$ 1474.0283, found 1474.0264.

CH_3CO-Lys-Lys-Val-Val-Lys(CO-C_5H_{11})-Trp-Val-Lys-Phe-Lys-NH_2 (BP427)

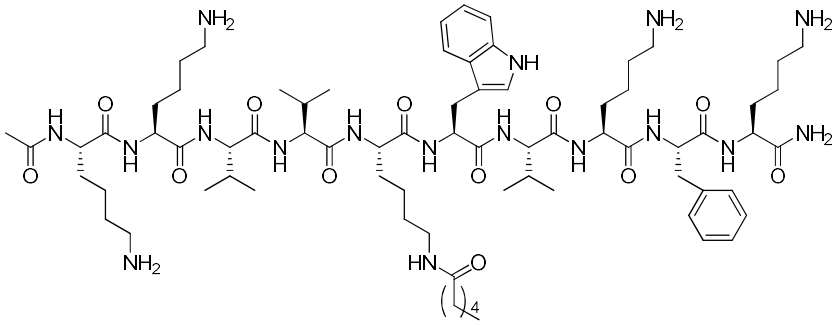

This peptide was synthesized from resin **6** following the strategy described above using hexanoic acid. The cleavage provided **BP427** in 43% HPLC purity. Elution with H_2O/CH_3CN (88:12) yielded **BP427** in >99% HPLC purity.

HPLC (λ = 220 nm): t_R = 6.33 min. ESI-MS (*m/z*): 715.1 $[M+2H]^{2+}$, 726.5 $[M+H+Na]^{2+}$; 1429.1 $[M+H]^+$, 1451.1 $[M+Na]^+$. HRMS (*m/z*): calculated for $C_{73}H_{123}N_{17}O_{12}$ $[M+2H]^{2+}$ 714.9763, found 714.9742; calculated for $C_{73}H_{122}N_{17}O_{12}Na$ $[M+H+Na]^{2+}$ 725.9673, found 725.9658; calculated for $C_{73}H_{121}N_{17}O_{12}Na_2$ $[M+2Na]^{2+}$ 736.9583, found 736.9569; calculated for $C_{73}H_{121}N_{17}O_{12}Na$ $[M+Na]^+$ 1450.9273, found 1450.9245.

CH_3CO-Lys-Lys-Val-Val-Lys(CO-C_3H_7)-Trp-Val-Lys-Phe-Lys-NH_2 (BP428)

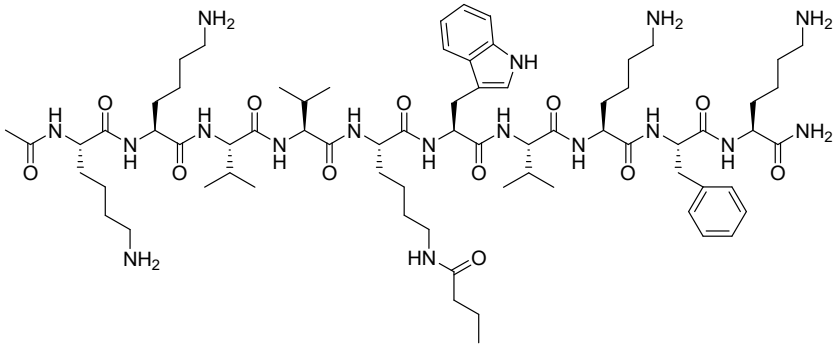

This peptide was synthesized from resin **6** following the strategy described above using butyric acid. The cleavage provided **BP428** in 46% HPLC purity. Elution with H_2O/CH_3CN (88:12) yielded **BP428** in >99% HPLC purity.

HPLC (λ = 220 nm): t_R = 6.12 min. ESI-MS (*m/z*): 701.1 $[M+2H]^{2+}$, 712.0 $[M+H+Na]^{2+}$; 1401.1 $[M+H]^+$, 1423.1 $[M+Na]^+$. HRMS (*m/z*): calculated for $C_{71}H_{120}N_{17}O_{12}$ $[M+3H]^{3+}$ 467.6429, found 467.6417; calculated for $C_{71}H_{119}N_{17}O_{12}$ $[M+2H]^{2+}$ 700.9607, found 700.9590; calculated for $C_{71}H_{118}N_{17}O_{12}Na$ $[M+H+Na]^{2+}$ 711.9516, found 711.9498; calculated for $C_{71}H_{117}N_{17}O_{12}Na_2$ $[M+2Na]^{2+}$ 722.9426, found 722.9411; calculated for $C_{71}H_{117}N_{17}O_{12}Na$ $[M+Na]^+$ 1422.8960, found 1422.8950.

CH_3CO-Lys-Lys-Val-Val-Lys(CO-$C_{11}H_{23}$)-Trp-Val-Lys-Phe-Lys-NH_2 (BP429)

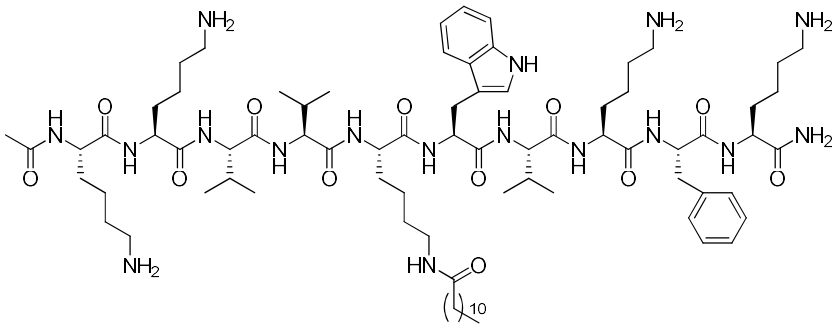

This peptide was synthesized from resin **6** following the strategy described above using lauric acid. The cleavage provided **BP429** in 57% HPLC purity. Elution with H_2O/CH_3CN (81:19) yielded **BP429** in >99% HPLC purity.

HPLC (λ = 220 nm): t_R = 7.21 min. ESI-MS (*m/z*): 505.1 $[M+3H]^{3+}$, 757.6 $[M+2H]^{2+}$, 768.1 $[M+H+Na]^{2+}$, 779.6 $[M+2Na]^{2+}$, 1514.2 $[M+H]^+$, 1535.2 $[M+Na]^+$. HRMS (*m/z*): calculated for $C_{79}H_{136}N_{17}O_{12}$ $[M+3H]^{3+}$ 505.0179, found 505.0172; calculated for $C_{79}H_{135}N_{17}O_{12}$ $[M+2H]^{2+}$ 757.0233, found 757.0216; calculated for $C_{79}H_{134}N_{17}O_{12}Na$ $[M+H+Na]^{2+}$ 768.0142, found 768.0116; calculated for $C_{79}H_{133}N_{17}O_{12}Na_2$ $[M+2Na]^{2+}$ 779.0052, found 779.0037; calculated for $C_{79}H_{133}N_{17}O_{12}Na$ $[M+Na]^+$ 1535.0212, found 1535.0194.

CH_3CO-Lys-Lys-Val-Lys(CO-C_5H_{11})-Phe-Trp-Val-Lys-Phe-Lys-NH_2 (BP430)

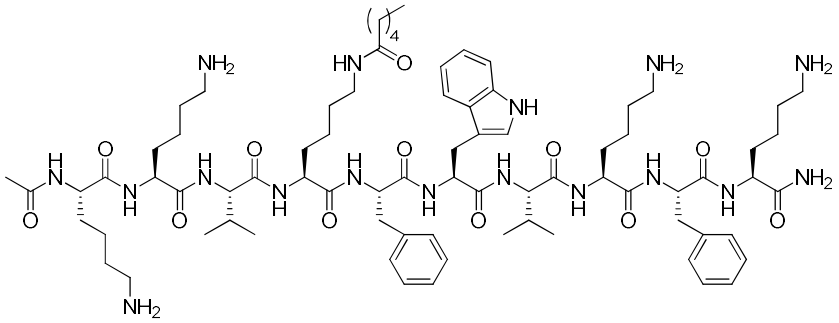

This peptide was synthesized from resin **7** following the strategy described above using hexanoic acid. The cleavage provided **BP430** in 74% HPLC purity. Elution with H_2O/CH_3CN (85:15) yielded **BP430** in >99% HPLC purity.

HPLC (λ = 220 nm): t_R = 6.46 min. ESI-MS (*m/z*): 739.1 $[M+2H]^{2+}$, 750.5 $[M+H+Na]^{2+}$; 1477.2 $[M+H]^+$, 1499.2 $[M+Na]^+$. HRMS (*m/z*): calculated for $C_{77}H_{124}N_{17}O_{12}$ $[M+3H]^{3+}$ 492.9866, found 492.9852; calculated for $C_{77}H_{123}N_{17}O_{12}$ $[M+2H]^{2+}$ 738.9763, found 738.9745; calculated for $C_{77}H_{122}N_{17}O_{12}Na$ $[M+H+Na]^{2+}$ 749.9673, found 749.9645; calculated for $C_{77}H_{121}N_{17}O_{12}Na_2$ $[M+2Na]^{2+}$ 760.9583, found 760.9565; calculated for $C_{77}H_{122}N_{17}O_{12}$ $[M+H]^+$ 1476.9453, found 1476.9429.

CH_3CO-Lys-Lys-Val-Lys(CO-C_3H_7)-Phe-Trp-Val-Lys-Phe-Lys-NH_2 (BP431)

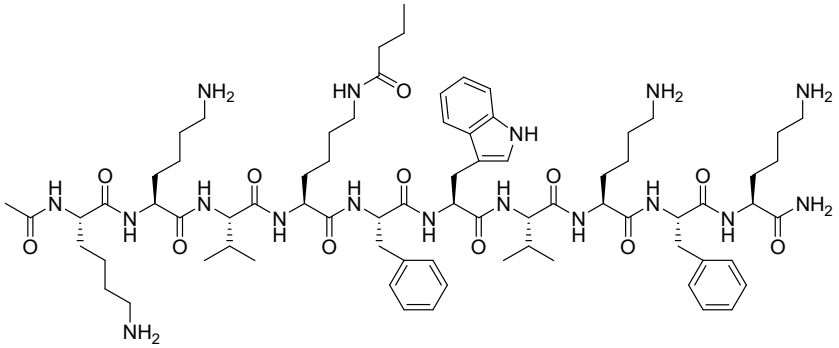

This peptide was synthesized from resin **7** following the strategy described above using butyric acid. The cleavage provided **BP431** in 58% HPLC purity. Elution with H_2O/CH_3CN (87:13) yielded **BP431** in >99% HPLC purity.

HPLC (λ = 220 nm): t_R = 6.26 min. ESI-MS (*m/z*): 725.1 $[M+2H]^{2+}$, 736.6 $[M+H+Na]^{2+}$; 1449.1 $[M+H]^+$, 1471.1 $[M+Na]^+$. HRMS (*m/z*): calculated for $C_{75}H_{120}N_{17}O_{12}$ $[M+3H]^{3+}$ 483.6429, found 483.6433; calculated for $C_{75}H_{119}N_{17}O_{12}$ $[M+2H]^{2+}$ 724.9607, found 724.9612; calculated for $C_{75}H_{118}N_{17}O_{12}Na$ $[M+H+Na]^{2+}$ 735.9516, found 735.9524; calculated for $C_{75}H_{117}N_{17}O_{12}Na_2$ $[M+2Na]^{2+}$ 746.9426, found 746.9434; calculated for $C_{75}H_{118}N_{17}O_{12}$ $[M+H]^+$ 1448.9140, found 1448.9144; calculated for $C_{75}H_{117}N_{17}O_{12}Na$ $[M+Na]^+$ 1470.8960, found 1470.8986.

CH_3CO-Lys-Lys-Val-Lys(CO-$C_{11}H_{23}$)-Phe-Trp-Val-Lys-Phe-Lys-NH_2 (BP432)

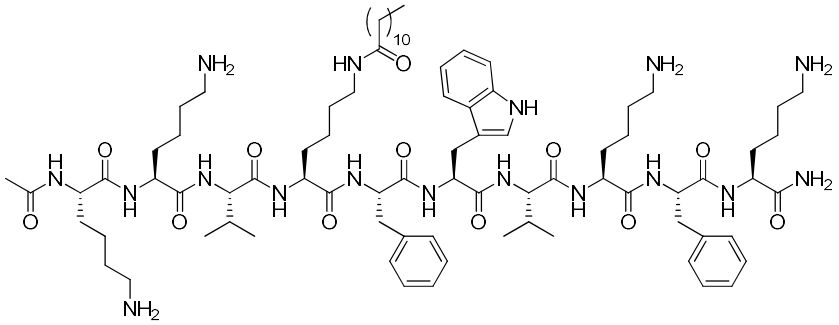

This peptide was synthesized from resin **7** following the strategy described above using lauric acid. The cleavage provided **BP432** in 80% HPLC purity. Elution with H_2O/CH_3CN (81:19) yielded **BP432** in >99% HPLC purity.

HPLC (λ = 220 nm): t_R = 7.26 min. ESI-MS (*m/z*): 781.6 $[M+2H]^{2+}$, 792.6 $[M+H+Na]^{2+}$, 1561.3 $[M+H]^+$, 1583.3 $[M+Na]^+$. HRMS (*m/z*): calculated for $C_{83}H_{136}N_{17}O_{12}$ $[M+3H]^{3+}$ 521.0179, found 521.0162; calculated for $C_{83}H_{135}N_{17}O_{12}$ $[M+2H]^{2+}$ 781.0233, found 781.0215; calculated for $C_{83}H_{134}N_{17}O_{12}Na$ $[M+H+Na]^{2+}$ 792.0142, found 792.0122; calculated for $C_{83}H_{133}N_{17}O_{12}Na_2$ $[M+2Na]^{2+}$ 803.0052, found 803.0036; calculated for $C_{83}H_{134}N_{17}O_{12}$ $[M+H]^+$ 1561.0392, found 1561.0347; calculated for $C_{83}H_{133}N_{17}O_{12}Na$ $[M+Na]^+$ 1583.0212, found 1583.0199.

CH_3CO-Lys-Lys-Lys(CO-C_5H_{11})-Val-Phe-Trp-Val-Lys-Phe-Lys-NH_2 (BP433)

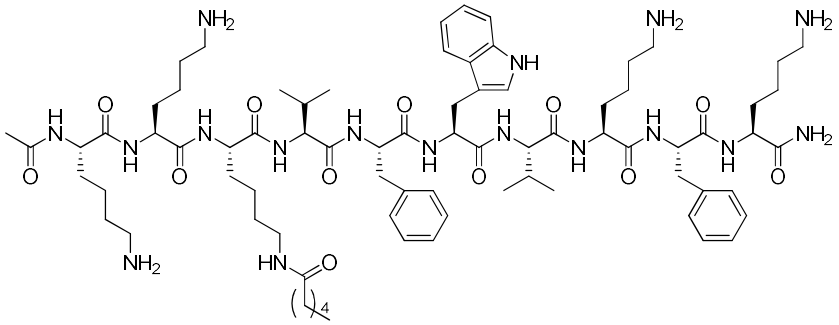

This peptide was synthesized from resin **8** following the strategy described above using hexanoic acid. The cleavage provided **BP433** in 63% HPLC purity. Elution with H_2O/CH_3CN (85:15) yielded **BP433** in >99% HPLC purity.

HPLC (λ = 220 nm): t_R = 6.46 min. ESI-MS (*m/z*): 739.1 $[M+2H]^{2+}$, 750.0 $[M+H+Na]^{2+}$; 1477.1 $[M+H]^+$, 1499.1 $[M+Na]^+$. HRMS (*m/z*): calculated for $C_{77}H_{124}N_{17}O_{12}$ $[M+3H]^{3+}$ 492.9866, found 492.9874; calculated for $C_{77}H_{123}N_{17}O_{12}$ $[M+2H]^{2+}$ 738.9763, found 738.9764; calculated for $C_{77}H_{122}N_{17}O_{12}Na$ $[M+H+Na]^{2+}$ 749.9673, found 749.9664; calculated for $C_{77}H_{121}N_{17}O_{12}Na_2$ $[M+2Na]^{2+}$ 760.9583, found 760.9580; calculated for

$C_{77}H_{122}N_{17}O_{12}$ $[M+H]^+$ 1476.9453, found 1476.9457; calculated for $C_{77}H_{121}N_{17}O_{12}Na$ $[M+Na]^+$ 1498.9273, found 1498.9280.

CH_3CO-Lys-Lys-Lys(CO-C_3H_7)-Val-Phe-Trp-Val-Lys-Phe-Lys-NH_2 (BP434)

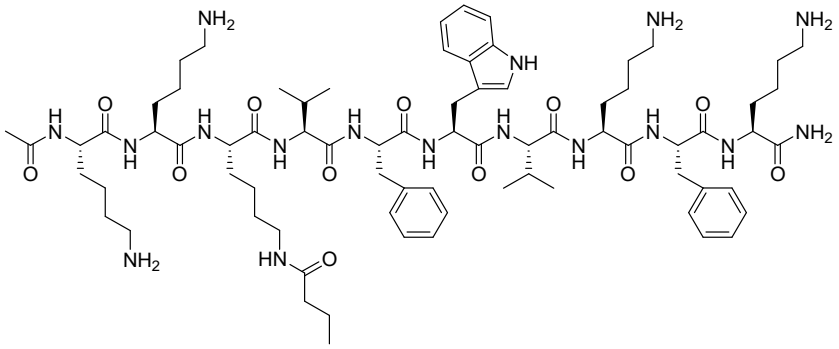

This peptide was synthesized from resin **8** following the strategy described above using butyric acid. The cleavage provided **BP434** in 46% HPLC purity. Elution with H_2O/CH_3CN (88:12) yielded **BP434** in >99% HPLC purity.

HPLC (λ = 220 nm): t_R = 6.26 min. ESI-MS (*m/z*): 725.5 $[M+2H]^{2+}$, 736.0 $[M+H+Na]^{2+}$, 1449.1 $[M+H]^+$, 1471.1 $[M+Na]^+$. HRMS (*m/z*): calculated for $C_{75}H_{120}N_{17}O_{12}$ $[M+3H]^{3+}$ 483.6429, found 483.6433; calculated for $C_{75}H_{119}N_{17}O_{12}$ $[M+2H]^{2+}$ 724.9607, found 724.9601; calculated for $C_{75}H_{118}N_{17}O_{12}Na$ $[M+H+Na]^{2+}$ 735.9516, found 735.9501; calculated for $C_{75}H_{118}N_{17}O_{12}$ $[M+H]^+$ 1448.9140, found 1448.9135; calculated for $C_{75}H_{117}N_{17}O_{12}Na$ $[M+Na]^+$ 1470.8960, found 1470.8966.

CH_3CO-Lys-Lys-Lys(CO-$C_{11}H_{23}$)-Val-Phe-Trp-Val-Lys-Phe-Lys-NH_2 (BP435)

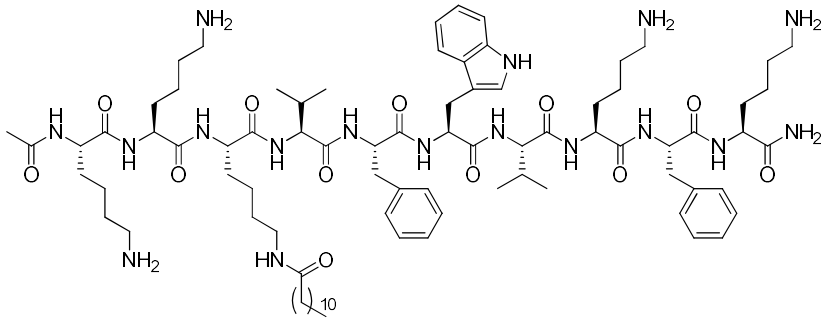

This peptide was synthesized from resin **8** following the strategy described above using lauric acid. The cleavage provided **BP435** in 70% HPLC purity. Elution with H_2O/CH_3CN (82:18) yielded **BP435** in >99% HPLC purity.

HPLC (λ = 220 nm): t_R = 7.27 min. ESI-MS (*m/z*): 781.6 $[M+2H]^{2+}$, 792.1 $[M+H+Na]^{2+}$; 1561.2 $[M+H]^+$, 1583.2 $[M+Na]^+$. HRMS (*m/z*): calculated for $C_{83}H_{136}N_{17}O_{12}$ $[M+3H]^{3+}$ 521.0179, found 521.0198; calculated for

$C_{83}H_{135}N_{17}O_{12}$ $[M+2H]^{2+}$ 781.0233, found 781.0247; calculated for $C_{83}H_{134}N_{17}O_{12}$ $[M+H]^{+}$ 1561.0392, found 1561.0409.

CH_3CO-Lys-Lys(CO-C_5H_{11})-Val-Val-Phe-Trp-Val-Lys-Phe-Lys-NH_2 (BP436)

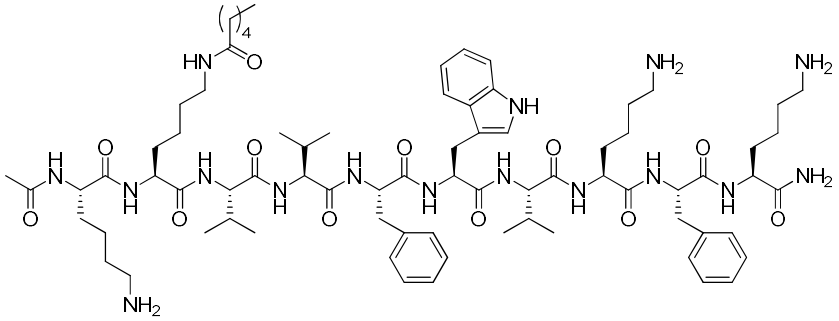

This peptide was synthesized from resin **9** following the strategy described above using hexanoic acid. The cleavage provided **BP436** in 63% HPLC purity. Elution with H_2O/CH_3CN (78:22) yielded **BP436** in >99% HPLC purity.

HPLC (λ = 220 nm): t_R = 6.85 min. ESI-MS (*m/z*): 724.5 $[M+2H]^{2+}$, 735.5 $[M+H+Na]^{2+}$; 1448.1 $[M+H]^{+}$, 1470.1 $[M+Na]^{+}$. HRMS (*m/z*): calculated for $C_{76}H_{121}N_{16}O_{12}$ $[M+3H]^{3+}$ 483.3111, found 483.3102; calculated for $C_{76}H_{120}N_{16}O_{12}$ $[M+2H]^{2+}$ 724.4630, found 724.4619; calculated for $C_{76}H_{119}N_{16}O_{12}Na$ $[M+H+Na]^{2+}$ 735.4540, found 735.4520; calculated for $C_{76}H_{119}N_{16}O_{12}$ $[M+H]^{+}$ 1447.9188, found 1447.9172; calculated for $C_{76}H_{118}N_{16}O_{12}Na$ $[M+Na]^{+}$ 1469.9007, found 1469.8977.

CH_3CO-Lys-Lys(CO-C_3H_7)-Val-Val-Phe-Trp-Val-Lys-Phe-Lys-NH_2 (BP437)

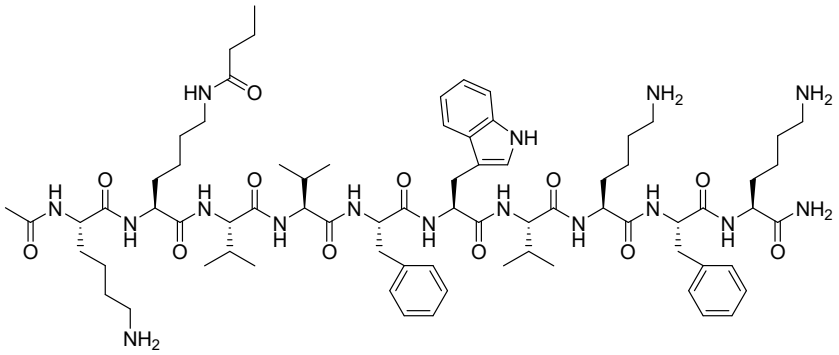

This peptide was synthesized from resin **9** following the strategy described above using butyric acid. The cleavage provided **BP437** in 49% HPLC purity. Elution with H_2O/CH_3CN (80:20) yielded **BP437** in 97% HPLC purity.

HPLC (λ = 220 nm): t_R = 6.62 min. ESI-MS (*m/z*): 710.5 $[M+2H]^{2+}$, 721.5 $[M+H+Na]^{2+}$; 1420.1 $[M+H]^{+}$, 1442.0 $[M+Na]^{+}$. HRMS (*m/z*): calculated for $C_{74}H_{117}N_{16}O_{12}$ $[M+3H]^{3+}$ 473.9673, found 473.9657; calculated for

$C_{74}H_{116}N_{16}O_{12}$ $[M+2H]^{2+}$ 710.4474, found 710.4447; calculated for $C_{74}H_{115}N_{16}O_{12}$ $[M+H]^{+}$ 1419.8875, found 1419.8844; calculated for $C_{74}H_{114}N_{16}O_{12}Na$ $[M+Na]^{+}$ 1441.8694, found 1441.8667.

CH_3CO-Lys-Lys(CO-$C_{11}H_{23}$)-Val-Val-Phe-Trp-Val-Lys-Phe-Lys-NH_2 (BP438)

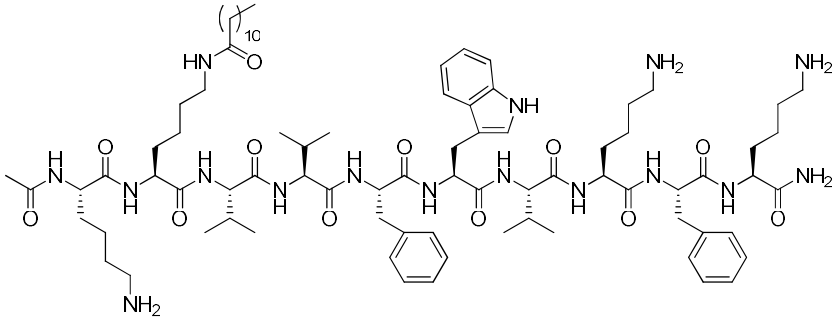

This peptide was synthesized from resin **9** following the strategy described above using lauric acid. The cleavage provided **BP438** in 73% HPLC purity. Elution with H_2O/CH_3CN (78:22) yielded **BP438** in 93% HPLC purity.

HPLC (λ = 220 nm): t_R = 7.74 min. ESI-MS (*m/z*): 766.6 $[M+2H]^{2+}$, 778.1 $[M+H+Na]^{2+}$; 1532.2 $[M+H]^{+}$, 1554.2 $[M+Na]^{+}$. HRMS (*m/z*): calculated for $C_{82}H_{133}N_{16}O_{12}$ $[M+3H]^{3+}$ 511.3424, found 511.3408; calculated for $C_{82}H_{132}N_{16}O_{12}$ $[M+2H]^{2+}$ 766.5100, found 766.5078; calculated for $C_{82}H_{131}N_{16}O_{12}Na$ $[M+H+Na]^{2+}$ 777.5010, found 777.4985; calculated for $C_{82}H_{130}N_{16}O_{12}Na_2$ $[M+2Na]^{2+}$ 788.4919, found 788.4897; calculated for $C_{82}H_{131}N_{16}O_{12}$ $[M+H]^{+}$ 1532.0127, found 1532.0079; calculated for $C_{82}H_{130}N_{16}O_{12}Na$ $[M+Na]^{+}$ 1553.9946, found 1553.9912.

CH_3CO-Lys(CO-C_5H_{11})-Lys-Val-Val-Phe-Trp-Val-Lys-Phe-Lys-NH_2 (BP439)

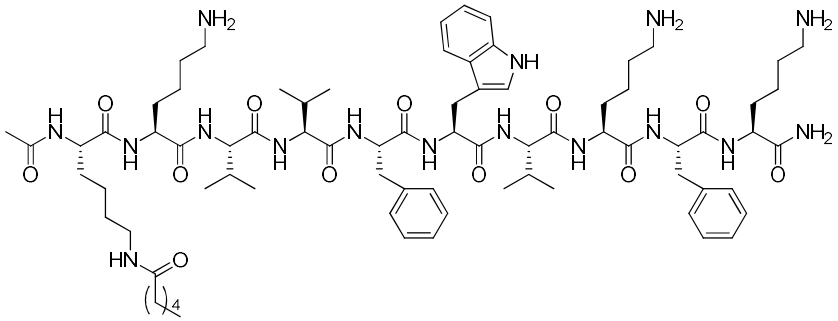

This peptide was synthesized from resin **10** following the strategy described above using hexanoic acid. The cleavage provided **BP439** in 62% HPLC purity. Elution with H_2O/CH_3CN (82:18) yielded **BP439** in >99% HPLC purity.

HPLC (λ = 220 nm): t_R = 6.81 min. ESI-MS (*m/z*): 725.0 $[M+2H]^{2+}$, 735.5 $[M+H+Na]^{2+}$; 1448.1 $[M+H]^{+}$, 1470.1 $[M+Na]^{+}$. HRMS (*m/z*): calculated for $C_{76}H_{121}N_{16}O_{12}$ $[M+3H]^{3+}$ 483.3111, found 483.3096; calculated for $C_{76}H_{120}N_{16}O_{12}$ $[M+2H]^{2+}$ 724.4630, found 724.4612; calculated for $C_{76}H_{119}N_{16}O_{12}Na$ $[M+H+Na]^{2+}$ 735.4540,

found 735.4514; calculated for $C_{76}H_{118}N_{16}O_{12}Na_2$ $[M+2Na]^{2+}$ 746.4450, found 746.4423; calculated for $C_{76}H_{119}N_{16}O_{12}$ $[M+H]^+$ 1447.9188, found 1447.9158; calculated for $C_{76}H_{118}N_{16}O_{12}Na$ $[M+Na]^+$ 1469.9007, found 1469.8973.

CH_3CO-Lys(CO-C_3H_7)-Lys-Val-Val-Phe-Trp-Val-Lys-Phe-Lys-NH_2 (BP440)

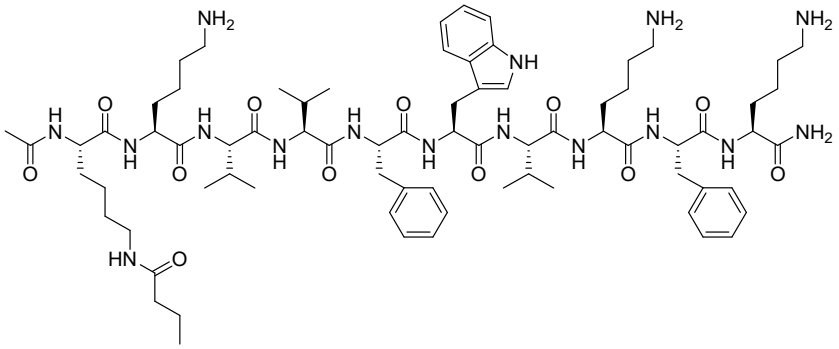

This peptide was synthesized from resin **10** following the strategy described above using butyric acid. The cleavage provided **BP440** in 50% HPLC purity. Elution with H_2O/CH_3CN (82:18) yielded **BP440** in >99% HPLC purity.

HPLC (λ = 220 nm): t_R = 6.58 min. ESI-MS (*m/z*): 710.5 $[M+2H]^{2+}$, 721.5 $[M+H+Na]^{2+}$; 1420.0 $[M+H]^+$, 1442.0 $[M+Na]^+$. HRMS (*m/z*): calculated for $C_{74}H_{117}N_{16}O_{12}$ $[M+3H]^{3+}$ 473.9673, found 473.9675; calculated for $C_{74}H_{116}N_{16}O_{12}$ $[M+2H]^{2+}$ 710.4474, found 710.4471; calculated for $C_{74}H_{115}N_{16}O_{12}Na$ $[M+H+Na]^{2+}$ 721.4384, found 721.4372; calculated for $C_{74}H_{114}N_{16}O_{12}Na_2$ $[M+2Na]^{2+}$ 732.4293, found 732.4279; calculated for $C_{74}H_{115}N_{16}O_{12}$ $[M+H]^+$ 1419.8875, found 1419.8878; calculated for $C_{74}H_{114}N_{16}O_{12}Na$ $[M+Na]^+$ 1441.8694, found 1441.8718.

CH_3CO-Lys(CO-$C_{11}H_{23}$)-Lys-Val-Val-Phe-Trp-Val-Lys-Phe-Lys-NH_2 (BP441)

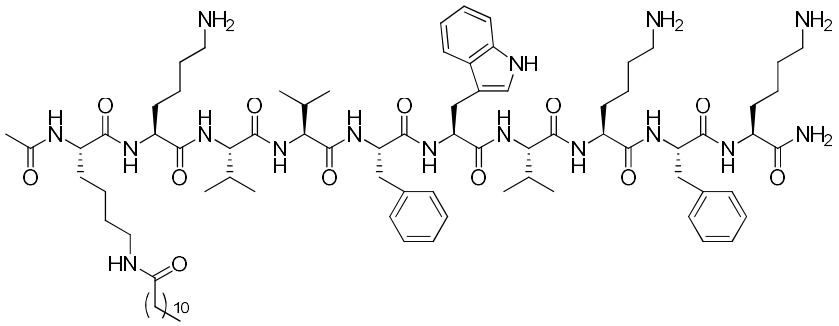

This peptide was synthesized from resin **10** following the strategy described above using lauric acid. The cleavage provided **BP441** in 65% HPLC purity. Elution with H_2O/CH_3CN (74:26) yielded **BP441** in >99% HPLC purity.

HPLC (λ = 220 nm): t_R = 7.73 min. ESI-MS (*m/z*): 511.7 $[M+3H]^{3+}$; 766.6 $[M+2H]^{2+}$; 1532.2 $[M+H]^{+}$, 1554.2 $[M+Na]^{+}$. HRMS (*m/z*): calculated for $C_{82}H_{133}N_{16}O_{12}$ $[M+3H]^{3+}$ 511.3424, found 511.3411; calculated for $C_{82}H_{132}N_{16}O_{12}$ $[M+2H]^{2+}$ 766.5100, found 766.5080; calculated for $C_{82}H_{131}N_{16}O_{12}Na$ $[M+H+Na]^{2+}$ 777.5010, found 777.4984; calculated for $C_{82}H_{130}N_{16}O_{12}Na_2$ $[M+2Na]^{2+}$ 788.4919, found 788.4902; calculated for $C_{82}H_{131}N_{16}O_{12}$ $[M+H]^{+}$ 1532.0127, found 1532.0116; calculated for $C_{82}H_{130}N_{16}O_{12}Na$ $[M+Na]^{+}$ 1553.9946, found 1553.9936.

5.4. General method for solid-phase peptide conjugates synthesis

The synthesis was carried out manually on solid-phase in polypropylene syringes equipped with a polyethylene filter. An orthogonal Fmoc/^{t}Bu strategy was followed. ChemMatrix resin (0.66 mmol/g) was used as solid support. The conditions used to swell the resin were MeOH (2 x 1 min), DMF (2 x 1 min), CH_2Cl_2 (2 x 1 min), CH_2Cl_2/TFA (99:1) (3 x 1 min), CH_2Cl_2/DIEA (19:1) (3 x 1 min), CH_2Cl_2 (3 x 1 min) and DMF (6 x 1 min). A Fmoc-Rink-amide linker was used for peptides with a C-terminal amide and a linker PAC was used for peptides with a C-terminal carboxylic acid. Once the ChemMatrix resin was swollen, it was treated with the corresponding linker (4 equiv), Oxyma (4 equiv) and DIPCDI (4 equiv) in DMF overnight. After this time, the resin was washed with DMF (6 x 1 min) and CH_2Cl_2 (3 x 1 min), and the completion of the reaction was checked with the Kaiser test (Kaiser 1970).

The sequence was synthesized through sequential Fmoc removal and coupling steps of the corresponding protected amino acids. The Fmoc removal step was carried out with piperidine/DMF (3:7, 1 x 2 min and 2 x 10 min). The coupling of the first amino acid (5 equiv) onto a PAC-ChemMatrix resin was performed in presence of *N,N*-diisopropylcarbodiimide (DIPCDI) (5 equiv), 4-dimethylaminopyridine (DMAP) (0.5 equiv) and *N,N'*-diisopropylethylamine (DIEA) (1 equiv) in DMF at room temperature for 2 h under stirring. This treatment was repeated twice and, then, the resin was washed with DMF (6 x 1 min) and CH_2Cl_2 (3 x 1 min), and dried with diethyl ether (3 x 2 min). The reaction was monitored using a Fmoc test. Then, the resin was acetylated with CH_2Cl_2/pyridine/acetic anhydride (18:1.35:1.35, 2 x 30 min) and washed with CH_2Cl_2 (3 x 2 min), DMF (3 x 2 min), MeOH (2 x 2 min), CH_2Cl_2 (2 x 2 min) and DMF (6 x 1 min). Coupling of the other amino acids were carried out by treating the resin with the corresponding protected amino acid (4 equiv), Oxyma (4 equiv) and DIPCDI (4 equiv) in DMF under stirring for 1 h at room temperature. After each coupling and Fmoc removal step, the resin was washed with DMF (6 x 1 min) and CH_2Cl_2 (3 x 1 min), and the reactions were monitored with the Kaiser test (Kaiser 1970) if the coupling was performed on a primary amine or with the chloranil test (Vojkovsky 1995) if the coupling was performed on a secondary amine. After the coupling of the fifth amino acid, NMP was employed instead of DMF. At the end of the synthesis, the Fmoc was removed and the peptide was cleaved from the resin by treatment with TFA/H_2O/TIS (95:2.5:2.5) for 2 h at room temperature. Peptides incorporating a tryptophan residue were cleaved with TFA/phenol/H_2O/TIS (92.5:2.5:2.5:2.5). Following evaporation of the acidic solution, the crude peptide was washed with cold diethyl ether. The mixture was centrifuged and the supernatant was removed. This procedure was repeated three times. The resulting peptide was dissolved in H_2O,

lyophilized, purified by reverse-phase chromatography with a CombiFlash® Rf equipment, analysed by HPLC, and characterized by ESI-MS and HRMS.

Lys-Lys-Leu-D-Phe-Lys-Lys-Ile-Leu-Lys-Tyr-Leu-Phe-Lys-Leu-Phe-Lys-Lys-Ile-Leu-Lys-Val-Leu-NH_2 **(BP143-BP13)**

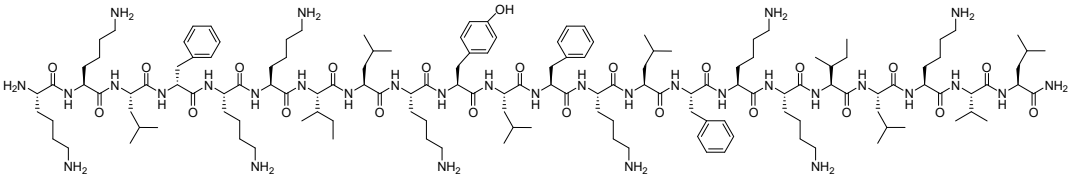

A Fmoc-Rink-ChemMatrix resin (200 mg, 0.66 mmol/g) was swollen with CH_2Cl_2 (1 x 20 min) and with DMF (1 x 20 min). Removal of the Fmoc group and coupling of the amino acids were performed using the conditions described in the above general method. The cleavage provided **BP143-BP13** in 86% HPLC purity. Elution with H_2O/CH_3CN (55:45) yielded **BP143-BP13** in >99% HPLC purity.

HPLC (λ = 220 nm): t_R = 8.23 min. ESI-MS (*m/z*): 1390.5 $[M+2H]^{2+}$, 1402.0 $[M+H+Na]^{2+}$, 2780.0 $[M+H]^+$, 2801.9 $[M+Na]^+$, 2817.8 $[M+K]^+$. HRMS (*m/z*): calculated for $C_{143}H_{249}N_{32}O_{23}$ $[M+5H]^{5+}$ 556.5854, found 556.5850; calculated for $C_{143}H_{248}N_{32}O_{23}$ $[M+4H]^{4+}$ 695.4800, found 695.4795; calculated for $C_{143}H_{247}N_{32}O_{23}$ $[M+3H]^{3+}$ 926.9708, found 926.9697; calculated for $C_{143}H_{246}N_{32}O_{23}$ $[M+2H]^{2+}$ 1389.9526, found 1389.9498.

Phe-Lys-Leu-Phe-Lys-Lys-Ile-Leu-Lys-Val-Leu-Lys-Lys-Leu-D-Phe-Lys-Lys-Ile-Leu-Lys-Tyr-Leu-NH_2 **(BP13-BP143)**

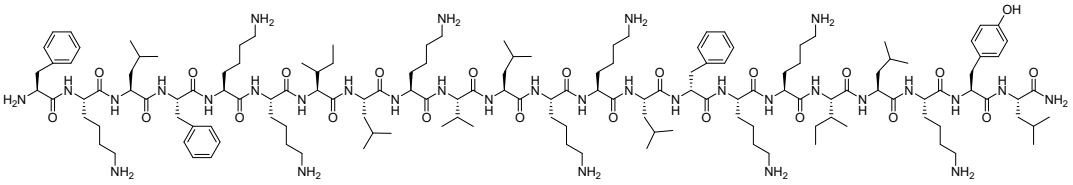

A Fmoc-Rink-ChemMatrix resin (200 mg, 0.66 mmol/g) was swollen with CH_2Cl_2 (1 x 20 min) and with DMF (1 x 20 min). Removal of the Fmoc group and coupling of the amino acids were performed using the conditions described in the above general method. The cleavage provided **BP13-BP143** in 70% HPLC purity. Elution with H_2O/CH_3CN (80:20) yielded **BP13-BP143** in >99% HPLC purity.

HPLC (λ = 220 nm): t_R = 8.22 min. ESI-MS (*m/z*): 1390.7 $[M+2H]^{2+}$, 1401.7 $[M+H+Na]^{2+}$, 1412.7 $[M+2Na]^{2+}$, 2780.3 $[M+H]^+$, 2802.3 $[M+Na]^+$. HRMS (*m/z*): calculated for $C_{143}H_{248}N_{32}O_{23}$ $[M+4H]^{4+}$ 695.48.00, found 695.4786; calculated for $C_{143}H_{247}N_{32}O_{23}$ $[M+3H]^{3+}$ 926.9708, found 926.9691; calculated for $C_{143}H_{246}N_{32}O_{23}$ $[M+2H]^{2+}$ 1389.9526, found 1389.9499.

Val-Trp-Asn-Gln-Pro-Val-Arg-Gly-Phe-Lys-Val-Tyr-Glu-Lys-Lys-Leu-D-Phe-Lys-Lys-Ile-Leu-Lys-Tyr-Leu-NH_2 **(Pep13-BP143)**

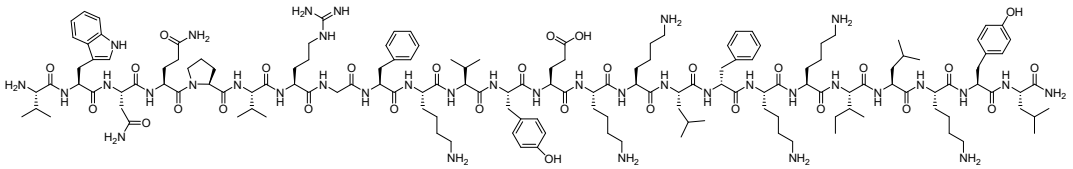

A Fmoc-Rink-ChemMatrix resin (200 mg, 0.66 mmol/g) was swollen with CH_2Cl_2 (1 x 20 min) and with DMF (1 x 20 min). Removal of the Fmoc group and coupling of the amino acids were performed using the conditions described in the above general method. The cleavage provided **Pep13-BP143** in 92% HPLC purity. Elution with H_2O/CH_3CN (70:30) yielded **Pep13-BP143** in >99% HPLC purity.

HPLC (λ = 220 nm): t_R = 7.11 min. ESI-MS (*m/z*): 605.9 $[M+5H]^{5+}$, 757.1 $[M+4H]^{4+}$, 1009.3 $[M+3H]^{3+}$, 1512.9 $[M+2H]^{2+}$, 1524.4 $[M+H+Na]^{2+}$, 1535.4 $[M+2Na]^{2+}$. HRMS (*m/z*): calculated for $C_{149}H_{240}N_{37}O_{30}$ $[M+5H]^{5+}$ 605.5673, found 605.5688; calculated for $C_{149}H_{239}N_{37}O_{30}$ $[M+4H]^{4+}$ 756.7073, found 756.7094; calculated for $C_{149}H_{238}N_{37}O_{30}$ $[M+3H]^{3+}$ 1008.6073, found 1008.6115; calculated for $C_{149}H_{237}N_{37}O_{30}$ $[M+2H]^{2+}$ 1512.4073, found 1512.4139.

Lys-Lys-Leu-D-Phe-Lys-Lys-Ile-Leu-Lys-Tyr-Leu-Val-Trp-Asn-Gln-Pro-Val-Arg-Gly-Phe-Lys-Val-Tyr-Glu-OH **(BP143-Pep13)**

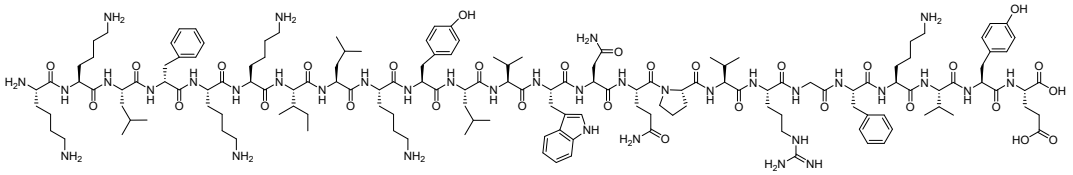

A PAC-ChemMatrix resin (200 mg, 0.66 mmol/g) was swollen with CH_2Cl_2 (1 x 20 min) and with DMF (1 x 20 min). Coupling of the amino acids and removal of the Fmoc group were performed using the conditions described in the above general method. The cleavage provided **BP143-Pep13** in 92% HPLC purity. Elution with H_2O/CH_3CN (70:30) yielded **BP143-Pep13** in >99% HPLC purity.

HPLC (λ = 220 nm): t_R = 6.92 min. ESI-MS (*m/z*): 606.1 $[M+5H]^{5+}$, 757.3 $[M+4H]^{4+}$, 1009.2 $[M+3H]^{3+}$, 1513.3 $[M+2H]^{2+}$. HRMS (*m/z*): calculated for $C_{149}H_{239}N_{36}O_{31}$ $[M+5H]^{5+}$ 605.7641, found 605.7628; calculated for $C_{149}H_{238}N_{36}O_{31}$ $[M+4H]^{4+}$ 756.9533, found 756.9520; calculated for $C_{149}H_{237}N_{36}O_{31}$ $[M+3H]^{3+}$ 1008.9353, found 1008.9342; calculated for $C_{149}H_{236}N_{36}O_{31}$ $[M+2H]^{2+}$ 1512.8993, found 1512.8990.

Arg-Ile-Asn-Ser-Ala-Lys-Asp-Asp-Ala-Ala-Gly-Leu-Gln-Ile-Ala-Lys-Lys-Leu-Phe-Lys-Lys-Ile-Leu-Lys-Lys-Leu-NH_2 **(flg15-BP16)**

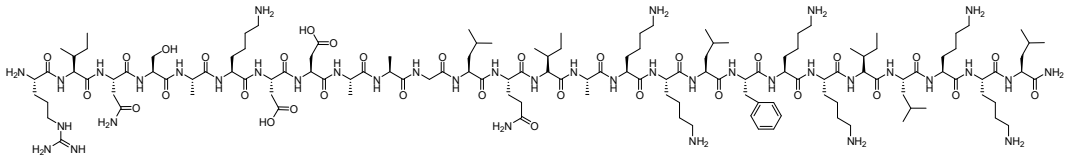

A Fmoc-Rink-ChemMatrix resin (200 mg, 0.66 mmol/g) was swollen with CH_2Cl_2 (1 x 20 min) and with DMF (1 x 20 min). Removal of the Fmoc group and coupling of the amino acids were performed using the conditions described in the above general method. The cleavage provided **flg15-BP16** in 56% HPLC purity. Elution with H_2O/CH_3CN (68:32) yielded **flg15-BP16** in >99% HPLC purity.

HPLC (λ = 220 nm): t_R = 6.94 min. ESI-MS (*m/z*): 1456.0 $[M+2H]^{2+}$, 2910.9 $[M+H]^{+}$. HRMS (*m/z*): calculated for $C_{133}H_{239}N_{39}O_{33}$ $[M+2H]^{2+}$ 1455.9120, found 1455.9087; calculated for $C_{133}H_{238}N_{39}O_{33}Na$ $[M+H+Na]^{2+}$ 1466.9030, found 1466.9029; calculated for $C_{133}H_{237}N_{39}O_{33}Na_2$ $[M+2Na]^{2+}$ 1477.8939, found 1477.8917.

Lys-Lys-Leu-Phe-Lys-Lys-Ile-Leu-Lys-Lys-Leu-Arg-Ile-Asn-Ser-Ala-Lys-Asp-Asp-Ala-Ala-Gly-Leu-Gln-Ile-Ala-OH **(BP16-flg15)**

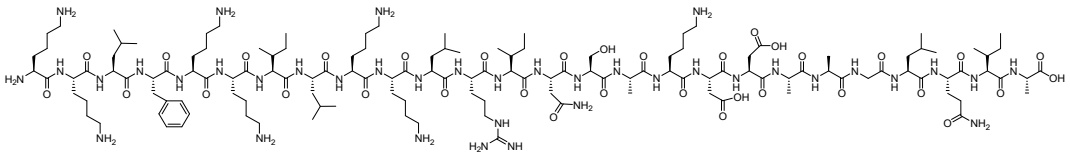

A PAC-ChemMatrix resin (200 mg, 0.66 mmol/g) was swollen with CH_2Cl_2 (1 x 20 min) and with DMF (1 x 20 min). Coupling of the amino acids and removal of the Fmoc group were performed using the conditions described in the above general method. The cleavage provided **BP16-flg15** in 75% HPLC purity. Elution with H_2O/CH_3CN (80:20) yielded **BP359 (BP16-flg15)** in >99% HPLC purity.

HPLC (λ = 220nm): t_R = 6.04 min. ESI-MS (*m/z*): 971.4 $[M+3H]^{3+}$, 986.2 $[M+H+2Na]^{3+}$, 993.7 $[M+3Na]^{3+}$, 1456.5 $[M+2H]^{2+}$, 1467.5 $[M+H+Na]^{2+}$, 1478.9 $[M+2Na]^{2+}$. HRMS (*m/z*): calculated for $C_{133}H_{238}N_{38}O_{34}$ $[M+2H]^{2+}$ 1456.4040, found 1456.4023; calculated for $C_{133}H_{237}N_{38}O_{34}Na$ $[M+H+Na]^{2+}$ 1467.3950, found 1467.3915.

Lys-Lys-Val-Val-Phe-Trp-Val-Lys-Phe-Lys-Arg-Ile-Asn-Ser-Ala-Lys-Asp-Asp-Ala-Ala-Gly-Leu-Gln-Ile-Ala-OH
(KSLW-flg15)

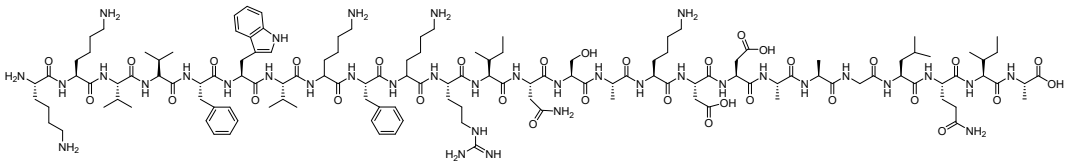

A PAC-ChemMatrix resin (200 mg, 0.66 mmol/g) was swollen with CH_2Cl_2 (1 x 20 min) and with DMF (1 x 20 min). Coupling of the amino acids and removal of the Fmoc group were performed using the conditions described in the above general method. The cleavage provided **KSLW-flg15** in 69% HPLC purity. Elution with H_2O/CH_3CN (75:25) yielded **KSLW-flg15** in >99% HPLC purity.

HPLC (λ = 220 nm): t_R = 6.47 min. ESI-MS (*m/z*): 1417.5 $[M+2H]^{2+}$, 2833.7 $[M+H]^{+}$. HRMS (*m/z*): calculated for $C_{132}H_{216}N_{36}O_{33}$ $[M+2H]^{2+}$ 1417.3174, found 1417.3209; calculated for $C_{132}H_{215}N_{36}O_{33}Na$ $[M+H+Na]^{2+}$ 1428.3084, found 1428.3120.

Arg-Ile-Asn-Ser-Ala-Lys-Asp-Asp-Ala-Ala-Gly-Leu-Gln-Ile-Ala-Lys-Lys-Val-Val-Phe-Trp-Val-Lys-Phe-Lys-NH_2
(flg15-KSLW)

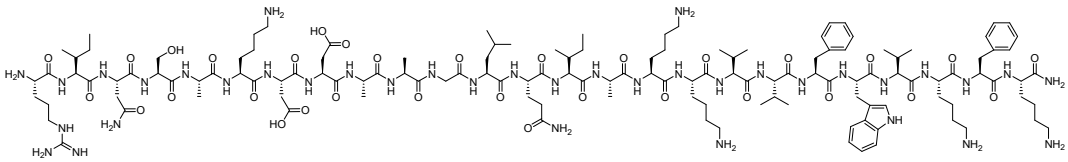

A Fmoc-Rink-ChemMatrix resin (200 mg, 0.66 mmol/g) was swollen with CH_2Cl_2 (1 x 20 min) and with DMF (1 x 20 min). Removal of the Fmoc group and coupling of the amino acids were performed using the conditions described in the above general method. The cleavage provided **flg15-KSLW** in 49% HPLC purity. Elution with H_2O/CH_3CN (75:25) yielded **flg15-KSLW** in >99% HPLC purity.

HPLC (λ = 220 nm): t_R = 6.59 min. ESI-MS (*m/z*): 1416.3 $[M+2H]^{2+}$, 1427.2 $[M+H+Na]^{2+}$, 1438.7 $[M+2Na]^{2+}$. HRMS (*m/z*): calculated for $C_{132}H_{217}N_{37}O_{32}$ $[M+2H]^{2+}$ 1416.8254, found 1416.8202; calculated for $C_{132}H_{216}N_{37}O_{32}Na$ $[M+H+Na]^{2+}$ 1427.8164, found 1427.8106; calculated for $C_{132}H_{215}N_{37}O_{32}Na_2$ $[M+2Na]^{2+}$ 1438.8073, found 1438.8016.

Lys-Lys-Leu-Phe-Lys-Lys-Ile-Leu-Lys-Tyr-Leu-Lys-Lys-Val-Val-Phe-Trp-Val-Lys-Phe-Lys-NH_2 **(BP100-KSLW)**

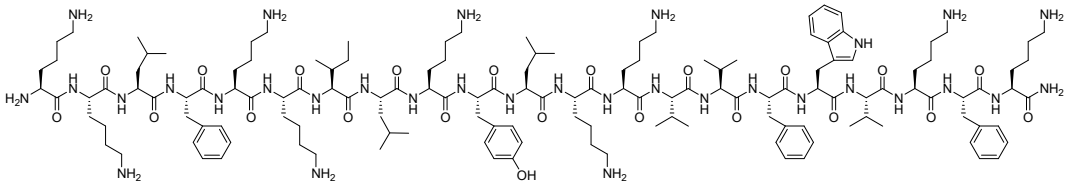

A Fmoc-Rink-ChemMatrix resin (200 mg, 0.66 mmol/g) was swollen with CH_2Cl_2 (1 x 20 min) and with DMF (1 x 20 min). Removal of the Fmoc group and coupling of the amino acids were performed using the conditions described in the above general method. The cleavage provided **BP100-KSLW** in 60% HPLC purity. Elution with H_2O/CH_3CN (71:29) yielded **BP100-KSLW** in >99% HPLC purity.

HPLC (λ = 220 nm): t_R = 6.91 min. ESI-MS (*m/z*): 904.7 $[M+3H]^{3+}$, 1355.9 $[M+2H]^{2+}$, 1366.9 $[M+H+Na]^{2+}$, 1377.8 $[M+2Na]^{2+}$. HRMS (*m/z*): calculated for $C_{140}H_{230}N_{32}O_{22}$ $[M+2H]^{2+}$ 1356.3941, found 1356.3920; calculated for $C_{140}H_{229}N_{32}O_{22}Na$ $[M+H+Na]^{2+}$ 1367.3850, found 1367.3825; calculated for $C_{140}H_{228}N_{32}O_{22}Na_2$ $[M+2Na]^{2+}$ 1378.3760, found 1378.3774.

Lys-Lys-Val-Val-Phe-Trp-Val-Lys-Phe-Lys-Lys-Lys-Leu-Phe-Lys-Lys-Ile-Leu-Lys-Tyr-Leu-NH_2 **(KSLW-BP100)**

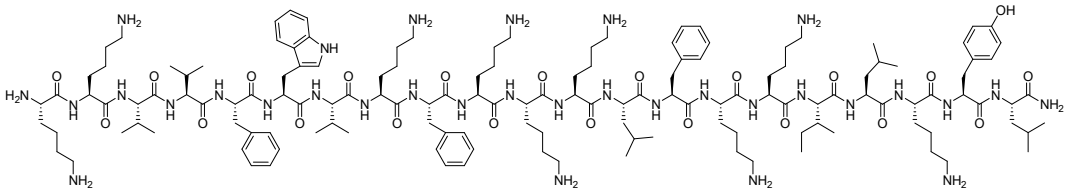

A Fmoc-Rink-ChemMatrix resin (200 mg, 0.66 mmol/g) was swollen with CH_2Cl_2 (1 x 20 min) and with DMF (1 x 20 min). Removal of the Fmoc group and coupling of the amino acids were performed using the conditions described in the above general method. The cleavage provided **KSLW-BP100** in 75% HPLC purity. Elution with H_2O/CH_3CN (80:20) yielded **KSLW-BP100** in >99% HPLC purity.

HPLC (λ = 220 nm): t_R = 6.74 min. ESI-MS (*m/z*): 1356.4 $[M+2H]^{2+}$, 1368.0 $[M+H+Na]^{2+}$, 2711.9 $[M+H]^{+}$, 2733.8 $[M+Na]^{+}$. HRMS (*m/z*): calculated for $C_{140}H_{230}N_{32}O_{22}$ $[M+2H]^{2+}$ 1356.3941, found 1356.3937; calculated for $C_{140}H_{229}N_{32}O_{22}Na$ $[M+H+Na]^{2+}$ 1367.3850, found 1367.3851; calculated for $C_{140}H_{228}N_{32}O_{22}Na_2$ $[M+2Na]^{2+}$ 1378.3760, found 1378.3778.

Phe-Lys-Leu-Phe-Lys-Lys-Ile-Leu-Lys-Val-Leu-Lys-Lys-Val-Val-Phe-Trp-Val-Lys-Phe-Lys-NH_2 **(BP13-KSLW)**

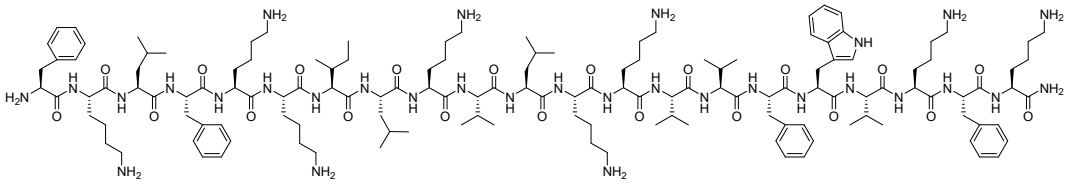

A Fmoc-Rink-ChemMatrix resin (200 mg, 0.66 mmol/g) was swollen with CH_2Cl_2 (1 x 20 min) and with DMF (1 x 20 min). Removal of the Fmoc group and coupling of the amino acids were performed using the conditions described in the above general method. The cleavage provided **BP13-KSLW** in 60% HPLC purity. Elution with H_2O/CH_3CN (67:33) yielded **BP13-KSLW** in >99% HPLC purity.

HPLC (λ = 220 nm): t_R = 7.49 min. ESI-MS (*m/z*): 1334.5 $[M+2H]^{2+}$, 1345.5 $[M+H+Na]^{2+}$, 1356.0 $[M+2Na]^{2+}$, 2667.0 $[M+H]^{+}$, 2688.9 $[M+Na]^{+}$. HRMS (*m/z*): calculated for $C_{139}H_{227}N_{31}O_{21}$ $[M+2H]^{2+}$ 1333.8833, found 1333.8812, calculated for $C_{139}H_{226}N_{31}O_{21}Na$ $[M+H+Na]^{2+}$ 1344.8743, found 1344.8720; calculated for $C_{139}H_{225}N_{31}O_{21}Na_2$ $[M+2Na]^{2+}$ 1355.8653, found 1355.8654.

Lys-Lys-Val-Val-Phe-Trp-Val-Lys-Phe-Lys-Phe-Lys-Leu-Phe-Lys-Lys-Ile-Leu-Lys-Val-Leu-NH_2 **(KSLW-BP13)**

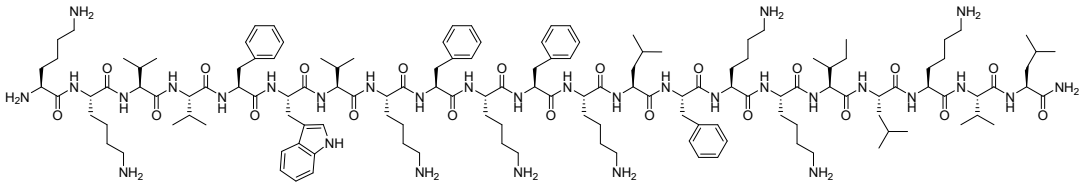

A Fmoc-Rink-ChemMatrix resin (200 mg, 0.66 mmol/g) was swollen with CH_2Cl_2 (1 x 20 min) and with DMF (1 x 20 min). Removal of the Fmoc group and coupling of the amino acids were performed using the conditions described in the above general method. The cleavage provided **KSLW-BP13** in 86% HPLC purity. Elution with H_2O/CH_3CN (70:30) yielded **KSLW-BP13** in >99% HPLC purity.

HPLC (λ = 220 nm): t_R = 7.03 min. ESI-MS (*m/z*): 2666.8 $[M+H]^{+}$, 2688.7 $[M+Na]^{+}$, 2705.7 $[M+K]^{+}$. HRMS (*m/z*): calculated for $C_{139}H_{227}N_{31}O_{21}$ $[M+2H]^{2+}$ 1333.8833, found 1333.8801; calculated for $C_{139}H_{226}N_{31}O_{21}Na$ $[M+H+Na]^{2+}$ 1344.8743, found 1344.8711.

Lys-Lys-Val-Val-Phe-Trp-Val-Lys-Phe-Lys-Tyr-Gly-Ile-His-Thr-His-NH_2 **(KSLW-Pip1)**

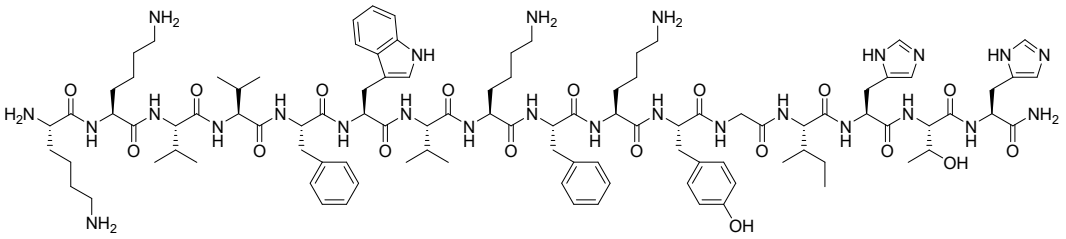

A Fmoc-Rink-ChemMatrix resin (200 mg, 0.66 mmol/g) was swollen with CH_2Cl_2 (1 x 20 min) and with DMF (1 x 20 min). Removal of the Fmoc group and coupling of the amino acids were performed using the conditions described in the above general method. The cleavage provided **KSLW-Pip1** in 47% HPLC purity. Elution with H_2O/CH_3CN (75:25) yielded **KSLW-Pip1** in >99% HPLC purity.

HPLC (λ = 220 nm): t_R = 6.17 min. ESI-MS (*m/z*): 1009.1 $[M+2H]^{2+}$, 2017.2 $[M+H]^+$, 2039.1 $[M+Na]^+$. HRMS (*m/z*): calculated for $C_{101}H_{152}N_{26}O_{18}$ $[M+2H]^{2+}$ 1008.5883, found 1008.5871; calculated for $C_{101}H_{151}N_{26}O_{18}$ $[M+H]^+$ 2016.1694, found 2016.1636.

Tyr-Gly-Ile-His-Thr-His-Lys-Lys-Val-Val-Phe-Trp-Val-Lys-Phe-Lys-NH_2 **(Pip1-KSLW)**

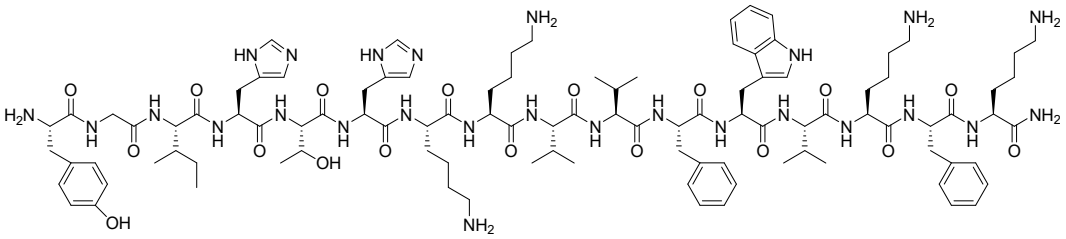

A Fmoc-Rink-ChemMatrix resin (200 mg, 0.66 mmol/g) was swollen with CH_2Cl_2 (1 x 20 min) and with DMF (1 x 20 min). Removal of the Fmoc group and coupling of the amino acids were performed using the conditions described in the above general method. The cleavage provided **Pip1-KSLW** in 78% HPLC purity. Elution with H_2O/CH_3CN (77:23) yielded **Pip1-KSLW** in >99% HPLC purity.

HPLC (λ = 220 nm): t_R = 6.15 min. ESI-MS (*m/z*): 1009.1 $[M+2H]^{2+}$, 2017.2 $[M+H]^+$, 2039.2 $[M+Na]^+$. HRMS (*m/z*): calculated for $C_{101}H_{152}N_{26}O_{18}$ $[M+2H]^{2+}$ 1008.5883, found 1008.5881; calculated for $C_{101}H_{151}N_{26}O_{18}$ $[M+H]^+$ 2016.1694, found 2016.1636.

Lys-Lys-Val-Val-Phe-Trp-Val-Lys-Phe-Lys-Lys-Lys-Leu-Phe-Lys-Lys-Ile-Leu-Lys-Lys-Leu-NH_2 **(KSLW-BP16)**

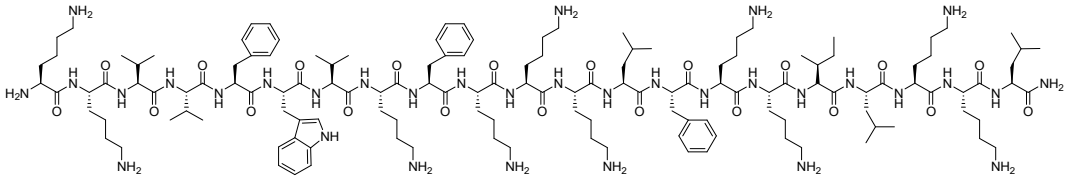

A Fmoc-Rink-ChemMatrix resin (200 mg, 0.66 mmol/g) was swollen with CH_2Cl_2 (1 x 20 min) and with DMF (1 x 20 min). Removal of the Fmoc group and coupling of the amino acids were performed using the conditions described in the above general method. The cleavage provided **KSLW-BP16** in 68% HPLC purity. Elution with H_2O/CH_3CN (70:30) yielded **KSLW-BP16** in >99% HPLC purity.

HPLC (λ = 220 nm): t_R = 6.53 min. ESI-MS (*m/z*): 1339.0 $[M+2H]^{2+}$, 1349.9 $[M+H+Na]^{2+}$, 1360.9 $[M+2Na]^{2+}$, 2676.8 $[M+H]^+$, 2698.8 $[M+Na]^+$, 2714.7 $[M+K]^+$. HRMS (*m/z*): calculated for $C_{137}H_{233}N_{33}O_{21}$ $[M+2H]^{2+}$ 1338.4084, found 1338.4063.

Lys-Lys-Leu-Phe-Lys-Lys-Ile-Leu-Lys-Lys-Leu-Lys-Lys-Val-Val-Phe-Trp-Val-Lys-Phe-Lys-NH_2 **(BP16-KSLW)**

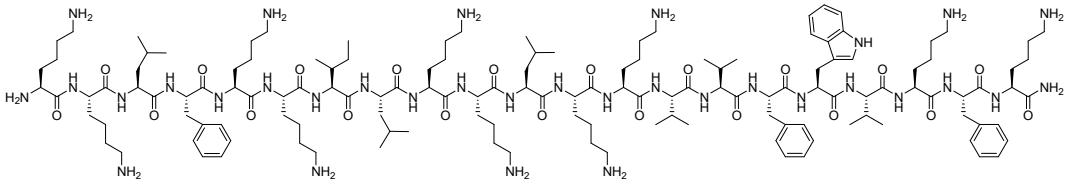

A Fmoc-Rink-ChemMatrix resin (200 mg, 0.66 mmol/g) was swollen with CH_2Cl_2 (1 x 20 min) and with DMF (1 x 20 min). Removal of the Fmoc group and coupling of the amino acids were performed using the conditions described in the above general method. The cleavage provided **BP16-KSLW** in 54% HPLC purity. Elution with H_2O/CH_3CN (81:19) yielded **BP16-KSLW** in >99% HPLC purity.

HPLC (λ = 220 nm): t_R = 6.61 min. ESI-MS (*m/z*): 893.0 $[M+3H]^{3+}$, 1338.9 $[M+2H]^{2+}$, 2676.9 $[M+H]^+$. HRMS (*m/z*): calculated for $C_{137}H_{233}N_{33}O_{21}$ $[M+2H]^{2+}$ 1338.4084, found 1338.4056.

Phe-Lys-Leu-Phe-Lys-Lys-Ile-Leu-Lys-Val-Leu-Lys-Lys-Leu-Phe-Lys-Lys-Ile-Leu-Lys-Lys-Leu-NH_2 **(BP13-BP16)**

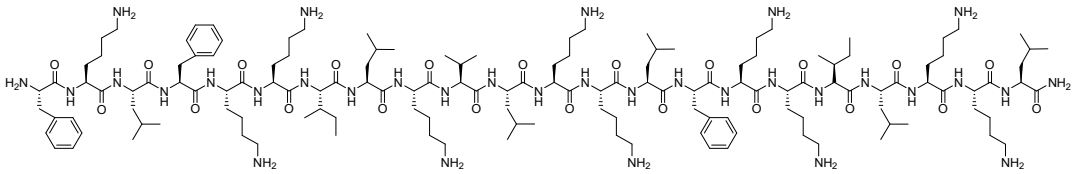

A Fmoc-Rink-ChemMatrix resin (200 mg, 0.66 mmol/g) was swollen with CH_2Cl_2 (1 x 20 min) and with DMF (1 x 20 min). Removal of the Fmoc group and coupling of the amino acids were performed using the conditions described in the above general method. The cleavage provided **BP13-BP16** in 82% HPLC purity. Elution with H_2O/CH_3CN (61:39) yielded **BP13-BP16** in >99% HPLC purity.

HPLC (λ = 220 nm): t_R = 8.05 min. ESI-MS (*m/z*): 1373.1 $[M+2H]^{2+}$, 1384.5 $[M+H+Na]^{2+}$, 2745.1 $[M+H]^+$, 2767.0 $[M+Na]^+$. HRMS (*m/z*): calculated for $C_{140}H_{249}N_{33}O_{22}$ $[M+2H]^{2+}$ 1372.4684, found 1372.4666.

Lys-Lys-Leu-Phe-LysLys-Ile-Leu-Lys-Lys-Leu-Phe-Lys-Leu-Phe-Lys-Lys-Ile-Leu-Lys-Val-Leu-NH_2 **(BP16-BP13)**

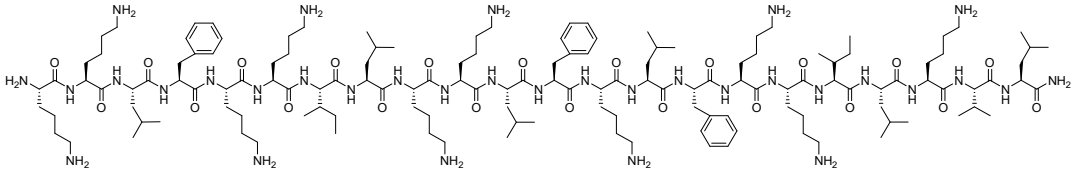

A Fmoc-Rink-ChemMatrix resin (200 mg, 0.66 mmol/g) was swollen with CH_2Cl_2 (1 x 20 min) and with DMF (1 x 20 min). Removal of the Fmoc group and coupling of the amino acids were performed using the conditions described in the above general method. The cleavage provided **BP16-BP13** in 73% HPLC purity. Elution with H_2O/CH_3CN (66:34) yielded **BP16-BP13** in >99% HPLC purity.

HPLC (λ = 220 nm): t_R = 8.04 min. ESI-MS (*m/z*): 1373.1 $[M+2H]^{2+}$, 1384.1 $[M+H+Na]^{2+}$, 2745.1 $[M+H]^+$, 2767.0 $[M+Na]^+$. HRMS (*m/z*): calculated for $C_{140}H_{249}N_{33}O_{22}$ $[M+2H]^{2+}$ 1372.4684, found 1372.4627.

Val-Trp-Asn-Gln-Pro-Val-Arg-Gly-Phe-Lys-Val-Tyr-Glu-Lys-Lys-Leu-Phe-Lys-Lys-Ile-Leu-Lys-Lys-Leu-NH_2 (**Pep13-BP16)**

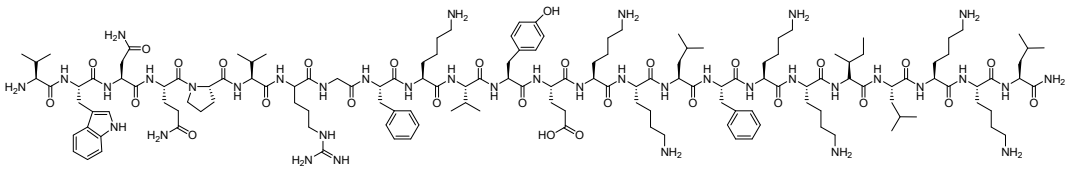

A Fmoc-Rink-ChemMatrix resin (200 mg, 0.66 mmol/g) was swollen with CH_2Cl_2 (1 x 20 min) and with DMF (1 x 20 min). Removal of the Fmoc group and coupling of the amino acids were performed using the conditions described in the above general method. The cleavage provided **Pep13-BP16** in 77% HPLC purity. Elution with H_2O/CH_3CN (72:28) yielded **Pep13-BP16** in >99% HPLC purity.

HPLC (λ = 220 nm): t_R = 6.63 min. ESI-MS (*m/z*): 1495.5 $[M+2H]^{2+}$, 2989.9 $[M+H]^+$. HRMS (*m/z*): calculated for $C_{146}H_{240}N_{38}O_{29}$ $[M+2H]^{2+}$ 1494.9231, found 1494.9216.

Lys-Lys-Leu-Phe-Lys-Lys-Ile-Leu-Lys-Lys-Leu-Val-Trp-Asn-Gln-Pro-Val-Arg-Gly-Phe-Lys-Val-Tyr-Glu-OH **(BP16-Pep13)**

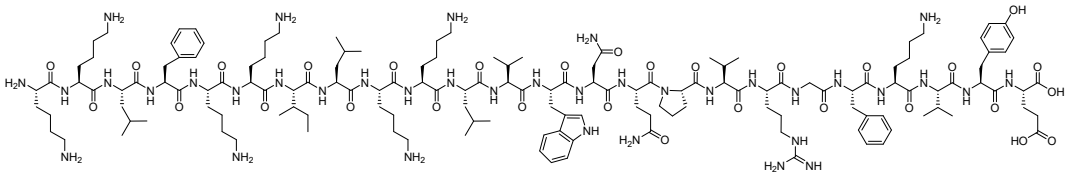

A PAC-ChemMatrix resin (200 mg, 0.66 mmol/g) was swollen with CH_2Cl_2 (1 x 20 min) and with DMF (1 x 20 min). Removal of the Fmoc group and coupling of the amino acids were performed using the conditions described in the above general method. The cleavage provided **BP16-Pep13** in 84% purity. Elution with H_2O/CH_3CN (75:25) yielded **BP16-Pep13** in >99% HPLC purity.

HPLC (λ = 220 nm): t_R = 6.24 min. ESI-MS (*m/z*): 1496.5 $[M+2H]^{2+}$, 2991.8 $[M+H]^+$. HRMS (*m/z*): calculated for $C_{146}H_{239}N_{37}O_{30}$ $[M+2H]^{2+}$ 1495.4151, found 1495.4161.

Phe-Lys-Leu-Phe-Lys-Lys-Ile-Leu-Lys-Val-Leu-Lys-Lys-Leu-Phe-Lys-Lys-Ile-Leu-Lys-Tyr-Leu-NH_2 **(BP13-BP100)**

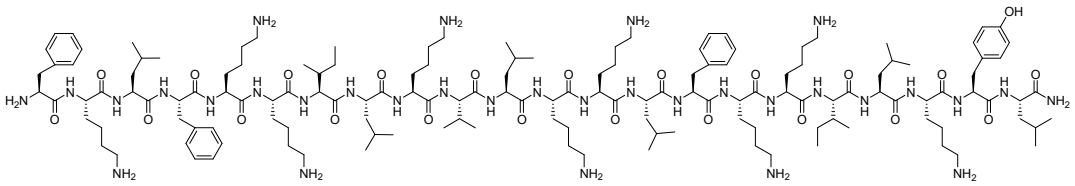

A Fmoc-Rink-ChemMatrix resin (200 mg, 0.66 mmol/g) was swollen with CH_2Cl_2 (1 x 20 min) and with DMF (1 x 20 min). Removal of the Fmoc group and coupling of the amino acids were performed using the conditions described in the above general method. The cleavage provided **BP13-BP100** in 51% HPLC purity. Elution with H_2O/CH_3CN (65:35) yielded **BP13-BP100** in >99% HPLC purity.

HPLC (λ = 220 nm): t_R = 8.29 min. ESI-MS (*m/z*): 927.4 $[M+3H]^{3+}$, 934.8 $[M+2H+Na]^{3+}$, 1390.6 $[M+2H]^{2+}$, 1401.6 $[M+H+Na]^{2+}$, 1412.6 $[M+2Na]^{2+}$. HRMS (*m/z*): calculated for $C_{143}H_{248}N_{32}O_{23}$ $[M+4H]^{4+}$ 695.4800, found 695.4794; calculated for $C_{143}H_{247}N_{32}O_{23}$ $[M+3H]^{3+}$ 926.9708, found 926.9693; calculated for $C_{143}H_{246}N_{32}O_{23}$ $[M+2H]^{2+}$ 1389.9526, found 1389.9360.

Lys-Lys-Leu-Phe-Lys-Lys-Ile-Leu-Lys-Tyr-Leu-Phe-Lys-Leu-Phe-Lys-Lys-Ile-Leu-Lys-Val-Leu-NH_2 **(BP100-BP13)**

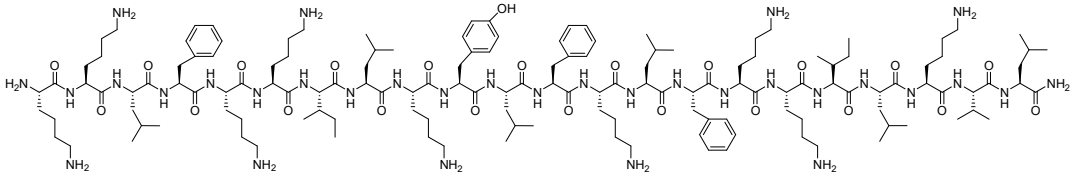

A Fmoc-Rink-ChemMatrix resin (200 mg, 0.66 mmol/g) was swollen with CH_2Cl_2 (1 x 20 min) and with DMF (1 x 20 min). Removal of the Fmoc group and coupling of the amino acids were performed using the conditions described in the above general method. The cleavage provided **BP100-BP13** in 72% HPLC purity. Elution with H_2O/CH_3CN (62:38) yielded **BP100-BP13** in >99% HPLC purity.

HPLC (λ = 220 nm): t_R = 8.18 min. ESI-MS (*m/z*): 1390.6 $[M+2H]^{2+}$, 1401.6 $[M+H+Na]^{2+}$, 1412.6 $[M+2Na]^{2+}$, 2780.2 $[M+H]^{+}$, 2802.2 $[M+Na]^{+}$. HRMS (*m/z*): calculated for $C_{143}H_{248}N_{32}O_{23}$ $[M+4H]^{4+}$ 695.4800, found 695.4811; calculated for $C_{143}H_{247}N_{32}O_{23}$ $[M+3H]^{3+}$ 926.9708, found 926.9719; calculated for $C_{143}H_{246}N_{32}O_{23}$ $[M+2H]^{2+}$ 1389.9526, found 1389.9537.

Lys-Lys-Leu-Phe-Lys-Lys-Ile-Leu-Lys-Tyr-Leu-Arg-Ile-Asn-Ser-Ala-Lys-Asp-Asp-Ala-Ala-Gly-Leu-Gln-Ile-Ala-OH **(BP100-flg15)**

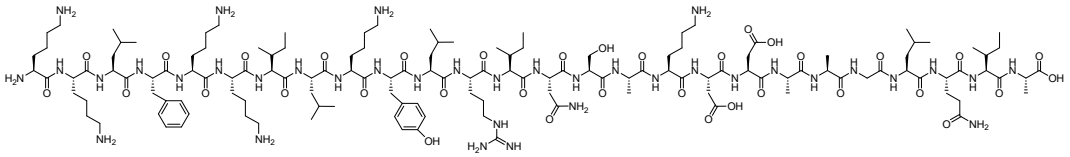

A PAC-ChemMatrix resin (200 mg, 0.66 mmol/g) was swollen with CH_2Cl_2 (1 x 20 min) and with DMF (1 x 20 min). Coupling of the amino acids and removal of the Fmoc group were performed using the conditions described in the above general method. The cleavage provided **BP100-flg15** in 97% HPLC purity. Elution with H_2O/CH_3CN (68:32) yielded **BP100-flg15** in >99% HPLC purity.

HPLC (λ = 220 nm): t_R = 6.36 min. ESI-MS (*m/z*): 983.0 $[M+3H]^{3+}$, 990.6 $[M+2H+Na]^{3+}$, 1473.9 $[M+2H]^{2+}$, 1484.9 $[M+H+Na]^{2+}$, 2945.8 $[M+H]^{+}$. HRMS (*m/z*): calculated for $C_{136}H_{236}N_{37}O_{35}$ $[M+3H]^{3+}$ 982.5936, found 982.5964; calculated for $C_{136}H_{235}N_{37}O_{35}$ $[M+2H]^{2+}$ 1473.3868, found 1473.3903.

Arg-Ile-Asn-Ser-Ala-Lys-Asp-Asp-Ala-Ala-Gly-Leu-Gln-Ile-Ala-Lys-Lys-Leu-Phe-Lys-Lys-Ile-Leu-Lys-Tyr-Leu-NH_2 **(flg15-BP100)**

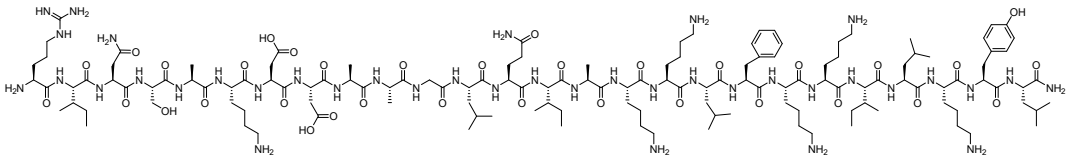

A Fmoc-Rink-ChemMatrix resin (200 mg, 0.66 mmol/g) was swollen with CH_2Cl_2 (1 x 20 min) and with DMF (1 x 20 min). Removal of the Fmoc group and coupling of the amino acids were performed using the conditions described in the above general method. The cleavage provided **flg15-BP100** in >99% HPLC purity. Elution with H_2O/CH_3CN (67:33) yielded **flg15-BP100** in >99% HPLC purity.

HPLC (λ = 220 nm): t_R = 7.02 min. ESI-MS (*m/z*): 590.0 $[M+5H]^{5+}$, 737.3 $[M+4H]^{4+}$, 982.6 $[M+3H]^{3+}$, 1473.3 $[M+2H]^{2+}$, 1484.8 $[M+H+Na]^{2+}$, 2944.8 $[M+H]^{+}$, 2966.7 $[M+Na]^{+}$. HRMS (*m/z*): calculated for $C_{136}H_{237}N_{38}O_{34}$ $[M+3H]^{3+}$ 982.2656, found 982.2687; calculated for $C_{136}H_{236}N_{38}O_{34}$ $[M+2H]^{2+}$ 1472.8948, found 1472.8977.

Lys-Lys-Leu-Phe-Lys-Lys-Ile-Leu-Lys-Tyr-Leu-Val-Trp-Asn-Gln-Pro-Val-Arg-Gly-Phe-Lys-Val-Tyr-Glu-OH (**BP100-Pep13)**

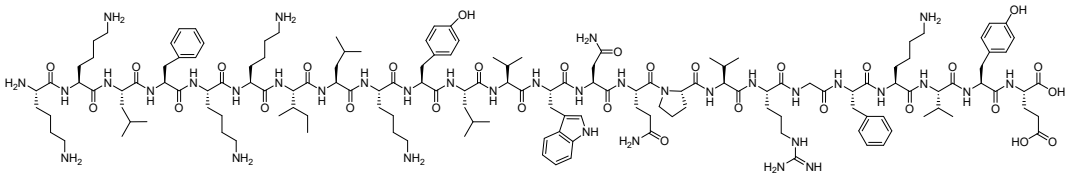

A PAC-ChemMatrix resin (200 mg, 0.66 mmol/g) was swollen with CH_2Cl_2 (1 x 20 min) and with DMF (1 x 20 min). Coupling of the amino acids and removal of the Fmoc group were performed using the conditions described in the above general method. The cleavage provided **BP100-Pep13** in >99% HPLC purity. Elution with H_2O/CH_3CN (75:25) yielded **BP100-Pep13** in >99% HPLC purity.

HPLC (λ = 220 nm): t_R = 6.44 min. ESI-MS (*m/z*): 606.0 $[M+5H]^{5+}$, 757.2 $[M+4H]^{4+}$, 1009.3 $[M+3H]^{3+}$, 1513.9 $[M+2H]^{2+}$, 1524.8 $[M+H+Na]^{2+}$, 1535.9 $[M+2Na]^{2+}$. HRMS (*m/z*): calculated for $C_{149}H_{238}N_{36}O_{31}$ $[M+4H]^{4+}$ 756.9533, found 756.9535; calculated for $C_{149}H_{237}N_{36}O_{31}$ $[M+3H]^{3+}$ 1008.9353, found 1008.9335; calculated for $C_{149}H_{236}N_{36}O_{31}$ $[M+2H]^{2+}$ 1512.8993, found 1512.8950.

Val-Trp-Asn-Gln-Pro-Val-Arg-Gly-Phe-Lys-Val-Tyr-Glu-Lys-Lys-Leu-Phe-Lys-Lys-Ile-Leu-Lys-Tyr-Leu-NH_2 **(Pep13-BP100)**

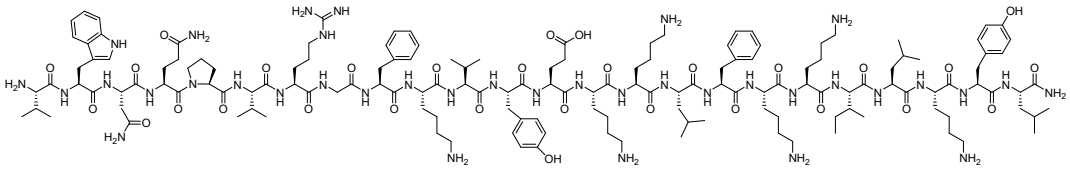

A Fmoc-Rink-ChemMatrix resin (200 mg, 0.66 mmol/g) was swollen with CH_2Cl_2 (1 x 20 min) and with DMF (1 x 20 min). Removal of the Fmoc group and coupling of the amino acids were performed using the conditions described in the above general method. The cleavage provided **Pep13-BP100** in 88% HPLC purity. Elution with H_2O/CH_3CN (72:28) yielded **Pep13-BP100** in >99% HPLC purity.

HPLC (λ = 220 nm): t_R = 6.85 min. ESI-MS (*m/z*): 1009.2 $[M+3H]^{3+}$, 1016.6 $[M+2H+Na]^{3+}$, 1512.9 $[M+2H]^{2+}$, 1523.9 $[M+H+Na]^{2+}$. HRMS (*m/z*): calculated for $C_{149}H_{239}N_{37}O_{30}$ $[M+4H]^{4+}$ 756.7073, found 756.7061; calculated for $C_{149}H_{238}N_{37}O_{30}$ $[M+3H]^{3+}$ 1008.6073, found 1008.6047; calculated for $C_{149}H_{237}N_{37}O_{30}$ $[M+2H]^{2+}$ 1512.4073, found 1512.4007.

Lys-Lys-Val-Val-Phe-Trp-Val-Lys-Phe-Lys-Val-Trp-Asn-Gln-Pro-Val-Arg-Gly-Phe-Lys-Val-Tyr-Glu-OH **(KSLW-Pep13)**

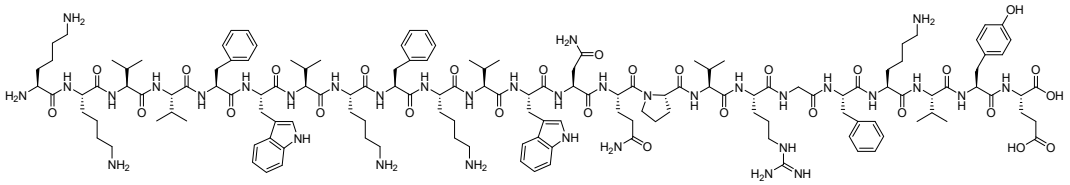

A PAC-ChemMatrix resin (200 mg, 0.66 mmol/g) was swollen with CH_2Cl_2 (1 x 20 min) and with DMF (1 x 20 min). Coupling of the amino acids and removal of the Fmoc group were performed using the conditions described in the above general method. The cleavage provided **KSLW-Pep13** in 73% HPLC purity. Elution with H_2O/CH_3CN (80:20) yielded **KSLW-Pep13** in >99% HPLC purity.

HPLC (λ = 220 nm): t_R = 6.66 min. ESI-MS (*m/z*): 971.6 $[M+3H]^{3+}$, 978.9 $[M+2H+Na]^{3+}$, 1456.8 $[M+2H]^{2+}$, 1467.8 $[M+H+Na]^{2+}$. HRMS (*m/z*): calculated for $C_{145}H_{219}N_{35}O_{29}$ $[M+4H]^{4+}$ 728.6679, found 728.6690; calculated for $C_{145}H_{218}N_{35}O_{29}$ $[M+3H]^{3+}$ 971.2214, found 971.2214; calculated for $C_{145}H_{217}N_{35}O_{29}$ $[M+2H]^{2+}$ 1456.3285, found 1456.3288.

Val-Trp-Asn-Gln-Pro-Val-Arg-Gly-Phe-Lys-Val-Tyr-Glu-Lys-Lys-Val-Val-Phe-Trp-Val-Lys-Phe-Lys-NH_2

(Pep13-KSLW)

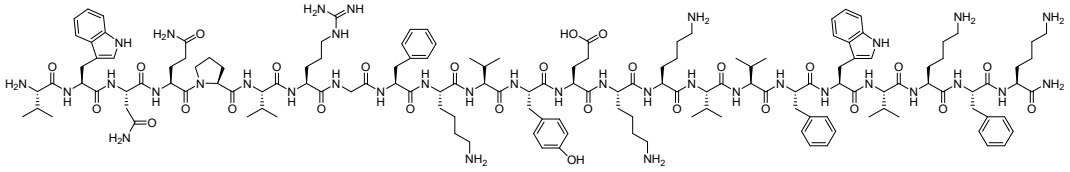

A Fmoc-Rink-ChemMatrix resin (200 mg, 0.66 mmol/g) was swollen with CH_2Cl_2 (1 x 20 min) and with DMF (1 x 20 min). Removal of the Fmoc group and coupling of the amino acids were performed using the conditions described in the above general method. The cleavage provided **Pep13-KSLW** in 77% HPLC purity. Elution with H_2O/CH_3CN (84:16) yielded **Pep13-KSLW** in >99% HPLC purity.

HPLC (λ = 220 nm): t_R = 6.75 min. ESI-MS (*m/z*): 1456.5 $[M+2H]^{2+}$, 2910.8 $[M+H]^{+}$. HRMS (*m/z*): calculated for $C_{145}H_{221}N_{36}O_{28}$ $[M+5H]^{5+}$ 582.9390, found 582.9387; calculated for $C_{145}H_{220}N_{36}O_{28}$ $[M+4H]^{4+}$ 728.4219, found 728.4214; calculated for $C_{145}H_{219}N_{36}O_{28}$ $[M+3H]^{3+}$ 970.8934, found 970.8935; calculated for $C_{145}H_{218}N_{36}O_{28}$ $[M+2H]^{2+}$ 1455.8365, found 1455.8384.

5.5. Synthesis of the cyclic decapeptides containing a tryptophan

5.5.1. Synthesis of the linear decapeptides library protected at the N- and C-terminus

The MBHA resin (200 mg, 0.4 mmol/g) was swollen with CH_2Cl_2 (1 × 20 min) and DMF (1 × 20 min), and washed with piperidine/DMF (3:7, 1 × 5 min), DMF (6 × 1 min) and CH_2Cl_2 (3 × 1 min). Then, the resin was treated with Fmoc-Rink-amide linker (4 equiv), Oxyma (4 equiv) and DIPCDI (4 equiv) in DMF overnight.

After this time, the resin was washed with DMF (6 × 1 min) and CH_2Cl_2 (3 × 1 min). After Fmoc removal with piperidine/DMF (3:7, 2 + 10 min) and washes with DMF (6 x 1 min) and CH_2Cl_2 (2 x 1 min), Fmoc-Glu-OAll (4 equiv) was coupled using Oxyma (4 equiv) and DIPCDI (4 equiv). This trifunctional amino acid allows peptide anchoring into the solid support and results in a Gln residue after peptide cleavage. The elongation of the peptide sequence was performed by sequential Fmoc removal and coupling steps. After the sixth coupling, NMP was employed instead of DMF. Once the linear sequence was completed, an aliquot of the resin was treated with TFA/phenol/H_2O/TIS (92.5:2.5:2.5:2.5) for 1.5 h. In this case, phenol was used to avoid the alkylation of the Trp residue of the sequence. The acidic solution was then removed using nitrogen and after diethyl ether extraction, the linear peptides were analysed by HPLC and characterized by ESI-MS.

Fmoc-Lys-Lys-Leu-Leu-Lys-Trp-Leu-Lys-Lys-Gln-OAll

HPLC (λ = 220 nm): t_R = 7.21 min (98% purity). ESI-MS (*m/z*): 526.0 $[M+3H]^{3+}$, 788.5 $[M+2H]^{2+}$, 799.5 $[M+H+Na]^{2+}$, 810.0 $[M+2Na]^{2+}$, 1575.0 $[M+H]^{+}$, 1597.0 $[M+Na]^{+}$.

Fmoc-Leu-Lys-Lys-Leu-Lys-Trp-Leu-Lys-Lys-Gln-OAll

HPLC (λ = 220 nm): t_R = 6.90 min (>99% purity). ESI-MS (*m/z*): 525.7 $[M+3H]^{3+}$, 788.0 $[M+2H]^{2+}$, 799.5 $[M+H+Na]^{2+}$, 810.5 $[M+2Na]^{2+}$, 1575.0 $[M+H]^{+}$, 1597.0 $[M+Na]^{+}$.

Fmoc-Lys-Leu-Leu-Lys-Lys-Trp-Leu-Lys-Lys-Gln-OAll

HPLC (λ = 220 nm): t_R = 7.08 min (>99% purity). ESI-MS (*m/z*): 525.9 $[M+3H]^{3+}$, 788.5 $[M+2H]^{2+}$, 799.0 $[M+H+Na]^{2+}$, 810.5 $[M+2Na]^{2+}$, 1575.0 $[M+H]^{+}$, 1597.0 $[M+Na]^{+}$.

Fmoc-Leu-Lys-Leu-Lys-Lys-Trp-Leu-Lys-Lys-Gln-OAll

HPLC (λ = 220 nm): t_R = 6.97 min (>99% purity). ESI-MS (*m/z*): 525.9 $[M+3H]^{3+}$, 788.0 $[M+2H]^{2+}$, 799.5 $[M+H+Na]^{2+}$, 810.0 $[M+2Na]^{2+}$, 1575.0 $[M+H]^{+}$, 1597.0 $[M+Na]^{+}$.

Fmoc-Leu-Leu-Lys-Lys-Lys-Trp-Leu-Lys-Lys-Gln-OAll

HPLC (λ = 220 nm): t_R = 6.93 min (>99% purity). ESI-MS (*m/z*): 525.7 $[M+3H]^{3+}$, 788.0 $[M+2H]^{2+}$, 799.5 $[M+H+Na]^{2+}$, 810.0 $[M+2Na]^{2+}$, 1575.0 $[M+H]^{+}$, 1597.0 $[M+Na]^{+}$.

Fmoc-Leu-Lys-Leu-Lys-Leu-Trp-Lys-Lys-Lys-Gln-OAll

HPLC (λ = 220 nm): t_R = 6.93 min (>99% purity). ESI-MS (*m/z*): 526.0 $[M+3H]^{3+}$, 788.0 $[M+2H]^{2+}$, 799.5 $[M+H+Na]^{2+}$, 810.5 $[M+2Na]^{2+}$, 1575.0 $[M+H]^{+}$, 1597.0 $[M+Na]^{+}$.

Fmoc-Leu-Leu-Lys-Leu-Lys-Trp-Lys-Lys-Lys-Gln-OAll

HPLC (λ = 220 nm): t_R = 7.07 min (>99% purity). ESI-MS (*m/z*): 525.7 $[M+3H]^{3+}$, 788.5 $[M+2H]^{2+}$, 799.0 $[M+H+Na]^{2+}$, 810.0 $[M+2Na]^{2+}$, 1575.0 $[M+H]^{+}$, 1597.0 $[M+Na]^{+}$, 1613.9 $[M+K]^{+}$.

Fmoc-Leu-Leu-Leu-Lys-Lys-Trp-Lys-Lys-Lys-Gln-OAll

HPLC (λ = 220 nm): t_R = 7.23 min (96% purity). ESI-MS (*m/z*): 788.5 $[M+2H]^{2+}$, 799.5 $[M+H+Na]^{2+}$, 810.5 $[M+2Na]^{2+}$, 1575.1 $[M+H]^{+}$, 1597.0 $[M+Na]^{+}$.

Fmoc-Lys-Leu-Leu-Leu-Lys-Trp-Lys-Lys-Leu-Gln-OAll

HPLC (λ = 220 nm): t_R = 7.37 min (97% purity). ESI-MS (*m/z*): 780.5 $[M+2H]^{2+}$, 792.0 $[M+H+Na]^{2+}$, 1560.9 $[M+H]^{+}$, 1582.0 $[M+Na]^{+}$.

Fmoc-Lys-Lys-Lys-Leu-Lys-Trp-Lys-Lys-Leu-Gln-OAll

HPLC (λ = 220 nm): t_R = 6.61 min (97% purity). ESI-MS (*m/z*): 796.0 $[M+2H]^{2+}$, 807.0 $[M+H+Na]^{2+}$, 818.0 $[M+2Na]^{2+}$, 1612.0 $[M+Na]^{+}$.

Fmoc-Leu-Leu-Leu-Lys-Lys-Trp-Lys-Lys-Leu-Gln-OAll

HPLC (λ = 220 nm): t_R = 6.94 min (>99% purity). ESI-MS (*m/z*): 781.0 $[M+2H]^{2+}$, 792.0 $[M+H+Na]^{2+}$, 802.5 $[M+2Na]^{2+}$, 1560.0 $[M+H]^{+}$, 1581.9 $[M+Na]^{+}$.

Fmoc-Lys-Lys-Leu-Lys-Lys-Trp-Lys-Lys-Leu-Gln-OAll

HPLC (λ = 220 nm): t_R = 6.64 min (96% purity). ESI-MS (*m/z*): 795.5 $[M+2H]^{2+}$, 806.5 $[M+H+Na]^{2+}$, 1590.0 $[M+H]^{+}$, 1612.0 $[M+Na]^{+}$, 1627.9 $[M+K]^{+}$.

Fmoc-Leu-Leu-Lys-Leu-Lys-Trp-Lys-Lys-Leu-Gln-OAll

HPLC (λ = 220 nm): t_R = 7.44 min (95% purity). ESI-MS (*m/z*): 781.0 $[M+2H]^{2+}$, 791.5 $[M+H+Na]^{2+}$, 1560.0 $[M+H]^{+}$, 1581.9 $[M+Na]^{+}$, 1597.9 $[M+K]^{+}$.

Fmoc-Lys-Leu-Lys-Lys-Lys-Trp-Lys-Lys-Leu-Gln-OAll

HPLC (λ = 220 nm): t_R = 6.67 min (93% purity). ESI-MS (m/z): 795.5 $[M+2H]^{2+}$, 806.5 $[M+H+Na]^{2+}$, 817.5 $[M+2Na]^{2+}$, 1590.0 $[M+H]^{+}$, 1612.0 $[M+Na]^{+}$.

Fmoc-Leu-Leu-Leu-Leu-Lys-Trp-Lys-Lys-Leu-Gln-OAll

HPLC (λ = 220 nm): t_R = 8.49 min (>99% purity). ESI-MS (m/z): 773.5 $[M+2H]^{2+}$, 784.0 $[M+H+Na]^{2+}$, 1545.0 $[M+H]^{+}$, 1567.0 $[M+Na]^{+}$, 1583.9 $[M+K]^{+}$.

Fmoc-Lys-Lys-Lys-Lys-Lys-Trp-Leu-Lys-Leu-Gln-OAll

HPLC (λ = 220 nm): t_R = 6.50 min (>99% purity). ESI-MS (*m/z*): 795.6 $[M+2H]^{2+}$, 806.6 $[M+H+Na]^{2+}$, 817.6 $[M+2Na]^{2+}$, 1590.2 $[M+H]^{+}$, 1612.2 $[M+Na]^{+}$.

Fmoc-Lys-Lys-Lys-Lys-Leu-Trp-Lys-Lys-Leu-Gln-OAll

HPLC (λ = 220 nm): t_R = 6.45 min (>99% purity). ESI-MS (*m/z*): 796.1 $[M+2H]^{2+}$, 806.6 $[M+H+Na]^{2+}$, 817.6 $[M+2Na]^{2+}$, 1590.2 $[M+H]^{+}$, 1612.2 $[M+Na]^{+}$.

Fmoc-Lys-Lys-Lys-Lys-Lys-Trp-Lys-Leu-Leu-Gln-OAll

HPLC (λ = 220 nm): t_R = 6.54 min (95% purity). ESI-MS (*m/z*): 796.1 $[M+2H]^{2+}$, 807.1 $[M+H+Na]^{2+}$, 818.1 $[M+2Na]^{2+}$, 1590.2 $[M+H]^{+}$, 1612.2 $[M+Na]^{+}$.

Fmoc-Lys-Lys-Lys-Leu-Leu-Trp-Leu-Lys-Leu-Gln-OAll

HPLC (λ = 220 nm): t_R = 6.94 min (>99% purity). ESI-MS (*m/z*): 780.6 $[M+2H]^{2+}$, 791.6 $[M+H+Na]^{2+}$, 802.6 $[M+2Na]^{2+}$, 1560.2 $[M+H]^{+}$, 1582.2 $[M+Na]^{+}$.

Fmoc-Lys-Lys-Lys-Lys-Leu-Trp-Leu-Lys-Lys-Gln-OAll

HPLC (λ = 220 nm): t_R = 6.30 min (>99% purity). ESI-MS (*m/z*): 795.6 $[M+2H]^{2+}$, 806.6 $[M+H+Na]^{2+}$, 818.1 $[M+2Na]^{2+}$, 1590.2 $[M+H]^{+}$, 1612.2 $[M+Na]^{+}$.

Fmoc-Lys-Leu-Lys- Lys-Leu-Trp-Leu-Lys-Leu-Gln-OAll

HPLC (λ = 220 nm): t_R = 7.15 min (>99% purity). ESI-MS (*m/z*): 780.7 $[M+2H]^{2+}$, 1560.2 $[M+H]^{+}$, 1582.2 $[M+Na]^{+}$, 1598.2 $[M+K]^{+}$.

Fmoc-Lys-Lys-Lys-Leu-Lys-Trp-Leu-Leu-Leu-Gln-OAll

HPLC (λ = 220 nm): t_R = 7.12 min (>99% purity). ESI-MS (*m/z*): 780.6 $[M+2H]^{2+}$, 792.1 $[M+H+Na]^{2+}$, 803.1 $[M+2Na]^{2+}$, 1560.2 $[M+H]^{+}$, 1582.2 $[M+Na]^{+}$.

Fmoc-Lys-Lys-Lys-Lys-Lys-Trp-Leu-Lys-Lys-Gln-OAll

HPLC (λ = 220 nm): t_R = 6.16 min (>99% purity). ESI-MS (*m/z*): 803.6 $[M+2H]^{2+}$, 814.1 $[M+H+Na]^{2+}$, 825.1 $[M+2Na]^{2+}$, 1605.2 $[M+H]^{+}$, 1627.2 $[M+Na]^{+}$.

Fmoc-Lys-Lys-Leu-Leu-Lys-Trp-Leu-Lys-Leu-Gln-OAll

HPLC (λ = 220 nm): t_R = 7.59 min (>99% purity). ESI-MS (*m/z*): 780.7 $[M+2H]^{2+}$, 1560.2 $[M+H]^{+}$, 1582.2 $[M+Na]^{+}$, 1598.2 $[M+K]^{+}$.

Fmoc-Leu-Lys-Lys-Lys-Leu-Trp-Leu-Lys-Leu-Gln-OAll

HPLC (λ = 220 nm): t_R = 7.15 min (99% purity). ESI-MS (*m/z*): 780.7 $[M+2H]^{2+}$, 1560.2 $[M+H]^{+}$, 1582.2 $[M+Na]^{+}$, 1598.2 $[M+K]^{+}$.

Fmoc-Lys-Lys-Lys-Lys-Lys-Trp-Lys-Leu-Lys-Gln-OAll

HPLC (λ = 220 nm): t_R = 6.22 min (>99% purity). ESI-MS (*m/z*): 803.6 $[M+2H]^{2+}$, 814.6 $[M+H+Na]^{2+}$, 825.1 $[M+2Na]^{2+}$, 1605.2 $[M+H]^{+}$, 1627.2 $[M+Na]^{+}$.

Fmoc-Lys-Lys-Lys-Leu-Lys-Trp-Leu-Lys-Lys-Gln-OAll

HPLC (λ = 220 nm): t_R = 6.41 min (98% purity). ESI-MS (*m/z*): 796.1 $[M+2H]^{2+}$, 806.6 $[M+H+Na]^{2+}$, 818.1 $[M+2Na]^{2+}$, 1590.2 $[M+H]^{+}$, 1612.2 $[M+Na]^{+}$, 1628.2 $[M+K]^{+}$.

Fmoc-Lys-Leu-Lys-Lys-Lys-Trp-Leu-Leu-Leu-Gln-OAll

HPLC (λ = 220 nm): t_R = 7.15 min (99% purity). ESI-MS (*m/z*): 780.7 $[M+2H]^{2+}$, 792.1 $[M+H+Na]^{2+}$, 1560.3 $[M+H]^{+}$, 1582.3 $[M+Na]^{+}$, 1598.2 $[M+K]^{+}$.

Fmoc-Lys-Lys-Lys-Lys-Leu-Trp-Lys-Lys-Lys-Gln-OAll

HPLC (λ = 220 nm): t_R = 6.16 min (>99% purity). ESI-MS (*m/z*): 803.6 $[M+2H]^{2+}$, 814.6 $[M+H+Na]^{2+}$, 825.6 $[M+2Na]^{2+}$, 1605.2 $[M+H]^{+}$, 1627.2 $[M+Na]^{+}$.

Fmoc-Lys-Leu-Leu-Lys-Lys-Trp-Leu-Lys-Leu-Gln-OAll

HPLC (λ = 220 nm): t_R = 7.50 min (>99% purity). ESI-MS (*m/z*): 780.7 $[M+2H]^{2+}$, 791.6 $[M+H+Na]^{2+}$, 1560.3 $[M+H]^{+}$, 1582.0 $[M+Na]^{+}$, 1598.2 $[M+K]^{+}$.

Fmoc-Lys-Lys-Leu-Lys-Lys-Trp-Lys-Leu-Lys-Gln-OAll

HPLC (λ = 220 nm): t_R = 6.54 min (94% purity). ESI-MS (*m/z*): 795.7 $[M+2H]^{2+}$, 806.7 $[M+H+Na]^{2+}$, 815.1 $[M+H+K]^{2+}$, 1590.3 $[M+H]^{+}$, 1612.3 $[M+Na]^{+}$, 1628.2 $[M+2Na]^{+}$.

Fmoc-Lys-Leu-Lys-Leu-Leu-Trp-Leu-Lys-Leu-Gln-OAll

HPLC (λ = 220 nm): t_R = 7.51 min (92% purity). ESI-MS (*m/z*): 773.1 $[M+2H]^{2+}$, 784.1 $[M+H+Na]^{2+}$, 795.1 $[M+2Na]^{2+}$, 1545.2 $[M+H]^{+}$, 1567.2 $[M+Na]^{+}$.

Fmoc-Lys-Leu-Lys-Leu-Lys-Trp-Leu-Leu-Leu-Gln-OAll

HPLC (λ = 220 nm): t_R = 7.56 min (>99% purity). ESI-MS (*m/z*): 773.1 $[M+2H]^{2+}$, 784.1 $[M+H+Na]^{2+}$, 795.1 $[M+2Na]^{2+}$, 1545.2 $[M+H]^{+}$, 1567.2 $[M+Na]^{+}$.

Fmoc-Leu-Lys-Lys-Leu-Leu-Trp-Leu-Lys-Leu-Gln-OAll

HPLC (λ = 220 nm): t_R = 7.61 min (>99% purity). ESI-MS (*m/z*): 773.1 $[M+2H]^{2+}$, 784.6 $[M+H+Na]^{2+}$, 795.1 $[M+2Na]^{2+}$, 1545.2 $[M+H]^{+}$, 1567.2 $[M+Na]^{+}$.

Fmoc-Lys-Lys-Lys-Leu-Lys-Trp-Lys-Leu-Lys-Gln-OAll

HPLC (λ = 220 nm): t_R = 6.44 min (92% purity). ESI-MS (*m/z*): 796.1 $[M+2H]^{2+}$, 806.6 $[M+H+Na]^{2+}$, 817.6 $[M+2Na]^{2+}$, 1590.2 $[M+H]^{+}$, 1612.2 $[M+Na]^{+}$.

Fmoc-Leu-Lys-Lys-Leu-Lys-Trp-Leu-Leu-Leu-Gln-OAll

HPLC (λ = 220 nm): t_R = 7.89 min (>99% purity). ESI-MS (*m/z*): 773.1 $[M+2H]^{2+}$, 784.6 $[M+H+Na]^{2+}$, 795.6 $[M+2Na]^{2+}$, 1545.2 $[M+H]^{+}$, 1567.2 $[M+Na]^{+}$.

Fmoc-Leu-Lys-Lys-Leu-Leu-Trp-Leu-Lys-Lys-Gln-OAll

HPLC (λ = 220 nm): t_R = 7.16 min (>99% purity). ESI-MS (*m/z*): 781.1 $[M+2H]^{2+}$, 791.6 $[M+H+Na]^{2+}$, 803.1 $[M+2Na]^{2+}$, 1560.2 $[M+H]^{+}$, 1582.2 $[M+Na]^{+}$.

5.5.2. Synthesis of the linear decapeptides protected at the N-terminus

Once the lineal sequence was completed, the allyl group at the C-terminus was removed by treatment with $Pd(PPh_3)_4$ in $CHCl_3$/AcOH/*N*-methylmorpholine (NMM) (3:2:1) for 3 h under nitrogen. After completion of the reaction, the resin was washed with tetrahydrofuran (3 x 2 min), DMF (3 x 2 min), DIEA/CH_2Cl_2 (1:19, 3 x 2 min), sodium *N,N*-diethyldithiocarbamate (0.03 M in DMF, 3 x 15 min) and DMF (10 x 1 min). An aliquot of the peptidyl resin was acidolytically cleaved using the conditions described in section 1.1. The residue was analysed by HPLC and characterised by ESI-MS.

Fmoc-Lys-Lys-Leu-Leu-Lys-Trp-Leu-Lys-Lys-Gln-OH

HPLC (λ = 220 nm): t_R = 7.26 min (>99% purity). ESI-MS (*m/z*): 512.3 $[M+3H]^{3+}$, 768.0 $[M+2H]^{2+}$, 779.5 $[M+H+Na]^{2+}$, 790.0 $[M+2Na]^{2+}$, 1535.0 $[M+H]^{+}$, 1557.9 $[M+Na]^{+}$.

Fmoc-Leu-Lys-Lys-Leu-Lys-Trp-Leu-Lys-Lys-Gln-OH

HPLC (λ = 220 nm): t_R = 7.04 min (93% purity).

Fmoc-Lys-Leu-Leu-Lys-Lys-Trp-Leu-Lys-Lys-Gln-OH

HPLC (λ = 220 nm): t_R = 7.21 min (>99% purity).

Fmoc-Leu-Lys-Leu-Lys-Lys-Trp-Leu-Lys-Lys-Gln-OH

HPLC (λ = 220 nm): t_R = 7.13 min (>99% purity).

Fmoc-Leu-Leu-Lys-Lys-Lys-Trp-Leu-Lys-Lys-Gln-OH

HPLC (λ = 220 nm): t_R = 7.12 min (>99% purity).

Fmoc-Leu-Lys-Leu-Lys-Leu-Trp-Lys-Lys-Lys-Gln-OH

HPLC (λ = 220 nm): t_R = 7.12 min (>99% purity).

Fmoc-Leu-Leu-Lys-Leu-Lys-Trp-Lys-Lys-Lys-Gln-OH

HPLC (λ = 220 nm): t_R = 7.29 min (>99% purity).

Fmoc-Leu-Leu-Leu-Lys-Lys-Trp-Lys-Lys-Lys-Gln-OH

HPLC (λ = 220 nm): t_R = 7.45 min (97% purity). ESI-MS (*m/z*): 768.0 $[M+2H]^{2+}$, 779.0 $[M+H+Na]^{2+}$, 790.5 $[M+2Na]^{2+}$, 1535.0 $[M+H]^{+}$, 1557.0 $[M+Na]^{+}$.

Fmoc-Lys-Leu-Leu-Leu-Lys-Trp-Lys-Lys-Leu-Gln-OH

HPLC (λ = 220 nm): t_R = 7.45 min (>99% purity). ESI-MS (*m/z*): 761.0 $[M+2H]^{2+}$, 771.5 $[M+H+Na]^{2+}$, 782.9 $[M+2Na]^{2+}$, 1519.9 $[M+H]^{+}$, 1542.0 $[M+Na]^{+}$.

Fmoc-Lys-Lys-Lys-Leu-Lys-Trp-Lys-Lys-Leu-Gln-OH

HPLC (λ = 220 nm): t_R = 6.65 min (>99% purity). ESI-MS (*m/z*): 776.0 $[M+2H]^{2+}$, 787.0 $[M+H+Na]^{2+}$, 797.5 $[M+2Na]^{2+}$, 1550.0 $[M+H]^{+}$, 1572.0 $[M+Na]^{+}$.

Fmoc-Leu-Leu-Leu-Lys-Lys-Trp-Lys-Lys-Leu-Gln-OH

HPLC (λ = 220 nm): t_R = 7.59 min (>99% purity). ESI-MS (*m/z*): 760.5 $[M+2H]^{2+}$, 771.5 $[M+H+Na]^{2+}$, 782.5 $[M+2Na]^{2+}$, 1520.0 $[M+H]^{+}$, 1542.0 $[M+Na]^{+}$.

Fmoc-Lys-Lys-Leu-Lys-Lys-Trp-Lys-Lys-Leu-Gln-OH

HPLC (λ = 220 nm): t_R = 6.67 min (>99% purity). ESI-MS (*m/z*): 775.5 $[M+2H]^{2+}$, 786.5 $[M+H+Na]^{2+}$, 798.0 $[M+2Na]^{2+}$, 1550.0 $[M+H]^{+}$, 1572.0 $[M+Na]^{+}$.

Fmoc-Leu-Leu-Lys-Leu-Lys-Trp-Lys-Lys-Leu-Gln-OH

HPLC (λ = 220 nm): t_R = 7.62 min (98% purity). ESI-MS (*m/z*): 761.0 $[M+2H]^{2+}$, 771.5 $[M+H+Na]^{2+}$, 782.9 $[M+2Na]^{2+}$, 1520.0 $[M+H]^{+}$, 1541.9 $[M+Na]^{+}$.

Fmoc-Lys-Leu-Lys-Lys-Lys-Trp-Lys-Lys-Leu-Gln-OH

HPLC (λ = 220 nm): t_R = 6.39 min (>99% purity). ESI-MS (*m/z*): 776.0 $[M+2H]^{2+}$, 786.5 $[M+H+Na]^{2+}$, 798.0 $[M+2Na]^{2+}$, 1550.0 $[M+H]^{+}$, 1572.0 $[M+Na]^{+}$.

Fmoc-Leu-Leu-Leu-Leu-Lys-Trp-Lys-Lys-Leu-Gln-OH

HPLC (λ = 220 nm): t_R = 8.33 min (93% purity).

Fmoc-Lys-Lys-Lys-Lys-Lys-Trp-Leu-Lys-Leu-Gln-OH

HPLC (λ = 220 nm): t_R = 6.26 min (>99% purity).

Fmoc-Lys-Lys-Lys-Lys-Leu-Trp-Lys-Lys-Leu-Gln-OH

HPLC (λ = 220 nm): t_R = 6.24 min (>99% purity)

Fmoc-Lys-Lys-Lys-Lys-Lys-Trp-Lys-Leu-Leu-Gln-OH

HPLC (λ = 220 nm): t_R = 6.33 min (>99% purity).

Fmoc-Lys-Lys-Lys-Leu-Leu-Trp-Leu-Lys-Leu-Gln-OH

HPLC (λ = 220 nm): t_R = 6.73 min (>99% purity).

Fmoc-Lys-Lys-Lys-Lys-Leu-Trp-Leu-Lys-Lys-Gln-OH

HPLC (λ = 220 nm): t_R = 6.20 min (>99% purity).

Fmoc-Lys-Leu-Lys- Lys-Leu-Trp-Leu-Lys-Leu-Gln-OH

HPLC (λ = 220 nm): t_R = 6.89 min (>99% purity). ESI-MS (*m/z*): 760.6 $[M+2H]^{2+}$, 771.6 $[M+H+Na]^{2+}$, 783.6 $[M+2Na]^{2+,}$ 1520.2 $[M+H]^{+}$, 1542.1 $[M+Na]^{+}$.

Fmoc-Lys-Lys-Lys-Leu-Lys-Trp-Leu-Leu-Leu-Gln-OH

HPLC (λ = 220 nm): t_R = 6.87 min (>99% purity).

Fmoc-Lys-Lys-Lys-Lys-Lys-Trp-Leu-Lys-Lys-Gln-OH

HPLC (λ = 220 nm): t_R = 6.08 min (>99% purity).

Fmoc-Lys-Lys-Leu-Leu-Lys-Trp-Leu-Lys-Leu-Gln-OH

HPLC (λ = 220 nm): t_R = 7.29 min (>99% purity). ESI-MS (*m/z*) = 760.6 $[M+2H]^{2+}$, 771.6 $[M+H+Na]^{2+}$, 1520.2 $[M+H]^{+}$, 1542.2 $[M+Na]^{+}$.

Fmoc-Leu-Lys-Lys-Lys-Leu-Trp-Leu-Lys-Leu-Gln-OH

HPLC (λ = 220 nm): t_R = 6.87 min (>99% purity).

Fmoc-Lys-Lys-Lys-Lys-Lys-Trp-Lys-Leu-Lys-Gln-OH

HPLC (λ = 220 nm): t_R = 6.12 min (>99% purity).

Fmoc-Lys-Lys-Lys-Leu-Lys-Trp-Leu-Lys-Lys-Gln-OH

HPLC (λ = 220 nm): t_R = 6.32 min (>99% purity).

Fmoc-Lys-Leu-Lys-Lys-Lys-Trp-Leu-Leu-Leu-Gln-OH

HPLC (λ = 220 nm): t_R = 6.84 min (>99% purity).

Fmoc-Lys-Lys-Lys-Lys-Leu-Trp-Lys-Lys-Lys-Gln-OH

HPLC (λ = 220 nm): t_R = 6.10 min (>99% purity).

Fmoc-Lys-Leu-Leu-Lys-Lys-Trp-Leu-Lys-Leu-Gln-OH

HPLC (λ = 220 nm): t_R = 7.21 min (>99% purity).

Fmoc-Lys-Lys-Leu-Lys-Lys-Trp-Lys-Leu-Lys-Gln-OH

HPLC (λ = 220 nm): t_R = 6.37 min (>99% purity).

Fmoc-Lys-Leu-Lys-Leu-Leu-Trp-Leu-Lys-Leu-Gln-OH

HPLC (λ = 220 nm): t_R = 7.24 min (91% purity).

Fmoc-Lys-Leu-Lys-Leu-Lys-Trp-Leu-Leu-Leu-Gln-OH

HPLC (λ = 220 nm): t_R = 7.24 min (>99% purity).

Fmoc-Leu-Lys-Lys-Leu-Leu-Trp-Leu-Lys-Leu-Gln-OH

HPLC (λ = 220 nm): t_R = 7.32 min (>99% purity).

Fmoc-Lys-Lys-Lys-Leu-Lys-Trp-Lys-Leu-Lys-Gln-OH

HPLC (λ = 220 nm): t_R = 6.29 min (>99% purity).

Fmoc-Leu-Lys-Lys-Leu-Lys-Trp-Leu-Leu-Leu-Gln-OH

HPLC (λ = 220 nm): t_R = 7.52 min (>99% purity).

Fmoc-Leu-Lys-Lys-Leu-Leu-Trp-Leu-Lys-Lys-Gln-OH

HPLC (λ = 220 nm): t_R = 7.02 min (>99% purity).

5.5.3. Solid-phase synthesis of the cyclic decapeptides

After Fmoc-removal of the corresponding linear peptidyl resin with piperidine/NMP (3:7, 1 x 2 min + 2 x 10 min), cyclization was performed by treating the resin with [ethylcyano(hydroxyimino)acetato-O^2] tri-1-pyrrolidinylphosphonium hexafluorophosphate (PyOxim), Oxyma and DIEA in NMP for 24 h. Following washes with NMP (6 x 1 min) and CH_2Cl_2 (2 x 1 min), cyclic peptides were cleaved from the resin by treatment with TFA/phenol/H_2O/TIS (92.5:2.5:2.5:2.5) for 2 h. The cleavage cocktail was then removed using nitrogen and after diethyl ether extraction, cyclic peptides were dissolved in H_2O, and lyophilized. All the peptides were analysed by HPLC and characterized by ESI-MS and HRMS.

c(Lys-Lys-Leu-Leu-Lys-Trp-Leu-Lys-Lys-Gln) (**BPC136W**)

HPLC (λ = 220 nm): t_R = 6.87 min (90% purity). ESI-MS (*m/z*): 1294.9 $[M+H]^+$, 1316.9 $[M+Na]^+$, 1332.9 $[M+K]^+$. HRMS (ESI) (*m/z*): calculated for $C_{64}H_{113}N_{17}O_{11}$ $[M+2H]^{2+}$ 647.9397, found 647.9401; calculated for $C_{64}H_{112}N_{17}O_{11}$ $[M+H]^+$ 1294.8722, found 1294.8697.

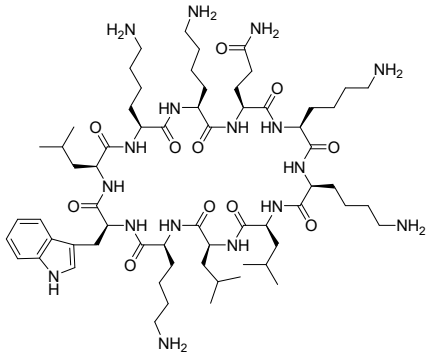

c(Leu-Lys-Lys-Leu-Lys-Trp-Leu-Lys-Lys-Gln) (**BPC140W**)

HPLC (λ = 220 nm): t_R = 6.95 min (81% purity). ESI-MS (*m/z*): 1296.0 $[M+H]^+$, 1317.0 $[M+Na]^+$. HRMS (ESI) (*m/z*): calculated for $C_{64}H_{113}N_{17}O_{11}$ $[M+2H]^{2+}$ 647.9397, found 647.9406; calculated for $C_{64}H_{112}N_{17}O_{11}$ $[M+H]^+$ 1294.8722, found 1294.8683.

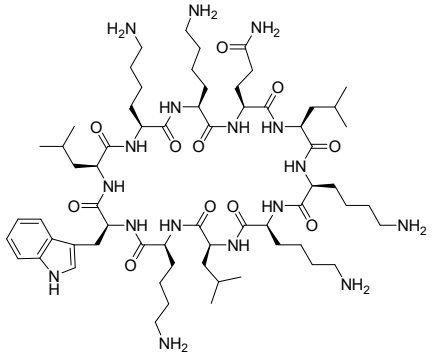

c(Lys-Leu-Leu-Lys-Lys-Trp-Leu-Lys-Lys-Gln) (**BPC142W**)

HPLC (λ = 220 nm): t_R = 6.76 min (87% purity). ESI-MS (*m/z*): 1295.0 $[M+H]^+$, 1317.0 $[M+Na]^+$, 1333.9 $[M+K]^+$. HRMS (ESI) (*m/z*): calculated for $C_{64}H_{113}N_{17}O_{11}$ $[M+2H]^{2+}$ 647.9397, found 647.9424; calculated for $C_{64}H_{112}N_{17}O_{11}$ $[M+H]^+$ 1294.8722, found 1294.8755.

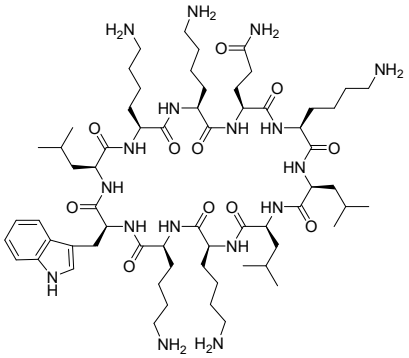

c(Leu-Lys-Leu-Lys-Lys-Trp-Leu-Lys-Lys-Gln) (**BPC144W**)

HPLC (λ = 220 nm): t_R = 6.72 min (87% purity). ESI-MS (*m/z*): 1294.8 $[M+H]^+$, 1316.7 $[M+Na]^+$. HRMS (ESI) (*m/z*): calculated for $C_{64}H_{113}N_{17}O_{11}$ $[M+2H]^{2+}$ 647.9397, found 647.9381; calculated for $C_{64}H_{112}N_{17}O_{11}$ $[M+H]^+$ 1294.8722, found 1294.8674.

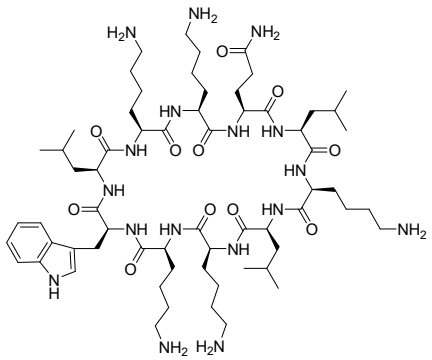

c(Leu-Leu-Lys-Lys-Lys-Trp-Leu-Lys-Lys-Gln) (**BPC146W**)

HPLC (λ = 220 nm): t_R = 6.45 min (90% purity). ESI-MS (*m/z*): 1294.8 $[M+H]^+$, 1316.8 $[M+Na]^+$. HRMS (ESI) (*m/z*): calculated for $C_{64}H_{113}N_{17}O_{11}$ $[M+2H]^{2+}$ 647.9397, found 647.9419; calculated for $C_{64}H_{112}N_{17}O_{11}$ $[M+H]^+$ 1294.8722, found 1294.8703.

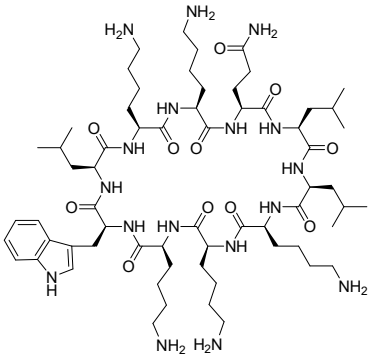

c(Leu-Lys-Leu-Lys-Leu-Trp-Lys-Lys-Lys-Gln) (**BPC156W**)

HPLC (λ = 220 nm): t_R = 6.37 min (>99% purity). ESI-MS (*m/z*): 1295.0 $[M+H]^+$, 1317.0 $[M+Na]^+$. HRMS (ESI) (*m/z*): calculated for $C_{64}H_{113}N_{17}O_{11}$ $[M+2H]^{2+}$ 647.9397, found 647.9422; calculated for $C_{64}H_{112}N_{17}O_{11}$ $[M+H]^+$ 1294.8722, found 1294.8723.

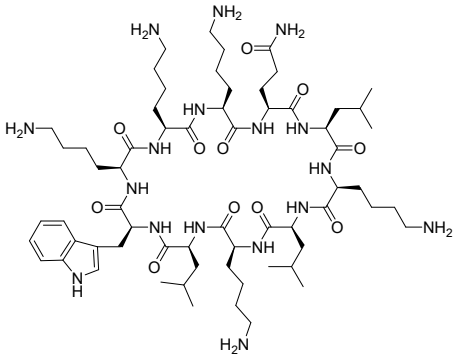

c(Leu-Leu-Lys-Leu-Lys-Trp-Lys-Lys-Lys-Gln) (**BPC164W**)

HPLC (λ = 220 nm): t_R = 6.38 min (>99% purity). ESI-MS (*m/z*): 1295.0 $[M+H]^+$, 1317.0 $[M+Na]^+$. HRMS (ESI) (*m/z*): calculated for $C_{64}H_{113}N_{17}O_{11}$ $[M+2H]^{2+}$ 647.9397, found 647.9417; calculated for $C_{64}H_{112}N_{17}O_{11}$ $[M+H]^+$ 1294.8722, found 1294.8723.

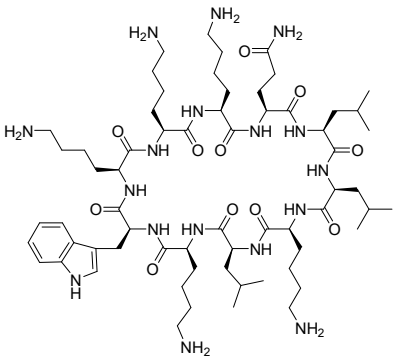

c(Leu-Leu-Leu-Lys-Lys-Trp-Lys-Lys-Lys-Gln) (**BPC166W**)

HPLC (λ = 220 nm): t_R = 6.38 min (90% purity). ESI-MS (*m/z*): 1294.9 $[M+H]^+$, 1316.9 $[M+Na]^+$, 1332.8 $[M+K]^+$. HRMS (ESI) (*m/z*): calculated for $C_{64}H_{113}N_{17}O_{11}$ $[M+2H]^{2+}$ 647.9397, found 647.9423; calculated for $C_{64}H_{112}N_{17}O_{11}$ $[M+H]^+$ 1294.8722, found 1294.8742.

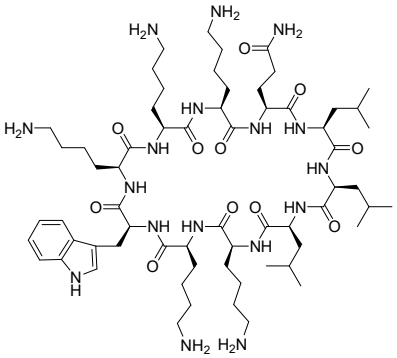

c(Lys-Leu-Leu-Leu-Lys-Trp-Lys-Lys-Leu-Gln) (**BPC184W**)

HPLC (λ = 220 nm): t_R = 6.97 min (93% purity). ESI-MS (*m/z*): 1279.9 $[M+H]^+$, 1301.8 $[M+Na]^+$, 1317.8 $[M+K]^+$. HRMS (ESI) (*m/z*): calculated for $C_{64}H_{112}N_{16}O_{11}$ $[M+2H]^{2+}$ 640.4343, found 640.4371; calculated for $C_{64}H_{111}N_{16}O_{11}$ $[M+H]^+$ 1279.8613, found 1279.8604.

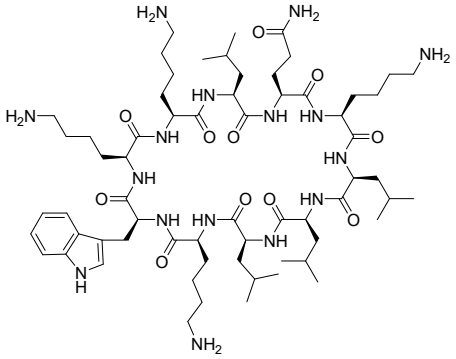

c(Lys-Lys-Lys-Leu-Lys-Trp-Lys-Lys-Leu-Gln) (**BPC186W**)

HPLC (λ = 220 nm): t_R = 5.94 min (>99% purity). ESI-MS (*m/z*): 1309.9 $[M+H]^+$, 1331.9 $[M+Na]^+$, 1347.8 $[M+K]^+$. HRMS (ESI) (*m/z*): calculated for $C_{64}H_{114}N_{18}O_{11}$ $[M+2H]^{2+}$ 655.4452, found 655.4473; calculated for $C_{64}H_{113}N_{18}O_{11}$ $[M+H]^+$ 1309.8831, found 1309.8832.

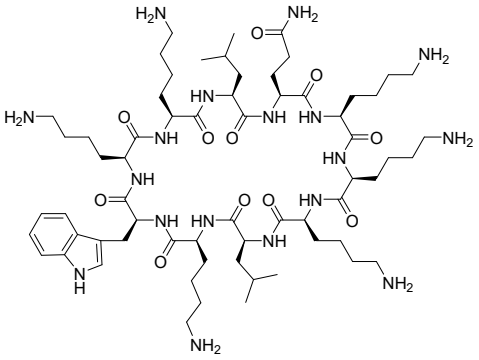

c(Leu-Leu-Leu-Lys-Lys-Trp-Lys-Lys-Leu-Gln) (**BPC188W**)

HPLC (λ = 220 nm): t_R = 6.97 min (93% purity). ESI-MS (*m/z*): 1279.9 $[M+H]^+$, 1301.9 $[M+Na]^+$. HRMS (ESI) (*m/z*): calculated for $C_{64}H_{112}N_{16}O_{11}$ $[M+2H]^{2+}$ 640.4343, found 640.4352; calculated for $C_{64}H_{111}N_{16}O_{11}$ $[M+H]^+$ 1279.8613, found 1279.8585.

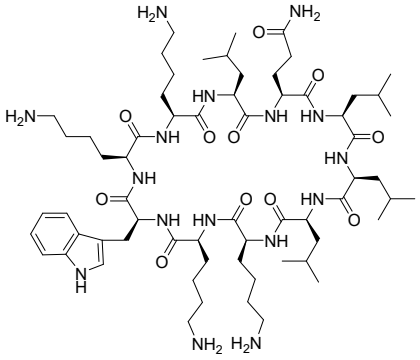

c(Lys-Lys-Leu-Lys-Lys-Trp-Lys-Lys-Leu-Gln) (**BPC194W**)

HPLC (λ = 220 nm): t_R = 6.21 min (91% purity). ESI-MS (*m/z*): 1309.9 $[M+H]^+$, 1331.9 $[M+Na]^+$, 1347.9 $[M+K]^+$. HRMS (ESI) (*m/z*): calculated for $C_{64}H_{114}N_{18}O_{11}$ $[M+2H]^{2+}$ 655.4452, found 655.4456; calculated for $C_{64}H_{113}N_{18}O_{11}$ $[M+H]^+$ 1309.8831, found 1309.8802.

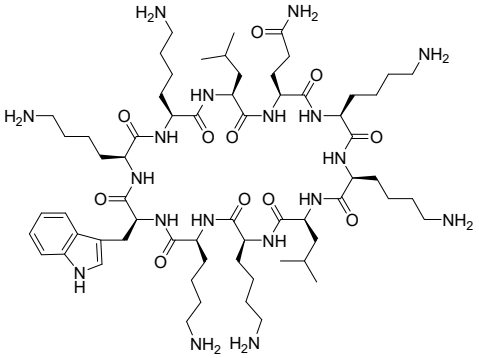

c(Leu-Leu-Lys-Leu-Lys-Trp-Lys-Lys-Leu-Gln) (**BPC196W**)

HPLC (λ = 220 nm): t_R = 6.60 min (99% purity). ESI-MS (*m/z*): 1279.9 $[M+H]^+$, 1301.9 $[M+Na]^+$. HRMS (ESI) (*m/z*): calculated for $C_{64}H_{112}N_{16}O_{11}$ $[M+2H]^{2+}$ 640.4343, found 640.4362; calculated for $C_{64}H_{111}N_{16}O_{11}$ $[M+H]^+$ 1279.8613, found 1279.8610.

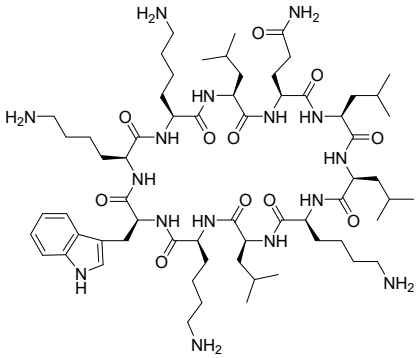

c(Lys-Leu-Lys-Lys-Lys-Trp-Lys-Lys-Leu-Gln) (**BPC198W**)

HPLC (λ = 220 nm): t_R = 6.26 min (93% purity). ESI-MS (*m/z*): 1309.8 $[M+H]^+$, 1331.8 $[M+Na]^+$. HRMS (ESI) (*m/z*): calculated for $C_{64}H_{114}N_{18}O_{11}$ $[M+2H]^{2+}$ 655.4452, found 655.4468; calculated for $C_{64}H_{113}N_{18}O_{11}$ $[M+H]^+$ 1309.8831, found 1309.8813.

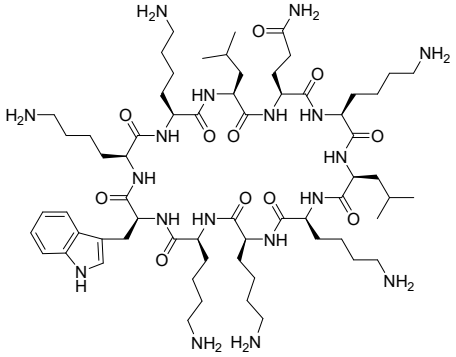

c(Leu-Leu-Leu-Leu-Lys-Trp-Lys-Lys-Leu-Gln) (**BPC200W**)

HPLC (λ = 220 nm): t_R = 7.40 min (96% purity). ESI-MS (*m/z*): 1264.8 $[M+H]^+$, 1286.7 $[M+Na]^+$. HRMS (ESI) (*m/z*): calculated for $C_{64}H_{112}N_{15}O_{11}$ $[M+3H]^{3+}$ 422.2883, found 422.2892; calculated for $C_{64}H_{111}N_{15}O_{11}$ $[M+2H]^{2+}$ 632.9288, found 632.9303; calculated for $C_{64}H_{110}N_{15}O_{11}$ $[M+H]^+$ 1264.8504, found 1264.8552.

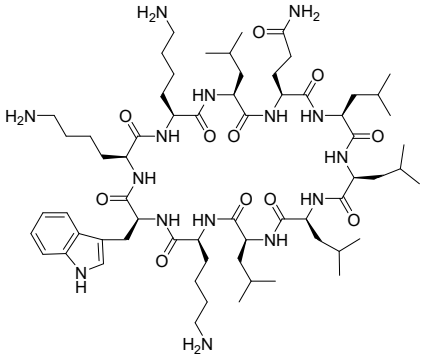

c(Lys-Lys-Lys-Lys-Lys-Trp-Leu-Lys-Leu-Gln) (**BPC870W**)

HPLC (λ = 220 nm): t_R = 5.95 min (>99% purity). ESI-MS (*m/z*): 1310.0 $[M+H]^+$, 1332.0 $[M+Na]^+$. HRMS (ESI) (*m/z*): calculated for $C_{64}H_{114}N_{18}O_{11}$ $[M+2H]^{2+}$ 655.4452, found 655.4470; calculated for $C_{64}H_{113}N_{18}O_{11}$ $[M+H]^+$ 1309.8831, found 1309.8828.

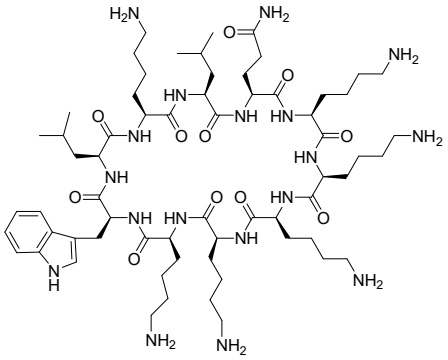

c(Lys-Lys-Lys-Lys-Leu-Trp-Lys-Lys-Leu-Gln) (**BPC872W**)

HPLC (λ = 220 nm): t_R = 5.96 min (>99% purity). ESI-MS (*m/z*): 1310.0 $[M+H]^+$, 1332.0 $[M+Na]^+$. HRMS (ESI) (*m/z*): calculated for $C_{64}H_{114}N_{18}O_{11}$ $[M+2H]^{2+}$ 655.4452, found 655.4454; calculated for $C_{64}H_{113}N_{18}O_{11}$ $[M+H]^+$ 1309.8831, found 1309.8806.

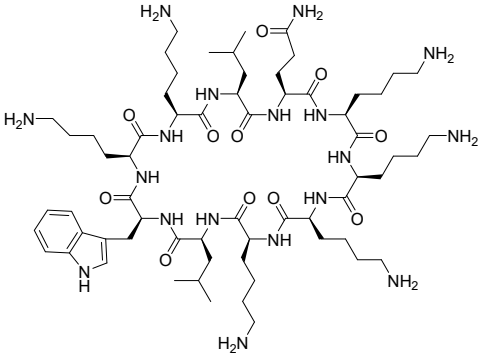

c(Lys-Lys-Lys-Lys-Lys-Trp-Lys-Leu-Leu-Gln) (**BPC874W**)

HPLC (λ = 220 nm): t_R = 5.96 min (>99% purity). ESI-MS (*m/z*): 1310.1 $[M+H]^+$, 1332.1 $[M+Na]^+$. HRMS (ESI) (*m/z*): calculated for $C_{64}H_{114}N_{18}O_{11}$ $[M+2H]^{2+}$ 655.4452, found 655.4446; calculated for $C_{64}H_{113}N_{18}O_{11}$ $[M+H]^+$ 1309.8831, found 1309.8804.

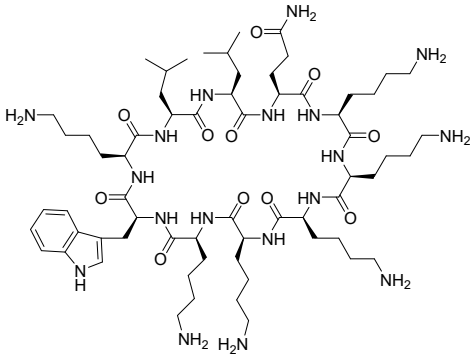

c(Lys-Lys-Lys-Leu-Leu-Trp-Leu-Lys-Leu-Gln) (**BPC876W**)

HPLC (λ = 220 nm): t_R = 6.37 min (>99% purity). ESI-MS (*m/z*): 1280.0 $[M+H]^+$, 1302.1 $[M+Na]^+$. HRMS (ESI) (*m/z*): calculated for $C_{64}H_{112}N_{16}O_{11}$ $[M+2H]^{2+}$ 640.4343, found 640.4344; calculated for $C_{64}H_{111}N_{16}O_{11}$ $[M+H]^+$ 1279.8613, found 1279.8603.

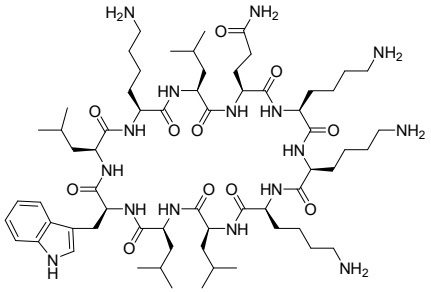

c(Lys-Lys-Lys-Lys-Leu-Trp-Leu-Lys-Lys-Gln) (**BPC878W**)

HPLC (λ = 220 nm): t_R = 5.75 min (>99% purity). ESI-MS (*m/z*): 1310.1 $[M+H]^+$, 1332.1 $[M+Na]^+$. HRMS (ESI) (*m/z*): calculated for $C_{64}H_{114}N_{18}O_{11}$ $[M+2H]^{2+}$ 655.4452, found 655.4451; calculated for $C_{64}H_{113}N_{18}O_{11}$ $[M+H]^+$ 1309.8831, found 1309.8810.

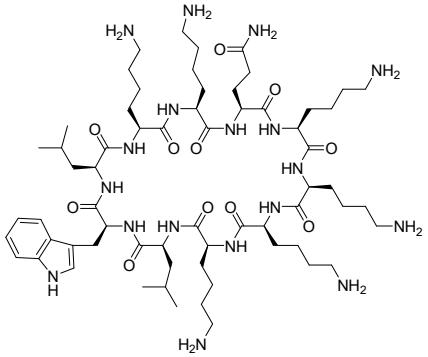

c(Lys-Leu-Lys- Lys-Leu-Trp-Leu-Lys-Leu-Gln) (**BPC880W**)

HPLC (λ = 220 nm): t_R = 6.88 min (93% purity). ESI-MS (*m/z*): 1279.9 $[M+H]^+$, 1301.9 $[M+Na]^+$. HRMS (ESI) (*m/z*): calculated for $C_{64}H_{112}N_{16}O_{11}$ $[M+2H]^{2+}$ 640.4343, found 640.4334; calculated for $C_{64}H_{111}N_{16}O_{11}$ $[M+H]^+$ 1279.8613, found 1279.8592.

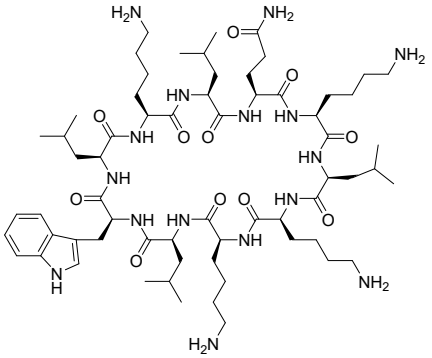

c(Lys-Lys-Lys-Leu-Lys-Trp-Leu-Leu-Leu-Gln) (**BPC882W**)

HPLC (λ = 220 nm): t_R = 6.53 min (99% purity). ESI-MS (*m/z*): 1280.1 $[M+H]^+$, 1302.0 $[M+Na]^+$. HRMS (ESI) (*m/z*): calculated for $C_{64}H_{112}N_{16}O_{11}$ $[M+2H]^{2+}$ 640.4343, found 640.4338; calculated for $C_{64}H_{111}N_{16}O_{11}$ $[M+H]^+$ 1279.8613, found 1279.8591.

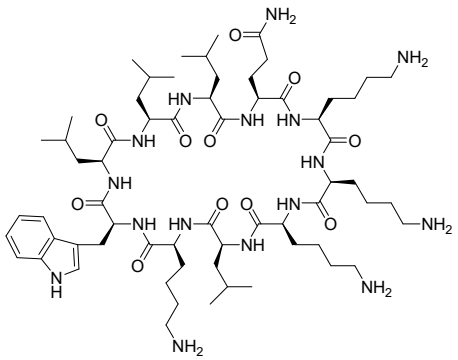

c(Lys-Lys-Lys-Lys-Lys-Trp-Leu-Lys-Lys-Gln) (**BPC884W**)

HPLC (λ = 220 nm): t_R = 5.60 min (99% purity). ESI-MS (*m/z*): 1324.9 $[M+H]^+$, 1346.9 $[M+Na]^+$. HRMS (ESI) (*m/z*): calculated for $C_{64}H_{115}N_{19}O_{11}$ $[M+2H]^{2+}$ 662.9506, found 662.9519; calculated for $C_{64}H_{114}N_{19}O_{11}$ $[M+H]^+$ 1324.8940, found 1324.8964.

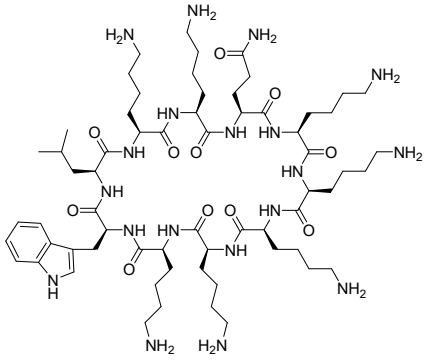

c(Lys-Lys-Leu-Leu-Lys-Trp-Leu-Lys-Leu-Gln) (**BPC886W**)

HPLC (λ = 220 nm): t_R = 7.04 min (80% purity). ESI-MS (*m/z*): 1279.9 $[M+H]^+$, 1301.9 $[M+Na]^+$. HRMS (ESI) (*m/z*): calculated for $C_{64}H_{112}N_{16}O_{11}$ $[M+2H]^{2+}$ 640.4343, found 640.4337; calculated for $C_{64}H_{111}N_{16}O_{11}$ $[M+H]^+$ 1279.8613, found 1279.8591.

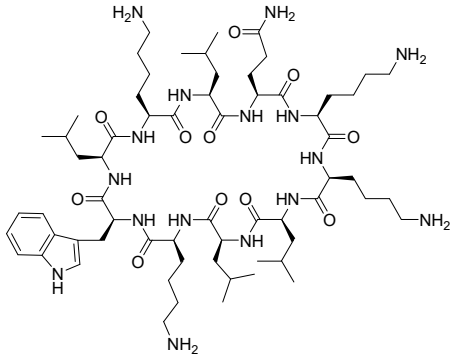

c(Leu-Lys-Lys-Lys-Leu-Trp-Leu-Lys-Leu-Gln) (**BPC888W**)

HPLC (λ = 220 nm): t_R = 6.41 min (91% purity). ESI-MS (*m/z*): 1279.9 $[M+H]^+$, 1301.9 $[M+Na]^+$. HRMS (ESI) (*m/z*): calculated for $C_{64}H_{112}N_{16}O_{11}$ $[M+2H]^{2+}$ 640.4343, found 640.4320; calculated for $C_{64}H_{111}N_{16}O_{11}$ $[M+H]^+$ 1279.8613, found 1279.8584.

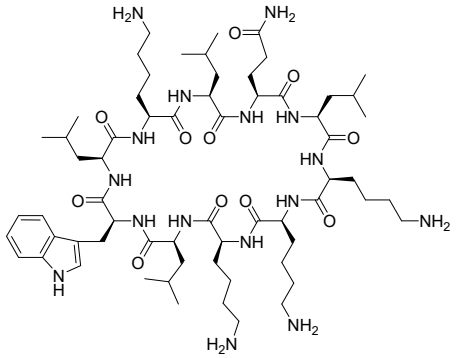

c(Lys-Lys-Lys-Lys-Lys-Trp-Lys-Leu-Lys-Gln) (**BPC890W**)

HPLC (λ = 220 nm): t_R = 5.71 min (>99% purity). ESI-MS (*m/z*): 1324.9 $[M+H]^+$, 1346.9 $[M+Na]^+$. HRMS (ESI) (*m/z*): calculated for $C_{64}H_{115}N_{19}O_{11}$ $[M+2H]^{2+}$ 662.9506, found 662.9522; calculated for $C_{64}H_{114}N_{19}O_{11}$ $[M+H]^+$ 1324.8940, found 1324.8913.

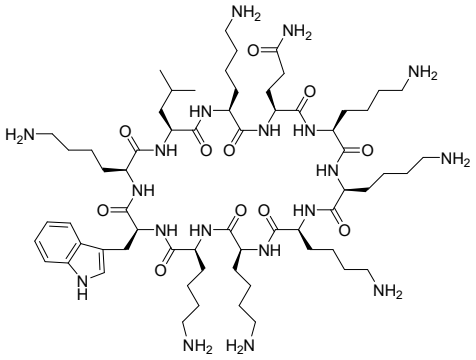

c(Lys-Lys-Lys-Leu-Lys-Trp-Leu-Lys-Lys-Gln) (**BPC892W**)

HPLC (λ = 220 nm): t_R = 5.95 min (>99% purity). ESI-MS (*m/z*): 1309.9 $[M+H]^+$, 1331.9 $[M+Na]^+$. HRMS (ESI) (*m/z*): calculated for $C_{64}H_{114}N_{18}O_{11}$ $[M+2H]^{2+}$ 655.4452, found 655.4479; calculated for $C_{64}H_{113}N_{18}O_{11}$ $[M+H]^+$ 1309.8831, found 1309.8813.

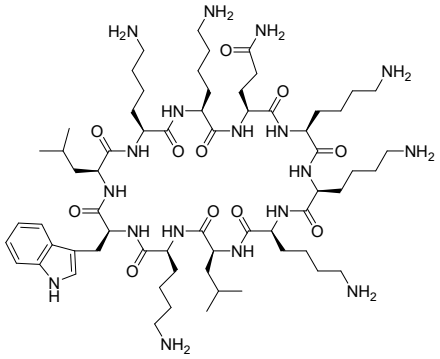

c(Lys-Leu-Lys-Lys-Lys-Trp-Leu-Leu-Leu-Gln) (**BPC894W**)

HPLC (λ = 220 nm): t_R = 6.59 min (96% purity). ESI-MS (*m/z*): 1280.0 $[M+H]^+$, 1302.0 $[M+Na]^+$, 1318.0 $[M+K]^+$. HRMS (ESI) (*m/z*): calculated for $C_{64}H_{112}N_{16}O_{11}$ $[M+2H]^{2+}$ 640.4343, found 640.4343; calculated for $C_{64}H_{111}N_{16}O_{11}$ $[M+H]^+$ 1279.8613, found 1279.8627.

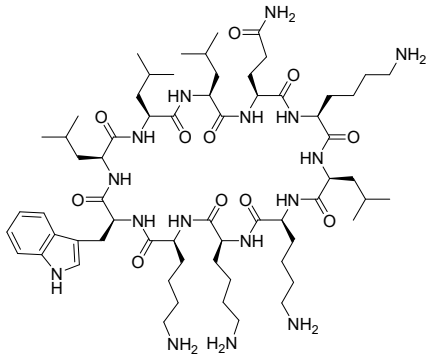

c(Lys-Lys-Lys-Lys-Leu-Trp-Lys-Lys-Lys-Gln) (**BPC896W**)

HPLC (λ = 220 nm): t_R = 5.59 min (>99% purity). ESI-MS (*m/z*): 1325.0 $[M+H]^+$, 1347.0 $[M+Na]^+$. HRMS (ESI) (*m/z*): calculated for $C_{64}H_{115}N_{19}O_{11}$ $[M+2H]^{2+}$ 662.9506, found 662.9532; calculated for $C_{64}H_{114}N_{19}O_{11}$ $[M+H]^+$ 1324.8940, found 1324.8937.

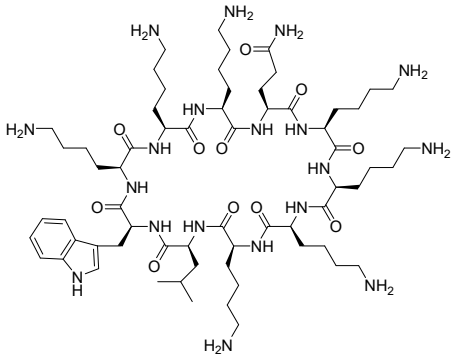

c(Lys-Leu-Leu-Lys-Lys-Trp-Leu-Lys-Leu-Gln) (**BPC898W**)

HPLC (λ = 220 nm): t_R = 7.04 min (92% purity). ESI-MS (*m/z*): 1280.1 $[M+H]^+$, 1302.0 $[M+Na]^+$. HRMS (ESI) (*m/z*): calculated for $C_{64}H_{112}N_{16}O_{11}$ $[M+2H]^{2+}$ 640.4343, found 640.4336; calculated for $C_{64}H_{111}N_{16}O_{11}$ $[M+H]^+$ 1279.8613, found 1279.8595.

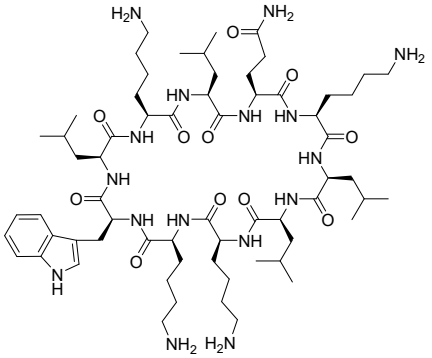

c(Lys-Lys-Leu-Lys-Lys-Trp-Lys-Leu-Lys-Gln) (**BPC900W**)

HPLC (λ = 220 nm): t_R = 5.88 min (>99% purity). ESI-MS (*m/z*): 1310.1 $[M+H]^+$, 1332.1 $[M+Na]^+$. HRMS (ESI) (*m/z*): calculated for $C_{64}H_{114}N_{18}O_{11}$ $[M+2H]^{2+}$ 655.4452, found 655.4471; calculated for $C_{64}H_{113}N_{18}O_{11}$ $[M+H]^+$ 1309.8831, found 1309.8859.

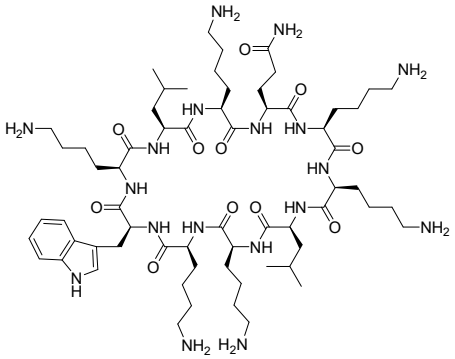

c(Lys-Leu-Lys-Leu-Leu-Trp-Leu-Lys-Leu-Gln) (**BPC902W**)

HPLC (λ = 220 nm): t_R = 7.05 min (>99% purity). ESI-MS (*m/z*): 1265.1 $[M+H]^+$, 1287.0 $[M+Na]^+$. HRMS (ESI) (*m/z*): calculated for $C_{64}H_{111}N_{15}O_{11}$ $[M+2H]^{2+}$ 632.9288, found 632.9297; calculated for $C_{64}H_{110}N_{15}O_{11}$ $[M+H]^+$ 1264.8504, found 1264.8507.

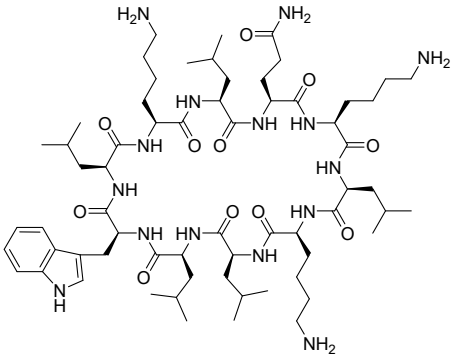

c(Lys-Leu-Lys-Leu-Lys-Trp-Leu-Leu-Leu-Gln) (**BPC904W**)

HPLC (λ = 220 nm): t_R = 6.92 min (>99% purity). ESI-MS (*m/z*): 1265.1 $[M+H]^+$, 1287.0 $[M+Na]^+$. HRMS (ESI) (*m/z*): calculated for $C_{64}H_{111}N_{15}O_{11}$ $[M+2H]^{2+}$ 632.9288, found 632.9283; calculated for $C_{64}H_{110}N_{15}O_{11}$ $[M+H]^+$ 1264.8504, found 1264.8495.

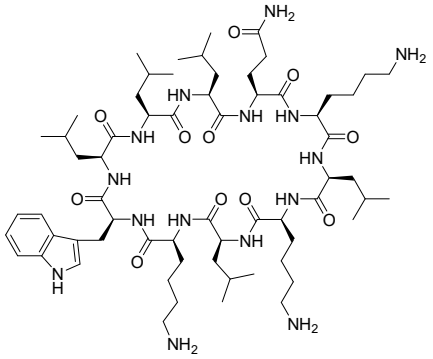

c(Leu-Lys-Lys-Leu-Leu-Trp-Leu-Lys-Leu-Gln) (**BPC906W**)

HPLC (λ = 220 nm): t_R = 7.04 min (99% purity). ESI-MS (*m/z*): 1264.8 $[M+H]^+$, 1286.8 $[M+Na]^+$. HRMS (ESI) (*m/z*): calculated for $C_{64}H_{111}N_{15}O_{11}$ $[M+2H]^{2+}$ 632.9288, found 632.9307; calculated for $C_{64}H_{110}N_{15}O_{11}$ $[M+H]^+$ 1264.8504, found 1264.8502.

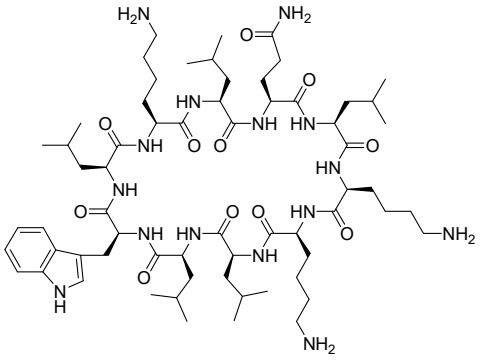

c(Lys-Lys-Lys-Leu-Lys-Trp-Lys-Leu-Lys-Gln) (**BPC908W**)

HPLC (λ = 220 nm): t_R = 5.91 min (92% purity). ESI-MS (*m/z*): 1309.9 $[M+H]^+$, 1331.9 $[M+Na]^+$. HRMS (ESI) (*m/z*): calculated for $C_{64}H_{114}N_{18}O_{11}$ $[M+2H]^{2+}$ 655.4452, found 655.4467; calculated for $C_{64}H_{113}N_{18}O_{11}$ $[M+H]^+$ 1309.8831, found 1309.8804.9

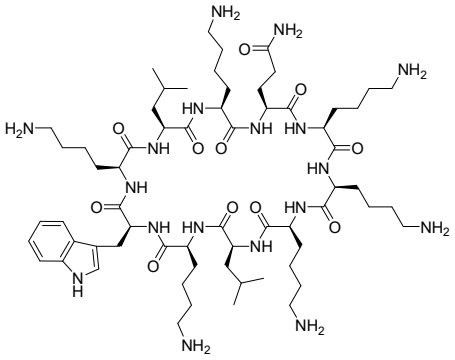

c(Leu-Lys-Lys-Leu-Lys-Trp-Leu-Leu-Leu-Gln) (**BPC910W**)

HPLC (λ = 220 nm): t_R = 7.60 min (93% purity). ESI-MS (*m/z*): 1264.9 $[M+H]^+$, 1286.8 $[M+Na]^+$. HRMS (ESI) (*m/z*): calculated for $C_{64}H_{111}N_{15}O_{11}$ $[M+2H]^{2+}$ 632.9288, found 632.9314; calculated for $C_{64}H_{110}N_{15}O_{11}$ $[M+H]^+$ 1264.8504, found 1264.8477.

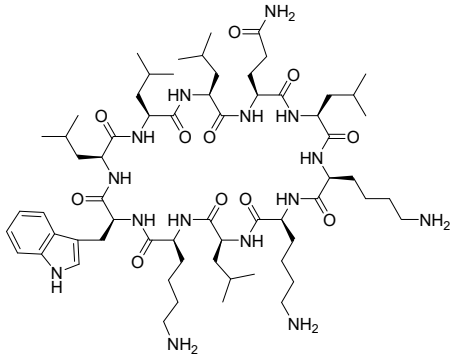

c(Leu-Lys-Lys-Leu-Leu-Trp-Leu-Lys-Lys-Gln) (**BPC912W**)

HPLC (λ = 220 nm): t_R = 6.82 min (84% purity). ESI-MS (*m/z*): 1279.9 $[M+H]^+$, 1301.8 $[M+Na]^+$. HRMS (ESI) (*m/z*): calculated for $C_{64}H_{112}N_{16}O_{11}$ $[M+2H]^{2+}$ 640.4343, found 640.4358; calculated for $C_{64}H_{111}N_{16}O_{11}$ $[M+H]^+$ 1279.8613, found 1279.8603.

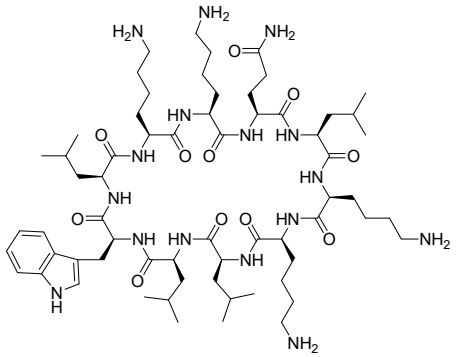

5.6. General conditions for biological tests

5.6.1. Bacterial strains and growth conditions

The following plant pathogenic bacterial strains were used: *Erwinia amylovora* PMV6076 (Institut National de la Recherche Agronomique, Angers, France), *Pseudomonas syringae* pv. syringae EPS94 (Institut de Tecnologia Agroalimentària, Universitat de Girona, Spain), *Xanthomonas axonopodis* pv. vesicatoria 2133-2, *Pseudomonas syringae* pv. actinidiae Psa3700.1.1, *Xanthomonas fragariae* Xf349-9A (Instituto Valenciano de Investigaciones Agrarias, Valencia, Spain), and *Xanthomonas arboricola* pv. pruni CFBP5563 (Collection Française de Bactéries associées aux Plantes, Angers, France). All bacteria except for *X. fragariae* were stored in Luria Bertani (LB) broth supplemented with glycerol (20%) and maintained at -80 °C. For *X. fragariae*, Medium B [49] was used instead of LB. *E. amylovora*, *X. arboricola* pv. pruni*, P. syringae* pv. syringae and *P. syringae* pv. actinidiae were scrapped from the agar media after growing for 24 at 25 °C, and *X. axonopodis* pv. *vesicatoria* and *X. fragariae* after growing for 48 h at 25 °C. The cell material was suspended in sterile water to obtain a suspension of 10^8 CFU mL^{-1}.

5.6.2. Antimicrobial activity

Lyophilized peptides were solubilized in sterile Milli-Q water to a final concentration of 1 mM and filter sterilized through a 0.22 μm pore filter. For minimum inhibitory concentration (MIC) assessment, dilutions of the peptides were made to obtain a stock concentration of 500, 250, 125, 62, 31, 16 and 8 μM. Twenty microlitres of each dilution were mixed in a microtiter plate well with 20 μL of the corresponding suspension of the bacterial indicator, 160 μL of Trypticase Soy Broth (TSB) (BioMèrieux, France) to a total volume of 200 μL. Three replicates for each strain, peptide and concentration were used. Bacterial growth was determined by optical density measurement at 600 nm (Bioscreen C, Labsystem, Helsinki, Finland). Microplates were incubated at 25 °C with 20 sec shaking before hourly absorbance measurement for 48 h. The experiment was repeated twice. The MIC was taken as the lowest peptide concentration with no growth at the end of the experiment.

5.6.3. Hemolytic activity

The hemolytic activity of the peptides was evaluated by determining hemoglobin release from erythrocyte suspensions of horse blood (5% vol/vol)(Oxoid) as previously described. Blood was centrifuged at 6000 g for 5 min, washed three times with TRIS buffer (10 mM TRIS, 150 mM NaCl, pH 7.2) and ten diluted.

Peptides were solubilized in TRIS buffer and mixed with horse erythrocytes and the final concentrations tested were 375, 250, 150 and 50 μM. The mixture was incubated under continuous shaking for 1 h at 37 °C. Then, the tubes were centrifuged at 3500g for 10 min, 80 μL aliquots of the supernatant transferred to 100-well microplates (Bioscreen), diluted with 80 μL water, and the absorbance measured at 540 nm (Bioscreen). Complete hemolysis was obtained by the addition of melittin at 100 μM (Sigma-Aldrich Corporation, Madrid, Spain). The percentage of hemolysis (*H*) was calculated using the equation: $H = 100\times[(Op-Ob)/(Om-Ob)]$, where *Op* was the density for a given peptide concentration, *Ob* for the buffer, and *Om* for the melittin positive control.

5.6.4. Effect of peptide infiltration on tobacco leaves

Peptide solutions of 50, 150 and 250 μM were infiltrated (100 μL) into the mesophylls of fully expanded tobacco leaves. Six independent inoculations were carried out in a single leaf, and at least three independent inoculations were performed per peptide and concentration randomly distributed in different leaves and plants. Control infiltrations with water (negative control) or melittin (positive control) at the same molar concentration were performed. The appearance of symptoms on the leaves was followed for 48 h after infiltration and measured as a lesion diameter.

6. REFERENCES

Abelleira, A.; Ares, A.; Aguin, O.; Peñalver, J.; Morente, M. C.; López, M.M.; Mansilla, J. P. *J. Appl. Microbiol*. **2015**, 1659–1671.

Agrios G.N. *Plant pathology*, 5th ed., 2005, Academic Press, San Diego, California.

Badosa, E.; Ferre, R.; Planas, M.; Feliu, L.; Besalú, E.; Cabrefiga, J.; Bardají, E.; Montesinos, E. *Peptides* **2007**, 2276-2285.

Badosa, E.; Moiset, G.; Montesinos, L.; Talleda, M.; Bardají, E.; Feliu, L.; Planas, M.; Montesinos, E. *PloS ONE* **2013**, e85515.

Bahar, A.A.; Ren, D. *Pharmaceuticals* **2013**, 1543-1575.

Bektas, Y.; Eulgem, T. *Front Plant Sci*. **2015**, 804.

Bernegossi, J.; Calixto, G. M. F.; Sanches, P. R. S.; Fontana, C. R.; Cilli, E. M.; Garrido, S. S.; Chorilli, M. *Molecules* **2016**, 37.

Blondelle, S.E.; Lohner, K. *Biopolymers* **2000**, 74-87.

Brogden, K. A. *Nat. Rev. Microbiol*. **2005**, 238–250.

Brotman, Y.; Makovitzki, A.; Shai, Y.; Chat, I.; Viterbo, A. *Appl. Environ. Microbiol*. **2009**, 5373-7379.

Brunner, F.; Rosahl, S.; Lee, J.; Rudd, J.J.; Geiler, C.; Kauppinen, S.; Rasmussen, G.; Scheel, D.; Nurnberger, T. *Embo J*. **2002**, 6681-6688.

Chan, D. I.; Prenner, E. J.: & Vogel, H. J. *Biochim. Biophys. Acta-Biomembr.* **2006**, 1184–1202.

Choi, J.; Baek, K.-H.; Moon, E. *Plant Pathol. J.* **2014**, 245–253.

Cirac, A. D.; Torné, M.; Badosa, E.; Montesinos, E.; Salvador, P.; Feliu, L.; Planas, M. *Molecules* **2017**, 1054.

Concannon, S. P.; Crowe, T. D.; Abercombie, J. J.; Molina, C. M.; Hou, T.; Sukumaran, D. K.; Raj, P. A.; Leung, K.-P. *J. Med. Microbiol*. **2003**, 1083-1093.

Conlon, J. M.; Mechkarska, M.; Radosavljevic, G.; Attoub, S.; King, J. D.; Lukic, M.; McClean, S. *Peptides* **2014**, 132-140.

Czihal, P.; Knappe, D.; Fritsche, S.; Zahn, M.; Berthold, N.; Piantavigna, S.; Müller, U.; Van Dorpe, S.; Herth, N.; Binas, A.; Köhler, G.; De Spiegeleer, B.; Martin, L. L.; Nolte, O.; Sträter, N.; Alber, G.; Hoffmann, R. *ACS Chem. Biol.* **2012**, 1281-1291.

Dathe, M.; Wieprecht, T. *Biochim. Biophys. Acta-Biomembr*. **1999**, 71-87.

de Veer, S.J.; Weidmann, J.; Craik, D.J. *Acc. Chem. Res*. **2017**, 1557-1565.

Domalaon, R.; Zhanel, G.G.; Schweizer, F. *Curr. Top. Med. Chem*. **2016**, 1217–1230.

European and Mediterranean Plant Protection Organization (EPPO). 2005.

Felix, G.; Duran, J.D.; Volko, S.; Boller, T. *Plant J*. **1999**, 265-276.

Felix, G.; Boller, T. J. *Biol. Chem*. **2003**, 6201-6208.

Gawande, P. V.; Leung, K. P.; Madhyastha, S. *Curr. Microbiol*. **2014**, 635-641.

Gour, S.; Kaushik, V.; Kumar, V.; Bhat, P.; Yadav, S. C.; Yadav. J. K. *J. Pept. Sci*. **2016**, 201-207.

Grant, G.A. *Synthetic Peptides. A User's Guide*, W.H. Freeman and Company: New York, 1992.

Grau-Campistany, A.; Manresa, A.; Pujol, M.; Rabanal, F.; Cajal, Y. *Biochim. Biophys. Acta.* **2016**, 333–343.

Grant, G.A. *Synthetic Peptides. A User's Guide*.; W.H. Freeman and Company: New York, 1992.

Güell, I.; Cabrefiga, J.; Badosa, E.; Ferre, R.; Talleda, M.; Bardají, E.; Planas, M.; Feliu, L.; Montesinos, E. *Appl. Environ. Microbiol.* **2011**, 2667-2675.

Güell, I.; Vilà, S.; Badosa, E.; Montesinos, E.; Feliu, L.; Planas, M. *Pept Sci*. **2017**, e23012.

Hale, J. D.; Hancock, R. E. *Expert Rev. Anti-Infect. Ther*. **2007**, 951–959.

Halim, V. A.; Altmann, S.; Ellinger, D.; Eschen-Lippold, L.; Miersch, O.; Scheel, D.; Rosahl, S. *Plant J.* **2009**, 230-242.

Hancock, R. E. *Peptide antibiotics*. **1997**, 418-422.

Hong, S. Y.; Oh, J. E.; Kwon, M. Y.; Choi, M. J.; Lee, J. H.; Lee, B. L.; Moon, H. M.; Lee, K. H. *Antimicrob. Agents Chemother*. **1998**, 2534-2541.

Hu, W.; Lee, K.-C.; Cross, T.A. *Biochemistry* **1993**, 7035–7047.

Jerala, R. *Expert Opin Investig Drugs*. **2007**, 1159-1169.

Ji, S.; Li, W.; Zhang, L.; Zhang, Y.; Cao, B. *Biochem. Biophys. Res. Commun.* **2014**, 650–655.

Kaiser E, Colescott RL, Bossinger CD, Cook P. *Anal Biochem*. **1970**, 595-598.

Kates, S.; Albericio, F., *Solid-phase synthesis a practical guide*. 2000. Nova York: Marcel Dekker.

Kim, Y.; Komoda, E.; Miyashita, M.; Miyagawa, H. *J. Agric. Food Chem*. **2014**, 5781-5788.

Kim, Y.; Miyashita, M.; Miyagawa, H. *J. Agric. Food Chem*. **2015**, 5894-5901.

Kim, Y.; Miyashita, M.; Miyagawa, H. *Biosci. Biotechnol. Biochem*. **2016**, 1054-1057.

Lacombe, S.; Rougon-Cardoso, A.; Sherwood, E.; Peeters, N.; Dahlbeck, D.; van Esse, H.P.; Smoker, M.; Rallapalli, G.; Thomma, B.P.H.J.; Staskawicz, B.; Jones, J.D.G.; Zipfel, C. *Nature Biotechnol*. **2010**, 365-369.

Landgraf, R.; Smolka, U.; Altmann, S.; Eschen-Lippold, L.; Senning, M.; Sonnewald, S.; Weigel, B.; Frolova, N.; Strehmel, N.; Hause, G.; Scheel, D.; Böttcher, C.; Rosahl, S. *Plant Cell*. **2014**, 3403-3415.

Lee, D.W.; Kim, V.S. *Plant Pathol. J.* **2015**, 1-11.

Lorenzón, E. N.; Cespedes, G. F.; Vicente, E. F.; Nogueira, L. G.; Bauab, T. M.; Castro, M. S.; Cilli, E. M. *Antimicrob. Agents Chemother*. **2012**, 3004–3010.

Makovitzki, A.; Avrahamai, D.; Shai, Y. *Proc Natl Acad Sci USA*. **2006**, 15997-16002.

Makovitzki, A.; Viterbo, A.; Brotman, Y.; Chet, I.; Shai, Y. *Appl Environ Microbiol.* **2007**, 6629-6636.

Malina, A.; Shai, Y. *Biochem. J.* **2005**, 695-702.

Mandal, S. M.; Dey, S.; Mandal, M.; Sarkar, S.; Maria-Neto, S.; Franco, O. L. *Peptides* **2009**, 633-637.

Mandal, S. M.; Barbosa, A. E. A. D.; Franco, O. L. *Biotechnol. Adv.*, **2013**, 338-345.

Mangoni, M.L.; Shai, Y. *Cell Mol Life Sci.* **2011**, 2267-2280.

Markus, A. *J. Exp. Bot*. **2013**, 5269-5279.

Matsuzaki, K. *Biochim. Biophys. Acta*. **2009**, 1687-1692.

Merrifield, R. B. *J. Am. Chem. Soc.* **1963**, 2149.

Mishra, B.; Leishangthem, G. D.; Gill, K.; Singh, A. K.; Das, S.; Singh, K.; Xess, I.; Dinda, A.; Kapil, A.; Patro, I. K.; Dey, S. *Biochim. Biophys. Acta*. **2013**, 677-686.

Mitrev, S.; i Kovačević, B. *J. Plant Pathol.* **2006**, 321-324.

Miyashita, M.; Oda, M.; Ono Y.; Komoda E.; Miyagawa, H. *ChemBioChem*. **2011**, 1323-1329.

Molhoek, E.M.; van Dijk, A.; Veldhuizen, E.J.A.; Dijk-Knijnenburg, H.; Mars-Groenendijk, R.H.; Boele, L.C.L.; Kaman-van Zanten, W.E.; Haagsman, H.P.; Bikker, F.J. *Int. J. Antimicrob. Agents.* **2010**, 271–274.

Monroc, S.; Badosa, E.; Feliu, L.; Planas, M.; Montesinos, E.; Bardají, E. *Peptides* **2006**, 2567-2574.

Monroc, S.; Badosa, E.; Besalú, E.; Planas, M.; Bardají, E.; Montesinos, E.; Feliu, L. *Peptides* **2006***,* 2575-2584.

Muñoz, A.; López-García, B.; Pérez-Payá, E.; Marcos, J. F. *Biochem. Biophys. Res. Commun*. **2007**, 172-177.

Muthamilarasan, M.; Prasad, M. *J. Biosci*. **2013**, 433–449.

Na, D. H.; Faraj, J.; Capan, Y.; Leung, K. P.; DeLuca, P. P. *Pharm. Res*. **2007**, 1544-1550.

Nan, Y.H.; Bang, J.-K.; Jacob, B.; Park, I.-S.; Shin, S.Y. *Peptides* **2012**, 239–247.

Ng-Choi, I.; Soler, M.; Güell, I.; Badosa, E.; Cabrefiga, J.; Bardají, E.; Montesinos, E.; Planas, M.; Feliu, L. *Prot. Pept. Lett*. **2014**, 357-367.

Nomura, K.; Mecey, C.; Lee, Y.-N.; Imboden, L. A.; Chang, J. H.; & He, S. Y. *Proc. Natl. Acad. Sci. USA*. **2011**, 10774–10779.

Nürnberger, T.; Nennstiel, D.; Jabs, T.; Sacks, W. R.; Hahlbrock, K.; Scheel, D. *Cell*. **1994**, 449-460.

Oerke, E.C*. J. Agric. Sci*. **2006**, 31–43.

Okubo, B.; Silva, O.; Migliolo, L.; Gomes, D; Porto, W.; Batista, C.; Ramos, C.; Holanda, H.; Dias, S.; Franco, O.; Moreno, S. *Plos One* **2012**, e33639.

Oh, D.; Shin, S.Y.; Lee, S.; Kang, J.H.; Kim, S.D.; Ryu, P.D. *Biochemistry* **2000**, 11855-11864.

Oren, Z.; Shai, Y. *Biochemistry* **1997**, 1826-1835.

Oren, Z.; Lerman, J. C.; Gudmundsson, G. H.; Agerberth, B.; Shai, Y. *Biochem. J.* **1999**, 501-513.

Ostorhazi, E.; Nemes-Nikodem, E.; Knappe, D.; Hoffmann, R. *Protein Pept. Lett*. **2014**, 368-373.

Pantic, J. M.; Radosavljevic, G. D.; Jovanovic, I. P.; Arsenijevic, N. N.; Conlon, J. M.; Lukic, M. L. *Peptides* **2015**, 269-275.

Pieterse, J.; Leon-Reyes, A.; Van der Ent, S.: Van Wees, M. *Nat. chem. biol*. **2009**, 308–316.

Piqué, N.; Miñana-Galbis, D.; Merino, S.; Tomás, J. M. *Int. J. Mol. Sci.* **2015**, 12836–12854.

Prabhu, S.; Dennison, S. R.; Mura, M.; Lea, R. W.; Snape, T. J.; Harris, F. *J. Pept. Sci*. **2014**, 909-915.

Rajasekaran, G.; Kamalakannan, R.; Shin, S.Y. *J. Pept. Sci.* **2015**, 779–785.

Russo, A.; Aiello, C.; Grieco, P.; Marasco, D. *Curr. Med. Chem*. **2016**, 748-762.

Saravanan, R.; Li, X.; Lim, K.; Mohanram, H.; Peng, L.; Mishra, B.; Basu, A.; Lee, J.-M.; Bhattacharjya, S.; Leong, S.S. *Biotechnol. Bioeng.* **2014**, 37–49.

Semlali, A.; Leung, K. P.; Curt, S.; Rouabhia, M. *Peptides* **2011**, 859-867.

Shai, Y. *Peptide Science* **2002**, 236-248.

Shang, D.; Yu, F.; Li, J.; Zheng, J.; Zhang, L.; Li, Y. *Zoolog. Sci*. **2009**, 220-226.

Silva, O. N.; Porto, W. F.; Migliolo, L.; Mandal, S. M.; Gomes, D. G.; Holanda, H. H. S.; Silva, R. S. P.; Dias, S. C.; Costa, M. P.; Costa, C. R.; Silva, M. R.; Rezende, T. M.; Franco, O. L. *Biopolymers* **2012**, 322-331.

Sistla, S. *Mol. Cell. Biochem*. **2013**, 29-38.

Srinivas, S.; Prakash, V. *Int. J. Pept. Res. Ther*. **2010**, 7-15.

Straus, S. K., i Hancock, R. E. *Biochim. Biophys Acta-Biomembr*. **2006**, 1215-1223.

Strömsted, A.A.; Pasupuleti, M.; Schmidtchen, A.; Malmsten, M. *Antimicrob. Agents Chemother.* **2009**, 593–602.

S. Vilà Roura, *Disseny i síntesi de lipopèptids conjugats derivats de BPC194*, Universitat de Girona, 2014.

Theberge, S.; Semlali, A.; Alamri, A.; Leung, K. P.; Rouabhia, M. *Microbiol.* **2013**, *13*, 246.

Toke, O. *Peptide Science* **2005**, 717-735.

Vandroemmeab, J.; Van Vaerenbergha, J; De Vosb, P.; Maesa, M. *Plant Pathology*. **2008**, 438–444

Vilà, S.; Badosa, E.; Montesinos, E.; Feliu, L; Planas, M. *Org. Biomol. Chem.* **2013**, 3365.

Vilà, S.; Badosa, E.; Montesinos, E.; Planas, M.; Feliu, L. *PLoS ONE* **2016**, e0151639.

Vojkovsky T. *Pept Res*. **1995,** 236-237.

Volke, D.; Krizsan, A.; Berthold, N.; Knappe, D.; Hoffmann, R. *J. Proteome Res*. **2015**, 3274-3283.

Wang, C.; Li, H.-B.; Li, S.; Tian, L.-L.; Shang, D.-J. *Biochimie*. **2012**, 434-441.

Wang, C.; Tian, L.-L.; Li, S.; Li, H.-B.; Zhou, Y.; Wang, H.; Yang, Q.-Z.; Ma, L.-J.; Shang, D.-J. *PLoS ONE* **2013**, e60462.

Wang, C.; Chen, Y.-W.; Zhang, L.; Gong, X.-G.; Zhou, Y.; Shang, D.-J. *J. Drug. Target*. **2016**, 548-556.

Wei, C.; Hsu, S.; Deng, W.; Wen, Y.; Huang, H. *PLoS ONE* **2012**, e41056.

Wessolowski, A.; Bienert, M.; Dathe, M. *J. Pept. Res.* **2004**, 159–169.

Wieprecht, T.; Dathe, M.; Krause, E.; Beyermann, M.; Maloy, W. L.; MacDonald, D. L.; Bienert, M. *FEBS Letters*. **1997**, 135-140.

Wu, M.; Maier, E.; Benz, R.; Hancock, R. E. *Biochemistry*. **1999**, 7235-7242.

Xiao, J.; Zhang, H.; Niu, L.; Wang, X. *J. Agric. Food Chem*. **2011**, 1145-1151.

Xie, J.; Zhao, U.; Li, S.; Yan, Z.; Li, J.; Li, Y.; Mou, L.; Zhang, B.; Yang, W.; Miao, X. *Chem. Biol. Drug Des.* **2017**, 1–13.

Yamaguchi, Y.; Huffaker, A. *Curr. Opin. Plant Biol*. **2011**, 351-357.

Yeaman, M. R.; Yount, N. Y. *Pharmacol. Rev*. **2003**, *55 (1)*, 27-55.